

Dissertation

**submitted to the
Combined faculties for the Natural Sciences and for Mathematics
of the Ruperto-Carola University of Heidelberg, Germany
for the degree of
Doctor of Natural Sciences**

presented by

Diplom-biologist

Jens Hrach

Born in:

Gross-Gerau, Germany

Oral-examination:

**Toxicogenomic approaches
for the prediction of hepatotoxicity *in vitro***

Referees: Prof. Dr. Thomas Holstein
PD Dr. Suat Özbek

ACKNOWLEDGEMENTS	2
ABBREVIATIONS	3
SUMMARY	5
ZUSAMMENFASSUNG	7
1 INTRODUCTION	9
1.1 Endeavors of modern toxicology.....	9
1.2 The liver morphology and its cell types	10
1.3 Hepatocytes and xenobiotic metabolism	12
1.4 Hepatotoxicity	18
1.5 <i>In vitro</i> liver models.....	19
1.6 Endpoints for the analysis of hepatocyte cultures	27
1.7 Toxicogenomics	28
1.8 Techniques for global gene expression analysis.....	31
1.9 Toxicoproteomics.....	35
1.10 Aim of this work.....	37
2 MATERIALS AND METHODS	38
2.1 Materials	38
2.1.1 Chemicals and reagents.....	38
2.1.2 Technical equipment and auxiliary material	40
2.1.3 Kits.....	42
2.1.4 Software	42
2.1.5 Culture media and supplements	43
2.1.6 Buffers and solutions.....	43
2.1.6.1 Perfusion buffers for rat liver perfusion	43
2.1.6.2 Buffers for SELDI-TOF-MS	44
2.1.6.3 Buffers for protein-preparation and immunodetection.....	44
2.1.6.4 Buffers and solutions for Illumina BeadChip arrays	45
2.1.6.5 Buffers and solutions for Affymetrix Gene Chips®	45
2.2 Methods	47
2.2.1 Cell culture	47
2.2.1.1 Isolation of primary rat hepatocytes	47
2.2.1.2 Trypan Blue exclusion test	48
2.2.1.3 Preparation of culture dishes.....	48

2.2.1.4	Plating of cells.....	49
2.2.1.5	Culture of FaO and HepG2-cells	50
2.2.1.6	Suspension culture	50
2.2.1.7	Precision cut liver slices	50
2.2.1.8	Isolation of primary human hepatocytes.....	51
2.2.1.9	HepaRG cells.....	51
2.2.2	Rat <i>in vivo</i> study	51
2.2.3	Biochemical methods and cell viability assays.....	52
2.2.3.1	CellTiter-Glo® Luminescent cell viability assay.....	52
2.2.3.2	WST-1-assay	53
2.2.3.3	LDH release.....	53
2.2.3.4	Cytochrome P450 isoform induction and activity	55
2.2.3.5	Canalicular transporter activity	56
2.2.4	Molecular biological methods	56
2.2.4.1	Isolation of RNA and proteins.....	56
2.2.4.2	Quantification and quality check of nucleic acids.....	57
2.2.4.3	TaqMan® Low Density Arrays (TLDA)	58
2.2.4.4	Processing of RNA for Illumina and Affymetrix Chips	61
2.2.5	Microarray data analysis.....	66
2.2.5.1	Data extraction and quality control from Illumina BeadChip arrays	66
2.2.5.2	Data extraction and quality control from Affymetrix arrays.....	67
2.2.6	Protein separation by SDS polyacrylamide gel electrophoresis (SDS-PAGE)	68
2.2.7	Protein detection by western blot analysis and immune detection.....	69
2.2.8	SELDI-TOF analysis.....	70
3	RESULTS AND DISCUSSIONS.....	73
3.1	Comparison of different global gene expression platforms.....	73
3.1.1	Results of the platform comparison study	76
3.1.1.1	Experimental layout	76
3.1.1.2	Intraplatform comparability	78
3.1.1.3	Interplatform comparability	80
3.1.1.4	Biological interpretation	85
3.1.2	Conclusions of the platform comparison study.....	97
3.2	Establishment of a longer term cell culture of primary rat and human hepatocytes.....	100
3.2.1	Morphological and functional characterization of primary rat hepatocytes	101
3.2.1.1	Morphological examinations	101
3.2.1.2	CYP inducibility.....	104
3.2.1.3	Canalicular transport	107
3.2.1.4	Conclusions of the morphological and functional data	108

3.3 Global expression studies with different human and rat cell culture systems	110
3.3.1 Initial changes introduced by the process of perfusion	114
3.3.1.1 Primary rat hepatocytes	114
3.3.1.2 Primary human hepatocytes.....	116
3.3.2 Temporal changes in global gene expression.....	119
3.3.3 Analysis of protein expression with SELDI-TOF	124
3.3.4 Gene expression in established cell lines used as reference	127
3.3.5 Changes of gene expression early in culture - Cellular adaptation processes in primary hepatocytes	129
3.3.5.1 Liver slices.....	134
3.3.6 Molecular mechanisms affected over time in culture	137
3.3.6.1 Overview of the affected mechanisms in rat hepatocytes.....	137
3.3.6.2 Response to wounding, oxidative stress and immune response	139
3.3.6.3 ECM, cytoskeleton and tissue remodelling	141
3.3.6.4 Metabolic competence	142
3.3.6.5 Intracellular signalling and transcription factors	144
3.3.6.6 Affected mechanisms in human hepatocytes.....	146
3.3.7 Confirmation of the microarray results with TaqMan PCR.....	148
3.3.8 Conclusions from the characterization of primary hepatocytes in culture.....	150
3.4 Development of an <i>in vitro</i> liver toxicity prediction model based on longer term primary hepatocyte culture	155
3.4.1 Introduction to the <i>in vitro</i> prediction model	155
3.4.2 Short description of the test compounds.....	155
3.4.3 Experimental setup and dose finding	159
3.4.4 Data Analysis and establishment of an <i>in vitro</i> prediction model for hepatotoxicity	163
3.4.5 Analysis of the top ranked genes of the prediction model	169
3.5 Insights into the mechanisms of action for selected compounds	171
3.5.1 EMD X	171
3.5.2 AAP	174
3.5.3 Dex	177
4 CONCLUDING REMARKS AND FUTURE PERSPECTIVES	179
5 REFERENCES	183
APPENDIX	201

ACKNOWLEDGEMENTS

I want to thank all the people who contributed directly or indirectly to this work!

A special thanks to my thesis adviser Prof. Dr. Thomas Holstein. He escorted me throughout my studies and raised my general interest in biological sciences with his enthusiasm and knowledge of the molecular processes in living organisms.

I am deeply grateful to Dr. Phil Hewitt for giving me the opportunity to do my PhD work in the laboratories of the institute for toxicology at Merck-Serono and for all his support and scientific advice throughout their duration. He encouraged me to work independently; discussions with him were an important factor in focusing my interest into the field of toxicogenomics and beyond.

I would also like to thank Dr. Stefan Müller for his interest, the helpful support and useful suggestions throughout my work. He has always been open for discussions and put my work into the right context.

For their willingness to serve as referee for my thesis, I would like to thank PD Dr. Suat Özbek and Prof. Ursula Kummer. Another thanks to Dr. Peter-Jürgen Kramer and Prof. Dr. Hans Harleman, heads of the institute of toxicology, for the interest in my PhD work and their helpful comments. Both of them permitted me not only to perform my studies in their institute but also enabled me to attend advanced trainings courses and scientific conferences.

I would like to thank all the people at Merck, especially, all the members of our group who contributed to this work by discussions, help and friendship. Dr. Anja von Heydebreck and Dr. Eike Staub for bioinformatical support, Jörg Hiller for solving (nearly) all my computer-problems, Klaudia Clement, Bettina von Eiff, Yvonne Walter, Margret Kling and Melanie Kühnl for all their support in the lab, Gregor Tuschl, Nadine Zidek, Julia Pieh, and all other previous, current and upcoming PhD-Students for making this an unforgettable part of my live.

Most of all, I want to thank my whole family for all their support and love throughout the years. Without their help in every possible way, this work wouldn't have been possible. A big hug and thank you to my wife, for all her grateful understanding, for encouraging me and for giving me the best time of my life.

ABBREVIATIONS

%	Percentage
[]	Concentration
+/- FCS	With or without the addition of fetal calf serum
°C	Centigrade
µl	Micro litre
ALDH	Aldehyde dehydrogenase
AN	Accession Number
BNF	Beta-naftoflavon
bp	Basepair
BROD	Benzyloxyresorufin O-debenzylase
BSA	Bovine Serum Albumin
Carboxi-DCFDA	5-(and-6)-carboxy-2',7'-dichlorofluorescein diacetate
CHAPS	3-[(3-Cholamidopropyl)-dimethylammonio]-1-propanesulfonate
CO ₂	Carbonic acid
Da	Dalton
Dex	Dexametasone
DMSO	Dimethyl sulfoxide
(c)DNA	(complementary) Desoxy ribonucleic acid
DTT	Dithiothreitol
ECVAM	European Centre for the Validation of Alternative Methods
EDTA	Ethylenediaminetetraacetic acid
EROD	7-ethoxyresorufin-O-deethylase
FBS	Fetal Bovine Serum
FC	Fresh cells (hepatocytes directly after perfusion)
FDA	Food and Drug Administration
g	Gram
GLP	Good Laboratory Practice
GSH	Glutathione
h	Hour
H&E	Hematoxylin and eosin stain
HepaRG	Human hepatoma cell line
HepG2	Human hepatoma cell line
Hz	Hertz (cycles per second)
i.p.	intraperitoneal
ITS	Insulin, Transferrin, Selenit
IVT	<i>In vitro</i> transcription reaction
k	Kilo

ABBREVIATIONS

kDa	kilodaltons
l	Litre
LDH	Lactate dehydrogenase
M	Molarity
mA	Mili-Ampere
min	Minute
ML	Monolayer culture
mm	millimetre
mRNA	Messenger Ribonucleic acid
MTD	Maximum tolerated dose
MW	Molecular Weight
nm	Nanometre
NRU	Neutral Red Uptake
OD	Optical density
ON	Over night
PAGE	Polyacrylamide gel electrophoresis
PB	Phenobarbital
PB1	Perfusion Buffer 1
PB2	Perfusion Buffer 2
PBS	Phosphate Buffered Saline
PCA	Principal Components Analysis
PCR	Polymerase Chain Reaction
PL	Plastic culture
rcf	Relative centrifugal force
REACH	Registration, Evaluation and Authorization of Chemicals
RMA	Robust multi-array average
(c) RNA	(complementary) Ribonucleic acid
rpm	rounds per minute
rRNA	Ribosomal Ribonucleic acid
RT	Room temperature
SDS	Sodium dodecyl sulphate
sec	Second
SELDI-TOF	Surface-enhanced laser desorption/ionization – time of flight
SOM	Self Organizing Map
Susp.	Suspension
SW	Sandwich culture
TLDA	TaqMan Low Density Array
WB	Washing buffer

SUMMARY

The pharmaceutical and chemical industry is interested to replace as much as possible *in vivo* experiments with alternative *in vitro* models which have improved capability to assess and predict the safety profile of their products. This is influenced by the 3R principles of reducing the number of tests, the refinement of existing experiments and the replacement of animal experiments with new and alternative methods (Russell & Burch, 1959). The latter is also supported by EU-programms, which ultimately will be reflected in new regulatory guidelines.

One major target in the safety testing of new chemical products is the liver. This is not surprising as the liver is the major organ for xenobiotic metabolism. Several different culture systems for primary hepatocytes are actually in use for the study of acute toxicity, the basic mechanisms of action, metabolism or enzyme induction. Yet, there is no established and standardized culture method maintaining hepatocyte specific functionality for longer term experiments. This PhD work has the aim of developing a longer-term sandwich culture model which maintains hepatocytes in their differentiated and metabolically active state. To elucidate advantages and disadvantages of this culture, it was compared to several currently used culture models. Functional tests revealed an improved metabolic activity and viability over time in culture. Global gene expression analysis showed common effects caused by the liver perfusion as well as individual differences in the different culture systems.

The improved sandwich culture was applied to a toxicologically relevant study in which the cells were dosed with fifteen well known model compounds (hepatotoxins and negative controls) and the global gene expression data was used to build a predictive discrimination model for hepatotoxicity based on a defined gene set of 724 genes. This model was successfully applied on a blinded compound and on acetaminophen, which both were correctly classified to be hepatotoxic.

The use of the new Illumina global gene expression platform enabled a detailed comparison with the current state of the art technologies from Affymetrix and TaqMan real time PCR. Several technical parameters were checked for concordance and sensitivity between both platforms and the biological interpretation of an *in vivo* and *in vitro* toxicogenomics study was compared. The results of these studies revealed a high concordance between both platforms making both of them equally applicable for toxicogenomics studies.

In conclusion, the field of toxicogenomics, applied to an *in vitro* test system proved to deliver reliable and promising results allowing new insights into the mechanism of compound toxicity. Additionally, the prediction of toxicity of new compounds, with the help of a classification model, based on a large dataset of model compounds, seems to be applicable for early screening in drug development.

ZUSAMMENFASSUNG

Die pharmazeutische und chemische Industrie ist daran interessiert, *in vivo* Experimente so weit wie möglich durch alternative *in vitro* Methoden mit Möglichkeiten zu ersetzen, die das Sicherheitsprofil ihrer Produkte besser erfassen. Dies wird beeinflusst durch die 3R-Prinzipien, das Reduzieren der Anzahl von Tierversuchen, die Verbesserung existierender Experimente und dem Ersetzen von Tierversuchen durch alternative Methoden (Russell & Burch, 1959). Letzteres wird ebenfalls durch EU geförderte Programme unterstützt und ist das Ziel verschiedener regulatorischer Richtlinien.

Ein zentrales Ziel der Sicherheitstestung neuer chemikalischer Produkte ist die Leber. Dies ist nicht überraschend, da die Leber das Hauptorgan des Fremdstoffmetabolismus ist.

Momentan werden viele verschiedene Primärhepatozyten-Kultursysteme die Untersuchung von akuter Toxizität, den zugrunde liegenden Mechanismen, dem Metabolismus oder der Enzym-Induktion eingesetzt. Zurzeit gibt es jedoch keine etablierte und standardisierte Kulturmethode, welche die hepatozytenspezifischen Funktionen erhält und somit Langzeitversuche ermöglichen würde. Die vorliegende Doktorarbeit hatte das Ziel solch eine Methode in Form der Sandwich-Kultur zu entwickeln und dadurch den Differenzierungsgrad der Zellen sowie deren metabolische Aktivität zu erhalten. Um Vor- und Nachteile dieser Kulturmethode zu beleuchten wurde sie mit anderen, momentan verwendeten Methoden verglichen. Die globale Genexpressionsanalyse zeigte gemeinsame, durch die Leber-Perfusion verursachte Effekte sowie individuelle Unterschiede der verschiedenen Zellkulturen.

Basierend auf diesem Wissen wurden toxikologisch relevante Studien mit dem Sandwich-Kultur-System durchgeführt. Dafür wurden die Zellen mit fünfzehn Modellsubstanzen behandelt, anhand ihrer globalen Genexpressionsprofile ein diskriminatives Prädiktionsmodell für Hepatotoxizität erstellt und ein Gen-Set von 724 prädiktiven Genen definiert. Dieses Modell wurde danach erfolgreich mit einer verblindeten Substanz und mit Acetaminophen getestet.

Die Nutzung einer neuen Plattform zur globalen Genexpressionsanalyse von Illumina ermöglichte den detaillierten Vergleich mit der zurzeit meistverwendeten Plattform (Affymetrix) sowie mit der TaqMan PCR. Hierbei wurden verschiedenste technische Parameter auf Übereinstimmung und Sensitivität überprüft und die biologische Interpretation von mit beiden Plattformen gemessenen *in vivo* und *in vitro* Studien verglichen. Die Ergebnisse dieser Studien zeigten die hohe Übereinstimmung

zwischen beiden Mess-Plattformen, die eine Anwendung beider in toxikogenomischen Studien erlaubt.

Zusammenfassend lässt sich sagen dass toxikogenomische Studien in Verbindung mit einem *in vitro* Test System verlässliche und viel versprechende Ergebnisse liefert, welche neue Einblicke in den Wirkmechanismus von Substanzen ermöglicht. Zusätzlich ermöglicht die Klassifizierung von Substanzen mit Hilfe des erstellten Prädiktionsmodells ein frühes Screening in der Medikamentenentwicklung.

1 INTRODUCTION

1.1 Endeavors of modern toxicology

Toxicology is the study of adverse effects of chemical and physical agents on living organisms and the environment. The basic assumption of toxicology is that there is a relationship between the dose, the concentration at the affected site, and the resulting adverse effects. The physician Theophrast von Hohenheim (Paracelsus, 1493-1541) said: "*Alle Ding sind Gift, und nichts ohn Gift; allein die Dosis macht, daß ein Ding kein Gift ist*"¹. As he was the first one to discover the relationship between dose and effect of substances he is often called the "father of toxicology".

The purpose of modern toxicology is to understand the character and dimension of toxic effects and to regulate the use of potentially toxic substances. Up to now, there is a general lack of knowledge regarding 99% of chemicals manufactured around the world. The distinction between so-called "existing" and "new" chemicals is based on the cut-off date of 1981. All chemicals that were on the European Community market between 1 January 1971 and 18 September 1981 are called "existing"². Prior to that date, no stringent health and safety tests were needed to market chemicals, it was up to the authorities to prove that a substance posed a threat before it could be withdrawn. Since then, 3,800 so-called "new" chemicals have gone through a more stringent safety screening process. New perceptions have now introduced the possibility that the incidence of diseases, such as cancer, could be linked to this multitude of chemicals already on the market (Irigaray et al., 2007) Therefore, in June 2007, the European Parliament introduced a new system of Registration, Evaluation and Authorisation of CHemicals (REACH). Central to the system is a requirement for producers and importers of chemicals to prove that their substances are safe before put on the market (reversal of burden of proof). "Existing" chemicals will have to be screened for health and safety reasons over a period of 11 years. Therefore, defined, standardized and validated assays have to be conducted and the results regulated by national and international commissions³.

¹ "All things are poisonous and nothing is without poison, only the dose permits something not to be poisonous."

² Around 100,000, listed in the European Inventory of Existing Commercial Chemical Substances (EINECS).

³ Umweltbundesamt, Dessau-Rosslau, Germany; European Chemicals Agency, Helsinki, Finland

Up to now, only few of these mandatory tests can be accomplished with animal-free alternative methods leading to the problem that a marked increase of animal testing will be of animals are required (Figure 1). This contradicts the simultaneous effort of reducing the number of animals used in experiments for ethical and cost reasons.

In 1959, Russel and Burch suggested the principle of the 3Rs in order to reduce animal experiments (Russell & Burch, 1959). It refers to the improvement of the animal welfare by reducing the number of tests realised, the refinement of existing experiments to reduce the suffering of the animals and to a replacement of animal experiments with new and alternative methods. Considering this, it is believed that *in vitro* toxicity testing methods can be a useful, time and cost-effective supplement or in some case even a replacement of toxicology studies in living animals. Certain endpoints of toxicity can be depicted quite well, although currently available *in vitro* tests are not adequate to entirely replace animals in toxicology testing. In 1991, the European Centre for the Validation of Alternative Methods (ECVAM) was founded to assist and coordinate the development and validation of alternative test methods under the guidance of the European Union.

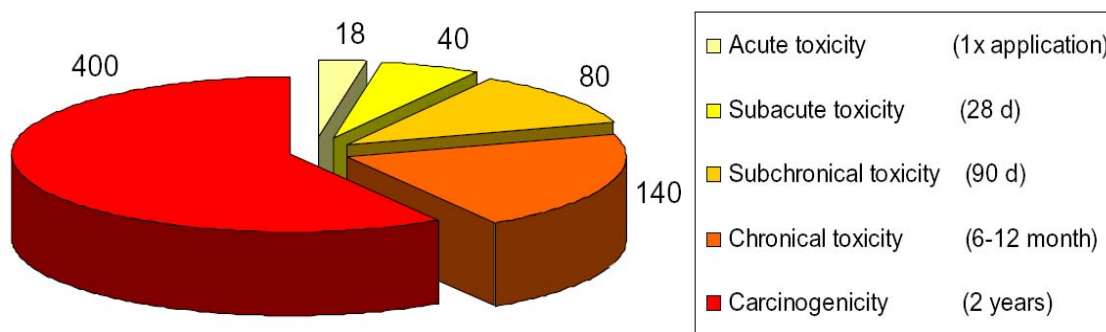


Figure 1: Increasing number of animals needed in toxicological testing procedure for one compound beginning with an acute toxicity study and ending with a 2-year carcinogenicity study.

1.2 The liver morphology and its cell types

The liver is the largest and most complex gland of the body. It is the main detoxifying organ in mammals, with large amounts of phase 1 and phase 2 metabolic enzymes and it is responsible for large parts of lipid and cholesterol metabolism, the production of hormones, phagocytosis of debris and bacteria as well as participating in iron metabolism. Additionally, it has an important role in many vital functions of the body, like the production of bile, the processing and storage of nutrients and Vitamin A and

the synthesis of blood proteins including albumin, lipoproteins, transferrin, growth factors and coagulation factors (LaBrecque, 1994; Kevresan et al., 2006).

In vertebrates, the liver is divided into four lobes, with each containing thousands of equally built lobules, and is served by two distinct blood supplies. The hepatic artery supplies oxygenated blood and the hepatic portal vein feeds blood from the intestinal system (including the pancreas and the spleen) and is rich in nutrients but is low in oxygen. The blood flows out of the liver via the hepatic vein in the direction of the inferior vena cava. Thereby, xenobiotics absorbed by ingestion have to pass the hepatocytes, the predominant cell type in liver, and can be taken up, metabolised and/or detoxified (first pass effect). The metabolites are excreted partly, depending on their chemical properties, into the bile canaliculi or via the venous blood into the urine. Hepatocytes, the liver parenchymal cells, account for about 80-90% of liver mass and 65% of cell number of a normal liver, Non-parenchymal cells like Kupffer cells (15%), endothelial cells, hepatic stellate cells or pit cells make up the remaining mass (Blouin, Bolender & Weibel, 1977; Widmann, Cotran & Fahimi, 1972; Wisse, 1977a, 1977b).

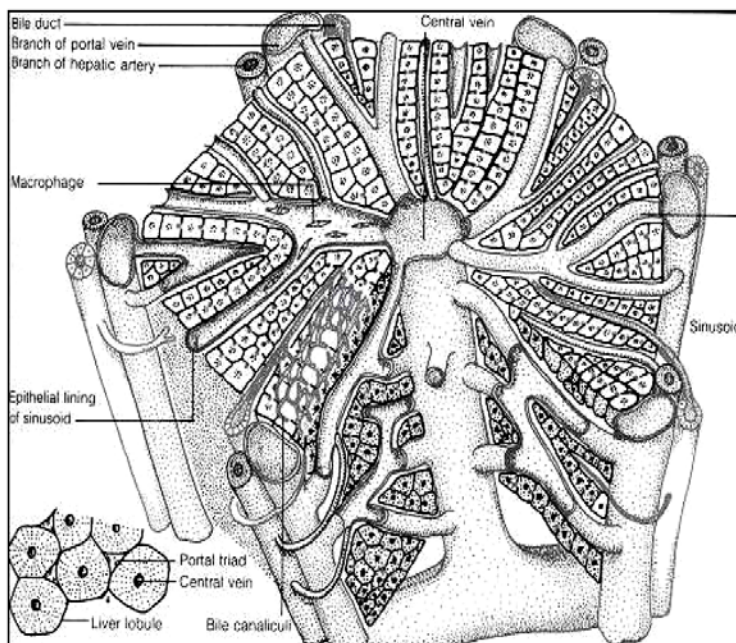


Figure 2: Schematic diagram of a normal liver lobule showing sheets of hepatocytes and the sinusoids which contain a variety of specialized cells like Ito-cells, Kupffer cells and endothelial cells. (Figure taken from www.ener-chi.com/d_liv.htm)

In a hexagonal shaped liver lobule, the central vein is surrounded by 4-6 portal areas (Matsumoto & Kawakami, 1982) and hepatocytes are arranged in cords radiating from the central vein (Figure 2). Hepatic endothelial cells form the walls of the sinusoidal, the capillaries between the cords of hepatocytes. Unlike other endothelial cells, they lack a basement membrane and the endothelial structures possess pores called fenestrae, allowing the blood to flow directly around the hepatocytes. They express several adhesion molecules facilitating inflammatory cell migration, usually as response to

activation by Kupffer cell signalling following liver damage (Ohira et al., 2003; Scoazec & Feldmann, 1994).

The Kupffer cells, resident macrophages in the liver, represent the second largest cell population of the liver. They are located in the hepatic sinusoids, in between or on top of endothelial cells, but they also make contact to the hepatocytes through their extensions. They exhibit several important functions, such as endocytosis of foreign material and bacteria, antigen presentation and secretion of biologically active products (e.g. nitric oxide and cytokines) and play an important role in immune and inflammatory responses involving cytokine-signalling (Winwood & Arthur, 1993).

Stellate cells are the fat-storing cells of the liver where they reside in the space of Disse between hepatocytes and endothelial cells. They store Vitamin A in lipid droplets, synthesize extracellular matrix proteins and it has been suggested that they contribute to liver fibrosis and immune response (Ogata et al., 1991; Friedman, 1997)

1.3 Hepatocytes and xenobiotic metabolism

As mentioned above, the liver is the main organ for endogenous and exogenous metabolism and detoxification of foreign compounds. The fenestrated endothelial allows the blood plasma to leak through the endothelial cell layer and come into close contact with the microvilli of the underlying hepatocytes in the space of Disse, providing optimal conditions for an extensive metabolic exchange (Enomoto et al., 2004). Hepatocytes are polygonally-shaped, polarized and highly differentiated cells with a turnover time *in vivo* of 300-400 days (Imai et al., 2001). There is an abundance of mitochondria and they often contain a second nucleus to manage their extensive roles in energy production, protein synthesis and metabolism/detoxification. Polyploidy is a general physiological process indicative of terminal differentiation (Sigal et al., 1999).

Each hepatocyte has a basolateral surface facing the lymph in the space of Disse and canalicular surfaces facing the bile duct. The basolateral membrane is rich in microvillus and expresses many transporters for uptake of organic anions, cations (OATPs and Oct1-3 respectively) and bile salts (NTCP, OST α and β). The canalicular membrane of neighbouring hepatocytes is sealed by tight junctions generating fine channels that run around the cells (Figure 3).

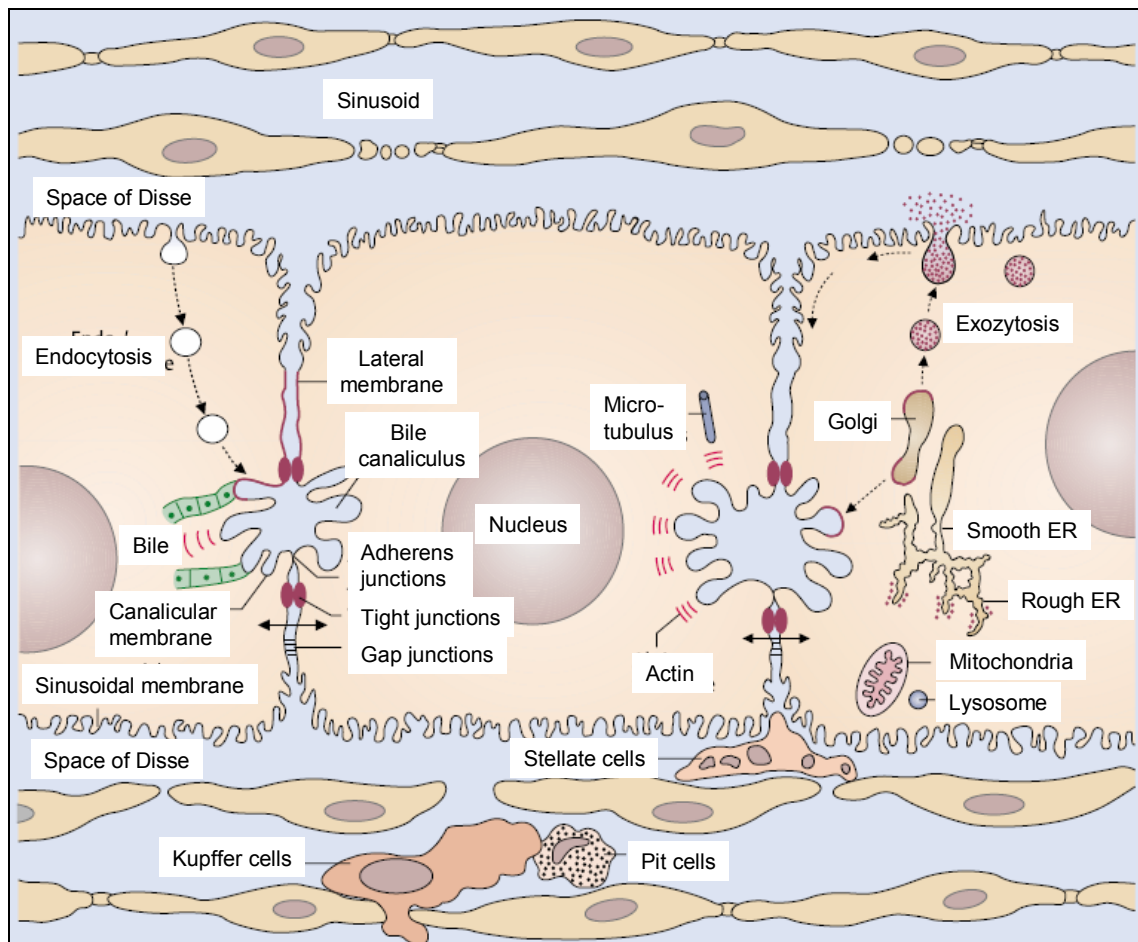


Figure 3: Ultrastructure of hepatocytes as polarized, secretory active cells with basolateral and apical surrounding (Figure adapted from Siegenthaler & Blum, 2006).

The hepatocyte membranes accommodate transporters which have overlapping substrate specificity (MDR 1-3, OATP) and are responsible for the export of bile salts or products of metabolic pathways (Figure 4). Hepatic export into the bile is an important function for the detoxification of foreign compounds entering the body and is therefore often referred to as phase 3 of xenobiotic metabolism (Makowski & Piłkuła, 1997; Yamazaki, Suzuki & Sugiyama, 1996). MRPs 1, 3 & 4 and OST α , β are basolaterally located, ATP-dependent, transporters. The shading of these transporters in Figure 4, and the white arrows in the pathways leading to and through them, symbolize their low activity in the normal hepatocyte. With hepatocellular disease or cholestasis, they are greatly up regulated, increasing the export of organic anions, thus limiting accumulation of toxic organic anions (e.g. bilirubin, bile salts) within the hepatocyte.

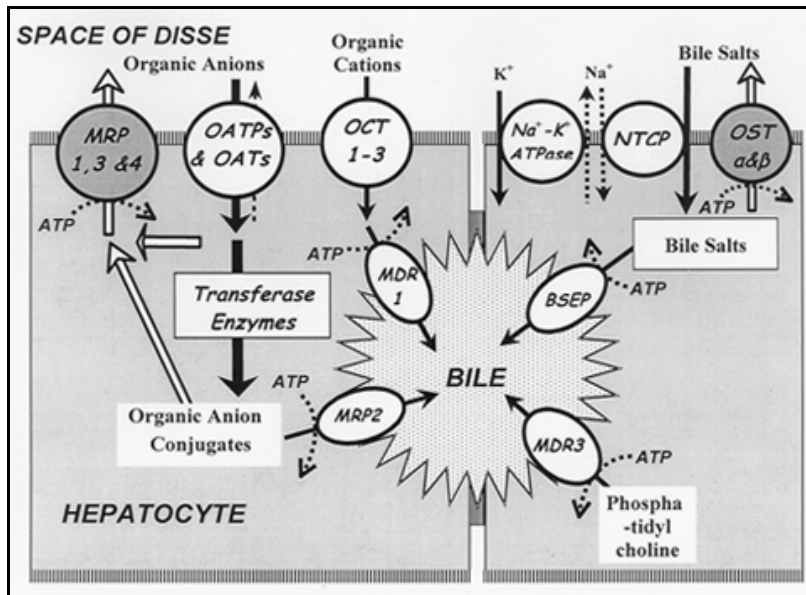


Figure 4: Schematic diagram of transport processes in hepatocytes. Shown are influx transporters, such as OATPs, OATs, NTCP and OCTs at the sinusoidal membrane, and efflux transporters, such as MDR1, MDR3, MRP2 and BSEP at the canalicular membrane. Additional efflux transporters such as MRP3, MRP4, and MRP6 at the basolateral membrane are not shown. (Figure taken from www.uwgi.org/gut/liver_05.asp)

There are different requirements, which the hepatocytes, as xenobiotic metabolizing cells, have to accomplish. The cells have to transform non-polar, lipophilic xenobiotics to more hydrophilic metabolites to facilitate their excretion into the bile or the urine (Figure 5). The resulting metabolites should be less biologically active (detoxified) and the metabolizing enzymes must have a broad, overlapping specificity so new and unknown compounds can be metabolized (Marquardt et al., 1999). For this reason, hepatocytes express a variety of metabolic enzymes, which are responsible for different types of reactions.

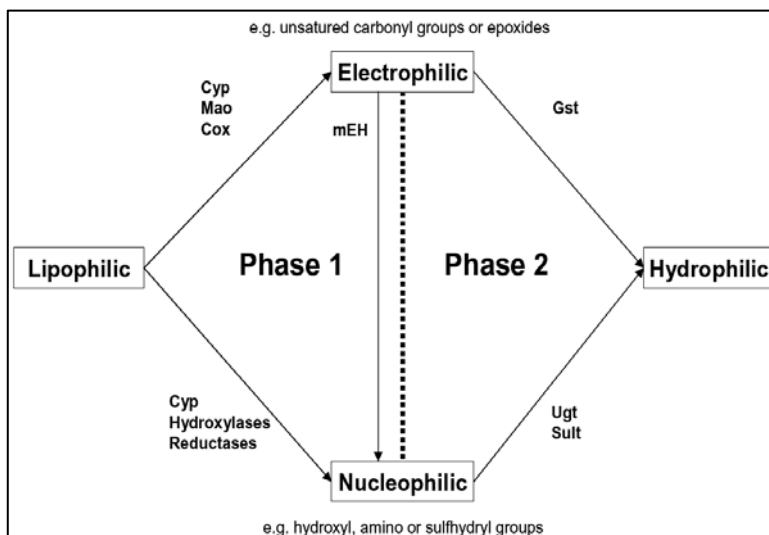


Figure 5: Phase model of xenobiotic metabolism. Lipophilic compounds are sequentially metabolized over electrophilic or nucleophilic intermediates to hydrophilic products that can afterwards be excreted renally or biliary. (Figure adapted from Marquardt & Schäfer, 2004).

Two main processes usually occur sequentially called phase 1 and phase 2. The former leads to an activation of the compound by introducing functional groups into the compound by oxidation, reduction or hydrolysis reactions. This is followed by phase 2 reactions, the conjugation of the active metabolite with a highly polar ligand like glucuronic acid or glutathione, leading to more hydrophilic products. As mentioned above, the directed transport of metabolites out of the cells by specialized transporters is often referred to as phase 3 of xenobiotic metabolism.

Typical phase 1 enzymes are listed in Table 1. The CYP enzymes, the predominant group of phase 1 enzymes in mammals, consist of at least 17 gene families with 50-60 individual isoforms (Guengerich, 2003; Waxman, 1999). The major human CYP enzymes involved in metabolism of drugs or exogenous toxins are Cyp3A4, Cyp1A1, Cyp1A2, Cyp2D6 and Cyp2C (Figure 6). The amount of each of these enzymes present in the liver reflects their importance in drug metabolism (Goodman et al., 1996).

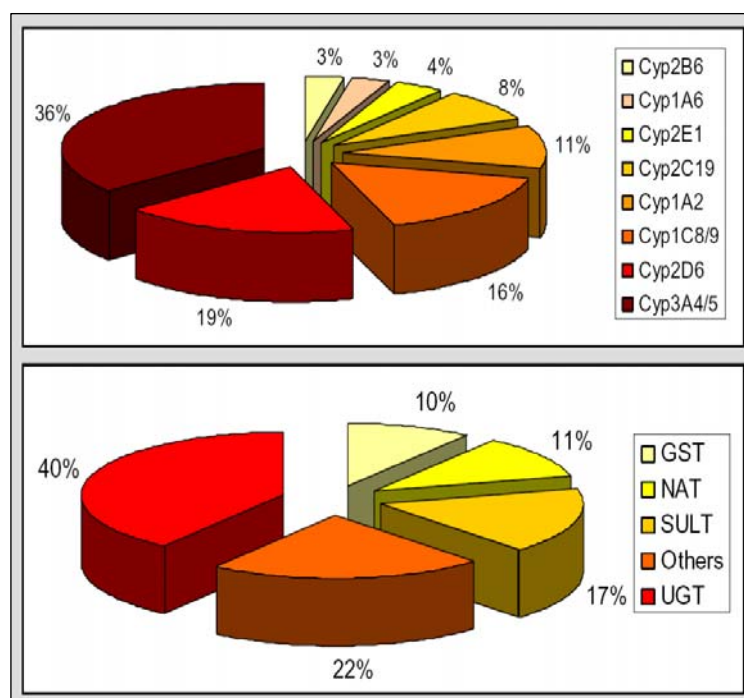


Figure 6: Proportion of drugs metabolized by cytochrome P450 isoenzymes (upper figure) and phase 2 enzymes (lower figure). Figures adapted from (Evans & Relling, 1999) and (Wrighton & Stevens, 1992).

Depending on the chemical properties of the introduced functional groups, phase 1 products can be classified as electrophilic or nucleophilic metabolites. Strong electrophilic metabolites are able to covalently bind to biological molecules like DNA, RNA or proteins and therefore have inherent cytotoxic or mutagenic potential (Besaratnia & Pfeifer, 2005). In contrast to this, nucleophiles can show biological activity by binding to cellular receptors and activating downstream reactions. Thus, the

metabolic activity of cells can lead not only to a detoxification but also, in certain cases, to a toxification of compounds.

The activation reaction is in most cases followed by a detoxifying phase 2 conjugation reaction. Thereby, the water solubility is increased allowing the cells to excrete the conjugates into the bile canaliculi and/or the blood plasma. Enzymes catalyzing phase 2 reactions are e.g. sulfotransferases (SULT), acetyltransferases (AT), glucuronyltransferases and Glutathione-S-Transferases (GST) (Figure 6).

Phase-1-Enzymes	Phase-2-Enzymes
Cytochrom-P450-dependent monooxygenases (CYP)	Transferases
Oxidoreduktases	Glutathiontransferases (GST)
Flavin-dependent monooxygenases (FMO)	UDP-glucuronosyltransferases (UGT)
Monoaminoxidasen (MAO)	Sulfotransferases (SULT)
Cyclooxygenases (COX)	Acetyltransferases (NAT)
Dihydrodioldehydrogenases	Methyltransferases
Alcohol- and aldehyddehydrogenases (ADH, ALDH)	Aminoacyltransferases
Esterases	
Amidasen	
Glucuronidasen	
Epoxidhydrolasen (EH)	
DT-Diaphorase (NQOR)	
Hydrolasen	
	Phase-3-Enzymes
	OATCs
	MDRs
	MRPs

Table 1: Example of enzyme classes involved in the three phases of xenobiotic metabolism.

Several factors can influence the efficiency of xenobiotic metabolism. The activation and inhibition of enzyme activity and the induction and repression of gene expression are the main elements of regulation. Inducers usually affect multiple enzymes from different steps of xenobiotic metabolism. Thereby, an entire metabolism cascade can be activated leading to the detoxification of the compound (Elias & Mills, 2007; Xu, Li & Kong, 2005). Responsible for this coordinated gene expressions are several forms of nuclear receptors which act in concert with other regulatory proteins (Figure 7). In their inactive form, they are present in the cytoplasm and, after binding of a substrate, are translocated into the nucleus in their active form as homo- or heterodimers. By binding to the DNA at different hormone response elements (HRE's) and recruiting other proteins, so called co-regulators, their effect can be modulated in various ways.

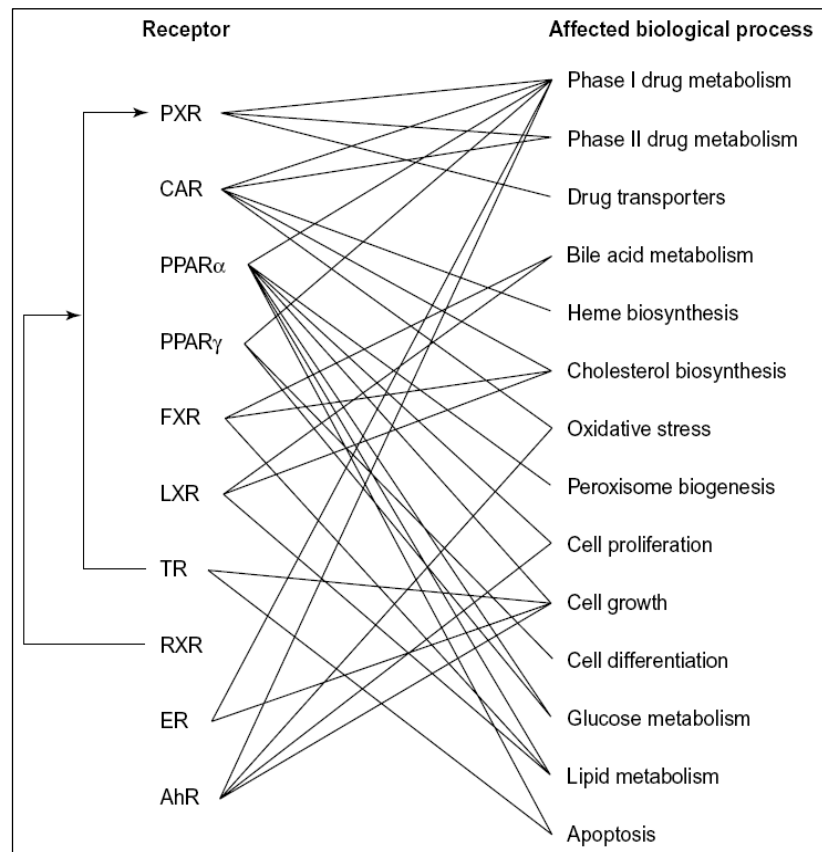


Figure 7: interaction of cellular transcription factors and their influence on several biological processes (Taken from Ulrich 2003).

Some receptors, so-called orphan receptors, do not have any known endogenous ligands but can bind metabolic intermediates with low affinity (Benoit et al., 2006). They are therefore thought to function as metabolic (*Peroxisome Proliverator activated receptors* (PPAR)) or xenobiotic (*pregnane X receptor* (PXR), *constitutively active receptor* (CAR)) sensors. Ligands for these kinds of receptors include lipophilic substances like hormones or xenobiotic compounds. They often build heterodimers with the *Retinoic X receptor* (RXR) or the *AHR-nuclear translocator* (Arnt) to activate the transcription of a wide range of metabolizing enzymes which in turn are often needed for further metabolisation of the initial substrate. This whole mechanism builds up an autoregulatory metabolic feedback-loop.

The expression of most metabolic enzymes, especially the CYP enzymes, is regulated in this way with the exception being CYP2E1, which is regulated in an even more complex manner. It is regulated on not only transcriptional but also pre-translational, translational, and posttranslational level with the stabilization of mRNA and protein as the most important steps (Ingelman-Sundberg et al., 1994)

1.4 Hepatotoxicity

Because of the central role the liver plays in the metabolism of xenobiotic compounds, hepatotoxicity is a major issue in pharmaceutical drug development (Ballet, 1997). Drug-induced liver injury is the major reason for attrition in clinical studies (Wysowski & Swartz, 2005) and hepatotoxic side effects are the main reason for drug withdrawals from the market (31%). A broad variety of liver pathophysiologies have been reported, including steatosis (fatty liver), cholestasis (obstruction of bile secretion), fibrosis (increased production and deposition of extracellular matrix components), hepatitis (inflammation), necrosis (cell death) or the formation of liver tumours. These pathological findings may arise from diseases affecting the liver, but also from xenobiotics, alcohol abuse or undesired drug-drug interactions. The pathological symptoms of certain liver diseases allow conclusions about the affected intracellular organelles. Although different histological changes can appear, a compound-class often displays a typical clinical or pathological appearance.

Xenobiotics administered orally first pass through the liver before entering the general blood circulation (first pass effect). Because the liver has multiple functions for the homeostasis of the whole body, drug induced liver toxicity can have severe consequences. Thirty to fifty percent of acute liver failures and fifteen percent of liver transplantations are related to chemical-induced hepatotoxicity (Andrade et al., 2004; Kaplowitz, 2001; Lewis, 2002). There is often a lack of reasonable understanding of the general molecular mechanisms of most drug-induced hepatotoxicities (Boelsterli, 2003; Jaeschke et al., 2002; Lee, 2003). The inhibition of mitochondrial function, disruption of intracellular calcium homeostasis, activation of apoptosis, oxidative stress, inhibition of specific enzymes or transporters and the formation of reactive metabolites that cause direct toxicity or immunogenic responses are some mechanisms that have to be considered.

The drug development process comprises a variety of steps to assess whether a test compound has adequate efficacy, appropriate physicochemical properties, metabolic stability, safety and bioreactivity in humans. Hepatotoxicity in humans has a poor correlation with regulatory animal toxicity tests (Olson et al., 1998; Olson et al., 2000). However, if assays identified a compound as a human liver-toxicant, there is more than 80% correlation to the corresponding findings in animals (Xu, Diaz & O'Brien, 2004). While *in vivo* models, limited by animal welfare/ethical concerns, are used to investigate systemic influences, cell culture models provide systems that can investigate specific mechanisms in a precisely controlled environment (Ulrich et al., 1995).

Although there are ways to analyse the many toxicological parameters individually *in vitro*, most have low predictive value for the detection of human hepatotoxicity. The poor predictivity and sensitivity of standard *in vitro* cytotoxicity assays is due to several reasons, including strong inter-species variation, the lack of a true physiological environment of *in vitro* experiments or the insufficient culturing conditions, resulting in a loss of e.g. metabolic capabilities (Olson et al., 1998). The *in vitro* assays usually measure lethal events in late stages of toxicity, but toxicity may not always be lethal per se. Cytotoxicity may take several days to appear (Olson et al., 1998; Slaughter, Thakkar & O'Brien 2002; Schoonen et al., 2005), demanding repeated drug administration. In contrast to directly active compounds (primary toxins), some compounds elicit their toxic potential only as a metabolite (secondary toxins) and usually cause damage in the organ where they are produced.

This of course raises the need for metabolically active long-term *in vitro* models that facilitate extended exposure times. Several models have been used for the detection of acute toxicity, but sub-chronic and chronic toxicities have not been addressed so far. Furthermore, standard tests generally investigate only one parameter whereas hepatotoxicity can develop via many different mechanisms and is considered a multi-factorial process. In order to improve sensitivity it will be necessary to analyse several morphological, biochemical and functional endpoints in parallel. Finally, tests should be performed not only with high concentrations, causing acute toxicity, but also with *in vivo* pharmacological concentrations.

1.5 *In vitro* liver models

In vitro tests have the advantage of allowing multiple testing of different compounds, doses and/or time points simultaneously under well-defined conditions. The simplicity of some *in vitro* systems, besides saving time, money and animals used for experimentation, provides the ability to specifically manipulate and analyze a small number of well-defined parameters. The most commonly used test systems include, the isolated perfused liver, liver slices, primary hepatocytes in suspension or culture, cell lines, transgenic cells and sub-cellular fractions such as S9 mix, microsomes, supersomes or cytosol (Table 2). The reduction in the complexity of the system and the increase in throughput offer the ability to study specific parameters more closely but create inherent constraints for each model (Figure 8). However, this limits their widespread use and acceptance by the regulatory authorities as an alternative for *in vivo* testing (Brandon et al., 2003). Although studies have shown that *in vitro*

cytotoxicity data can be used to identify appropriate doses for *in vivo* studies (Scholz et al., 1999)

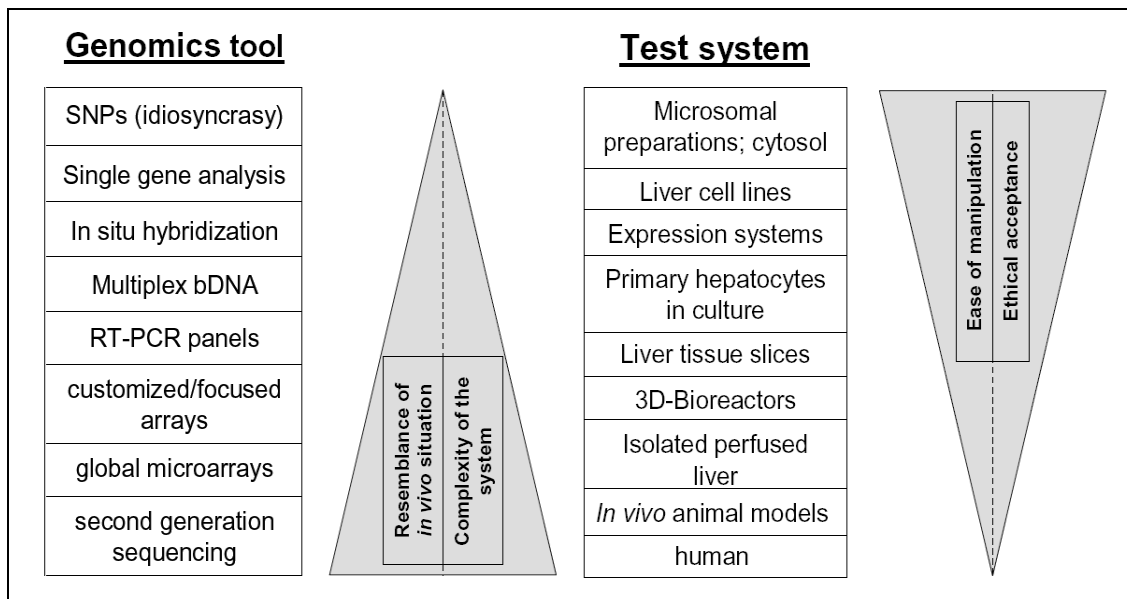


Figure 8: Models and genomic tools used for drug development, ordered by the correlation of the complexity of experiments conducted, the expressiveness, and the complexity of an *in vitro* model. (Adapted and modified from Brandon et al., 2003)

One major obstacle for some *in vitro* models is their limited metabolic competence, mainly due to the down regulation of CYP enzymes over time (Ching et al., 1996; De Smet et al., 1998). This is especially important since phase 1 and phase 2 metabolic conversions of chemicals can greatly influence their toxicity (Holme, 1985). To overcome these problems, new and innovative strategies are being developed in order to find reliable markers that are involved not only in early toxic responses but also in chronic toxicities, also occurring at sub-lethal doses of a test compound. Furthermore, there is a strong need for a robust long-term *in vitro* screening system that allows the characterisation of drug/chemical induced toxicities and helps to reduce the use of animals in toxicity testing.

Isolated perfused liver

Ideally, an *in vitro* test system should adequately represent the *in vivo* situation as closely as possible. Most liver specific features are preserved in whole isolated and perfused livers, first developed in 1972 by Gordon and colleagues (Gordon et al., 1972). Especially, the three-dimensional architecture of the liver, the cell-cell, cell-matrix interactions and functional bile canaliculi are maintained. Additionally, all liver cell types are present and the communication between them can play an important role in mediating toxicity. Despite all these advantages, the isolated perfused liver model is

difficult to handle and retains its functional integrity for only a few hours. Moreover, reproducibility is low, the use of animals is not significantly reduced and human organs are rarely available.

Precision-cut liver slices

First used in 1923 by Otto Warburg and improved over the following decades (Warburg, 1923; Krumdieck, dos Santos & Ho, 1980), precision-cut liver slices have the advantage of partially conserved liver cyto-architecture, cell-cell, cell-matrix contacts and the presence of different cell types (Lerche-Langr & Toutain, 2000). The preparation of slices from different parts of the liver facilitates lobe and zone specific analysis of metabolism and toxicity. In addition, since many slices can be prepared from the same human or animal donor, reproducibility and throughput can be increased significantly. Another major advantage is the possibility to conduct histopathological examinations, as well as biochemical and molecular biological studies from the same tissue. Due to the thickness of liver slices, 200-250 μm resembling 10-20 cell layers, the adequate supply of nutrients and oxygen from the incubation medium is only maintained for the outer cell layers. Therefore, liver slices are only useful for short-term toxicity studies due to their limited viability and the rapid decline of liver specific functions. The metabolic activity of tissue slices are reported to be preserved for 1-2 days in culture (Ekins et al., 1995).

Cell lines and sub-cellular fractions

Cell lines, isolated hepatocytes or whole liver cell suspensions are used as the starting material for a variety of *in vitro* models of different complexity and throughput. The simplest liver *in vitro* models are sub-cellular fractions, such as organ homogenates, microsomes, mitochondria or nuclei. Most sub-cellular fractions can be prepared and separated relatively easily by homogenisation of the tissue and sequential centrifugation. They are commercially available for a large number of species, including human. Nevertheless, they are only suitable for short-term studies with specific questions, such as enzyme inhibition, covalent binding or clearance studies. For example, liver supernatants ("S9") are used as an activation system for xenobiotics in *in vitro* genotoxicity assays (e.g., Ames-assay (Ames, Lee & Durston, 1973)). Mitochondria are added for the analysis of drug effects on respiration, ATP-synthesis and fatty acid oxidation. To acquire increased metabolic activity, animals are often induced by treatment with Arochlor 1254 or a Phenobarbital/beta-naphthoflavone (PB/BNF) mixture prior to S9 preparation (Callander et al., 1995), leading to elevated and unphysiological expression levels of metabolic enzymes. Most systems are supplemented with cofactors to preserve enzymatic activity. Other disadvantages

include the absence of complete enzyme systems like for phase 2 enzymes in microsomes.

The usage of different cell lines is one step forward in complexity. They are used for a variety of toxicological applications, but since most hepatic cell lines originate from tumours, they have lost the high degree of differentiation seen in hepatocytes and their gene expression pattern is distinctively different from normal liver cells. In addition, many cell lines display genetic instability. For example, the frequently used human hepatoma cell line HepG2 lacks expression of several CYP isoforms and phase 2 enzymes, making them insensitive to secondary toxic compounds (Knasmüller et al., 2004). To complicate matters, different sources of HepG2 cells can have very different enzyme profiles (Hewitt & Hewitt, 2004). Several transfected variants of HepG2 have been constructed which express increased levels of drug metabolising enzymes, including CYP1A1, CYP1A2, CYP2E1 and glutathione-S-transferases (Knasmüller et al., 2004), but *in vivo* relevance may not always be assumed because expression of the cloned enzymes is not at physiological levels and only single enzyme functions can be analyzed. Recently, the human hepatoma cell line HepaRG has been described. It is a naturally immortalized cell line from human liver with liver progenitor properties (Parent et al., 2004). After application of a differentiation protocol (Chapter 2.2.1.9, Page 51), HepaRG cells display hepatocyte like morphology and expression of drug metabolising enzymes at near *in vivo* levels (Gripon et al., 2002; Parent & Beretta, 2008). However, these novel cell lines still have to be confirmed and validated as a reasonable alternative cell-based assay for use in toxicological studies.

Cultures of isolated primary liver cells

To overcome the dilemma of non physiological gene expression and genomic instability, freshly isolated hepatocytes are often used for toxicological research. Although these are mostly mono-factorial systems which do not take into account the interactions between cell types or even whole organs in the body, cultures of primary rat and human hepatocytes are used in a variety of pharmacological and toxicological experiments, for example the evaluation of hepatic drug uptake and metabolism, drug-drug interactions and hepatotoxicity (Brandon et al., 2003; Gebhardt et al., 2003; Cross & Bayliss, 2000).

Fresh liver cells can be obtained by different procedures, all of which involve perfusion of the liver with Ca²⁺-free buffers combined with enzymes/proteases which disintegrate the extracellular matrix, leading to the separation of the cells from each other (Seglen, 1976; Howard et al., 1967). The isolation of liver cells is routinely performed for many species used in toxicity testing, but also with tissue from partial liver resections and

non-transplantable whole livers from human donors (LeCluyse et al., 2005; Richert et al., 2004)

In suspension, the survival of cells is short lived, normally not longer than 6 hours. Although the system is relatively high throughput, easy to use and preserves most of the metabolising enzymes at *in vivo* levels for a short time, it is only useable for acute toxicology or metabolism studies because the loss of contact to surrounding cells and the ECM environment has severe influence on the defined cell polarization and shape (Gebhardt et al., 2003). By capturing the cells into beads of alginate, the survival time can be prolonged to 24 hours. However, the lack of functional bile canaliculi, cell polarity and cell-cell contacts limits the use of alginate-embedded cells for drug transporter studies (Rialland et al., 2000).

The survival time in culture can be increased if hepatocytes are cultured on adhesive surfaces, for example, tissue culture dishes coated with ECM components. The most commonly used models are the monolayer culture (ML) where hepatocytes are usually attached to dried films of collagen I or Matrigel, a laminin-rich preparation from the Engelbreth-Holm-Swarm mouse sarcoma (Berthiaume et al., 1996).

During the perfusion procedure the cells are already primed for proliferation and can easily be forced to proliferate by the addition of mitogenic compounds, for example epidermal growth factor (EGF), allowing longer culturing (Etienne et al., 1988). However, this causes a down regulation of metabolic enzymes and thereby induces dedifferentiation associated with a loss of many liver specific functions and defined cell polarity (Luttringer et al., 2002; Skett & Bayliss, 1996; Paine & Andreacos, 2004; LeCluyse et al., 2000). Additionally, it is known that the typical phenotypic change of hepatocytes in monolayer culture, the “spreading” of the cells, has a negative effect on liver specific gene expression (Miranti, 2002). Intracellular signalling is closely connected to the interaction between ECM, cell-adhesion molecules and the cytoskeleton and therefore has a major impact on gene expression and the metabolic capacity of the cells. Altogether, this processes lead to a loss of up to 80-90% of phase 1 and about 50% of phase 2 metabolic activity during the first 24h in culture (Rodríguez-Antona et al., 2002; Wilkening, Stahl & Bader, 2003).

Culturing hepatocytes in a sandwich configuration (SW), embedded between two layers of gelled ECM proteins (e.g., collagen I or Matrigel), has prolonged the time in culture displaying hepatocyte-specific functions dramatically (LeCluyse et al., 2000; Dunn, Tompkins & Yarmush, 1991; Richert et al., 2002; Dunn et al., 1989). Cells adapted and maintained their physiologically occurring polygonal shape and bile canalicular-like structures could be observed for up to 14 days in culture (Tuschl & Müller, 2006). The same study showed less alterations of known stress-markers like

Gadd45 α in serum free sandwich culture compared to others and the expression of some marker genes involved in hepatocyte function were more stable. Additionally, SW cultured hepatocytes were successfully used for metabolism and induction studies (Kern et al., 1997; LeCluyse et al., 1999) indicating that the collagen overlay does not interfere with the test compounds. The development of long-term primary hepatocyte cultures is an essential step towards the study of chronic effects *in vitro*.

Another factor greatly influencing the morphological development and cell survival of hepatocytes in culture is the medium formulation and the addition/omission of serum, specified hormone mixtures or other supplements (Sidhu, Liu & Omiecinski, 2004; Pascussi et al., 2000; Turncliff, Meier & Brouwer, 2004). Among the most frequently used basal media, Dulbecco's modified Eagle medium (DMEM), modified Chee's medium (MCM) and Williams' medium E (WME), the DMEM/F12 mix seems most appropriate to maintain liver-specific functions and to help rebuild bile canaliculi (Turncliff, Tian & Brouwer, 2006). In culture, the addition of the glucocorticoid dexamethasone (DEX), at nanomolar concentrations, is essential for the long-term preservation of hepatocyte specific functions like polygonal hepatocyte morphology, structural integrity of cytoplasmic membranes, bile canaliculi-like structures and by maintaining the expression of liver specific transcription factors. Insulin enhances the glucose uptake of cells and contributes to maintaining liver specific gene expression. Selenium, a structural component of the enzyme glutathione peroxidase, which plays an essential role in the neutralization of metabolically generated peroxides, has also been shown to be beneficial when added to the medium (Yamada et al., 1980; Laishes & Williams, 1976; Müller & Pallauf, 2003). Since it is well known that serum enhances the surface attachment ability of hepatocytes (Williams, Bermudez & Scaramuzzino, 1977), cells are generally seeded in medium containing fetal calf serum, regardless of the subsequent culture conditions.

Co-cultures, spheroid cultures and 3 d bioreactor cultures

Hepatocytes make up about 60-70% of the cells in the intact liver. However, liver toxicity may not always originate from these cells. Therefore, co-cultures of hepatocytes with other non-parenchymal liver cells, such as endothelial, Kupffer, or stellate cells and also stable cell lines or fibroblasts can be applied to reflect a more physiological situation. For example, the excretion of TNF α or nitric oxide by Kupffer cells can lead to inflammatory reactions or apoptosis (El-Bahay et al., 1999; Kmiec, 2001).

Spheroids (spherical multicellular aggregates) will form if a crude liver cell suspension is prevented from adherence to the surface by continuous shaking. Cell-cell contacts are re-established, hepatocytes are located on the inside, non-parenchymal cells on

the outside and the deposition of ECM is seen throughout the spheroids. Alginate or other materials can be added to make up the internal structure of the spheres. Several studies showed the positive effect of this culture method on the expression of hepatotypic genes and the maintenance of metabolic capacity (Guigoz et al., 1987; Landry et al., 1985). The maintenance of prolonged functional activity has been related to the restoration and stability of cell polarity and close cell-to-cell contacts (Lu et al., 2005). However, the formation of these spheroids leads to hypoxic and necrotic cells dying at their centre. Additional problems arise from the accumulation of bile in the centre of spheroids.

Another skilful attempt to mimic a liver-like environment *in vitro* is the bioartificial liver system (3 d-bioreactors). Their major advantage is the re-establishment of the 3 d liver cyto-architecture with cell-cell contacts and a three-dimensional ECM environment, combined with continuous medium perfusion, providing a constant supply of oxygen and nutrients. Today a variety of culture systems are being used for bioreactor setups (Bader et al., 1998; Powers et al., 2002). Different studies have shown an improvement in some hepatocyte-specific functions in co-culture with other cell types, in spheroids and in 3D-bioreactors (Sivaraman et al., 2005). A very new and promising attempt to transfer and rebuild liver specific properties was developed by Linke et al (Linke et al., 2007). They co-cultured primary hepatocytes and microvascular endothelial cells by seeding them into a decellularized porcine jejunal segment with preserved vascular structures. The supply with nutrients was accomplished by perfusion of the blood vessels with culture medium. Biochemical testing showed metabolic and morphological stability for up to three weeks. However, the preparation of these cultures is quite elaborate, therefore their use as a high throughput tool for toxicological screening tests is unlikely.

Model	Advantages	Disadvantages
Isolated Perfused Liver	<ul style="list-style-type: none"> - liver specific functions close to <i>in vivo</i> - three dimensional cytoarchitecture - functional bile canaliculi - lobular structure preserved - collection of bile possible - short-term kinetic studies 	<ul style="list-style-type: none"> - not a high throughput system - hepatic function only preserved for a few hours - complicated to use - study of human liver difficult/impossible - best suited for liver of small animals - no significant reduction in the number of animals used
Liver Tissue Slices	<ul style="list-style-type: none"> - <i>in vivo</i> cytoarchitecture preserved - reasonably high throughput - functional drug metabolising enzymes, transporters and bile canaliculi - zone specific metabolism and toxicity may be studied - lobular structure preserved, selective effects detectable - human tissue slices more easily available than whole organs 	<ul style="list-style-type: none"> - hepatic function preserved for no more than 24 h - bile cannot be collected and analysed - necrotic cells / scar tissue at edges of the slice - presence of necrotic cells might affect the performance of the culture
3 d-Bioreactors (Bioartificial Liver Systems)	<ul style="list-style-type: none"> - long-term use possible - re-establishment of 3 d cytoarchitecture - continuous perfusion with medium - specific gene expression closer to <i>in vivo</i> than in hepatocyte cultures 	<ul style="list-style-type: none"> - very low throughput - difficult to standardize
Spheroids	<ul style="list-style-type: none"> - re-establishment of 3 d cytoarchitecture - presence of non-parenchymal cells on outer layer of and extra-cellular matrix throughout the spheroids 	<ul style="list-style-type: none"> - necrotic and hypoxic cells in centre of spheroids - accumulation of bile in centre of spheroids possible - not usable for long-term investigations (disaggregation and dedifferentiation)
Primary Hepatocyte Cultures	<ul style="list-style-type: none"> - reasonably high throughput - viability and differentiation preserved for up to 2 weeks - potential for use of long-term cultures in chronic toxicity - analysis of human samples possible - functional drug metabolising enzymes, transporters and bile canaliculi, - co-culture with other liver cells possible 	<ul style="list-style-type: none"> - culture may need special supplements in media - survival, differentiation status and function depends on culture conditions - no culture system is able to preserve all the different liver specific functions <i>in vitro</i> - difficult to regain cells for FACS analysis
Hepatocytes in Suspension	<ul style="list-style-type: none"> - reasonably high throughput - most drug metabolising enzymes well-preserved at <i>in vivo</i> levels - zone specific metabolism and toxicity may be studied - cryopreservation possible - analysis of human samples possible 	<ul style="list-style-type: none"> - limited use for drug transporter studies - lack of functional bile canaliculi - short-term viability (2-4 h.) - lack of cell-cell and cell-matrix contacts - variations in samples from different human donors
Cell Lines	<ul style="list-style-type: none"> - unlimited availability - some liver specific functions have been shown to be maintained - easy to use - reasonably high throughput 	<ul style="list-style-type: none"> - lacks <i>in vivo</i> phenotype - only a small set of hepatic functions expressed at levels different from liver - genotypic instability

Model	Advantages	Disadvantages
S9-Mix	<ul style="list-style-type: none"> - contains microsomal and cytosolic fractions - phase 1 and phase 2 activity 	<ul style="list-style-type: none"> - cofactors required for activity - lower enzyme activity compared to microsomes or cytosol
Microsomes, Supersomes, Baculosomes,	<ul style="list-style-type: none"> - high throughput system - maintain expression of phase 1 enzymes - can be recovered from frozen tissue - production of metabolites for structural analysis possible - use for drug inhibition, covalent binding and clearance studies - available from several species (including human) - one or more human enzymes (CYPs, UGTs) can be specifically expressed 	<ul style="list-style-type: none"> - lacks phase 2 and other cytosolic enzymes - short-term studies - cofactors required for activity - inadequate representation of the diversity of hepatic functions - UGT-reaction partly impaired
Mitochondria	<ul style="list-style-type: none"> - high throughput - analysis of the effect of drugs on respiration and ATP synthesis and fatty acid oxidation 	<ul style="list-style-type: none"> - only very short-term studies
Cytosol	<ul style="list-style-type: none"> - soluble phase 2 enzymes (GST, ST, NAT) can be studied separately depending on added cofactors 	<ul style="list-style-type: none"> - cofactors required for activity - no CYPs, UGTs
Cloned Expression Systems	<ul style="list-style-type: none"> - high throughput - one or more human enzymes can be specifically expressed - unlimited cell number 	<ul style="list-style-type: none"> - studies may lack <i>in vivo</i> relevance - no physiologic levels of expressed enzymes - only single (some) enzymes can be analyzed
The Virtual Hepatocyte	<ul style="list-style-type: none"> - mathematical modelling of cellular events - prediction of unknown interactions may be possible 	<ul style="list-style-type: none"> - limited computational power - still in experimental stage

Table 2: Overview of *in vitro* methods used for toxicology (adapted and expanded from Sahu, 2008)

1.6 Endpoints for the analysis of hepatocyte cultures

The list of tests used to gain insight into the effect of a test-substance on cells and to assess functional and biochemical parameters of cultured cells is extensive. These range from standardised tests, e.g. cell viability measurements or morphology-based approaches, to hepatocyte specific activity tests such as bile production, CYP activity or drug transport. In addition, the analysis of gene or protein expression with established molecular methods like real-time PCR, microarray technologies, mass spectrometry or immune detection is commonly applied.

Some chemically induced changes in cellular functions may be irreversible, ultimately leading to cell death, whereas others may be transient. Irreversible endpoints include the induction of apoptosis, measured by increased caspase activity, or the loss of plasma membrane integrity. Plasma membrane damage can be analysed by the detection of cytoplasmic enzyme release (e.g., lactate dehydrogenase, LDH) or the

uptake of specific dyes such as neutral red and trypan blue into the cytoplasm. In addition, alterations in general hepatocyte functions like albumin synthesis and urea or bile secretion provide information on the impairment of cellular processes. The energy status of the cell is often used to determine cytotoxicity by studying the ATP content of cells or the mitochondrial or enzymatic capacity to reduce tetrazolium salts (XTT, MTT, WST) (Berridge, Herst & Tan, 2005). Compound induced oxidative stress can lead to glutathione (GSH) depletion. GSH is considered one of the primary antioxidant molecules for sustaining the intracellular redox status by scavenging peroxides and the reduction of oxidized molecules. Additionally, it is used in phase 2 reactions for neutralizing strong oxidants, by the formation of glutathinyl adducts which is catalyzed by various glutathione S-transferases (GSTs) and plays a vital role in rescuing cells from apoptosis. The cytosolic GSH content can be measured with specific glutathione detection kits. Drug transport is studied by fluorescent dyes or with the analysis of the bile acid transport by HPLC (High Performance Liquid Chromatography) (Kostrubsky et al., 2003; Liu et al., 1999).

1.7 Toxicogenomics

Traditional toxicological studies, e.g. the 2-year carcinogenicity rodent study, are time consuming and expensive together with a high requirement for laboratory animals. They focus on evaluating classical endpoints like gain of body- or organ-weight, death rate, tumour incidence, serum markers or histological changes, making safety assessment one of the bottlenecks in the pharmaceutical drug developmental process. New methods and processes like genomics, proteomics, lipidomics or metabonomics are being used to improve the drug development process (Ballet, 1997; Brandon et al., 2003) and the “-omics” field is rapidly growing. Toxicogenomics is defined as a scientific sub-discipline that combines toxicology (the study of the nature and effects of poisons) with genomics (the investigation of the way that our genetic make-up, the genome, translates into biological functions). It is the study of the structure and output of the genome as it responds to adverse xenobiotic exposure and the identification of their putative mechanisms of action. The analysis of changes in gene expression caused by exposure to a test-compound together with strong bioinformatics and toxicological knowledge form the basis of toxicogenomics (Khor, Ibrahim & Kong, 2006; Nuwaysir et al., 1999; Chin & Kong, 2002). Central to genomic studies in toxicology is the assumption that compounds with a common endpoint can be classified based on related changes in gene expression. This allows extrapolation of toxic effects from known model compounds to unknown compounds by comparison of their expression

profiles (Hamadeh et al., 2002a; 2002b; Zidek et al., 2007; Ellinger-Ziegelbauer et al., 2004). Several open source or commercial attempts (e.g., GENELOGIC (USA), ICONIX Biosciences Inc. (USA)) have been made to develop databases based on expression profiles of reference compounds in order to classify chemicals. It should not be forgotten that many internal databases in the pharmaceutical industry are only used for in house purposes and are not made accessible to the public (Mattes et al., 2004). There are several statistical methods to discriminate compounds on the basis of their gene expression profiles, some of which are discussed later (Page 33). In principle, they try to find single genes or gene sets that can discriminate between different treatment groups. These highly informative gene clusters can then be used to predict the class membership of a new unknown sample (Hamadeh et al., 2002a; Simon et al., 2003). The reported results are very encouraging but also show the need for large gene expression databases and effective analysis models to allow their future implementation into the drug development process.

Mechanistic studies are performed to increase the understanding of the function and regulation of genes that lead to compound specific toxicity. In most cases, the changes in gene and protein expression precede the physiological effects. This means that there is a great potential to extrapolate from changes in gene expression to long term toxicological endpoints such as liver necrosis, inflammation, steatosis or tumour neogenesis (Pennie, 2000; Burchiel et al., 2001; Fielden & Zacharewski, 2001). The detection of both the underlying mechanism of toxicity and the molecular basis of the response to exposure in an early stage of drug development will have a great impact on safety evaluation. Recent studies showed the possibility to define different toxic mechanisms, including tumour formation, inflammatory effects, oxidative stress, impairment of cellular signalling and induction of apoptosis (Bulera et al., 2001; Lettieri, 2006). Warring and his coworkers have shown a correlation between a physiological response to a toxicant and changes in the genomic profile, allowing the interpretation of gene expression data with respect to specific organotypic endpoints. This concept is referred to as "phenotypic anchoring" (Waring et al., 2001; Orphanides, 2003).

There have been numerous attempts to find new biomarkers for the early identification of hepatocarcinogenesis with the use of toxicogenomics and proteomics methods (Ellinger-Ziegelbauer et al., 2004; Fella et al., 2005). There is hope that these new methods will make it possible to detect intrinsic changes in the molecular pattern ("genetic fingerprint") that are indicative of the pathological endpoint before he becomes histopathologically detectable (Aardema & MacGregor, 2002). Besides the improvement of the drug development process, this could also facilitate a considerable reduction in the time needed to obtain results and the number of animals used in

toxicity testing (Kroeger, 2006). Although most data is generated from *in vivo* liver samples, there are efforts to build databases for the screening of hepatotoxicity based on primary hepatocyte cell culture experiments by genomic and proteomic approaches. Therefore, it is necessary to carefully characterise the cell culture model used.

In order to understand the mechanisms behind any compound induced change of gene expression, it is essential to know the basal gene expression in the test system. In the case of primary hepatocytes, it is not only the individual differences but also the effects of time and the conditions of culturing which have to be taken into account. Therefore, a comprehensive analysis of gene expression changes in rat and human hepatocytes and different cell culture systems (liver slices, suspension culture, primary hepatocytes cultured on plastic surface, on collagen I ML and in SW culture as well as different cell lines) has been carried out as part of this thesis.

Not every cell culture system is appropriate for every toxicological endpoint, as liver specific functions gradually decrease over time. *In vivo*, they are supported by liver architecture, cell-cell and cell-matrix interactions and the complex hormonal signalling of the body. It is impossible to mimic these conditions in culture and great endeavours are being made to maintain liver specific functions and attributes for as long as possible (LeCluyse et al., 2005; Richert et al., 2004; Turncliff et al., 2006; Vinken et al., 2006). Evaluating the basal gene expression pattern will help to understand the processes of dedifferentiation and will allow the interpretation of gene expression changes caused by xenobiotics and to extrapolate to mechanisms *in vivo*.

However, one has to be aware of the limitations of these techniques. Some compounds directly effect cellular macromolecules causing damage without changing gene expression. Often expression changes may reflect secondary effects following after the primary direct toxicity of the compound. The dimension of changes in gene expression is also dependent on dose, duration of exposure to the toxicant and on time from dosing to sampling (Gatzidou, Zira & Theocharis, 2007). Not all changes in gene expression have a direct impact on the corresponding protein content of a cell. Due to the variety of epigenetic control mechanisms there can be significant differences in gene and protein expression. Additionally, changes in protein activity, caused for example by phosphorylation or ubiquitinylation, can not be addressed and other , proteomic techniques have to be considered (Pennie et al., 2000; Merrick & Madenspacher, 2005). With this in mind, toxicogenomics can be a powerful tool. The extrapolation from data generated from animals to potential human activity could be enhanced by finding species-overlapping biomarkers (Aardema & MacGregor, 2002). Even the generation of human data is achievable and relatively straight forward.

1.8 Techniques for global gene expression analysis

The new and developing field of microarray technology evolved from E.M. Southern's realization that labelled nucleic acid molecules can be hybridized to their counterparts and therefore be used to detect their existence and amount in the original sample (Southern, 1975). The sequencing of whole genomes from human, as well as of many "laboratory" animal species, quickened the development of new technologies for the measurement of several thousand genes in a single experiment (Brown & Botstein, 1999; Schena, 1996). Meanwhile, these microarray technologies are used for a wide spectrum of issues, like drug discovery, basic research and target discovery, biomarker determination, pharmacology, toxicology, target selectivity, development of prognostic tests and disease-subclass determination (Butte, 2002). A wide range of different platforms for global gene expression are currently available. Although they all are either cDNA or oligonucleotide based, they differ in distinct properties such as the type of probes (short/long oligonucleotides, cDNA), the number of genes, probe selection and design, competitive versus non-competitive hybridization, labeling methods or the methods of production (*in situ* polymerization, spotting, microbeads). In the following paragraphs, the bead chip technology of Illumina Inc. and the Affymetrix Gene Chip, used during this work, are introduced.

Illumina BeadChip arrays

Illumina Inc. developed in 2003 a bead based technology for global gene expression analysis (Gunderson et al., 2004). The chips are based on a silicon wafer with 3 μm sized beads on their surface and covalently bound 50mer oligonucleotide probes. One single probe-type representing one gene is bound to each bead type with more than 100,000 copies per bead. All the bead types are pooled and put onto the surface of a silicon wafer (Figure 9). This wafer was previously prepared by plasma etching to provide wells at a regular distance of 5 μm . Each array contains about 900,000 beads so statistically on a whole genome array, each bead-type is represented ~ 30 times on average. This redundancy allows up to 30,000 genes to be detected simultaneously per array. Because of the random arrangement of the beads and their high redundancy, local area effects (scratches, impurity and intensity variation) are of minor consequence, but this feature also raises the need for an initial decoding step. Therefore, the probes consist not only of the gene specific part (50 nt) but also a 23 nt-long address sequence. Decoding is performed by Illumina Inc. by sequential hybridizations with differently coloured probes and is at the same time an important quality control step (Gunderson et al., 2004).

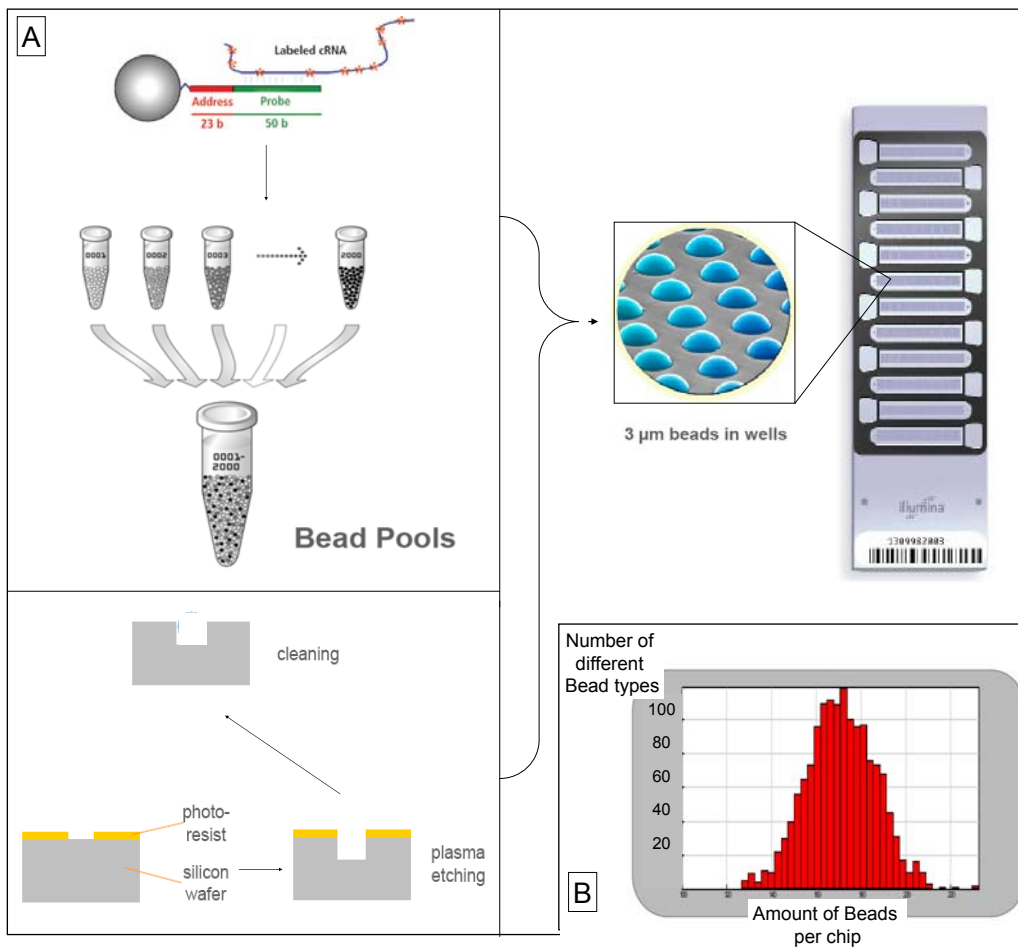


Figure 9: The production process of an Illumina BeadChip array. A) Depicts the structure of a single bead, the generation of a bead pool and the combination with a previously etched silicon wafer to a complete BeadChip. B) Shows a histogram of the average abundance of bead types per chip.

Affymetrix gene expression arrays

Affymetrix arrays are based on in situ synthesis of oligonucleotides directly on to the array surface. The probes are 25 nt long and are directly synthesized onto a silicon wafer via a combination of photolithography and combinational chemistry (McGall & Fidanza, 2001). For each gene, Affymetrix uses 11 to 20 probe sets, a probe set consisting of a 25 nt perfect match and a 25 nt mismatch oligonucleotide, to guarantee statistical relevance and certainty. After scanning, the intensity differences between perfect match and mismatch probes are calculated to give both quantitative (signal intensity) and qualitative (statistical significance) measurements (Figure 10).

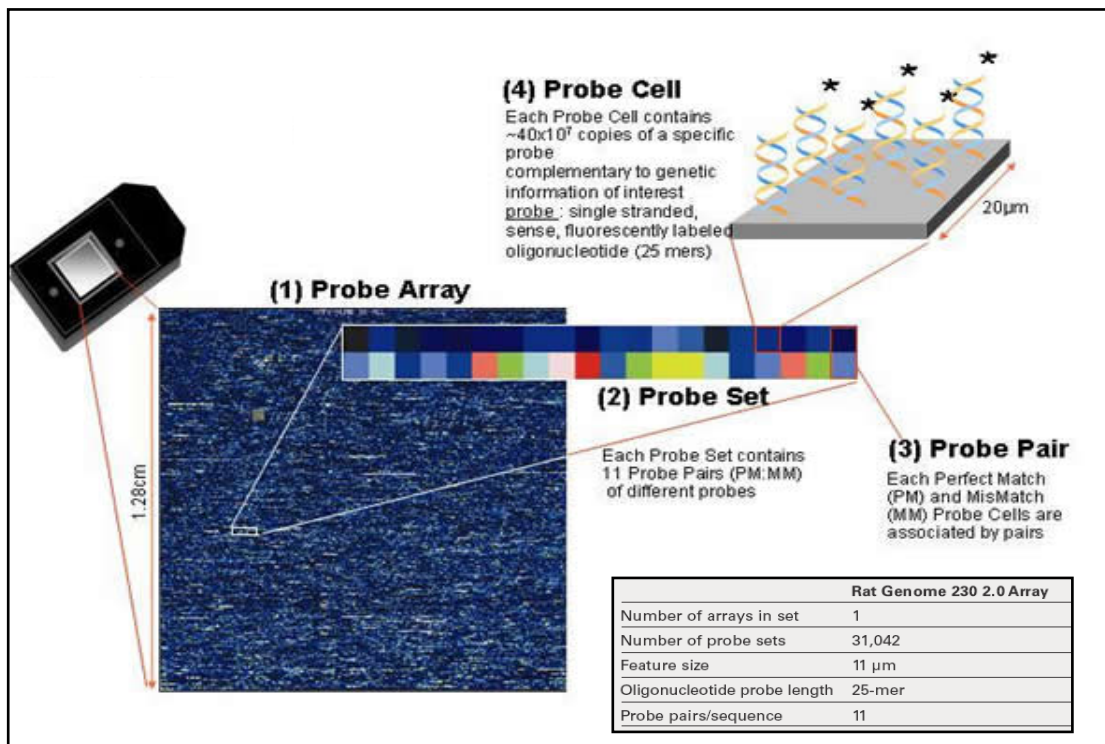


Figure 10: Scheme of the process and the architecture of an Affymetrix gene expression array (Taken from the Affymetrix homepage, www.affymetrix.com).

The RNA samples have to be isolated from the sample and reverse transcribed in order to produce biotinylated cRNA before hybridizing them to arrays of both suppliers, Illumina and Affymetrix. This procedure allows detection and quantification which otherwise wouldn't be possible. After scanning, raw data must be preprocessed before statistical analysis and the relative expression level of each gene can be determined by comparing the intensities of the genes to each other or to a control. With respect to the technical aspects and the experiment layout, each set of microarray data has to be normalized in an appropriate way. Further details of both techniques used will be discussed in detail in chapter 3.1.

Methods of data analysis

DNA microarray technology has made it possible to generate millions of data-points in a relatively short time. The analytical steps needed to convert the noisy data into reliable and interpretable biological information are challenging and error prone. Due to their great number, only an overview of the most common and important methods and algorithms used during these studies are presented. In principle, there are two main statistical approaches to identify genes or patterns of interest from microarray data. Supervised methods are used to identify patterns of gene expression, e.g. for the

identification of marker genes or the classification of compounds. Unsupervised methods identify signatures in the data set without input of data specific knowledge and can be used to summarize and to reduce the complexity of the multidimensional data. Important unsupervised tools include Principal Components Analysis (PCA), Hierarchical Clustering, Correlation and Self Organizing Maps (SOM) (Butte, 2002). PCAs are an attempt to reduce the multi-dimensional data of microarrays. Therefore, vectors (so called "Eigenvektoren") are calculated, each representing the greatest amount of variance of the data cloud within one certain experiment (Figure 11). The largest, and therefore statistically most relevant, Eigenvektoren are plotted resulting in one single point per sample in two- or three-dimensional space and is therefore a good tool for data reduction and display (Yeung & Ruzzo, 2001).

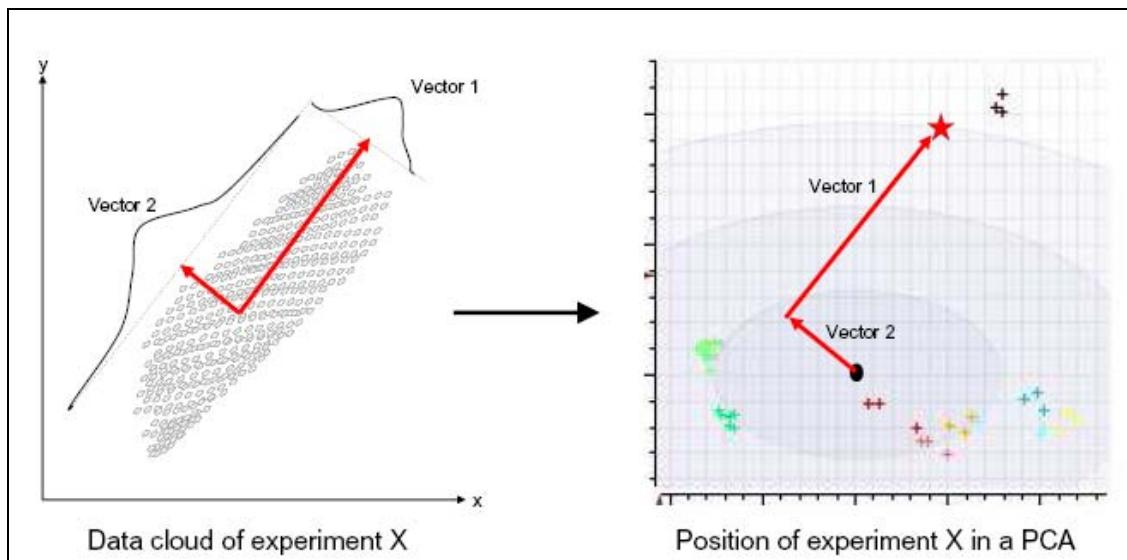


Figure 11: Graphical representation of a PCA transformation in two dimensions (x and y). The variance of the data in the original space (x, y) is best captured by the basis vectors v_1 and v_2 , which in turn are used as basis for the localization of the experiment in the appertaining PCA.

Several different algorithms can be applied depending on the structure of the dataset and the aim of the analysis. Hierarchical clustering calculates the distance of the sample or gene profiles from each other and visualizes this in form of a dendrogram-tree. Experiments closer to each other are more similar to each other than those further away. During a correlation analysis, the correlation of samples or genes to each other are calculated and then visualized in a heat map with a defined colour code. A two dimensional output is also produced by SOM Clustering, also termed as Kohonen-Maps after its inventor (Kohonen, 1997). This statistical method is a type of artificial neural network that is trained using unsupervised learning. During the presented work

SOM was used to group genes according to their expression profile (Nikkilä et al., 2002).

Supervised methods include t-test and the Analysis of Variance (ANOVA). T-test was applied to detect differences between empirical mean values of two datasets giving statistical confidence to the detected values. ANOVA was used to identify genes in a multivariate model whose expression is significantly altered between different biological samples. First described by R.A. Fisher in the 1920s, an ANOVA partitions the observed variance into components due to different explanatory variables and allows the effects of two or more treatment variables to be studied simultaneously. Other supervised methods include classification methods, such as Support Vector Machine or K-nearest-neighbour analysis. These algorithms “learn” to classify the data into preset categories from a training set and are able to match new data to the existing classifier (Raudys, 2000). Additionally, the minimum amount of genes needed for this discrimination can be calculated by ranking.

1.9 Toxicoproteomics

Marc Wilkins first used the term “proteome” in 1994. He defined it as the totality of all proteins produced at a certain moment by a cell and encoded by a genome. Like the transcriptome it depends on broadly diverse factors and is highly dynamic. The analysis of proteins, of the total proteome especially, is very challenging because of its extreme heterogeneity. Proteins range from relatively small peptides to large multi-enzyme complexes and are built up out of amino acids, which can, due to their side chains, develop multiple interactions and carry different charges. Several mechanisms of post-translational modification are known which enhance and increase this complexity of the proteome. It is believed that about 30,000 genes are encoded by the human genome. These genes result, via alternative splicing, in about 100,000 different transcripts. Further modifications are achieved by mechanisms such as nuclear transport, posttranscriptional modifications, gene silencing, changes in mRNA stability and in post-translational modifications like glycosylations, phosphorylations, methylations, enzymatic cleaving, changes in protein stability or intracellular transport mechanisms.

The abundance of proteins in the cell can be very heterogeneous. Some proteins are present only in a low copy number (e.g. some cellular receptors) whereas others are highly abundant (e.g. structural proteins) (Smith, 2000). The dynamic range of protein expression encompasses more than seven orders of magnitude (Anderson & Anderson, 2002). It is obvious then that the analysis of the proteome has high

demands on the techniques applied for their exploration. To date none of the techniques can acquire the analysis of the whole proteome. Each method has certain advantages and drawbacks and depicts only a small part of the whole picture.

Similar to genomic studies, proteomic methods can be used to examine early changes due to treatment with xenobiotics on a molecular level. Occurring prior to changes on histopathological level or classical toxicological endpoints, these changes can help in candidate selection, mechanistic studies, finding new biomarkers or the classification of compounds (Bandara & Kennedy, 2002). The classification of compounds is possible even without further mechanistic knowledge on the basis of “molecular signatures” (Wetmore & Merrick, 2004). One technique to collect such signatures of protein expression is the Surface Enhanced Laser Desorption and Ionisation (SELDI) Chip Technology (Bio-Rad, Hercules, CA, USA). This method was invented in 1993 by Hutchens and Yip and is a mixture of chromatographic surfaces and mass spectrometry (Hutchens & Yip, 1993). Samples of proteins are bound to a chromatographic surface (e.g. anionic, cationic, hydrophobic, hydrophilic or metal-binding) due to their physical properties and are afterwards analyzed via time of flight mass spectrometry. The resulting spectrum of masses resembles a so called “proteomic fingerprint” (Veenstra & Conrads, 2003).

A drawback of this method is the lack of fragmentation of the proteins. Therefore, an identification of the proteins detected with SELDI is complicated and needs additional efforts. Complex mixtures of proteins, like cell lysates, have to be intensely cleaned up as far as possible and enzymatically digested. Afterwards, they can be used for downstream analysis with “normal” MS or MS/MS techniques.

1.10 Aim of this work

The aim of this work was the development and characterization of the sandwich culture of primary rat and human hepatocytes as a tool for *in vitro* toxicology studies. Moreover, the gene expression changes in response of compound treatment of the cells in culture were addressed and used to build a predictive classification model.

Primarily, a thorough optimization of the culture conditions was performed with the main goal to enhance the differentiation status of cells and to prolong their time in culture. Besides the insurance of cells displaying liver-typical functionality over a long period of time, a clear definition of changes over time on different levels, the cell morphology and viability, gene and protein expression, metabolic activity and inducibility, were part of this project.

The main part of this work was concerned with the extensive characterization of the global gene expression changes over time in culture. Therefore, several culture systems were analyzed and compared with regard to their similarities and differences in gene expression over time.

The ability to establish a predictive hepatotoxicity model was examined by conducting toxicological studies with the new sandwich *in vitro* culture system. Cells were dosed with reference compounds (Chapter 3.4.2, Figure 58), changes in gene expression were analyzed and used to calculate a novel predictive model based on the global expression profile. Additionally, a predictive subset of discriminative genes should be found. The gene expression profile of two blinded compounds should be conducted as a preliminary verification of this model.

As the new platform from Illumina was used for these experiments, it was important to compare the results gained from these experiments to a well established platform (Affymetrix) and to TaqMan PCR, as the quality standard, in terms of reliability, sensitivity and concordance.

2 MATERIALS AND METHODS

2.1 Materials

2.1.1 Chemicals and reagents

Chemical/ Reagent	Provider
Secondary antibodies (Rabbit, Sheep)	GE Healthcare Europe GmbH, Freiburg, Germany
ECL Detection-Reagents and Hyperfilm	GE Healthcare Europe GmbH, Freiburg, Germany
Neutral Red	Sigma-Aldrich, Taufkirchen, Germany
Carboxi-DCFDA	Invitrogen, Karlsruhe, Germany
Acetic Acid ($\text{CH}_3\text{CO}_2\text{H}$)	Invitrogen, Karlsruhe, Germany
Ammonium bicarbonate (NH_4HCO_3)	Merck KGaA, Darmstadt, Germany
Ammonium persulfate ($(\text{NH}_4)_2\text{S}_2\text{O}_8$)	Merck KGaA, Darmstadt, Germany
Anti-Streptavidin Antibody (goat), biotinylated	Vector Laboratories, Burlingame, USA
Benzyloxy-Resorufin	Sigma-Aldrich, Taufkirchen, Germany
Biotin-16-UTP, 10 mm	PerkinElmer Life and Analytical Sciences, Waltham, USA
Bovine serum albumin (BSA), acetylated, 20 mg/ml	Ambion - An Applied Biosystems Business, Austin, USA
Calcium chloride hexahydrate ($\text{CaCl}_2 \cdot 6\text{H}_2\text{O}$)	Sigma-Aldrich, Taufkirchen, Germany
CHAPS ($\text{C}_{32}\text{H}_{58}\text{N}_2\text{O}_7\text{S}$)	Merck KGaA, Darmstadt, Germany
Chloroform LiChrosolv [®] (CHCl_3)	Merck KGaA, Darmstadt, Germany
Coomassie Brilliant Blue G250	Serva, Heidelberg, Germany
E1BC Buffer	Buffer Illumina, San Diego, USA
ECL-Detection Kit	Amersham, Buckinghamshire, UK
EDTA-Solution (0.5M)	Ambion - An Applied Biosystems Business, Austin, USA
Ethanol LiChrosolv [®] ($\text{CH}_3\text{CH}_2\text{OH}$)	Merck KGaA, Darmstadt, Germany
Ethoxy-Resorufin	Sigma-Aldrich, Taufkirchen, Germany
Cy3 [™] labelled streptavidin (1 mg/ml)	Amersham Biosciences, Buckinghamshire, UK (GE Healthcare)
Formamide, deionised (HCONH_2)	Ambion - An Applied Biosystems Business, Austin, USA
HEPES ($\text{C}_8\text{H}_{18}\text{N}_2\text{O}_4\text{S}$)	Merck KGaA, Darmstadt, Germany
Herring sperm DNA (10 mg/ml)	Promega Corporation, Madison, USA

2 MATERIALS AND METHODS

HybE1 Buffer	Buffer Illumina, San Diego, USA
NuPage 4-12% Bis-Tris Gel	Invitrogen - Molecular Probes, Eugene, USA
Isopropanol, LiChrosolv [®] ((CH ₃) ₂ CHOH)	Merck KGaA, Darmstadt, Germany
Calcium chloride (CaCl ₂)	Sigma-Aldrich, Taufkirchen, Germany
Potassium sulfate (KH ₂ SO ₄)	Sigma-Aldrich, Taufkirchen, Germany
Potassium chloride (KCl)	Merck KGaA, Darmstadt, Germany
Potassium phosphate monobasic (KH ₂ PO ₄)	Merck KGaA, Darmstadt, Germany
Liberase Blendzyme 2	Roche Applied Biosciences, Basel, Suisse
Magnesium sulfate (MgSO ₄)	Sigma-Aldrich, Taufkirchen, Germany
MES (2-[N-Morpholino]ethanesulfonic acid, C ₆ H ₁₃ NO ₄ S)	Sigma-Aldrich, Taufkirchen, Germany
Magnesium sulfate monohydrate (MgSO ₄ • 7 H ₂ O)	Sigma-Aldrich, Taufkirchen, Germany
Sodium phosphate dibasic (Na ₂ HPO ₄)	Sigma-Aldrich, Taufkirchen, Germany
Sodium chloride (NaCl)	Sigma-Aldrich, Taufkirchen, Germany
Sodium acetate (CH ₃ COONa)	Merck KGaA, Darmstadt, Germany
Sodium hydrogen carbonate (NaHCO ₃)	Merck KGaA, Darmstadt, Germany
Sodium hydroxide (NaOH)	Merck KGaA, Darmstadt, Germany
Trypan Blue 0.5% (w/v) in PBS	Biochrome AG, Berlin, Germany
Nuclease free water	Ambion - An Applied Biosystems Business, Austin, USA
Pentoxyl-Resorufin	Sigma-Aldrich, Taufkirchen, Germany
RNA 6000 Ladder	Ambion - An Applied Biosystems Business, Austin, USA
Hydrochloric acid (HCl)	Merck KGaA, Darmstadt, Germany
β-Mercaptoethanol	Sigma-Aldrich, Taufkirchen, Germany
SSPE (3 M NaCl, 0.2 M NaH ₂ PO ₄ , 0.02 M EDTA)	BioWhittaker Molecular Applications, Rockland, USA
Streptavidin Phycoerythrin (SAPE)	Invitrogen - Molecular Probes, Eugene, USA
Trichloroacetic acid (TCA, Cl ₃ CCOOH)	Merck KGaA, Darmstadt, Germany
Triton X-100	Serva, Heidelberg, Germany
TRI Reagent [™]	Sigma-Aldrich, Taufkirchen, Germany
Tween20 (10%)	Merck KGaA, Darmstadt, Germany

2.1.2 Technical equipment and auxiliary material

Equipment	Provider
PBSII ProteinChip Reader	Ciphergen
ABI Prism 7000	Applied Biosystems, Foster City, USA
Agilent 2100 Bioanalyzer	Agilent Technologies, Waldbronn, Germany
Autoclave	H&P Labortechnik, Oberschleißheim, Germany
Axon GenePix® 4000B Microarray Scanner	Molecular Devices (Axon Technologies), Union City, USA
Bead Station 500	Illumina, San Diego, USA
BeadChip® Hyb Cartridge	Illumina, San Diego, USA
BeadChip® Hyb Wheel	Illumina, San Diego, USA
BeadChip® Staining Dish	Illumina, San Diego, USA
BeadChip® Wash Trays	Illumina, San Diego, USA
Bottle-top filter, 0.2µm	Nalge Nunc International, Rochester, USA
Syringes	MT Braun, Melsungen, Germany
Cell scraper (25 cm, sterile)	Greiner-Bio One, Frickenhausen, Germany
Centrifuge 5415R	Eppendorf, Hamburg, Germany
Fluidic Station 450	Affymetrix, Santa Clara, USA
Digital camera CC 12	Olympus, Hamburg, Germany
iBlot™ Dry Blotting System	Invitrogen, Karlsruhe, Germany
Fluorescent-Spectralphotometer (RF-1502)	Shimadzu Europa, Duisburg, Germany
Fuchs-Rosenthal-Chamber (Neubauer improved)	Paul Marienfeld GmbH & Co., Lauda-Königshofen, Germany
Gene Chip® Fluidic Station 450	Affymetrix, Santa Clara, USA
Gene Chip® Human Genome U133 Plus 2.0 Array	Affymetrix, Santa Clara, USA
Gene Chip® Rat Expression Array (RAE) 230 2.0	Affymetrix, Santa Clara, USA
Gene Chip® Scanner 3000	Affymetrix, Santa Clara, USA
Glassware	Schott Glas, Mainz, Germany
Heat block Thermo Stat Plus	Eppendorf, Hamburg
HP GeneArray™ Scanner	Affymetrix, Santa Clara, USA
HumanRef-8 v2 Expression BeadChip	Illumina, San Diego, USA
NuPAGE® MES Running Buffer	Invitrogen, Karlsruhe, Germany
NuPAGE® Novex Bis-Tris-Gele	Invitrogen, Karlsruhe, Germany
NuPAGE® Reducing Agent	Invitrogen, Karlsruhe, Germany
Hybridization Oven 650	Affymetrix, Santa Clara, USA
Incubator	Kendro Laboratory, Hanau, Germany
Krumdieck-Tissue-Slicer	Alabama R&D Corp., Munford, USA

2 MATERIALS AND METHODS

Microscope	Zeiss, Jena, Germany
Microtiterplates (96 well, 24 well and 6 well)	Nalge Nunc, Rochester, USA
Molecular Imager	BIORAD, München, Germany
NanoDrop ND-1000	NanoDrop Technologies, Wilmington, USA
Nitrocellulose membrane	Schleicher & Schuell, Dassel, Germany
Microscope Olympus IX70	Olympus, Hamburg, Germany
Peristaltic Pump 313S	Watson-Marlow, Birmingham, UK
Petri-dishes TC (100 mm, 60 mm)	Greiner-Bio One, Frickenhausen, Germany
pH-Meter	Knick, Berlin, Germany
Pipettboy	Hirschmann Laborgeräte, Eberstadt,
Plastic ware	Nalge Nunc, Rochester, USA
Plastic tubes	15/50 ml Greiner-Bio One, Frickenhausen, Germany
RatRef-12 Expression BeadChip	Illumina, San Diego, USA
Reaction-cups (0.2 / 1.5 / 2 ml), Nuclease free	Eppendorf, Hamburg, Germany
Scale	Sartorius, Göttingen, Germany
Sentrix BeadChip custom array	Illumina, San Diego, USA
Speed-Vac Concentrator 5301	Eppendorf, Hamburg
Spectrophotometer TM3000	Bio-Rad, Hercules, USA
Steel beads	Qiagen, Hilden, Germany
Sterile Workbench	Kendro Laboratory, Hanau, Germany
Sterile filters (0.2 µM)	Nalge Nunc, Rochester, USA
Surgical instruments	Braun, Melsungen, Germany
Thermocycler	Eppendorf, Hamburg, Germany
TissueLyser	Qiagen, Hilden, Germany
Multifuge [®] 3 S-R	Thermo Fisher Scientific (Heraeus), Waltham, USA
U-RFL-T Power Supply Unit	Olympus, Hamburg, Germany
Vortex	Scientific Industries, Bohemia, USA
Varioclav Steam Sterilyzer	ThermoFisher Scientific, Schwerte, Germany
Water bath	Lauda GmbH & Co. KG, Lauda, Germany
Water bath SW 21	Julabo Labortechnik, Seelbach, Germany
Centrifuge	Kendro Laboratory, Hanau, Germany

2.1.3 Kits

Chemical/ Reagent	Provider
Apo-ONE [®] Homogeneous Caspase-3/7 assay	Promega Corporation, Madison, USA
BeadChip Buffer Kit	Illumina, San Diego, USA
CellTiter-Glo [®] Luminescent Cell Viability Assay	Promega Corporation, Madison, USA
CytoTox-ONE [™] Homogeneous Membrane Integrity Assay	Promega Corporation, Madison, USA
Gene Chip [®] Hybridization Control Kit	Affymetrix, Santa Clara, USA
Gene Chip [®] IVT Labeling Kit	Affymetrix, Santa Clara, USA
Gene Chip [®] One-Cycle cDNA Synthesis Kit	Affymetrix, Santa Clara, USA
Gene Chip [®] Poly-A RNA Control Kit	Affymetrix, Santa Clara, USA
Gene Chip [®] Sample Cleanup Module	Affymetrix, Santa Clara, USA
Glutathione (GSH) Detection Kit	Chemicon International, Tamecula, CA
MessageAmp [™] II aRNA Amplification Kit	Ambion- An Applied Biosystems Business, Austin, USA
P450Glo [®] (3A4 and 2C9) Assay Kit	Promega Corporation, Madison, USA
Primer and Probes for TaqMan [®] -RT-PCR	Applied Biosystems, Foster City, USA
QIAquick PCR Purification Kit	Qiagen, Hilden, Germany
RNA 6000 Nano LabChip [®] Kit	Agilent Technologies, Waldbronn, Germany
RNeasy Mini Kit	Qiagen, Hilden, Germany
WST-1-Assay	Roche, Mannheim, Germany

2.1.4 Software

Software	Provider
GECOS	Affymetrix, Santa Clara, USA
AnalySIS cell imaging	Soft Imaging System, Münster, Germany
2100 Expert Software	Agilent Technologies, Waldbronn, Germany
ABI Prism 7000 SDS	Applied Biosystems, Foster City, USA
BeadScan	Illumina, San Diego, USA
BeadStudio	Illumina, San Diego, USA
Expressionist [®] Pro	Genedata, Basel, Swisse
Gene Chip [®] Operating Software (GCOS)	Affymetrix, Santa Clara, USA
GenePix [™] Pro	Molecular Devices, UnionCity, USA
KC4	Bio-Tek Instruments, Vermont, USA
MetaCore [™]	GeneGO, St. Joseph, USA
OriginLab	OriginLab, Northampton, USA

2.1.5 Culture media and supplements

Media/ Supplement	Provider
After-shipment media for HepaRG-cells	Biopredic international, Rennes, France
Albumin Solution 35%	Sigma-Aldrich, Taufkirchen, Germany
Bovine serum albumin (BSA)	Merck KGaA, Darmstadt, Germany
Collagen I (Rat Tail)	Roche, Mannheim, Germany
D-MEM/F-12 (1:1) (1X), liquid - with GlutaMAX™ I	Invitrogen, Karlsruhe, Germany
D-MEM/F-12 (1:1) (1X), liquid - with L-Glutamine, without Phenol Red	Invitrogen, Karlsruhe, Germany
D-MEM/F-12, powder, 1:1	Invitrogen, Karlsruhe, Germany
DMSO ((CH ₃) ₂ SO)	Sigma-Aldrich, Taufkirchen, Germany
Fetal Bovine Serum (Research Grade)	HyClone, South Logan, USA
HEPARG culture medium	Biopredic international, Rennes, France
Insulin	Novo Nordisk Pharma, Mainz, Germany
ITS	Invitrogen, Karlsruhe, Germany
L-Glutamine	Ferak, Berlin, Germany
PBS	Invitrogen, Karlsruhe, Germany
Penicillin [10000 U/ ml]	Sigma-Aldrich, Taufkirchen, Germany
Streptomycin [10 mg/ml]	Sigma-Aldrich, Taufkirchen, Germany

2.1.6 Buffers and solutions

2.1.6.1 Perfusion buffers for rat liver perfusion

Stock solution	
6.30 g	NaCl
0.32 g	KCl
0.27 g	MgSO ₄ • 7 H ₂ O
0.15 g	KH ₂ PO ₄
1.81 g	NaHCO ₃
3.58 g	HEPES
1.50 g	D-Glucose
Add H ₂ O to 1 l	

Washing buffer	
0.58 g	CaCl ₂ •2 H ₂ O
20.00 g	BSA
Add H ₂ O to 1 l and calibrate to pH 7.2	

For Perfusion Buffer 1, add	
0.038 g	EGTA
Calibrate to pH 7.2	

For Perfusion Buffer 2, add	
0.58 g	CaCl ₂ •2 H ₂ O
Calibrate to pH 7.2 and add Liberase Blendzyme to 300 ml	

Trypan-blue solution	
500 µl	Trypanblue-Solution (0.5 %)
500 µl	Wash buffer

2 MATERIALS AND METHODS

modified Williams' Medium E	
1 mg	Ampicillin
125 mg	Gentamicin
29.2 mg	L-Glutamin
345 mg	Insulin
10 mg	Tylosin
Add 100 ml Williams' Medium E and calibrate to pH 7.4	

Krebs-Henseleit-Buffer	
60 mm	NaCl
2.4 mm	KCl
0.6 mm	KH ₂ PO ₄
0.6 mm	MgSO ₄ × 7 H ₂ O
12.5 mm	NaHCO ₃
0.625 mm	CaCl ₂ × 6 H ₂ O
12.6 mm	HEPES
50 mg/l	Gentamycin
Add H ₂ O to 1 l and calibrate to pH 7.4	

2.1.6.2 Buffers for SELDI-TOF-MS

Pre-activation buffer WCX	
10 mM	HCl (1 M)
Add H ₂ O to 1 l	

Binding buffer WCX	
0.1 M	Natriumacetat pH 4.5
0.05% (v/v)	Triton X-100

2.1.6.3 Buffers for protein-preparation and immunodetection

Lysis buffer for resuspending of Proteins	
6.3 g	Urea
2.3 g	Thio-urea
0.48 g	CHAPS
600 µl	DTT (1 M)
300 µl	Spermin (1 M)
Add H ₂ O to 12 ml	

PBS-Tween-Buffer	
10% (v/v)	PBS (10x)
0,1-5% (v/v)	Tween 20
85-89,9%	Aqua purificata

Coating-Solution	
5% (m/v)	Magermilchpulver
	PBS-Tween-Buffer

2.1.6.4 Buffers and solutions for Illumina BeadChip arrays

First strand synthesis mastermix (8 samples)	
2.2 μ l	T7(dT)Primer, 10 pmol/ μ L
4.4 μ l	10X 1st-strand buffer
8.8 μ l	dNTP mix
2.2 μ l	RNase Inhibitor
2.2 μ l	Reverse Transcriptase
24.2 μ l	Nuclease free water

Second strand synthesis mastermix (8 samples)	
22 μ l	10X 2nd-strand buffer
8.8 μ l	dNTP mix
4.4 μ l	DNA polymerase
2.2 μ l	RNaseH, 2U/ μ L
140 μ l	nuclease free water

Heat Wash buffer	
50 ml	Heat wash buffer
450 ml	Nuclease free water

IVT-Reaction	
8.8 μ l	10X reaction buffer
8.8 μ l	ATP, 75 mM
8.8 μ l	CTP, 75 mM
8.8 μ l	GTP, 75 mM
4.4 μ l	UTP, 75 mM
33 μ l	Biotin-16-UTP, 10 mM
8.8 μ l	T7 Enzyme Mix
6.6 μ l	nuclease free water

Wash buffer E1BC	
1.5 ml	E1BC Buffer
500 ml	Nuclease free water
Heat to 55°C over night	

Cy3 staining solution	
2 ml	Blocker™ Casein in PBS (1% m/v)
2 μ l	FluoroLink™ Cy™3 labelled streptavidin (1 mg/ml)

2.1.6.5 Buffers and solutions for Affymetrix Gene Chips®

first strand mastermix	
4 μ l	5x First Strand Reaction Mix Buffer
2 μ l	DTT [0.1M]
1 μ l	dNTP Mix [10 mM]

IVT Mastermix	
4 μ l	10x IVT Labeling Buffer
12 μ l	IVT Labeling NTP Mix
4 μ l	IVT Labeling Enzyme Mix

Second strand Mastermix	
30 μ l	5x Second Strand Reaction Mix Buffer
3 μ l	dNTP Mix [10 mM]
1 μ l	E. coli DNA Ligase (10 U/ μ l)
4 μ l	E. coli DNA Polymerase I (10 U/ μ l)
1 μ l	RNase H (2 U/ μ l)
91 μ l	nuclease free water

2 MATERIALS AND METHODS

Hybridization mix	
20 µl	fragmentede cRNA (15 µg)
5 µl	Control-Oligonucleotide B2 (5 nm)
3 µl	Herring-sperm DNA [10 mg/ml]
15 µl	100x Control-cRNA-Cocktail
3 µl	acetylated BSA [50 mg/ml]
150 µl	MES-Hybridising buffer
104 µl	DEPC-H ₂ O
Add H ₂ O to 12 ml	

MES-buffer for chip staining	
41.7 ml	12x MES
92.5 ml	5 M NaCl
2.5 ml	Tween20 (10 %)
Add H ₂ O to 1 l	

SAPE- buffer	
600 µl	2x MES-buffer
120 µl	acetylated BSA (20 mg/ml)
12 µl	SAPE (1 mg/ml)
468 µl	Nuclease free Water
Centrifuge 5 min at 9,000 x g	

Non-stringent washing buffer	
300 ml	20x SSPE
1 ml	Tween20 (10 %)
Add H ₂ O to 1 l	

Stringent washing buffer	
83.3 ml	20x SSPE
5.2 ml	5 M NaCl
1.0 ml	Tween20 (10 %)
Add H ₂ O to 1 l	

Antibody detection solution	
300 µl	2x MES-buffer
60 µl	acetylated BSA (20 mg/ml)
6.0 µl	Goat IgG (10 mg/ml in 150 mM NaCl)
3.6 µl	Anti-Streptavidin Antibody, biotinylated (0.5 mg/ml)
230.4 µl	nuclease free water

2.2 Methods

2.2.1 Cell culture

2.2.1.1 Isolation of primary rat hepatocytes

Male Wistar-rats with a weight between 200 to 300 g were used for the isolation of hepatocytes. The animals were kept according to animal welfare regulations⁴ and the perfusion was done with authorization from the local authorities⁵. The rats had free access to food and water and were kept at a constant temperature of 20°C and a light dark cycle of 12 h each.

The perfusion was carried out using a modification of the two-step perfusion method described by Seglen (Seglen, 1976). Before that, the rats were weighed, and anesthetised by a mixture of Ketanest S and Rampun 2% at a concentration of 100 mg/kg bodyweight and 15 mg/kg bodyweight, respectively. The anesthetized rats were mounted facing backwards and the abdominal wall was opened. A syringe was inserted into the portal vein and fixed with a ligature. The syringe was connected to a pumping system and the perfusion buffers by a flexible tube.

During the first step of perfusion the liver was flushed with perfusion buffer 1 (PB1) with a flow rate of 50 ml/min for 2 min and afterwards with a flow rate of 40 ml/min for another 3 min. To guaranty the complete removal of blood and to allow the perfusion buffers to flow trough the liver, the inferior vena cava, which is located behind the liver, was opened. PB1 is Ca²⁺ free and contains EGTA, which complexes the remaining Ca²⁺-ions which are important for cellular adhesion. During this procedure, the colour of the liver changes from red to pink.

Secondly, perfusion buffer 2 (PB2) was used at a flow rate of 45 ml/min for 5-7 min. PB2 contains Liberase Blendzyme 2, a mixture of Thermolysin (a neutral protease) and a collagenase. The dissociation of the tissue and thereby the separation of the cells was indicated by the appearance of a fine network on the surface of the liver. The liver was transferred into an ice cold washing buffer (WB), the liver capsule was opened and the separated cells were released. The cell suspension was filtered through a coarse gaze to remove bigger cell clumps. To remove non-parenchymal cells, the cell suspension was three times centrifuged (500rpm, 4°C for 2 min) to pellet the hepatocytes, the supernatant containing the other cell types of the liver was aspirated and the pellet was resuspended with cold WB.

⁴ Deutsches Tierschutzgesetz

⁵ Approval-Nr. v54-19c20/15 [DA4/Anz271E]

2.2.1.2 Trypan Blue exclusion test

Cell viability and cell number of freshly isolated hepatocytes was assessed by the trypan blue exclusion test. It is based on the principle that live cells possess intact cell membranes that exclude trypan blue, whereas dead cells do not.

50 µl Cell suspension was incubated with 1 ml trypan blue solution (500 µl Trypan blue, 0.5% + 500 µl WB1) for 1 min at RT. Afterwards, viable and dead cells were counted in a Fuchs-Rosenthal-Chamber by counting 3 fields with 16 squares each. The determined numbers of living and dead cells were used to calculate the viability, as well as the total number of cells.

$$Cells / ml = Cells_{Viable} \cdot D \cdot 5000 \qquad \%_{(Viability)} = \frac{Cells_{Viable}}{Cells_{Dead}} \cdot 100$$

D= Dilution Factor

The outcome per perfusion usually was in between 5×10^8 and 1×10^9 hepatocytes and the viability had to be greater than 85% for the cells to be used for further studies.

2.2.1.3 Preparation of culture dishes

Cells were plated onto either uncoated or collagen I coated culture plates for the plastic- and monolayer cultures and on a collagen-gel for sandwich cultures. This required different pre-processing of the culture dishes, except for the plastic cultures, where the culture-dishes were used as delivered.

The dishes for the monolayer cultures (ML) were coated by adding an acidic collagen I solution [10µg/ml] and letting it dry either over night (ON) or for two days (Table 3).

Cell culture plate	Area/well	Volume	Concentration	Time to dry
96 well plate	0.32 cm ²	110 µl	20 µg/ml	2 d
24 well plate	2 cm ²	125 µl	100 µg/ml	ON
6 well plate	9.6 cm ²	600 µl	100 µg/ml	ON
60 mm dish	28 cm ²	1.8 ml	100 µg/ml	ON

Table 3: Scheme of pipetting for coating of culture dishes for monolayer culture

For the sandwich cultures (SW) a layer of gelled collagen had to be prepared prior to the seeding of the cells. An ice-cold acidic solution of collagen I [83 µg/ml] was mixed

with 1/10th volume 10x DMEM-F12 media resulting in a final collagen-concentration of 75 µg/ml. This was then neutralized to a pH of 7.2 to 7.4, with a 1M sodium hydroxide solution and directly transferred to the culture dishes/plates (Table 4). By incubation in an incubator at 37°C for at least 30 min, the collagen was allowed to gelatinize.

Cell culture plate	Volume
24 well plate	75 µl
6 well plate	200 µl
60 mm dish	500 µl

Table 4: Volume of collagen I solution used for each layer of sandwich culture.

2.2.1.4 Plating of cells

After isolation, hepatocytes were plated as fast as possible. Cells were mixed with plating media (DMEM/F12 medium (Gibco)) supplemented with 10% (v/v) FBS, sodium pyruvate, antibiotics and insulin and dispensed uniformly onto the dishes (Table 5).

Cell culture plate	Cells/ ml	Volume	Total number of cells
96 well plates	500 *10 ³	100 µl	50 *10 ³
24 well plates	500 *10 ³	0.5 ml	250 *10 ³
6 well plates	1 *10 ⁶	1.5 ml	1.5 *10 ⁶
60 mm dishes	1.5 *10 ⁶	3 ml	4.5 *10 ⁶

Table 5: The media volumes and the amount of cells used for seeding.

Cells were allowed to attach to the culture surfaces at 37°C and 5% CO₂ in a humidified atmosphere for 4 h. Cultures were subsequently washed with cooled PBS to remove dead and damaged cells. Specific media, according to the experiment type, was added (medium with FBS (above) or serum-free medium supplemented with 0.1% BSA, dexamethasone and ITS) and cells were cultured in an incubator as described above.

After attachment (3-6 h) SW cultures were overlaid with a second layer of collagen I in the same manner as the first layer and incubated at 37°C for additional 30 min to allow the second layer to gelatinize. Medium was added afterwards and either changed daily for the time course experiments or every second day for the experiments with compound treatment.

2.2.1.5 Culture of FaO and HepG2-cells

The human hepatoma cell line HepG2 and the rat hepatoma cell line FaO were grown in DMEM/F12 medium (Gibco) supplemented with 10% (v/v) FBS, sodium pyruvate, antibiotics and insulin at 37°C and 5% CO₂ in a humidified atmosphere to 90% confluency, washed with PBS and lysed with Trizol for subsequent RNA isolation.

2.2.1.6 Suspension culture

The preparation and cultivation of rat and human suspension cultures was performed by Biopredic International. After perfusion, rat and human hepatocytes were purified, suspended in DMEM supplemented with fetal calf serum (5%), insulin (4 mg/l), hydrocortisone (10⁻⁶ mM), and gentamycin (50 mg/l) and incubated at 37 °C, 5% CO₂ on a mixer at 300 rpm. At each time point used for later analysis, cells were collected, shock frozen in liquid nitrogen and stored for subsequent RNA isolation with Trizol.

2.2.1.7 Precision cut liver slices

The preparation and cultivation of rat liver slices was performed in the laboratory of Prof. Müller⁶. 33-40 Day old male Wistar-rats from the institutes own breeding facility were kept according to the actual rules of animal welfare⁷ at a light dark rhythm of 12 h, 22°C and free access to water and food (Altromin 1316, Altromin GmbH, Lage, Germany). Animals were sacrificed by decapitation after being anaesthetized with ether and liver slices were cut according to the method of Müller (Müller et al., 1998).

Briefly after dissection, the liver was flushed with and then transferred into ice-cold Krebs-Henseleit-Buffer. Cylinders of 8 mm diameter were cut out and a Krumdieck-Tissue-Slicer was used to cut liver slices with a thickness of about 200-250µm. Four slices per 25 ml Erlenmeyer flask were incubated in 5 ml modified Williams' E Medium for 2 h, 6 h, 1 d and 2 d at 37°C, gassed with carbogen (95% O₂ and 5% CO₂) and bidirectionally shaken (100 hz). Change of media was made after 2 h and 24 h. At the mentioned time points, liver slices were transferred into 1.5 ml reaction tubes, shock-frozen in liquid nitrogen and stored at -80°C until RNA isolation.

⁶ Institute of Pharmacology and Toxicology of the Friedrich-Schiller-University of Jena

⁷ Deutsches Tierschutzgesetz

2.2.1.8 Isolation of primary human hepatocytes

Primary human hepatocytes were prepared from lobectomy segments resected from adult patients for medically required purposes by KaLy Cell⁸. Cells were checked for viability and seeded in culture wells in either ML culture or on a collagen gel as preparation for SW configuration. After incubation over night to ensure attachment of the cells, they were sent to Merck KGaA and used for further analyses. Cells designated for SW cultures were overlaid with a second layer of collagen gel as described in 2.2.1.4 and cells were incubated for another night at 37°C to allow the cells to recover from the transport procedure.

2.2.1.9 HepaRG cells

Cells were seeded and pre-incubated by Biopredic International⁹ and delivered as confluent ML cultures. After receipt, the media was changed to “after-shipment” media and cells were incubated at 37°C and 5% CO₂ in a humidified atmosphere for three days to allow regeneration. Following this incubation, media was changed to either basal media or to basal media supplemented with 2% DMSO and incubated for another two days. During this time, cells differentiated to their “hepatocyte-like” phenotype and were then used for time course experiments.

2.2.2 Rat *in vivo* study

Liver samples from rats treated with tetracycline (Tet) or vehicle control were taken from a short term toxicity study performed by phase-1 Molecular Toxicology Inc.¹⁰ The study was run according to the official guideline of animal welfare¹¹ and “Good laboratory Practices” (GLP)¹² compliance.

Male Sprague Dawley (CrI:CD[®]) rats with a body weight between 300 g and 400 g were kept under regular light-dark cycle of 12:12 hours with food (PMI Feeds Inc., Purina Milla, Richmond, USA) and water ad libitum. The rats were separated in groups of three animals per time point. Each group was treated once with vehicle control

⁸ KaLy Cell, 2500 Besançon, France

⁹ Biopredic International, 35000 RENNES, FRANCE

¹⁰ PHASE 1 MOLECULAR TOXICOLOGY INC., Santa Fe, USA

¹¹ United States Department of Agriculture (USDA) Animal Welfare Act (9 CFR Parts 1, 2, 3)

¹² Good Laboratory Practice refers to a system of management controls for laboratories and research organisations to ensure the consistency and reliability of results as outlined in the OECD Principles of GLP and national regulations. The FDA has rules for GLP in 21CFR58

(sodium chloride solution), low or high doses of tetracycline by i.p. injection. The high dose was 150 mg/kg and as low dose, one third of it was chosen (50 mg/kg). Dose finding was done by phase-1 Molecular Toxicology Inc. and was based on both published and unpublished data.

Treatment groups of three rats were sacrificed at 6 h, 1 d or 3 d by exposure to CO₂. After bleeding of the rats, the livers were withdrawn and divided into two pieces and cut into small pieces, shock-frozen in liquid nitrogen and stored at -80°C for later RNA extraction.

2.2.3 Biochemical methods and cell viability assays

There are a variety of assays to test for the number of dead cells (cytotoxicity assays), the number of living cells (viability assays), the total number of cells or the mechanism of cell death (e.g., apoptosis). Here, a number of different tests were used to address several of these different parameters. These tests were used to assess hepatocyte viability after perfusion (Trypan blue Test) or to characterize the different cell-cultures and their change over incubation time and to determine the kinetics of cell death caused by compound treatment. Results of the latter experiments were used to calculate the final concentrations used in the gene expression experiments.

2.2.3.1 CellTiter-Glo[®] Luminescent cell viability assay

For the detection of cell viability, the CellTiter-Glo[®] Luminescent Cell Viability Assay was used. This test is based on a luciferase reaction (Figure 12 Figure 12) to measure the amount of ATP in cells. This correlates directly with the number of cells and their viability because cells lose the ability to synthesize ATP directly after e.g. loss of membrane integrity or a cytotoxic event. The protocol was adapted to 24 well plates and to the different culture conditions resulting in a standardized protocol which is described below. Cell lysis, inhibition of endogenous ATPases and detection of ATP was performed by adding the CellTiter-Glo[®] Reagent to the culture wells. Per well, 100 µl reagent were mixed with the same volume of DMEM-F12 Medium. Lysing of the cells took place by 10 min incubation at RT and moderate shaking. Three times 50 µl cell lysate was transferred into a white 96 well plate to eliminate stray light, and the bioluminescence was measured.

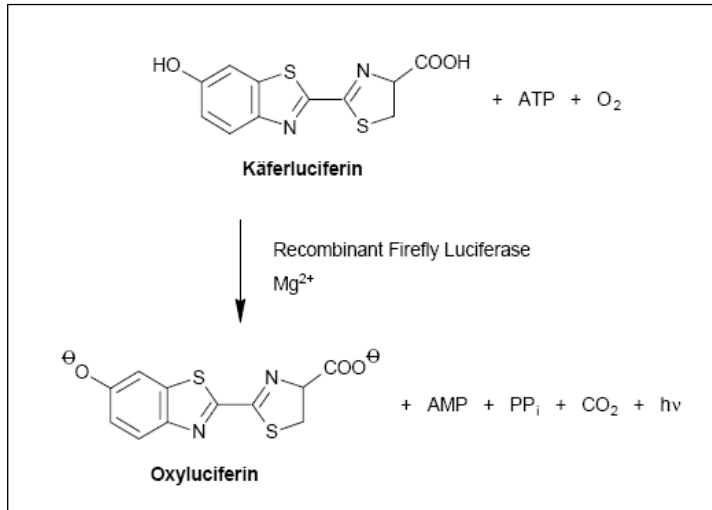


Figure 12: Chemical reaction of the CellTiter-Glo® Luminescent Cell Viability Assay. The reagent contains recombinant luciferase that uses the likewise contained luciferin as a substrate and reacts under the consumption of cellular ATP with the release of luminescence (Adapted from Assay Manual).

2.2.3.2 WST-1-assay

This test is based on the reduction of a tetrazolium salt that can be used for cell proliferation or cell viability assays. The rate of WST-1 cleavage by mitochondrial dehydrogenases correlates with the number of viable cells in the culture (Figure 13).

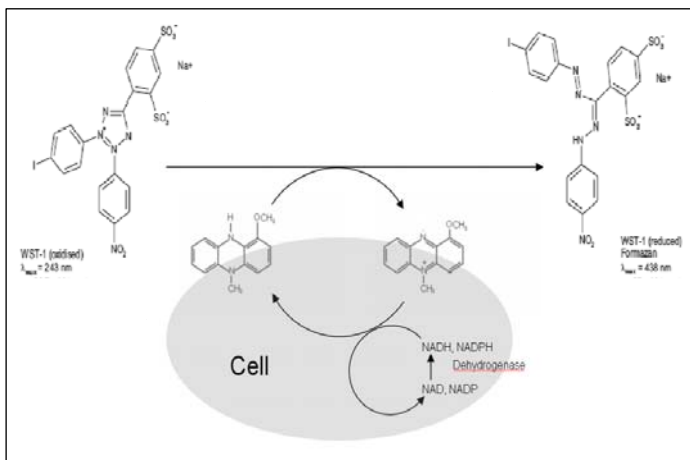


Figure 13: Assay mechanism of WST-1 conversion by dehydrogenases in viable cells. The water-soluble tetrazolium salt WST-1 is reduced to the coloured dye formazan by mitochondrial dehydrogenase enzymes with the intermediate electron acceptor PMS (Adapted from Assay Manual).

After aspiration of the culture wells, 350 µl of a mixture of DMEM F-12 media and WST-1 reagent (1/10th volume) was added to the cells and, following 4 hours incubation at 37°C, absorbance at 450 nm was measured.

2.2.3.3 LDH release

If cells get damaged or die, they lose their membrane integrity, releasing, among others, cytoplasmic proteins like lactate dehydrogenase (LDH) into the surrounding media. Based on the CytoTox-ONE™ Homogeneous Membrane Integrity Assay, a

standardized protocol was developed to measure the release of LDH from damaged hepatocytes as an indicator of cytotoxicity.

LDH catalyzes the conversion of lactate to pyruvate with the simultaneous production of NADH. The CytoTox-ONE™ Reagent contains substrates as well as cofactors for this reaction and for the conversion of resazurin to resorufin using NADH as an energy source. The emerging fluorescence is relative to the amount of LDH released into the media and was optically measured at 544 nm excitation and 595 nm emission wavelengths (Figure 14).

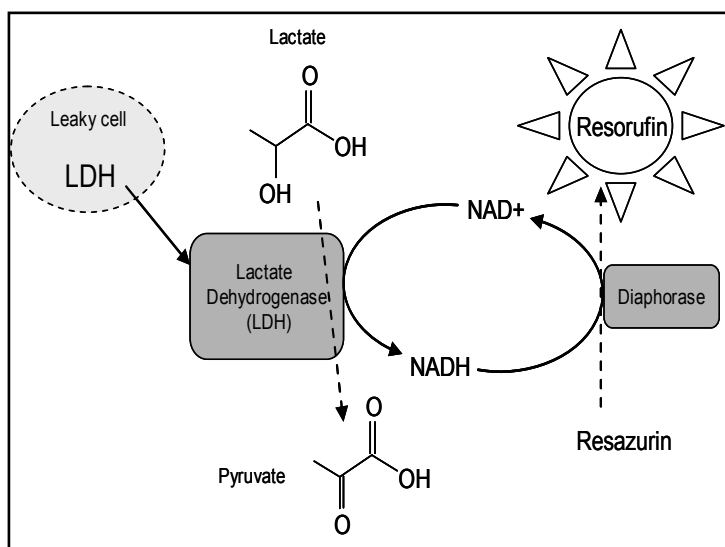


Figure 14: Principal behind the CytoTox-ONE™- Homogeneous Membrane Integrity Assay. Released LDH of damaged cells catalyzes the conversion of Lactate to Pyruvate under production of NADH in the culture media. This NADH is used to drive the diaphorase-catalyzed production of the resorufin product from resazurin.

Three times 50 μ l culture media per well were transferred to a black 96 well plate, mixed with the same volume of CytoTox-ONE™ Reagent and incubated for 10 min at RT. The reaction was stopped by adding 25 μ l Stop Solution and the fluorescence intensity was measured. Meanwhile, the remaining reaction media was aspirated and cells were lysed with 200 μ l 0.1% TritonX100 in PBS (v/v) for 10 min at RT. Again, three times 50 μ l were transferred to a black 96 well plate, the reaction was carried out and the fluorescence was measured as described above.

The LDH content of treated cells relative to the controls (time matched or fresh cells), which is an indication for the membrane integrity and cell viability, was calculated as follows:

$$\% LDH_{retained} = \left(\frac{LDH_{released}}{LDH_{released} + LDH_{cellular}} \right)_{Control} \div \left(\frac{LDH_{released}}{LDH_{released} + LDH_{cellular}} \right)_{Sample} \bullet 100$$

2.2.3.4 Cytochrome P450 isoform induction and activity

2.2.3.4.1 Induction of Cyp isoforms

Hepatocytes in ML and SW culture were induced with known inducers for the expression of CYP 1A, 2B, 2C and 3A isoforms. Cells were cultured as previously described and dosed at 0 h, 3 d and 9 d with the appropriate inducer for 48 h. CYP 1A1 was induced with β -naphthoflavone (BNF; 10 μ M), CYP 2B and 2C with phenobarbital (PB; 500 μ M) and CYP 3A with dexamethasone (Dex; 50 μ M). The concentrations of the inducers used in this experiment were selected based on preliminary experiments to obtain the largest enzyme induction without causing toxicity (data not shown).

2.2.3.4.2 Detection of Cytochromes P4503A7 and 2C9 isoform activity

The activity and induction of cytochrome P450s 3A7 and 2C9 were measured with the P450-Glo™ Assays (Promega). These tests are based on the CYP450-isoenzyme specific conversion of derivatives of beetle luciferin to a luciferin product that can be detected in a second reaction with a Luciferin Detection Reagent via the generation of luminescence. The amount of light produced is proportional to the activity of the CYP450-isoform (Figure 15).

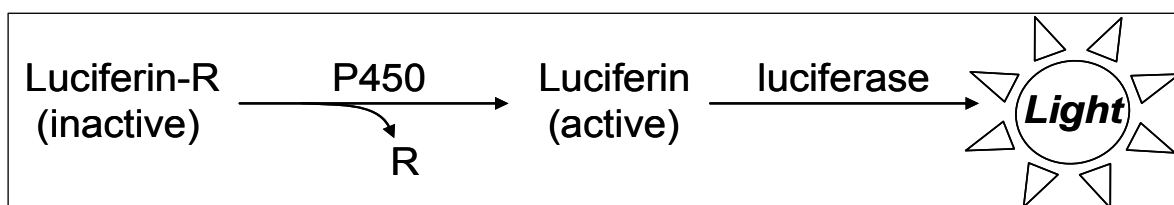


Figure 15: Conversion of P450-Glo™ substrate by cytochrome P450. Cytochrome P450 isoenzymes act specifically on a substrate to produce a luciferin product that generates light with the Luciferin Detection Reagent (modified from assay-manual).

The luciferin substrate (5 mM) was diluted in an appropriate Media (1:50) and culture media was replaced by 100 μ l of this mixture. Cells were incubated for 4 h at 37°C and 5% CO₂ for the progress of the biochemical reaction. Afterwards 2x 40 μ l were transferred into a white 96 well plate and the same volume of the P450-Glo™ Luciferin Detection Reagent was added. The reagent simultaneously stops the CYP450 reaction and initiates a luminescent signal, which was measured after 20min incubation at RT with a luminescence plate reader.

2.2.3.4.3 **Detection of Cytochromes P450 1A1 and 2B6 isoform activity**

Cytochrome P450 1A1 and Cytochrome P450 2B6 isoform activities and induction were characterized with either 7-ethoxyresorufin-O-deethylase (EROD) or benzyloxyresorufin-O-debenzylase (BROD). The reaction product was measurable with an excitation wavelength of 544 nm and an emission wavelength of 595 nm (Burke et al., 1985).

The cell culture media of cells cultured in a 24 well plate was aspirated and replaced by 150 μ l salicylamide solution (0.3M). Cells were incubated for 10 min at 37°C and 5% CO₂ and subsequently 150 μ l substrate solution was added (concentration of EROD was 5 μ M, BROD was 10 μ M). After 20 min incubation at 37°C, 3x 75 μ l were transferred into a black 96well plate and fluorescence was measured in a fluorescence plate reader.

2.2.3.5 **Canalicular transporter activity**

The functional activity of the canalicular transporter multidrug resistance associated protein (Mrp2) was studied with carboxy-DCFDA. This diacetate exhibits only weak fluorescence but is, after penetrating through the plasma membrane, rapidly metabolized to the fluorescent product carboxydichlorofluorescein. This fluorescent bile acid is known to be a substrate for this hepatocellular transporter (Heredi-Szabo et al., 2008) and therefore the dye efflux from hepatocytes cultured in either ML or SW culture could be determined over time.

Per well of a 24 well plate, the culture media was replaced by 500 μ l carboxy-DCFDA (diluted in PBS to a concentration of 5 μ M). The cells were incubated for 20min at 37°C and 5% CO₂, subsequently washed three times with warm PBS and observed with a fluorescence microscope at an excitation wavelength of 480 nm and a 530 nm filter for detection of the emitted light.

2.2.4 **Molecular biological methods**

2.2.4.1 **Isolation of RNA and proteins**

The isolation of RNA and proteins was conducted with TRI Reagent. TRI Reagent contains phenol and guanidine thiocyanate to maintain nucleotide and protein integrity during cell/tissue homogenization while at the same time disrupting and breaking down cells and cell components. All steps of the procedure were conducted according to the manufacturers' manual (Sigma).

Cells in culture were lysed by replacing the culture media with the appropriate volume of TRI reagent and the lysate was transferred into a 15 ml reaction tube. Tissue slices were homogenized by the addition of a nuclease free steel bead and the appropriate volume of TRI reagent with the Tissue Lyzer for 1 min with a frequency of 25 Hz. All samples were incubated for 10 min at RT, afterwards 200 µl chloroform per 1 ml TRI reagent were added, mixed by shaking and incubated for another 10 min. For the separation of the phases, this mixture was centrifuged for 15 min at 12,000 x g and 4°C. The upper aqueous phase containing the RNA was transferred into new reaction tube containing 500 µl ice cold isopropanol per ml TRI reagent, mixed by vortexing and incubated for 10 min at RT. Another centrifugation step precipitated the RNA. The pellet was washed with 1.5 ml ethanol (75%), the supernatant discarded, the pellet dried for 5-10 min and finally resolved in nuclease free water.

The proteins, which are contained in the organic lower phase, were isolated by discarding the white interphase containing the genomic DNA, precipitated by adding 1.5 ml isopropanol per 1 ml of TRI reagent used for initial homogenization and incubation for 10 min at room temperature. The proteins were sedimented by centrifugation at 12000 x g for 10 min at 4°C. The protein pellet was washed 3 times for 20 min at RT in 0.3 M guanidine hydrochloride in 95% ethanol (2 ml per ml TRI reagent) and once in 100% ethanol with centrifugation steps of 7500 x g for 5 min at 4°C to re-acquire the pellet. After this final wash step, the protein pellet was air dried for 5-10 min at RT and resuspended in 200-300 µl lysis buffer by using the tissue lyzer. After complete solubilization, the protein solution was stored at -20°C.

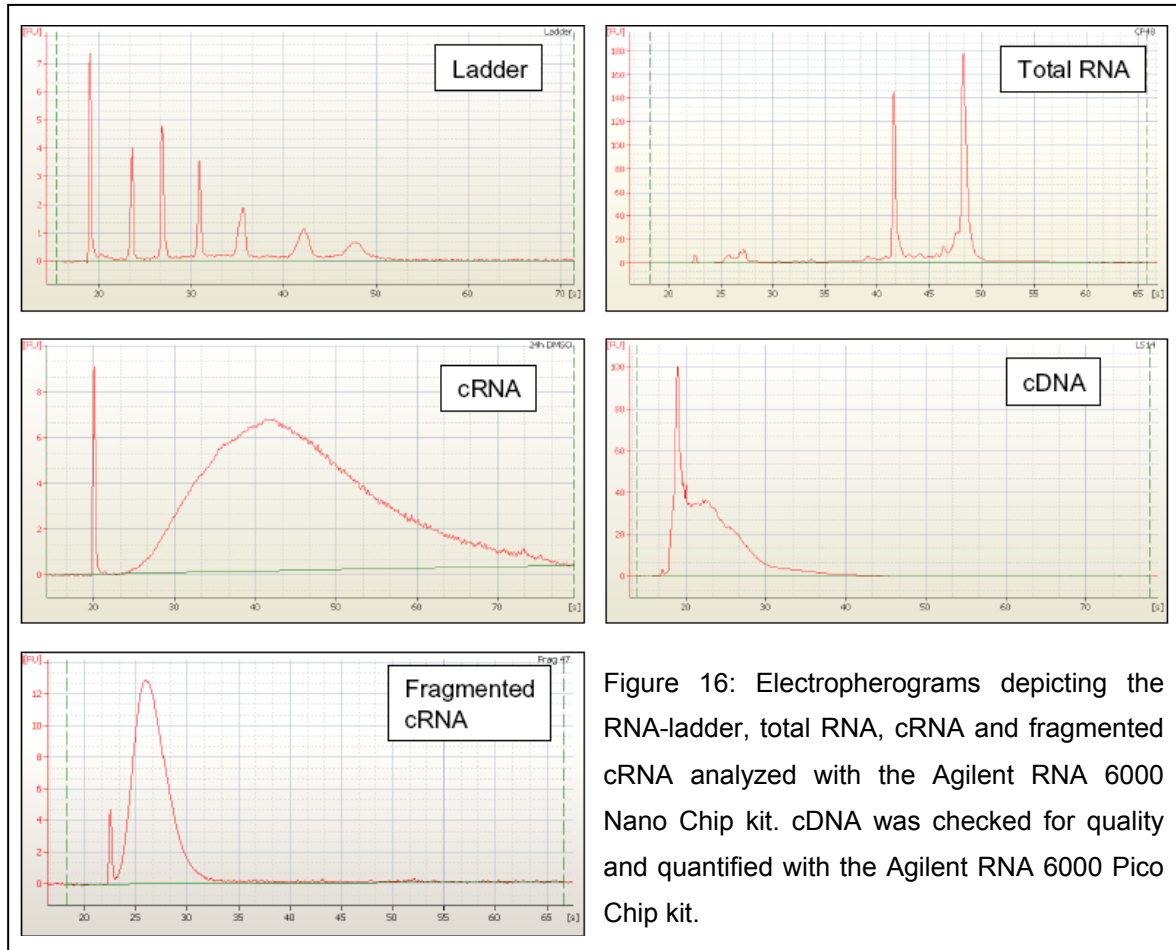
2.2.4.2 Quantification and quality check of nucleic acids

The quantification of isolated nucleic acids and the check for absence of protein was done by measuring the absorbance at 260 nm and 280 nm with a UV-spectrophotometer (NanoDrop ND-1000). The ratio between the two resulting values must be 1.8 or higher to guarantee a protein-free solution. With the help of the Lambert-Beer-Law and the molar extinction-coefficient, the concentration of the RNA in solution was calculated as follows:

$$c = \frac{\log_{10} \frac{I_0}{I}}{\varepsilon \cdot d}$$

c = Concentration, I_0 = Intensity of the initial light beam, I = Intensity of the transmitted light, $\log_{10} I_0/I$ = Absorption, ε = Extinction coefficient, d = Thickness of the cell

The quality of the nucleic acids was checked with the RNA 6000 Nano LabChip Kit II on the Agilent 2100 bioanalyzer according to the manufacturers' recommendations. This assay is based on capillary electrophoresis so the RNA was separated according to their length and detected by fluorescent labeling. The resulting electropherograms (Figure 16) were checked for signs of RNA degradation.



2.2.4.3 TaqMan® Low Density Arrays (TLDA)

2.2.4.3.1 Quantification of mRNA with TaqMan® Low Density Arrays (TLDA)

TaqMan real time PCR is based on the principle of a linear amplification and the 5' exonuclease activity of DNA polymerase during the PCR (Lawyer et al., 1993). TaqMan® probes contain a reporter dye (6-FAM™) linked to the 5' end of the probe and a non-fluorescent quencher (NFQ) at the 3' end of the probe. When the probe is intact, the proximity of the reporter dye to the quencher results in suppression of the reporter fluorescence, primarily due to Förster energy transfer (Förster, 1948).

During PCR, the TaqMan[®] probe anneals specifically to the middle of the amplified sequence. These probes are cleaved by the 5' exonuclease activity of the DNA polymerase during amplification whereby the reporter dye is separated from the quencher, resulting in an increase in fluorescence (Figure 17). The amount of fluorescence produced is measured at each amplification cycle, providing a real-time estimation of the amount of mRNA. This increase in fluorescent signal occurs only if the probe was bound to the target sequence which is amplified during PCR. The assays are designed to span exon junctions to eliminate the possibility of detecting genomic DNA, which may still be present in the cDNA sample.

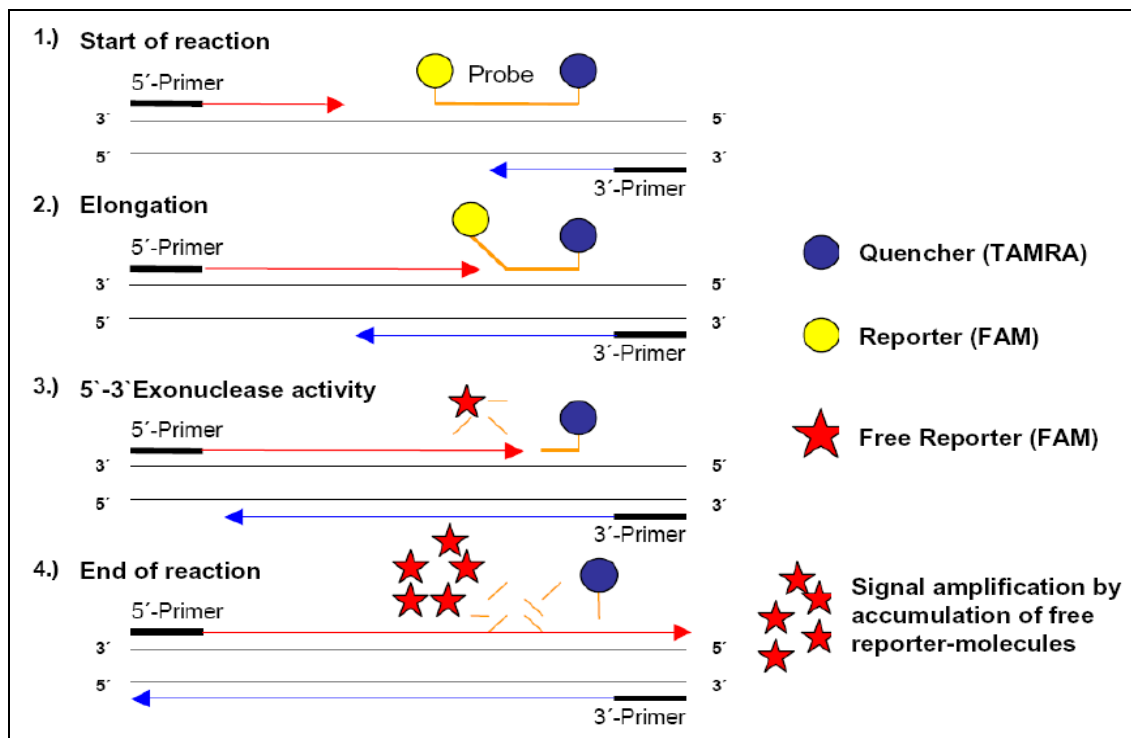


Figure 17: Principle of TaqMan-PCR. Additionally to the two amplification primers, a third gene specific primer, carrying a reporter and a quencher, hybridizes to the amplified gene. During amplification, this primer is degraded by the exonuclease activity of the Taq-polymerase, the reporter separates from the quencher and a fluorescent signal can be measured (modified from assay-manual).

TLDA's are a high throughput application of TaqMan PCR. A 384 well micro fluidic card enables 384 simultaneous real-time PCR reactions to be run in parallel across 12 to 384 targets. They are pre-loaded with optimized primers and probes and can be customized. A list of genes measured for the verification of microarray experiments can be found in the Appendix (Appendix 5 and Appendix 6).

2.2.4.3.2 cDNA synthesis for TaqMan® Low Density Arrays (TLDA)

For cDNA synthesis, the Transcriptor First Strand cDNA Synthesis Kit for RT-PCR (AMV) was used with random hexamers. 1 µg Total RNA in a volume of 11 µl was mixed with 9 µl reverse transcription mastermix and transcribed as follows:

Incubation	10 min	25°C
Reverse transcription	60 min	50°C
RT-Inactivation	5 min	85°C

Table 6: cDNA synthesis reaction for TaqMan® by RT-PCR

The success of the reverse transcription was reviewed and cDNA was quantified with the Agilent 2100 Bioanalyzer using the RNA 6000 Pico LabChip Kit according to the manufacturers manual (Figure 16).

The area under the curve (AUC) from the ladder and samples was used to calculate the concentrations of cDNA. One µl Ladder represents an AUC of 100 and a cDNA concentration of 1 ng/µl.

$$[cDNA] = 10 \text{ pg} / \mu\text{l} \cdot \frac{AUC_{Ladder}}{100} \cdot AUC_{Sample}$$

2.2.4.3.3 Conduction of TaqMan® Low Density Arrays (TLDA)

10 ng cDNA of each sample were made up to 50 µl with nuclease free water, mixed with the same volume qPCR™ Mastermix Plus (Eurogentec) and transferred into the sample reservoirs of the TLDA card. By centrifugation (2 min at 331 g), the samples were distributed into the sample wells and finally, the card was sealed to avoid mixing of the samples and reagents.

The cards were measured using the ABI Prism 790 hT Sequence Detection System controlled by the AB Prism 7900 h SDS Software 2.1 according to the manufacturers' recommendations (Applied Biosystems). Following time scale was used with 45 cycles:

Initial phase	2 min	50°C
Activation of Taq-Polymerase	10 min	94.5°C
Denature cDNA	30 sec	97°C
Annealing and Elongation	1 min	59.7°C

Table 7: Cycle-scheme of TLDA-cards, step 2-4 were repeated 45 times.

2.2.4.3.4 Evaluation of TaqMan[®] Low Density Arrays (TLDA)

Changes in gene expression were calculated relative to a constitutively expressed housekeeping gene such as 18s ribosomal RNA, and additionally compared to a control sample of fresh liver or a time matched vehicle control. Under optimal conditions, the amplification is exponential corresponding to a doubling of the amplified sequence during each cycle. Because this is not always the case, the efficiency corrected Δ CT method of Pfaffl was used (Pfaffl, 2001). The CT value is defined as the number of cycles in the exponential phase of amplification

$$Ratio = \frac{(E_{Target})^{\Delta CT_{Target} (Control - Target)}}{(E_{Control})^{\Delta CT_{Control} (Control - Target)}}$$

E = Efficiency of reverse transcription

Δ CT = Change in the number of cycles between sample and control

To calculate the efficiency of reverse transcription, a titration series of a standard cDNA over four orders of magnitude (0.1 ng - 100 ng) was prepared and amplified. The resulting CT values for each gene were plotted against the amount of cDNA inserted and a standard curve for each gene was calculated. The slope of this curve (m) was used to calculate the transcription efficiency as follows:

$$E = 10^{\left(-\frac{1}{m}\right)}$$

2.2.4.4 Processing of RNA for Illumina and Affymetrix Chips

To enable signal detection and quantification after hybridization to the microchips, the sample RNA has to be labelled. In this case, this was done for both techniques used (Affymetrix and Illumina) by incorporation of biotin-labelled nucleotides during an *in vitro* transcription reaction after an initial cDNA generation from total RNA. The labeling kits were purchased and enzymatic reactions were carried out as recommended by the suppliers.

2.2.4.4.1 cRNA Synthesis from total RNA for Illumina BeadChips

For the cRNA synthesis, the MessageAmp II aRNA Amplification Kit (Ambion Inc.), the RNeasy[®] MiniKit and the QIAquick[®] PCR Purification Kit (both Qiagen) were used. Per sample, 500ng total RNA were dried in a 0.2 ml PCR tube in a vacuum centrifuge concentrator at RT prior to the first strand synthesis.

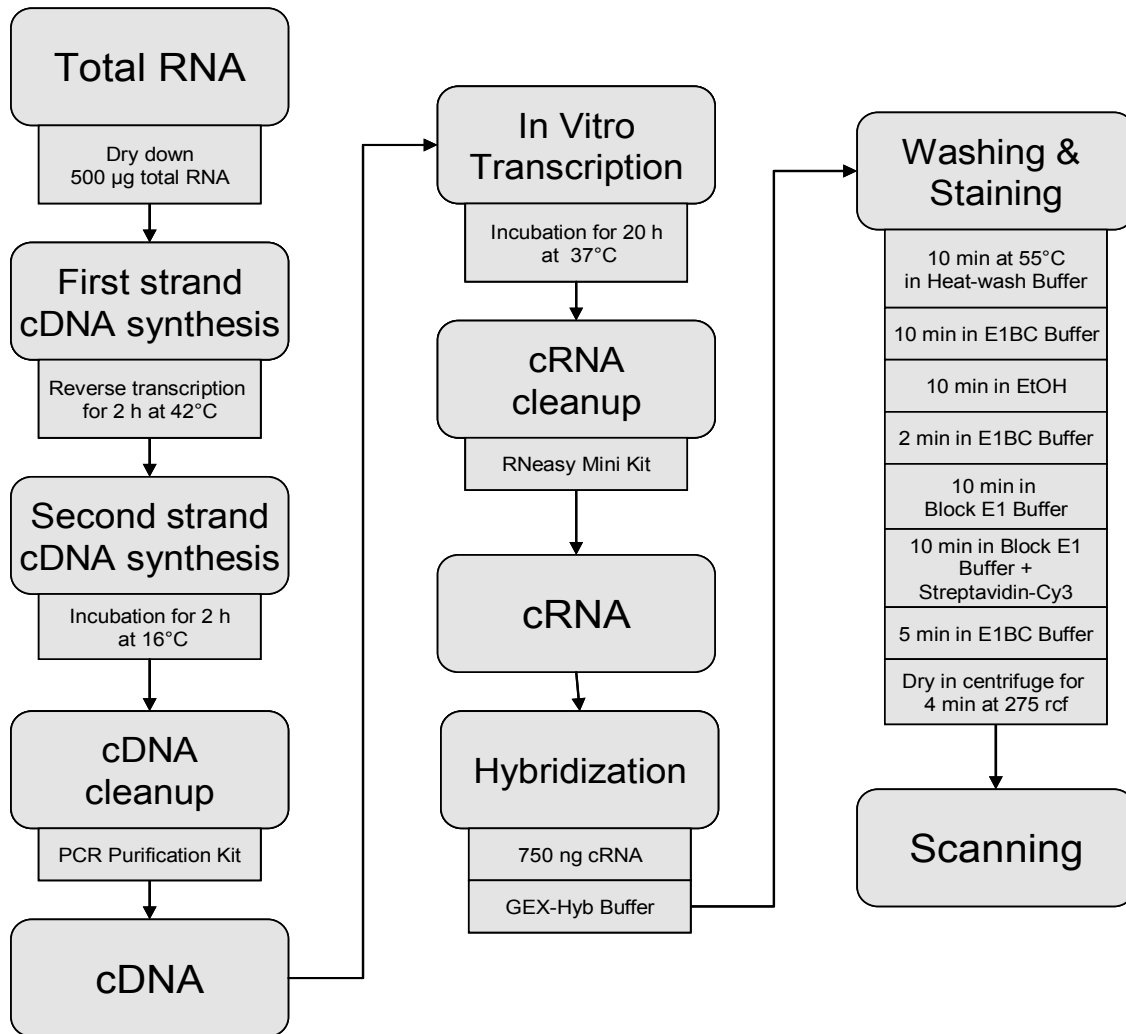


Figure 18: Workflow for the conduction of Illumina BeadChip arrays

During the first strand synthesis step, a single stranded cDNA from the mRNA-containing total RNA sample was synthesized with oligo-dT-primers and a reverse transcriptase. 5µl 1st strand synthesis master mix were dispensed into each sample tube, mixed to dissolve the dried RNA and incubated at 42°C for two hours.

In the 2nd strand synthesis step, the single stranded cDNA from the previous step was converted to double-stranded cDNA; the second strand master mix was prepared directly prior to use. 20 µl of this solution were dispensed into each sample tube and samples were incubated at 16°C for a further two hours.

For the clean up of the sample, the QIAquick PCR Purification Kit was used according to the manufacturers' instructions up to the point of elution which was done with 50 μ l nuclease free water. The double stranded cDNA was dried down in a vacuum centrifuge concentrator at RT prior to *in vitro* transcription (IVT).

During IVT, multiple copies of cRNA were created from every cDNA molecule and additionally, biotinylated UTP-nucleotides were incorporated into the cRNA. 10 μ l IVT mastermix were dispensed into each sample and the reaction was incubated at 37°C for 20 hours.

Following the IVT, samples were cleaned using the RNeasy Mini Kit (QIAGEN) according to the provided manual up to the point of elution. The cRNA was eluted from the columns by washing twice with 50 μ l nuclease free water and quantified and checked for quality as described under 2.2.4.2.

2.2.4.4.2 Hybridizing, staining and detection on Illumina BeadChips

For hybridization, 750ng of the biotin labelled cRNA of each sample was made up to a volume of 5 μ l with Nuclease free water and mixed with 10 μ l GEX-HYB buffer (provided by Illumina). Each mixture was then preheated at 65°C for 5 minutes, allowed to cool down to RT again and dispensed into a separate sample port on the chip (Figure 19). The RatRef-12_v1 chip allows 12 samples to be hybridized simultaneously, Human_RefSeq-8_v2 arrays can be loaded with 8 samples. Each BeadChip simultaneously assays 22,523 probes per sample, targeting genes and known alternative splice variants derived from the National Center for Biotechnology Information Reference Sequence (NCBI RefSeq) database (Build 36.2, Release 22 for human and Release 16 for rat)

Each BeadChip was placed into a BeadChip hybridization chamber, prepared with 200 μ l GEX HCB in each of the two humidifying buffer reservoirs. Hybridization chambers were sealed and incubated for 20 hours at 58°C with a rocker speed of 5.

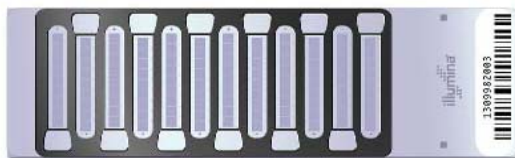


Figure 19: The RatRef-12 Expression BeadChip with IntelliHyb Seal contains 12 rat specific whole genome gene expression arrays, allowing 12 samples to be hybridized to a single chip. Each array probes 21,910 genes and contains 22,523 probes.

To guarantee a consistent quality and fluorescence intensity, several washing steps were performed after hybridization. A high stringency washing step with high

temperature wash buffer to remove unbound and mismatched cRNA, low stringency washing steps with Wash E1BC solution and ethanol, a blocking step with Block E1 buffer, the detection with Prepare Block E1 buffer containing streptavidin-Cy3 [1 mg/ml] and final wash steps with Wash E1BC solution were performed according to the manufacturers protocol. Finally, the BeadChips were dried by centrifugation at 275g at RT for 4 minutes. Scanning was done directly afterwards with the Illumina BeadStation500x at 532 nm and a resolution of 3µm. Three BeadChips could be scanned at once, data extraction was performed simultaneously during the scanning process by the BeadScan control software and the intensity data was exported.

2.2.4.4.3 cRNA synthesis from total-RNA for Affymetrix microarrays

During the whole process of generating cRNA the Gene Chip® One-Cycle cDNA Synthesis Kit, the Gene Chip® Sample Cleanup Module and the Gene Chip® IVT Labeling Kit supplied by Affymetrix were used. All enzymes and buffers used were included in these kits and all steps were accomplished according to the manufacturers' recommendations.

For the reverse transcription, 5µg of total RNA were used in 8 µl nuclease free water. 2 µl Poly-A RNA spike in controls and 2 µl T7 Oligo(dT) Primer [50 mM] were added to make a final volume of 12 µl and incubated for 10 min at 70°C.

7 µl First strand mastermix was added and the mixture was heated up to 42°C for 2 min. Finally, 1 µl enzyme (Superscript II™ [200µM]) was added and the reaction was incubated for 1 h at 42°C.

The single stranded cDNA resulting from the first strand synthesis reaction was used completely for the second strand synthesis. Therefore, 130 µl second strand synthesis mastermix was added and the reaction was incubated for 2 h at 16°C. The reaction was started by adding 2 µl T4-DNA-polymerase (5U/ µl), incubation for another 5 min at 16°C and stopped by the addition of 10 µl EDTA-solution (0.5 M). The clean up was done with the Gene Chip® Sample Cleanup Module and the cDNA was eluted from the columns with 14 µl nuclease free water.

Based on the double stranded cDNA, the biotinylated cRNA was synthesized with the Gene Chip® IVT Labeling Kit. 12 µl cDNA were made up to 20 µl with nuclease free water, mixed with 20 µl IVT-mastermix and incubated for 16 h at 37°C. The cleanup was again performed with the Gene Chip® Sample Cleanup Module and the elution was done in two steps with 11 µl and 10 µl nuclease free water. Quantification and quality control of the synthesized cRNA was performed as described in 2.2.4.2.

Prior to hybridization, the cRNA was fragmented to 200–300mers by metal-induced hydrolysis in fragmentation buffer (supplied with Sample Cleanup Module). 15µg cRNA

was made up to 32 μ l with nuclease free water, mixed with 8 μ l 5x Fragmentation Buffer and heated up to 94°C for 35 min. The fragmentation was checked on the Agilent Bioanalyzer 2100.

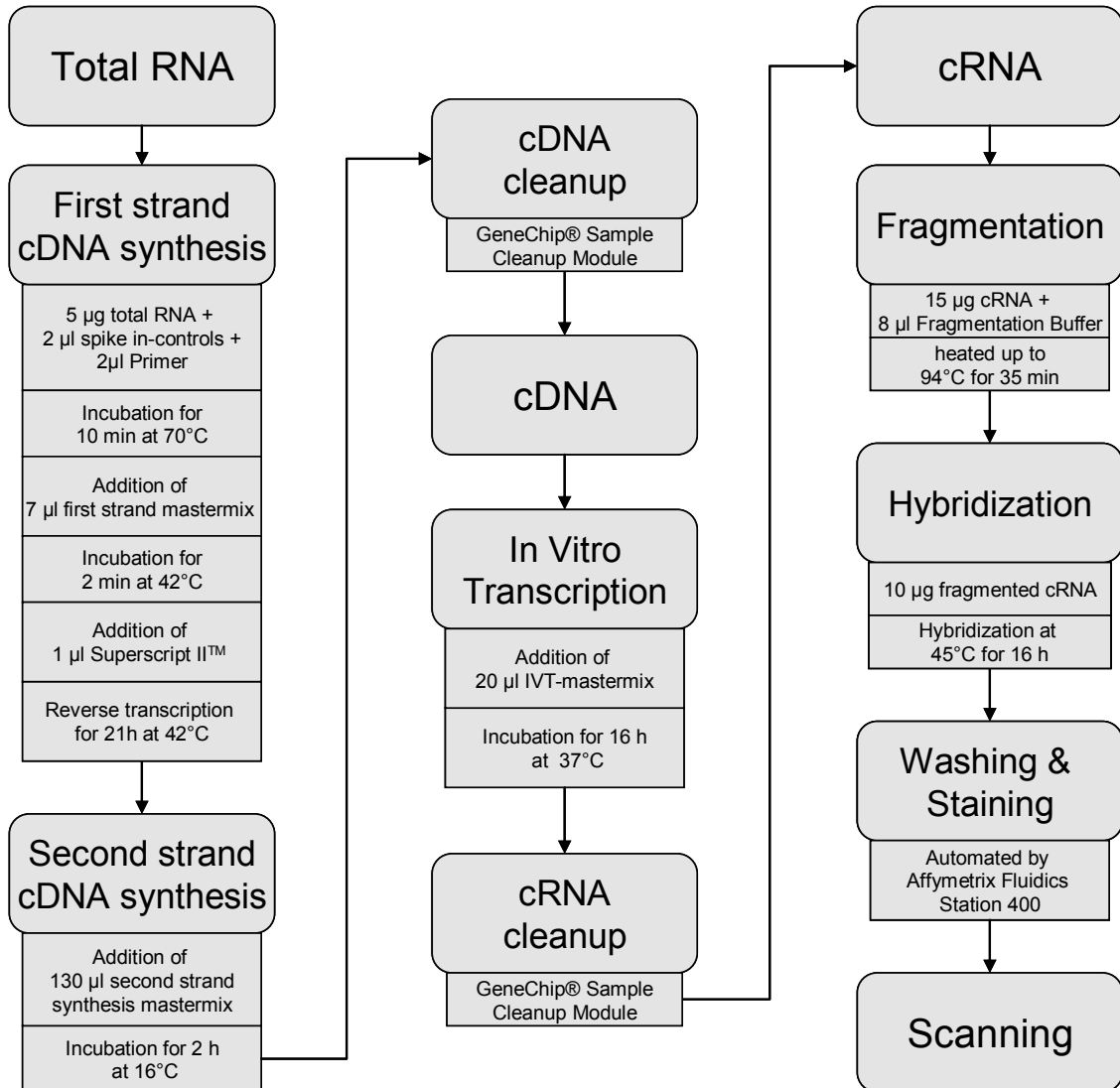


Figure 20: Scheme of the whole workflow for the conduction of Affymetrix Gene Chips®.

2.2.4.4.4 Hybridizing, staining and detection on Affymetrix microarrays

15 μ g fragmented cRNA (40 μ l) were mixed with 260 μ l hybridization mastermix, incubated for 5 min first at 99°C followed by 5min at 45°C and afterwards centrifuged at maximum speed for 5 min. The Affymetrix Chips used (either Gene Chip® Rat Expression Array(RAE) 230 2.0 or Gene Chip® Human Genome U133Plus 2.0Array) were pre-hybridized with 200 μ l 1x MES-Hybridization Buffer for 10 min at 45°C and at a rotation speed of 60rpm. The 1 x MES-Hybridization Buffer was replaced by 200 μ l of the cRNA-hybridization-mastermix (10 μ g) and the Chips were hybridized for 16 h at the same rotation speed.

The washing and staining steps were performed automatically by the Affymetrix Fluidics Station 400. Therefore, the precast washing program EukGE WS5, including the initial low and high stringency wash steps with wash buffers A and B, staining with SAPE-staining solution, antibody solution and a final wash step again with wash buffer A (Figure 20), was used.

The scanning took place in a Gene Chip[®] Scanner 3000 at 570 nm wavelength and a resolution of 3 μm controlled by the GCOS-Software which was used for data extraction and quality control afterwards, too.

2.2.5 Microarray data analysis

The data extraction for Illumina BeadChips and for Affymetrix Genome arrays was performed with specific vendor software.

2.2.5.1 Data extraction and quality control from Illumina BeadChip arrays

Data extraction for Illumina BeadChips was performed by the supplied BeadScan software during the process of scanning and data was exported. The intensity values for every bead were aligned with the decoding data, which was delivered together with each chip (Gunderson et al., 2004, Chapter 1.8). The data from all beads with the same probe bound to their surface were condensed to one value. Simultaneously, for each bead type, a p-Value was calculated indicating the probability to be able to discriminate between negative controls and the samples. Each array on the BeadChips contained also various controls which could be analyzed and used to confirm the quality of the data. Three different hybridization controls with low, medium and high concentration, contained in the hybridization buffer, were used to identify the overall quality of the hybridization, independent from the sample cRNA. Perfect match and mismatch controls were used to detect unspecific hybridizations and, together with a GC-rich probe, to ensure the stringency of the hybridization. Also contained in the hybridization buffer were two biotin-labelled oligonucleotides to control the fluorescence intensity and negative controls with random sequences to identify the background intensity level. Arrays which did not fulfil defined quality parameters were removed and sample hybridization was repeated. In some cases the BeadStudio software was used to normalize the data. Further statistical analyses were conducted in the software Expressionist[®] Analyzer of Genedata and will be discussed in later chapters.

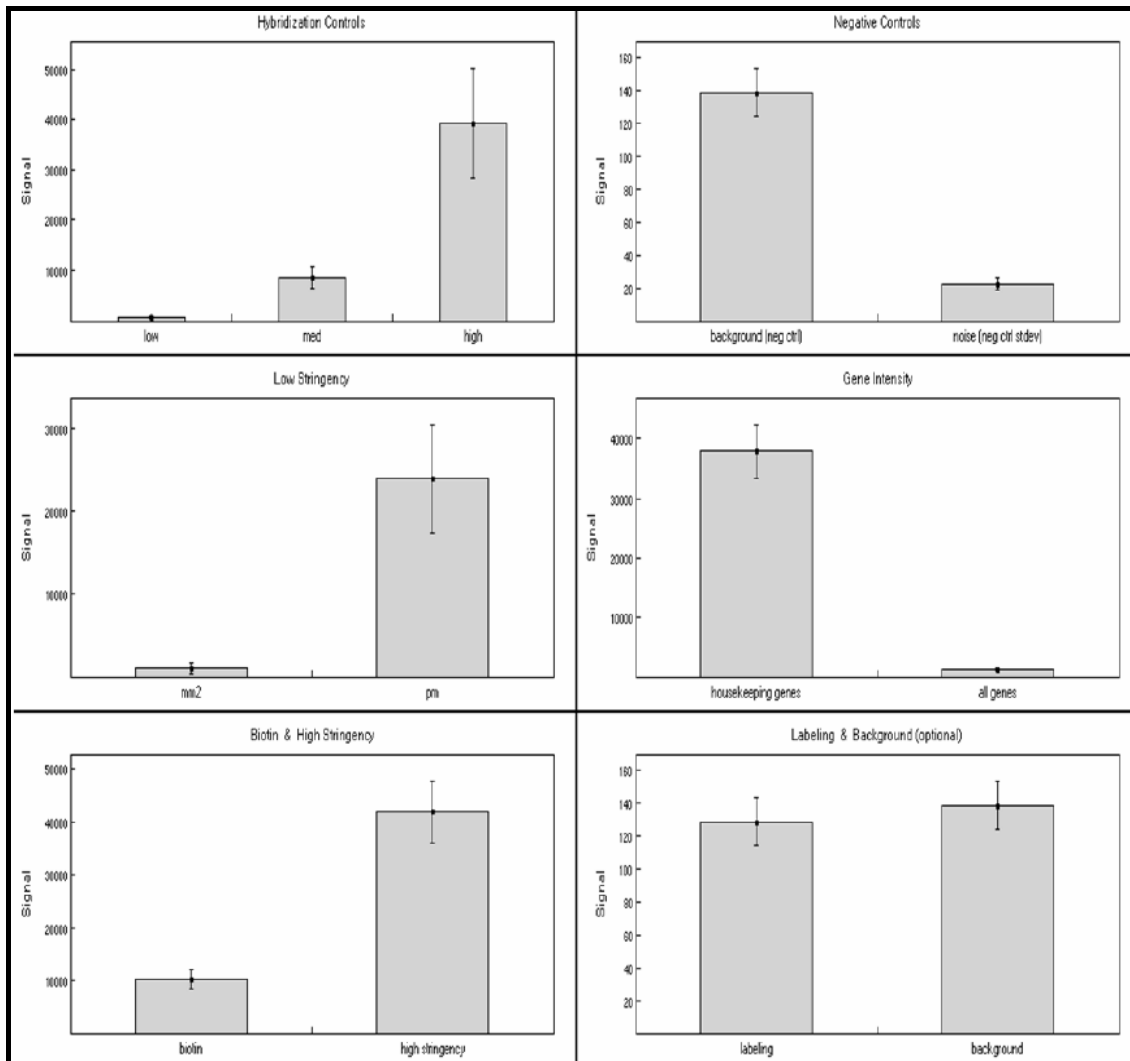


Figure 21: Overview of the hybridization controls for Illumina BeadChips. Mean values for all arrays analyzed are shown together with the standard deviation for low, medium and high abundant controls, a perfect and a mismatch control, a biotin control, the background intensity and the overall intensity for housekeepers and all genes. Together, these controls ensure the high quality of the data used for later analyses.

2.2.5.2 Data extraction and quality control from Affymetrix arrays

For each probe cell on the array, a single value was generated by the GCOS software. Because of the layout with eleven perfect match and eleven mismatch probe-cells per gene, a condensing step was included in the data extraction process, so only a single value per probe set was computed. The overall intensity and the intensity of the spike-in controls were visualized and checked for quality. The created .cel-files were uploaded into and processed with the Expressionist[®]Refiner software from Genedata. Therein, an automated workflow, including several quality controls and a RMA-normalization, was performed (Irizarry et al., 2003). This normalization method uses

only the perfect match data to perform background correction, normalization and expression value estimation. This results in lower variation coefficients and enhances the comparability between experiments (Irizarry et al., 2003).

At the end of each workflow and as a result of the controls, each Array was classified by the software in the quality parameters as either good, medium or bad (Figure 22). Chips classified as good were used in the analysis, chips classified as bad were repeated. The medium classification was checked manually and the decision if the data was used was made on a case-by-case basis.

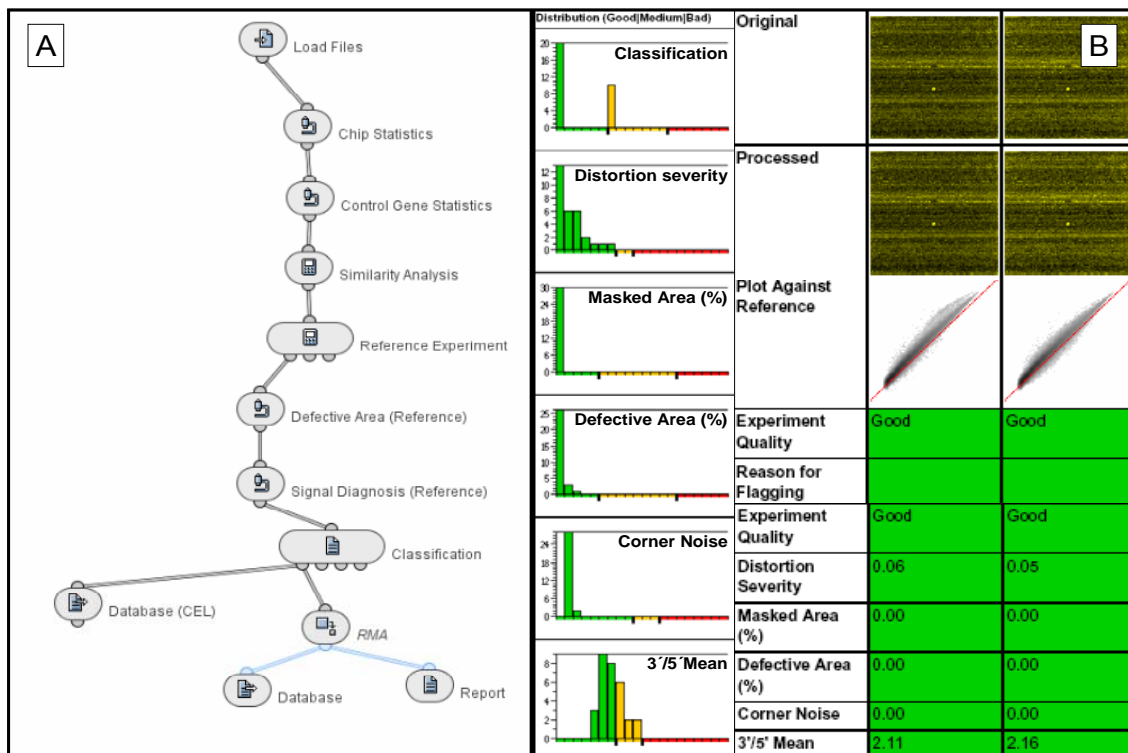


Figure 22: A) Overview of the Refiner workflow including chip statistics, quality controls, classification and RMA-normalization. B) Detail of the result report of a refiner analysis. The classification indicates the overall quality with a colour code; additional details for each Chip are shown on the right side.

2.2.6 Protein separation by SDS polyacrylamide gel electrophoresis (SDS-PAGE)

Isolated proteins and cell lysates were separated by SDS-PAGE. 5-50 µg Protein with a volume of 20-25 µl were mixed with 5 µl LDS sample buffer and 2 µl of reducing agent and heated for 10 min at 70°C. Each sample was transferred into a pocket of a NuPAGE® Novex 4-12% Bis-Tris-gel in an incubation tray assembled in accordance with the manufacturers' recommendations (Invitrogen). The separation was performed

at 200 V and 125 mA per gel for 60 min. 10 μ l Molecular marker were always run in one slot of the gel to allow an estimation of protein size.

2.2.7 Protein detection by western blot analysis and immune detection

Blotting of proteins from polyacrylamide gels to nitrocellulose membranes (0.2 μ m) was performed with the iBlot™ Dry Blotting System (Invitrogen) according to the manufacturers' recommendations. This system enables rapid protein transfers by the use of a shortened distance between electrodes, high field strength and high currents. The ion reservoirs are incorporated into the gel matrix instead of the buffer tanks or soaked papers. Transfer membranes and the copper electrodes (anode and cathode) are included into the iBlot™ Gel Transfer Stacks (Figure 23).

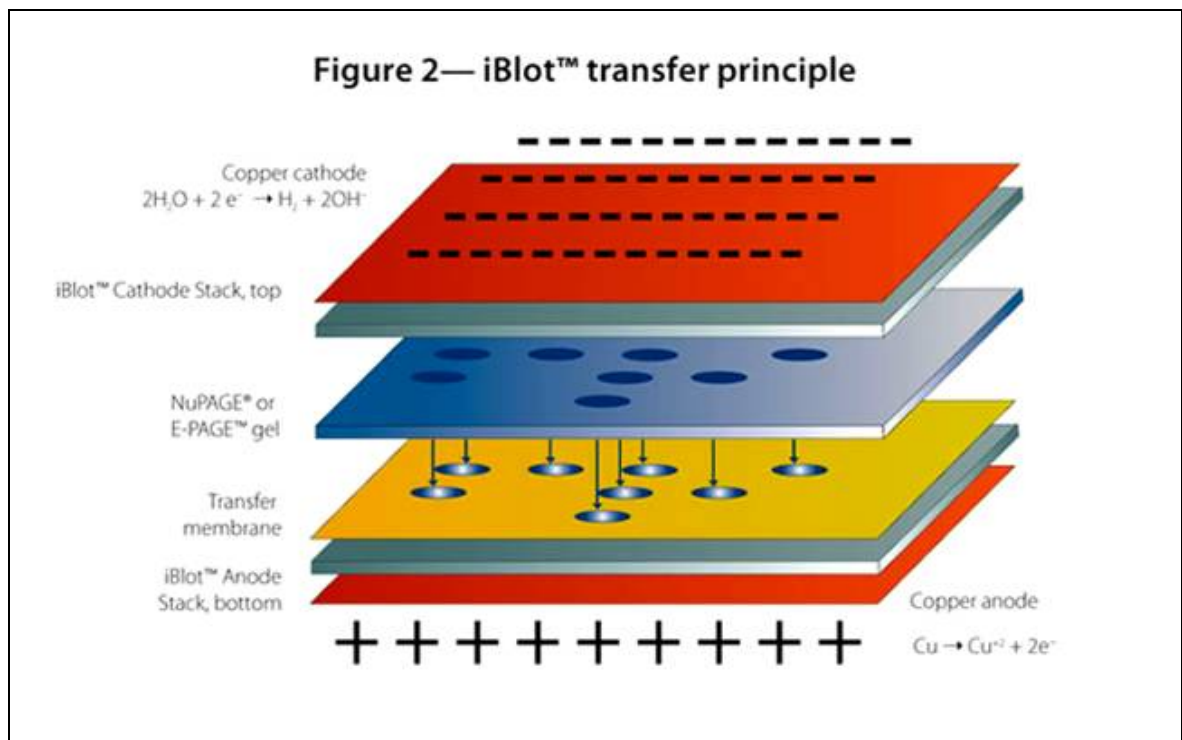


Figure 23: Principle of the iBlot™ Dry Blotting System (taken from the system manual).

Membranes were blocked by incubation with coating solution (5% milk solution in PBS-Tween buffer) for 1 h. The primary antibodies were diluted and incubated together with the membranes as follows:

Antibody	Organism	Provider	Time of incubation	Dilution
Primary antibodies				
Cytochrome P450 3A1	Mouse	abcam	1h	1:3,000
Cytochrome P450 2B1/2	Mouse	abcam	1h	1:3,000
Cytochrome P450 1A1	Rabbit	abcam	1.5h	1:3,000
Secondary antibodies				
Peroxidase conjugated (HRP) anti-rabbit IgG	Sheep	GE Healthcare (#329616)		1:5,000
Peroxidase conjugated (HRP) anti-mouse IgG	Rabbit	GE Healthcare (#328634)		1:5,000

Table 8: Antibodies used for immunodetection.

The membrane was washed with PBS-Tween buffer 3x 10 min, incubated with the adequate secondary antibody, also diluted in PBS-Tween buffer, for another hour and finally washed again as previously mentioned.

The detection was performed with ECL solution which was freshly prepared directly before use according to the manufacturers' recommendations (ECL-Kit, Amersham Biosciences). A chemoluminescent signal is produced by an enzymatic reaction between the secondary antibody-coupled horseradish peroxidase and the reagent which can be used to detect and quantify the specific protein.

The ECL solution was spread out on the membrane and incubated for 1min. The membrane was put into a film cassette together with a detection Film (Hyperfilm ECL, Amersham Biosciences), the time of exposure ranged from 2 min to 5 h. The processing of the films was performed automatically with a Hyper processor (Amersham Biosciences).

2.2.8 SELDI-TOF analysis

SELDI-TOF (Surface-enhanced laser desorption/ionization - time of flight) retains the target proteins on a solid-phase chromatographic surface array, where they are vaporized by ionization using a laser and fly through a "time-of-flight" tube where they separate based on mass and charge (Figure 24). To allow ionization, sinapinic acid was applied to each array. As the solvent evaporates, the proteins co-crystallize with the sinapinic acid. By absorbing the laser energy these crystals raise ionized proteins

which can then be detected. In these experiments cation exchange ProteinChip CM10 arrays were used to bind positively charged proteins, containing for example lysine, arginine or histidine, with weak anionic carboxylate groups.

The chip surface was pre-activated for 10 min with 50 μl pre-activation binding buffer, afterwards 50 to 500 μg isolated protein sample were applied onto the chip surface in 150 μl citrate binding buffer and centrifuged in a special chip processor for 1 h at 270 rpm and RT. The chip surface was washed three times with 300 μl binding buffer for 7 min at 270 rpm to remove unbound proteins. Washing was finalized by incubation with 300 μl H_2O for 1 min and drying for 15 – 20 min. Two times 0.5 μl sinapinic acid, freshly diluted in a 1:1 mix of acetonitrile and TFA [1%] were applied onto the chip surface and allowed to dry.

After drying, chips were placed into the *PBSII ProteinChip Reader* (CIPHERGEN) and measured in the linear mode. The ionisation of the sample was achieved with a N_2 -laser beam at (337 nm) with one warming shot with energy of 2,100 nJ and 10 data shots with 2,000 nJ. The mass range accomplished was 2 to 30 kDa, with a focus mass of 10 kDa. These settings were kept constant across all chips in an experiment. The ProteinChip Reader is directly linked to the *ProteinChip Software* for data analysis. The generated protein profiles were analysed by a multiple comparison of all spectra's. The *Biomarker Wizard*. A software tool allows clustering of the detected mass to charge (m/z) signals for all spectra. Similar m/z signals were matched to a cluster and afterwards relatively quantified. Significant intensity changes of single mass-ion-peaks were detected using non-parametric Mann–Whitney statistical analysis ($p\text{-Value} \leq 0.01$). Signals with a deregulation of more than two fold were accepted as differentially expressed. The visualisation of the differences between different groups was accomplished by plotting the signal intensities against the m/z -values of the clusters.

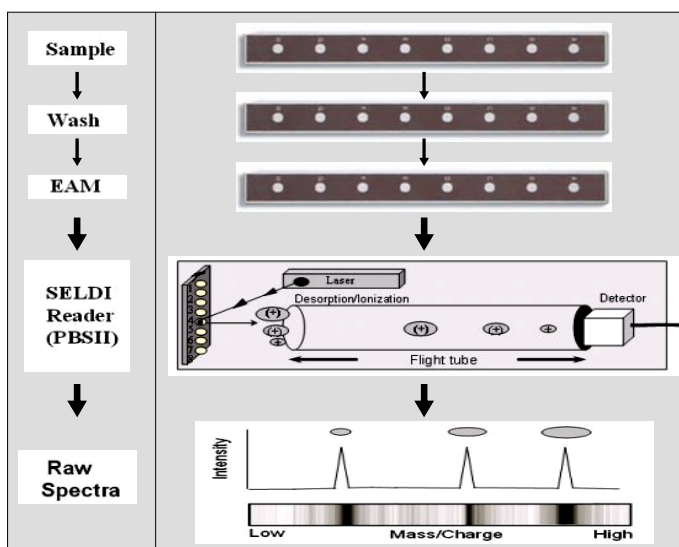


Figure 24: Scheme of the SELDI-workflow.

3 RESULTS AND DISCUSSIONS

3.1 Comparison of different global gene expression platforms

Microarray technology is one of the fastest evolving and most promising fields in molecular biology. Over the last decade, this technology has basically changed the way of addressing biological interrogations and opens new perspectives in monitoring cellular mechanisms and processes on a global level. There are applications in almost every field of biology and medicine and the number is still growing. The analysis of genomic data has become more and more important in modern toxicology and drug development, enabling researchers to identify changes in global gene expression as well as specifically affected pathways. Also the computing power was no longer a limitation, allowing the implementation of larger and more realistic models. The FDA and the EPA (US Environmental Protection Agency) have defined pharmaco- and toxicogenomics as key opportunities to personalized medicine and risk assessment (Dix et al., 2006; Lesko & Woodcock, 2004).

The use of microarrays to obtain insight into cellular processes and to monitor molecular interactions is a well-established method and has enabled scientists to understand cellular mechanisms in extreme detail and complexity. As illustrated in Figure 25, the amount of data in public databases, together with the molecular knowledge has tremendously increased over the last years. In the past, there were no official guidelines for conducting these types of experiments and so, the vast majority were performed without internal controls or accepted standards. The comparison of data within each platform and of results gained with other platforms gave quite conflicting results, showing either agreement (Li, Pankratz & Johnson, 2002; Parrish et al., 2004) or disagreement (Kuo et al., 2006; Mah et al., 2004) between the outcomes. This fact has driven the development of more rigid quality standards and guidelines not only in the manufacturing process but also on the handling and processing of the resulting data. The Implementation of MIAME (Minimal Information About a Microarray Experiment) was the first step towards a common standard. The FDA initiated a comprehensive project to look at microarray quality control and cross-platform comparisons (MAQC). The aim of this study was to learn how to handle existing microarray data in respect to reliability, comparability, repeatability and how the various

sources of variance, like intra- and interplatform and interlaboratory differences, affect the resulting data (Shi et al., 2006).

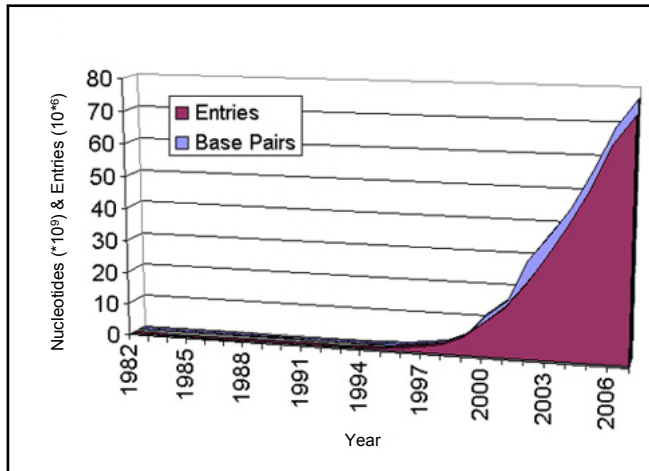


Figure 25: Growth of public gene bank databases. Shown are the number of nucleotides and entries submitted to the Genbank database from 1982 to 2006 (Data courtesy of NCBI).

Several providers have developed diverse variants of this technique and although the basic principle, measuring the amount of transcripts, is elementary, there are various differences in commercially available microarray platforms. Variability can be caused by multiple factors like the type of probes (*in situ* polymerization, spotting, microbeads), the probe selection and design, the number of probes (short/long oligonucleotides, cDNA), different labeling methods or competitive versus non-competitive hybridization. Affymetrix and Illumina both provide platforms allowing one sample to be hybridized per array. Array-to-array variability is minimized by highly standardized manufacturing and hybridization procedures. The degree of variation between replicates is an important issue for the experimental design and the interpretation of the results.

Results of gene expression experiments are often used for the development of large databases. Right now, great efforts are taking place to test the ability of integrating data generated with different types of platforms (Roter, 2005). An important aspect is the understanding of the influence that the technology has on the data itself, data handling and processing and of course the overlap of genes common to these technologies. Therefore, the reliability and accuracy of gene expression measurements are a quality attribute and an elementary requirement.

With this study, we wanted to investigate the comparability of a new global rat gene expression platform provided by Illumina Inc. with the well-established and accepted technique provided by Affymetrix. We therefore analyzed data generated from samples simultaneous on Illumina RatRef-12 Expression BeadChips (Illumina) and the Affymetrix Gene Chip[®] Rat Genome 230 2.0 Arrays.

The study comprised two sets of samples to elucidate the technical and biological differences/similarities. A titration series with RNA extracted from control liver and

kidney was generated for the more technically based comparison to test the linearity and the detection sensitivity of both platforms. Additionally, we investigated liver samples from rats treated with the model compound tetracycline as well as primary rat hepatocytes treated with tetracycline hydrochloride (both will be called Tet in the following to simplify reading). This setup enabled not only the direct comparison of results of both platforms but also to compare the changes in gene expression *in vivo* with the reaction of the hepatocytes cultured *in vitro*.

Our study design gave us the option to analyze the comparability of both platforms by means of technical concordance but also on the level of the biological interpretation of the data. The evaluation of intra-laboratory variation is important for future experimental design as are the number of replicates (biological and technical) needed. Additionally, by comparing *in vivo* and *in vitro* data, we gained deeper insights into the compound-specific mechanism of action and the possibility to mimic these effects *in vitro*.

The key questions of this study were:

- 1) Do we find a high concordance in the results of both platforms and if not, to what extent do they vary?
- 2) Is the biological interpretation of the data nevertheless the same?
- 3) Are both types of gene expression platforms equally qualified to measure samples with such a variety of origins?

Tet is an antibiotic that is produced by streptomycetes in nature. It inhibits bacterial growth by reversibly binding to the 16S subunit of the bacterial ribosome, inhibiting the binding of amino-acyl-tRNA to the ribosomal A site and thereby translation. In higher doses, this effect has been proven to take place in mammalian cells (McKee et al., 2006). In addition, Tet and its derivatives exert anti-inflammatory and immunomodulatory effects that are completely separate from its antimicrobial action (Gabler & Creamer, 1991). A toxic side effect of Tet is the causing of microvesicular steatosis in the liver, which occurs dose dependent through inhibition of mitochondrial β -oxidation of fatty acids and cholesterol biosynthesis (Fréneaux et al., 1988). Hepatic microvesicular steatosis can have severe consequences in some people (Westphal, Vetter & Brogard, 1994). Known molecular mechanisms include the inhibition of mitochondrial β -oxidation and peroxisome proliferator receptors (PPARs), and, in high doses, protein synthesis. Other genes affected play roles in cell proliferation, nucleoside metabolism and signal transduction. Additionally, Tet inhibits the induction of IL-1-converting enzyme and reduces cyclooxygenase-2 expression and prostaglandin E₂ production. Also the Poly(ADP-ribose) polymerase-1 (PARP-1), which promotes both cell death and

inflammation when activated by DNA damage, is inhibited (Yin et al., 2006). The clear dose and time dependent mode of action enables us to examine if the same biological interpretations following Tet treatment can be inferred from different platforms.

3.1.1 Results of the platform comparison study

3.1.1.1 Experimental layout

Technical comparison (Figure 26A)

RNA was isolated from a male Wistar rat and the titration series was performed with dilution steps of initially 10% and for the later steps 20% resulting in 7 samples, ranging from pure liver to pure kidney RNA (100%:0%, 90%:10%, 70%:30%, 50%:50%, 30%:70%, 10%:90%, 0%:100%; Liver:Kidney). Each sample was hybridized in technical triplicates on both platforms. The combination of biological differences in gene expression and the known inverse titration of both organs allow the assessment of the relative accuracy of each platform based on differentially detected genes and dilution effects.

Biological comparison (Figure 26B)

Liver samples from rats treated with low (50 mg/kg) or high (150 mg/kg) doses of Tet or a vehicle control were taken 6 h; 1 d or 3 d after treatment. RNA extraction was conducted as already described (see chapter 2 for details).

To obtain the *in vitro* samples, livers of male Wistar rats were perfused, primary hepatocytes isolated and cultured in SW format. Cells were treated with either vehicle control (0.5% DMSO) or Tet (low dose 40 μ M or high dose 200 μ M) twice, 72 h and 120 h after seeding. Cells were collected 6 h, 24 h and 72 h after the initial treatment. All samples were split, labelled according to the manufacturers' manuals and hybridized to either the Illumina RatRef-12 array or the Affymetrix Rat Genome 230 v2.0 array.

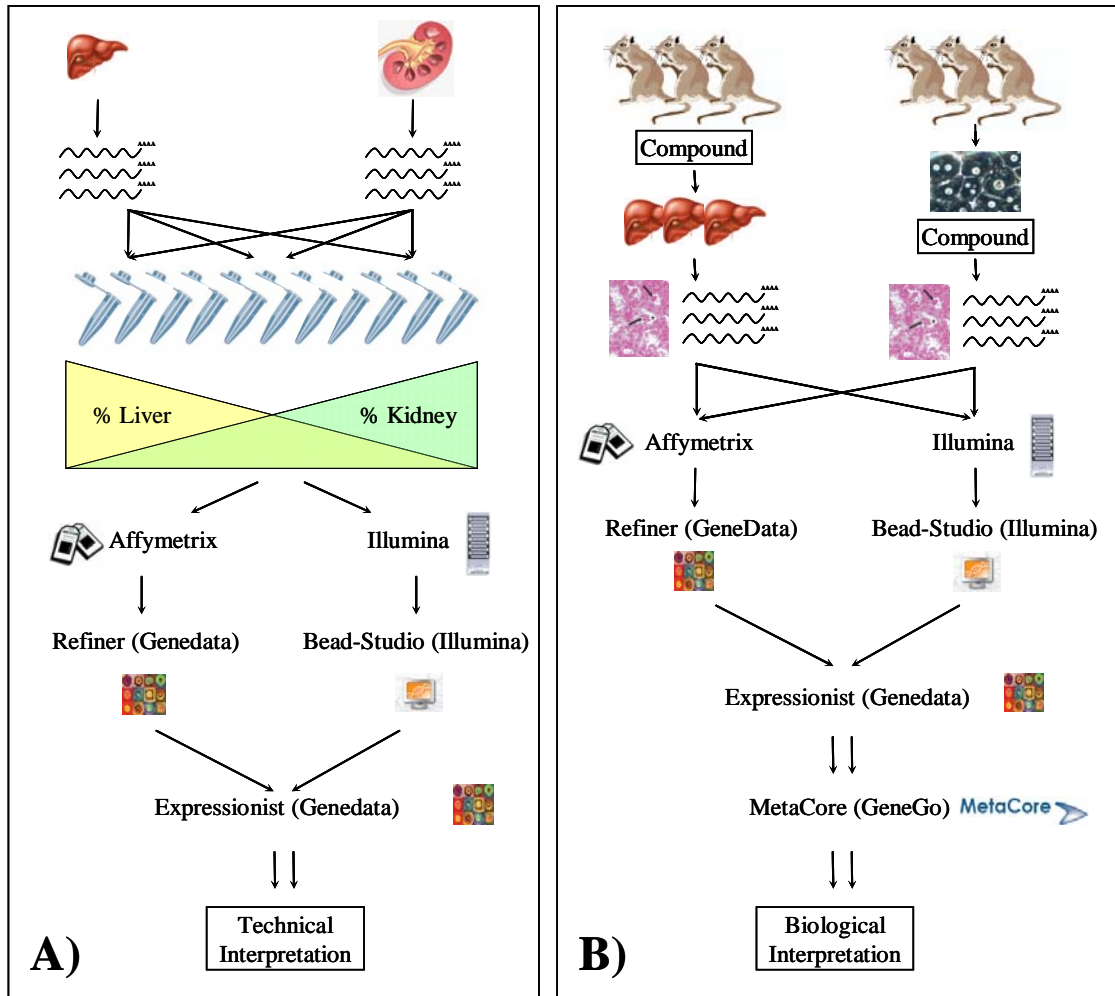


Figure 26: Experimental layouts of the studies conducted for comparing Affymetrix and Illumina global gene expression platforms. A) Technical comparison, a titration series between total RNA isolated from liver and kidney (100%:0%, 90%:10%, 70%:30%, 50%:50%, 30%:70%, 10%:90%, 0%:100%; liver:kidney). B) Biological comparison, an in vivo and an in vitro toxicogenomics studies were compared. Three biological replicates of either animals or hepatocytes in SW culture were treated with Tet at two doses.

Data extraction and probe mapping

Affymetrix data was extracted by the GCOS-Software, normalized with the RMA method and checked for quality parameters within the Expressionist®- Refiner software. Illumina data was processed and checked for quality in BeadStudio (Illumina). Data was imported into separate sessions of Expressionist®Analyst (Genedata), Illumina data was normalized with the LOESS-method, and both datasets were analysed in an analogous manner.

Because of their differences in probe design and the fact that they are based on different versions of sequence databases, it is necessary to map the probe sequences

contained on both chips to a common database version. This step was required because gene identifiers can change between different versions of the database due to new knowledge about specific genes or splice variants. There is a need to assure the identifiers of both platforms to characterize the same gene. Therefore, probe sequences from each platform were mapped to transcript sequences from RefSeq Release 19 (downloaded from ftp://ftp.ncbi.nih.gov/refseq/R_norvegicus/mRNA_Prot). A probe was defined as valid if it perfectly matched a transcript sequence and did not perfectly match any other transcript sequence with a different gene symbol. For Affymetrix probe sets, individual probes were determined to be valid by applying the definition above. Then probe sets were defined as valid if at least 80% of the probes within the set were valid. This procedure resulted in a gene list of 7,271 valid probes common on both platforms which was used in subsequent studies.

3.1.1.2 Intraplatform comparability

Due to technical differences the data produced by Illumina and Affymetrix contrast strongly in their intensity values. Therefore, the intraplatform comparability was examined by comparing the coefficients of variance (CV). The CV was used instead of the standard deviation because it is a dimensionless number and independent from the mean. CVs were calculated for each of the 7,271 valid genes using the 3 technical replicates for all samples of the titration series as well as the 3 biological replicates of the toxicogenomic dataset. The distribution of the replicate CV values of both platforms is shown as a series of box plots in Figure 27. The technical variance is directly compared to the biological variance arising from the individual differences of the animals used.

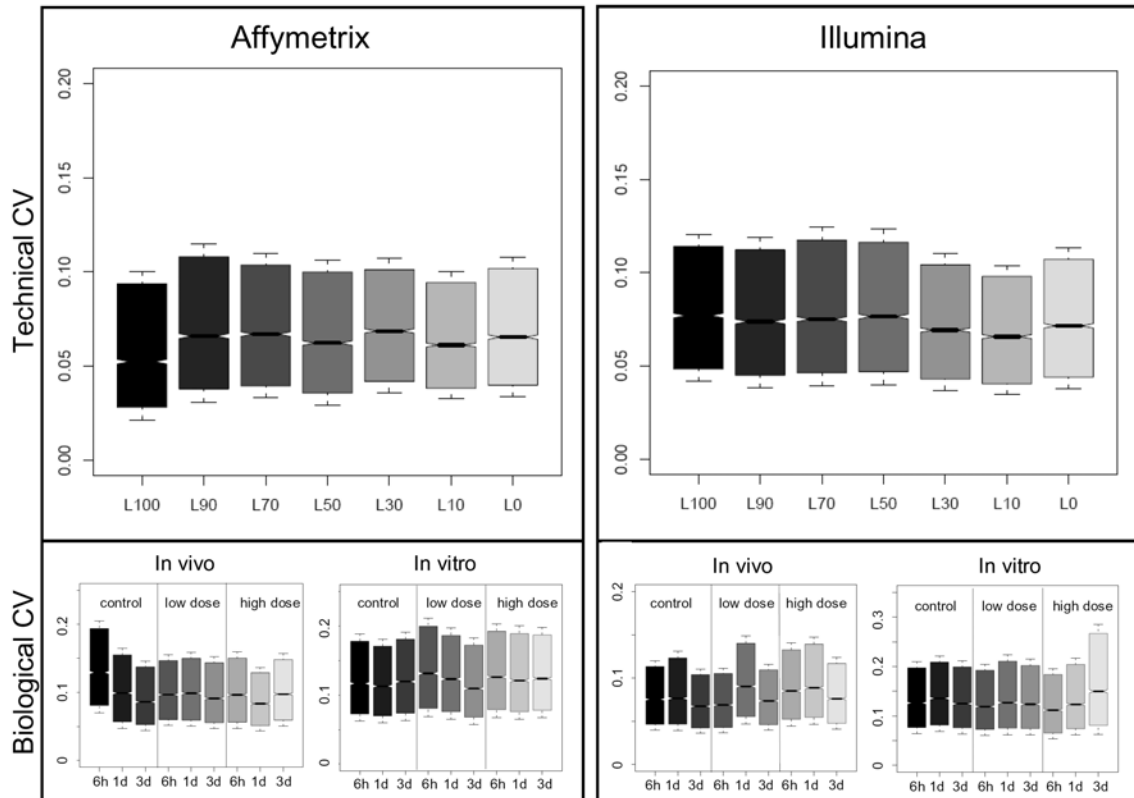


Figure 27: Box plots showing the distribution of the coefficients of variance (CV) for the 7,271 identically detected genes for the technical and biological replicates. The constriction of the bars denotes the median CV, the bars themselves include 50% of all CV values and the whiskers an additional 10%. The x-axis indicates the samples, the amount of liver RNA in the titration sample (L100 to L0) for the technical comparison and the time points of control, low and high dose for the biological comparison.

The median value of the technical variance for three replicates demonstrated analogous rates for both platforms. For Illumina, the CV was, with 7.3%, slightly higher than for Affymetrix (6.3%). The distribution of the CV values was also comparable and showed an asymmetrical shape. Thereby, the nature of the sample (Liver or Kidney) seems to have no effect on the result.

The median value for the biological variance ranged from 6.7% to 13.6%. For the *in vitro* samples measured with Illumina, it was only slightly higher than the median of the technical variance (7.8%). In contrast to this, the distribution of the CV values per gene was broader. Although the median of CV values is higher for *in vivo* samples measured with Affymetrix (9.8%), their distribution is in the same range as for Illumina. The *in vitro* samples showed slightly, but not significantly, increased median CV values compared with the *in vivo* samples for both platforms (12.1% for Affymetrix and 12.7% for Illumina). The Isolation of hepatocytes and the time of incubation seem to be an

additional factor that introduces variability into the gene expression data, although it is still within acceptable limits.

These findings correlate well with the results of the MAQC consortium (Shi et al., 2006; Klebanov & Yakovlev, 2007), where 5% to 15% of variance was reported for different global gene expression platforms (Affymetrix and Illumina were both below 10%).

Several reasons are responsible for these differences in the signal detection. Affymetrix and Illumina have fundamental differences in probe design and number of probes. Whereas Affymetrix uses a set of eleven 25mer oligonucleotides probes with perfect match and mismatch controls, Illumina instead uses 50mer oligonucleotides as probes in 30-fold redundancy. Sequence variations in the probe sets that target the same gene at different locations, the GC content, sequence length, intraplatform cross-match opportunities and the location of the probe sequence in relation to the 3'-end of the target gene might additionally cause different strengths of binding and therefore contribute to different levels of signal intensity. It has been shown that probes with complete sequence matches yield concordant results across platforms. There is a direct correlation between probe sequences and signal intensities for probes that target the same gene on different platforms (Pusztai, 2006).

3.1.1.3 Interplatform comparability

The interplatform comparison could only be performed indirectly. Due to their differences in probe sequences, labeling and hybridizing techniques, the resulting intensity values are fundamentally different. To overcome this problem, relative expression values between the titration samples and the 100% liver sample were calculated and compared. The relative expression values from the 7,271 commonly detected were collectively imported into Expressionist[®]Analyst and analyzed for common changes. Genes which had a more than 2-fold expression difference between liver and kidney samples and a pValue lower than 0.05 (ANOVA) were grouped according to their profile over the titration series with the help of SOM clustering (see chapter 2.2.5).

Six groups of genes were identified by SOM clustering (Figure 28). Groups E and F showed genes with a medium level expression in both tissues and a rising or falling expression profile with each dilution step and a close to linear slope in both platforms. Groups A and B were similar but showed higher expressed genes reaching the saturation of intensity measurement. This results in a nonlinear increase of intensity.

A subset of genes, contained in groups C and D, had showed no correlated or contradicting expression between both platforms. The intensity values of many (but not all) of those genes were close to the background level. Small variations in intensity

therefore result in large fold change values and no clear concentration dependency can be detected.

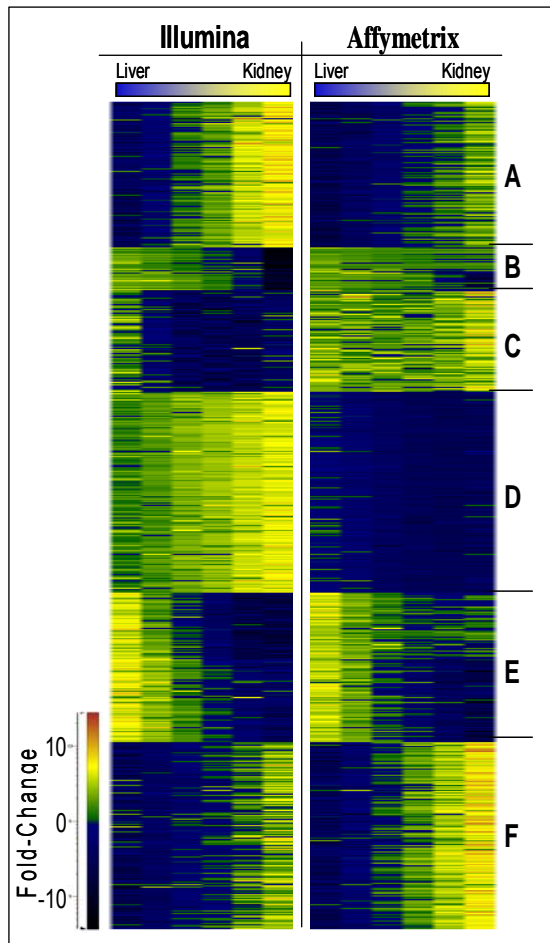


Figure 28: HeatMap generated by SOM-clustering of genes according to their fold change profile relative to the liver. The 7,271 commonly detected genes were filtered by a fold change ≥ 2 and a pValue of ≤ 0.05 between liver and kidney samples to retain only genes with a linear dependency. Clusters A, B, E and F contain genes shown to have equal tendencies across both Platforms, clusters C and D are a subset of genes with either no clear or contradictory tendency between both platforms.

The histogram shown in Figure 29 depicts the distribution of CVs of the titration experiment for both platforms. The value 1 indicates a perfect correlation and that the intensity values of the genes demonstrated the same behavior in the samples measured, -1 resembles negative correlation which means an inverse behavior. For Affymetrix, about 75% of the genes have a correlation of 1 to 0.9 and -1 to -0.9, for Illumina this value is 69%. The genes in between have lower linear dependency to the titration samples.

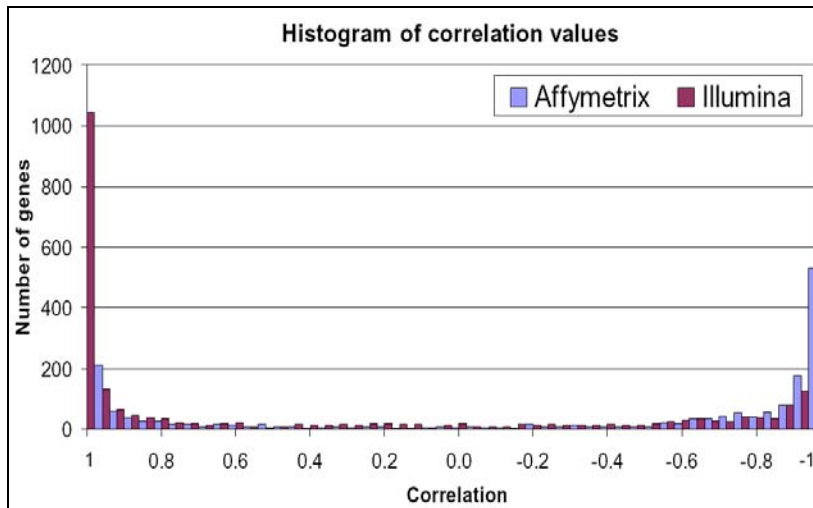


Figure 29: Histogram of the correlation coefficients of genes to the titration curve. The number of genes, found to have a more than 2 fold different expression levels in both tissues was plotted against their correlation values.

To further explore and validate these findings, the rat Tet toxicogenomics dataset was analyzed. Fold change values and pValues of this dataset were calculated for both platforms and each dose, time point and experiment type (*in vivo* or *in vitro*) relative to the time matched vehicle controls. The resulting gene lists were ranked either by the pValue (Figure 30A) or by the fold change (Figure 30B). The comparability between the gene lists was quantified using the “OrderedList” functionality of the Bioconductor R software (Lottaz et al., 2006).

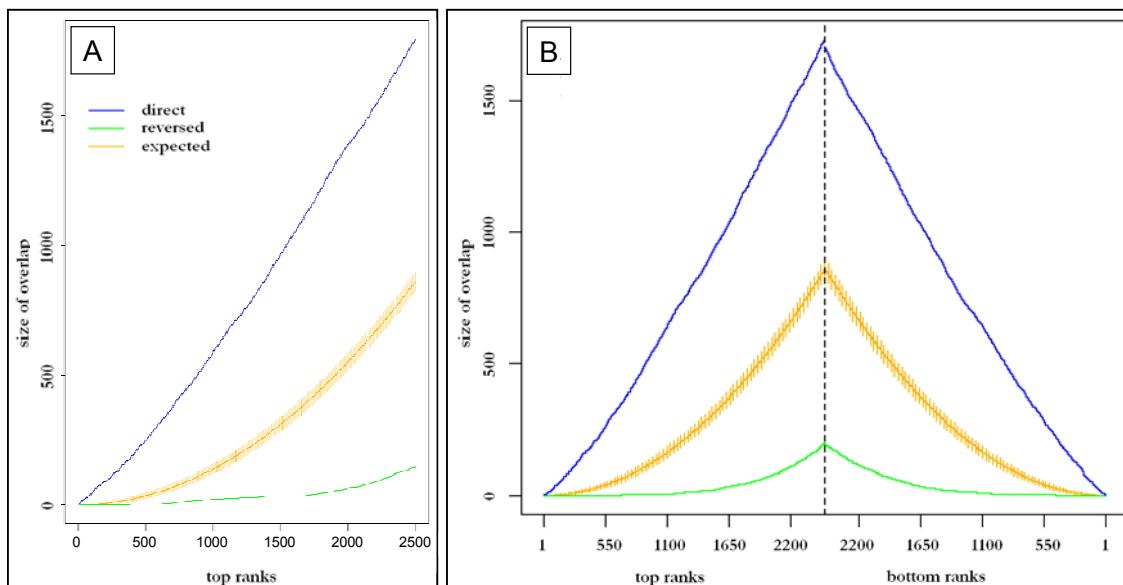


Figure 30: Gene list comparison (example shown for the *in vitro* experiment, high dose, 24 h). Genes have been ranked according to the p-Value (A) and to the extent of the fold change (B). The size of overlap of the top 500, 1000, 1500 etc. (labeling of the axis) genes of these lists were computed and compared to an overlap expected just by chance (orange line) and to the result obtained by reversing one of the two lists (green line).

Ranked gene lists were searched from the top (pValue ranked lists) or from both sides simultaneously (fold change ranked lists) for commonly occurring genes. The background of genes overlapping just by chance was calculated by comparing randomly perturbed gene lists 1,000 times. The negative control was obtained by inverting one of the two gene lists and comparing the top of one list with the bottom of the other.

The p-Values for the possibility to derive the obtained results just by chance were calculated (Appendix 2 and Appendix 13). The results show that the lists of top-ranked genes are highly saturated with genes detected by both platforms. Differences in the score indicating the overlap between the gene lists were detected and are plotted in Figure 31. The degree of overlap is strongly influenced by the nature of the samples. Gene lists of samples treated with low doses of Tet generally showed a lower analogy than others treated with high doses. In addition, time effects were seen *in vivo* and *in vitro*. The overlap of gene lists from both platforms is small 72 h after dosing compared to earlier time points. This can be explained by time dependent effects of Tet. The differences in scores between high and low doses of Tet *in vivo* or *in vitro* generally showed the same trend.

The highest overlap between the platforms for lists of genes was detected *in vivo* 6 h and *in vivo* and *in vitro* 24 h after high dose treatment. These are exactly the time points where the highest effect of the treatment was expected and are therefore best suited to analyze the effect of the compound on gene expression. Initial changes (6 h after dosing) leading to a high gene list overlap might be due to acute inflammatory effects. This would explain the discrepancy between *vivo* and *in vitro*. The latter is missing non parenchymal liver cell types, e.g. Kupffer cells, which are important for the induction and maintenance of inflammatory mechanisms.

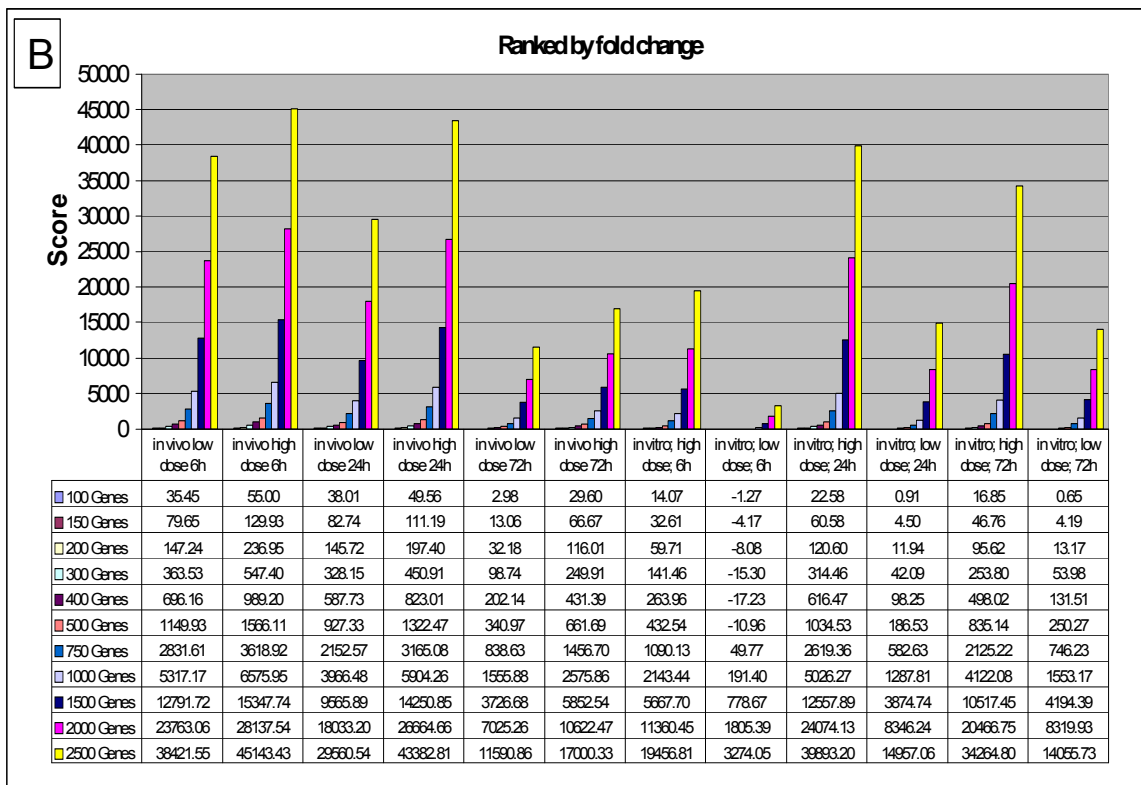
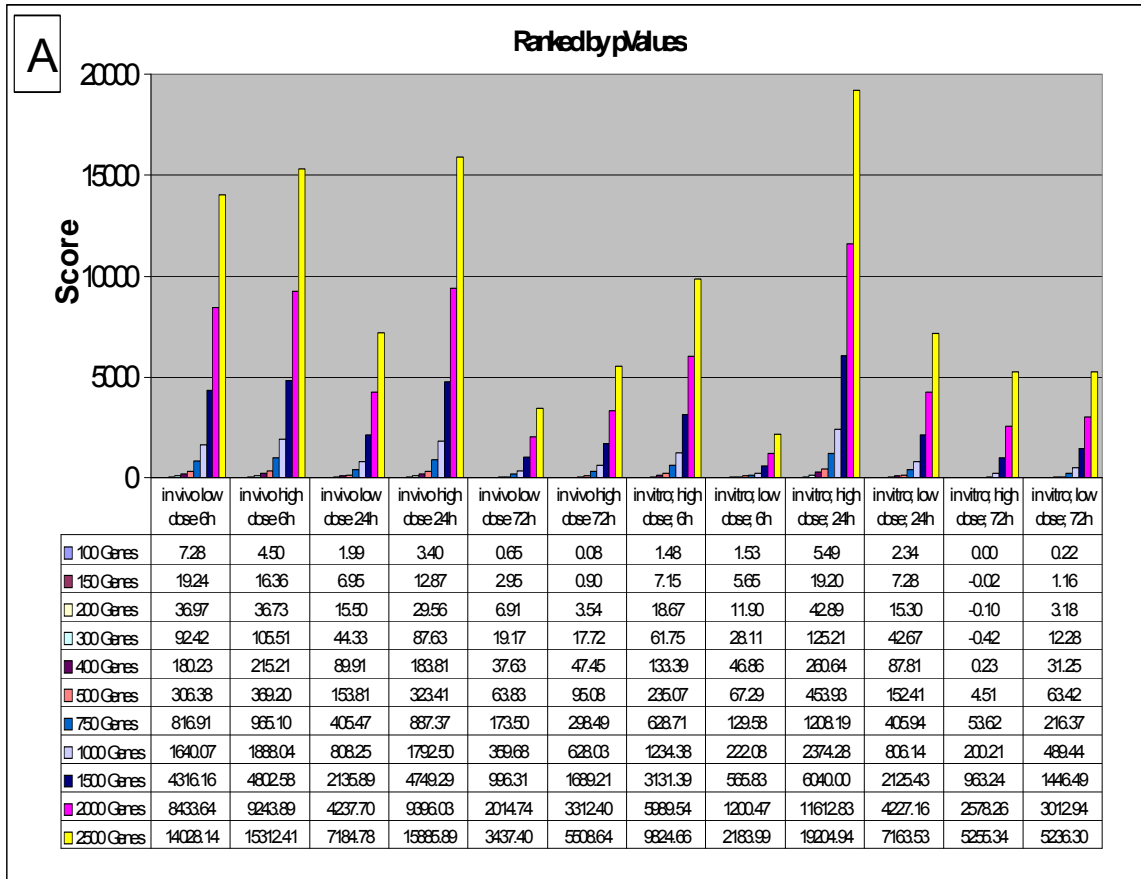


Figure 31: The difference of the scores calculated by the gene list overlap and the negative control were plotted for all the experiments. Scores were computed on the basis on the number of overlapping genes and reflect in principle a weighted sum of these values. A) Genes have been ranked by pValue; B) Genes have been ranked by fold change

These results were confirmed by a correlation analysis (Figure 32). Both platforms showed a high concordance, with high correlation coefficients, between each other. There were only minor differences in the correlation coefficients compared to the vehicle control for the 72 h time point and the 24 h time point (low dose). Significantly lower correlation coefficients were detected 6 h after treatment for both doses and 24 h after treatment with the high dose.

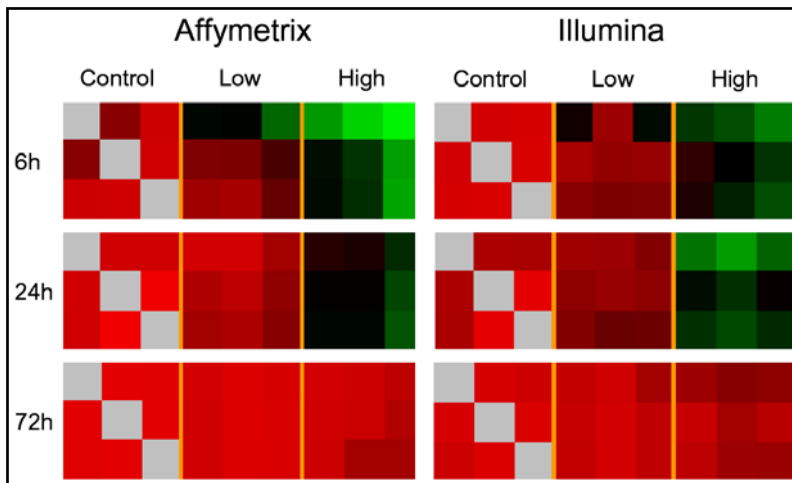


Figure 32: Correlation map of *in vivo* samples of tetracycline treated cells. Each square resembles one experiment; red is positive correlation, green represents a negative correlation.

Genes found to be changed in expression after treatment with Tet *in vivo* and *in vitro* (≥ 2 -fold, $pV \leq 0.05$) were common within both platforms. Lowering the fold change value to 1.5 lowered the platform concordance to 88.2%. In most cases not only the direction but also the extent of deregulations was very analogous between both platforms.

These results show that the variance across technical replicates is in a satisfactory range and even the individual differences of biological replicates caused only a slight increase. Conducting biological replicates instead of technical replicates helps to increase the statistical significance and therefore the match between the results of Illumina and Affymetrix.

3.1.1.4 Biological interpretation

Whereas the histopathological analysis of the *in vivo* samples showed no abnormality (data not shown, see Zidek et al., 2007, the morphological analysis of Tet treated primary rat hepatocytes showed a clear accumulation of lipid droplets over time (Figure 33) Cells treated with high doses of Tet were more affected and showed additional signs of cellular damage. This proved that the mechanisms leading to microvesicular steatosis *in vivo* are also present *in vitro* and that the sandwich culture model therefore is a qualified tool to analyze the mechanistic basis of the toxic effects of Tet.

The effect of treatment on gene expression can largely be seen 6 h after dosing *in vivo* and 24 h after dosing *in vivo* and *in vitro*. Whereas the effects endure *in vitro*, a recovery of the animals can be seen *in vivo*. Further analyses were accomplished within the Expressionist® Analyst software from Genedata and the biological interpretation was supported with MetaCore™ pathway analysis tools from GeneGo.

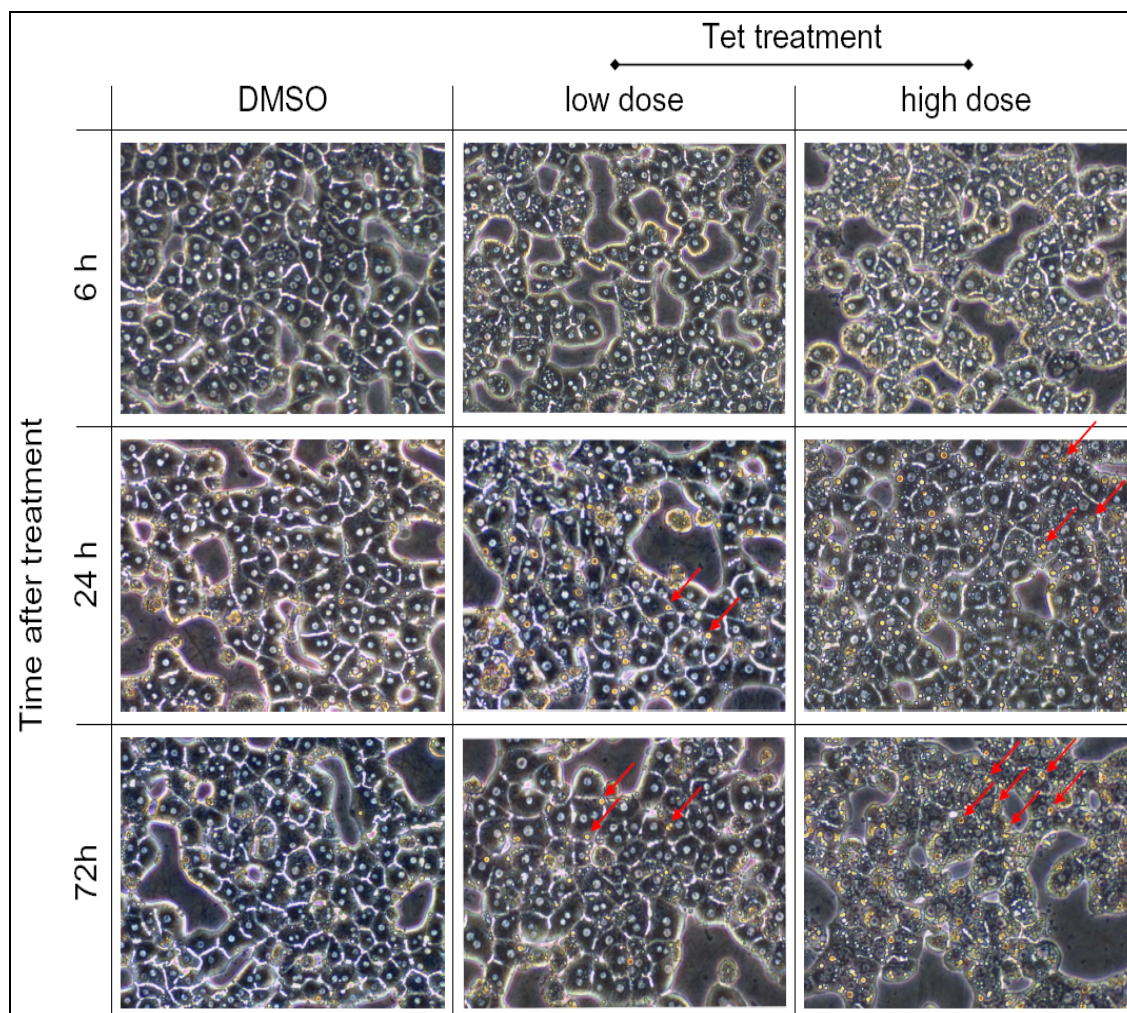


Figure 33: Primary rat hepatocytes treated with either DMSO (vehicle control) or low and high doses of Tet for 6/24/72 h. Cells were pre-cultured in sandwich culture for two days to acclimatise to the culture conditions and subsequently dosed with either 40 μ M or 200 μ M Tet. Both doses caused an accumulation of lipid droplets inside the cells and this effect was more pronounced in the high dose (See red arrows).

Figure 34 shows a PCA which separated samples from both platforms of the *in vivo* (A and B) and *in vitro* (C and D) experiments. The PCA analysis shows the basic tendencies within the data, which resembles the biological effects of treatment.

The time and dose dependent effects were observed *in vivo* and *in vitro*. Vehicle controls, low dose treatment groups 24 h and 72 h after treatment and high dose group

72 h after treatment clustered closely together *in vivo*. Two separate clouds, one containing both dosing groups 6 h after treatment and the other with the high dose experiments 24 h after treatment, indicate a change in gene expression in these animals. Whereas both treatment groups caused similar gene expression changes after 6 h the gene expression of the low dose animals returned to the control level after 24 h. The high dose group after 24 h separated from all groups indicating more severe effects. After 72 h even high dose animals appeared to have returned to normal animal gene expression levels. This can be explained with the single dose treatment of the animals and the reversible effect of Tet.

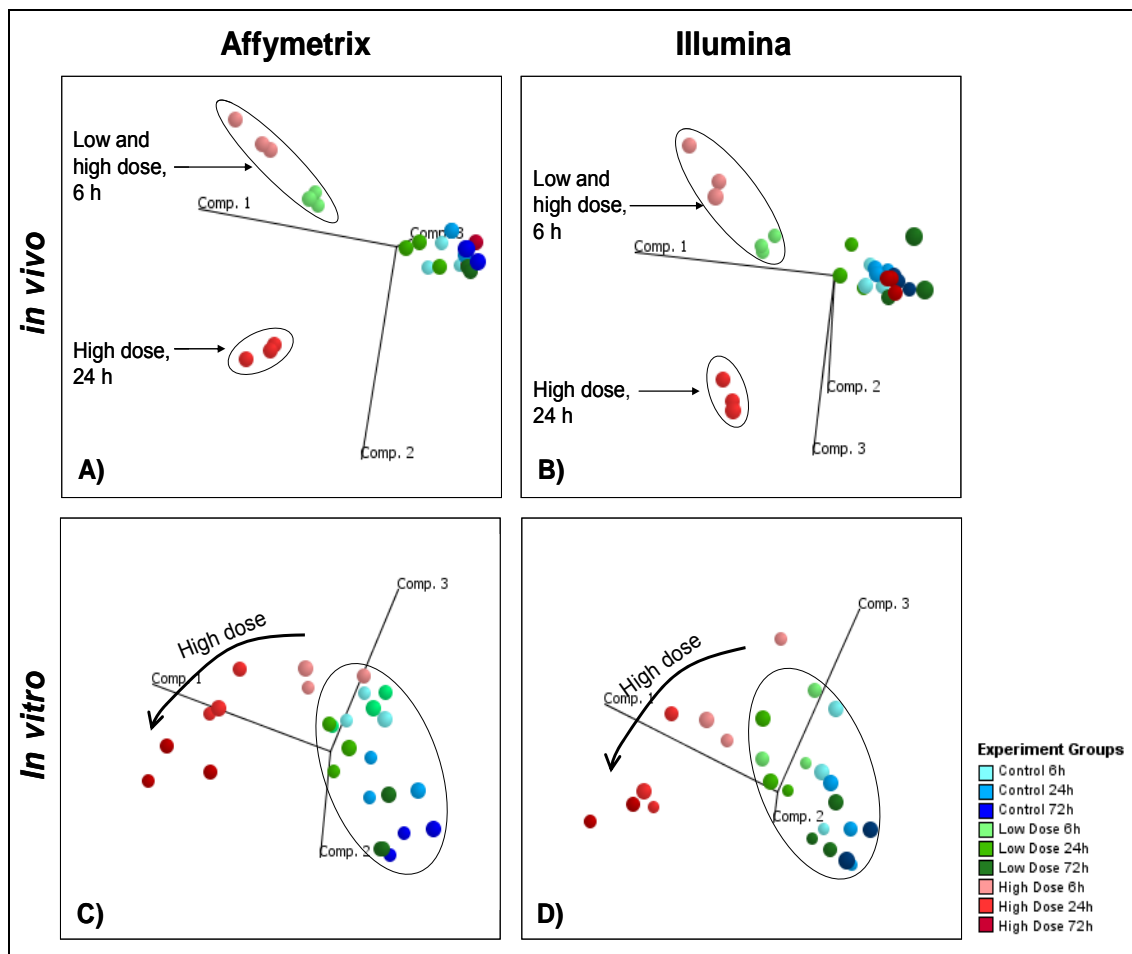


Figure 34: Principal components analysis (PCA) of the same datasets measured with Affymetrix Rat Genome 230 2.0 Array (A and C) and Illumina RatRef-12 Expression BeadChip arrays (B and D). Each point resembles the principal expression characteristics of all 7,271 common genes. The Tet *in vivo* study shows a clear separation of the experiments from the control group for both doses after 6 h and the high dose 24 h after treatment. *In vitro*, the separation is less clear after 6 h but high doses also separate at later time points.

In vitro (Figure 34 C and D) experiments showed related, but not identical, results to the *in vivo* samples. Due to the study design, where hepatocytes were dosed a second time 48 h after the first treatment, no regeneration effects were seen at 72 h. In fact, at 72 h even stronger effects were observed, indicating an increasing degeneration of these hepatocytes. The low dose experiments were not clearly separated from the controls, although they showed a tendency into the direction of the high dose experiments, indicating only a weak response to treatment.

The data from both *in vivo* and *in vitro* experiments are consistent across both platforms, which showed a high concordance of the 7,271 common genes. The high similarity between the PCAs show that not only the basal level but also any changes in gene expression after treatment were detected reliably by both Affymetrix and Illumina. The extent of these changes can be explained by the expected toxicity of Tet. The initial treatment caused an acute immune response in the animals, which was over in the low dose animals by 24 h. *In vitro*, the initial effects were less pronounced but subsequently, analogous tendencies were observed.

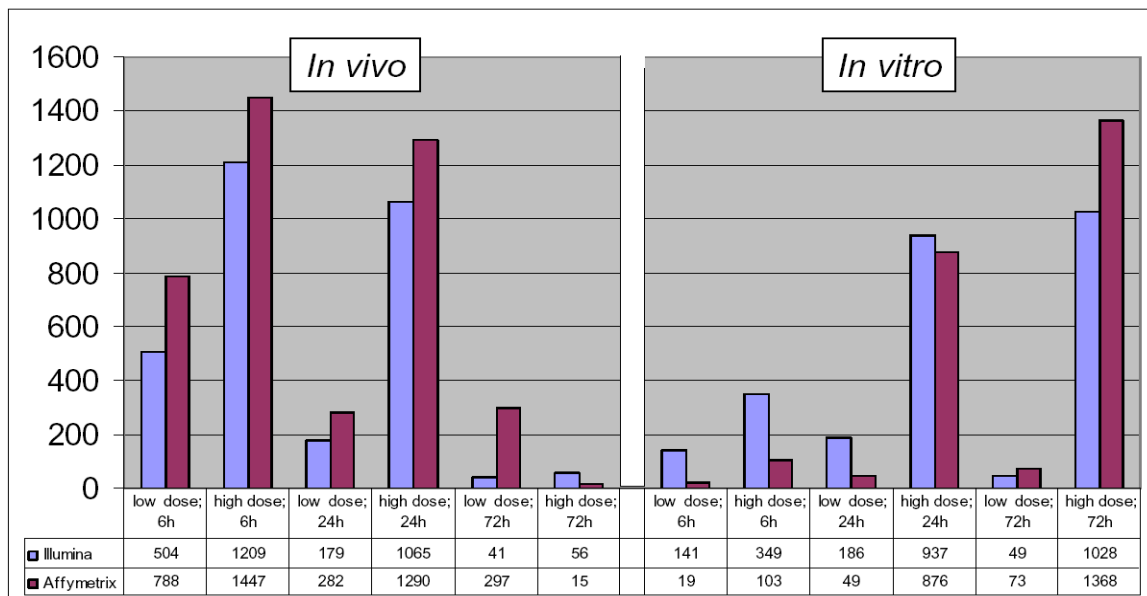


Figure 35: Number of genes significantly deregulated by treatment with Tet in either *in vivo* or *in vitro* experiments

The findings of the previous analysis were reflected by the number of genes deregulated after treatment (Figure 35). *In vivo*, already 6 h after treatment a substantial number of genes were deregulated and the high dose had a greater impact than the low dose. 24 h After treatment, the high dose still showed strong deregulations *in vivo* whereas the low dose showed only minor alterations. After 72 h only slight disturbances in gene expression were observed.

The number of significantly deregulated genes *in vitro* rose only in the cells treated with high dose Tet over time. Cells treated with low doses were not noticeably affected. The early time point showed no substantial deregulation, indicating technical differences between *in vivo* and *in vitro* mechanisms. 24 h After the initial treatment, the number of genes deregulated rose to 937 (Illumina) and 876 (Affymetrix) and after 72 h a maximum of 1028/1368 deregulated genes was reached.

To get insights into the molecular mechanisms of Tet activity, the significantly deregulated genes (fold change > 1.5 and pValue < 0.05), measured with Affymetrix and Illumina, were analyzed using the MetaCore™ pathway analysis tool (GeneGo). To account for time as well as dose dependency, two different time points, 6 h and 24 h, and both doses were analyzed for the *in vitro* samples and 24 h and 72 h time points were analyzed for the *in vivo* experiments. Results were examined for biological affects and both platforms compared

Gene expression changes caused by Tet treatment were involved in a variety of cellular processes (Table 9). The most affected pathways were associated with lipid metabolism followed by genes involved in signal transduction and cation homeostasis, inflammation, nucleotide and nucleic acid metabolism, protein and amino acid metabolism and cell cycle.

Down regulated		Up regulated	
GeneGo „maps“	GO processes	GeneGo „maps“	GO processes
Cholesterol Biosynthesis	Lipid metabolic process	PDGF signalling via STATs and NF-kB	Nucleotide and nucleic acid metabolic process
Regulation of lipid metabolism via LXR, NF- γ and SREBP	Cellular lipid metabolic process	Histamine H1 receptor signalling in immune response	RNA metabolic process
Regulation of fatty acid synthase activity in hepatocytes	Positive regulation of chondrocyte differentiation	Immune response_IL1 signalling pathway	Biopolymer metabolic process
Triacylglycerol metabolism	Organic acid metabolic process	TPO signalling via JAK-STAT pathway	Primary metabolic process
Role of CDK5 in cell adhesion	Alcohol metabolic process	MIF-mediated glucocorticoid regulation	Macromolecule metabolic process
Glycolysis and gluconeogenesis	Steroid metabolic process	Apoptosis and survival_TNFR1 signalling pathway	Regulation of cellular metabolic process
Unsaturated fatty acid biosynthesis	Carboxylic acid metabolic process	Leptin signalling via intracellular cascades	Cellular metabolic process

Table 9: Top 7 “maps” and GO processes significantly affected 6 h after treatment *in vivo* (here only the results from Affymetrix are shown, Illumina generally delivered resembling results). Thresholds: Fold change \geq 1.5; P-value \geq 0.05.

Whereas no severe morphological effects could be detected 6 h after treatment, more than 500 genes were significantly deregulated more than 1.5-fold. Listed in Table 9 are the top seven up and down regulated pathway maps and GO processes. Already at this early stage, cholesterol, lipid and energy metabolism were inhibited by high dose treatment of Tet. At the same time, inflammatory processes, such as the JAK/STAT signalling, the immune response and the metabolism of nucleic acids were activated. Altogether, this suggests early perturbations may lead to the accumulation of fatty acids and triglycerides in the cell and to a loss of energy production. Early responses to cellular stress combined with an up regulation of nucleotide, RNA and protein synthetic process was also observed. The latter might be a compensatory process due to the inhibition of protein synthesis by high doses of Tet on the level of translation. The fact that the inflammatory response is mainly mediated by hepatic macrophages, the Kupffer cells, explains the lack of an early inflammatory response *in vitro*.

24 h After treatment, Tet caused concordant changes in gene expression *in vivo* and *in vitro*. Table 10 shows the top ranked commonly affected maps and GO processes for both conditions. Besides the already consistent down regulation of lipid metabolism, amino acid metabolism was also affected. When there is a lack of energy in the cells, amino acids are used for energy production (Woolfson, 1983) and, because of the relationship between energy and nitrogen metabolism, an increase of urea synthesis. Accordingly, genes involved in protein catabolic pathways, such as proteosomal subunits, were activated and amino acid anabolic processes were inhibited.

Many intracellular signaling cascades were up regulated 24 h after dosing leading to large changes in gene expression (Table 10). The WNT signalling pathway is known to play multiple roles in hepatocytes, influencing the cytoskeletal composition, liver zonation and metabolism. Radisavljevic and González-Flecha showed in 2004 that oxidative stress activates signalling cascades essential for cell proliferation via sequential induction of mitogenic signalling genes, like phosphatidylinositol-3-kinase (PI3K), Akt and Ran (Radisavljevic & González-Flecha, 2004). Ran is a small GTPase that is essential for the translocation of RNA and proteins through the nuclear pore complex during interphase and has regulatory capabilities of mitotic spindle formation.

Also noticeable is the collective increase of several aminoacyl-tRNA synthetases and proteins involved in RNA processing and ribosomal biogenesis. This can be considered as a cellular reaction to the inhibition of protein synthesis.

Altogether, *in vivo* as well as *in vitro*, severe impairments of cellular metabolism, energy homeostasis and translation were detected and was consistent across both microarray platforms.

Down regulated		Up regulated	
GeneGo „maps“	GO processes	GeneGo „maps“	GO processes
Tryptophan metabolism	Carboxylic acid metabolic process	TGF, WNT and cytoskeletal remodelling	Nucleotide and nucleic acid metabolic process
Regulation of lipid metabolism via PPAR, RXR and VDR	Organic acid metabolic process	Signalling via PI3K/AKT and MAPK cascades	RNA processing
Peroxisomal branched chain fatty acid oxidation	Monocarboxylic acid metabolic process	RAN regulation pathway	tRNA metabolic process
Cholesterol biosynthesis	Lipid metabolic process	Cytoskeleton remodelling	Cellular metabolic process
PPAR regulation of lipid metabolism	Cellular lipid metabolic process	Signal transduction, AKT signalling	Ribosome biogenesis and assembly
Mitochondrial long chain fatty acid beta-oxidation	Fatty acid metabolic process	Chemokines and adhesion	Smooth endoplasmic reticulum calcium ion homeostasis
Leucine, isoleucine and valine metabolism	Nitrogen compound metabolic process	Aminoacyl-tRNA biosynthesis in cytoplasm	Endoplasmic reticulum calcium ion homeostasis

Table 10: Top seven “maps” and GO processes significantly affected *in vivo* and *in vitro* 24 h after treatment with Tet. (Only the results from Affymetrix are shown, Illumina generally delivered resembling results) Thresholds: Fold change \geq 1.5; P-value \geq 0.05.

Hepatocytes were dosed a second time and therefore, no signs of recovery as seen in the animals from the *in vivo* experiments, were expected. Again, the top ranked pathways and GO processes illustrate the heavy impact of Tet on lipid and energy metabolism. The up regulation of ribosomal RNA production in the cells increases the need for new synthesized nucleotides indicated by the increased expression of genes involved in their synthesis (Table 11).

Down regulated		Up regulated	
GeneGo „maps“	GO processes	GeneGo „maps“	GO processes
Cholesterol Biosynthesis	Lipid metabolic process	Aminoacyl-tRNA biosynthesis in cytoplasm	RNA processing
Cytoskeleton remodelling	Cellular lipid metabolic process	Cell cycle_Role of SUMO in p53 regulation	Primary metabolic process
Cell adhesion_Plasmin signalling	Carboxylic acid metabolic process	Signal transduction_AKT signalling	Cellular metabolic process
Chemokines and adhesion	Organic acid metabolic process	GTP-XTP metabolism	Metabolic process
TGF, WNT and cytoskeletal remodelling	Monocarboxylic acid metabolic process	ATM/ATR regulation of G1/S checkpoint	Biosynthetic process
Propionate metabolism	Fatty acid metabolic process	CTP/UTP metabolism	tRNA metabolic process
Integrin outside-in signalling	Carbohydrate metabolic process	ATP/ITP metabolism	Cellular biosynthetic process

Table 11: Top seven Maps and GO processes significantly affected *in vitro* 72 h after treatment with tetracycline. Thresholds: Fold change \geq 1.5; P-value \geq 0.05. (Again, only the results from Affymetrix are shown, Illumina generally delivered resembling results).

Both microarray platforms detected deregulations of genes involved in the cholesterol biosynthesis pathway. Although some of the genes could not be detected in all experiments, the biological interpretation from each was consistent. Cholesterol biosynthesis is closely associated with the metabolism of lipids. It is an extremely important biological molecule that has roles in membrane structure as well as being a precursor for the synthesis of steroid hormones and bile acids. The rate limiting step of this process is the conversion of acetyl-CoA to 3-hydroxy-3-methyl glutaryl-CoA by HMG-CoA synthase. This gene has a complex regulation and was found, together with other key-genes in this pathway, to be down regulated at multiple time points. One source for the acetyl-CoA molecules needed for the synthesis of cholesterol is the mitochondrial β -oxidation of fatty acids (Figure 36). Massive interruption of this process was observed by both platforms, which may be one trigger that caused the deposition of fatty acids and triglycerides in the cell. Fatty acid binding protein (FABP) was one of the few genes that were affected differentially *in vitro* and *in vivo*. Whereas it was down regulated *in vitro*, a strong induction *in vivo* was detected. *In vivo*, the regulation of

FABP is closely connected to cholesterol biosynthesis and the cholesterol level in the cells (Montoudis et al., 2008). Even though this important protein was oppositely regulated, an accumulation of lipid droplets in cultured hepatocytes was taking place.

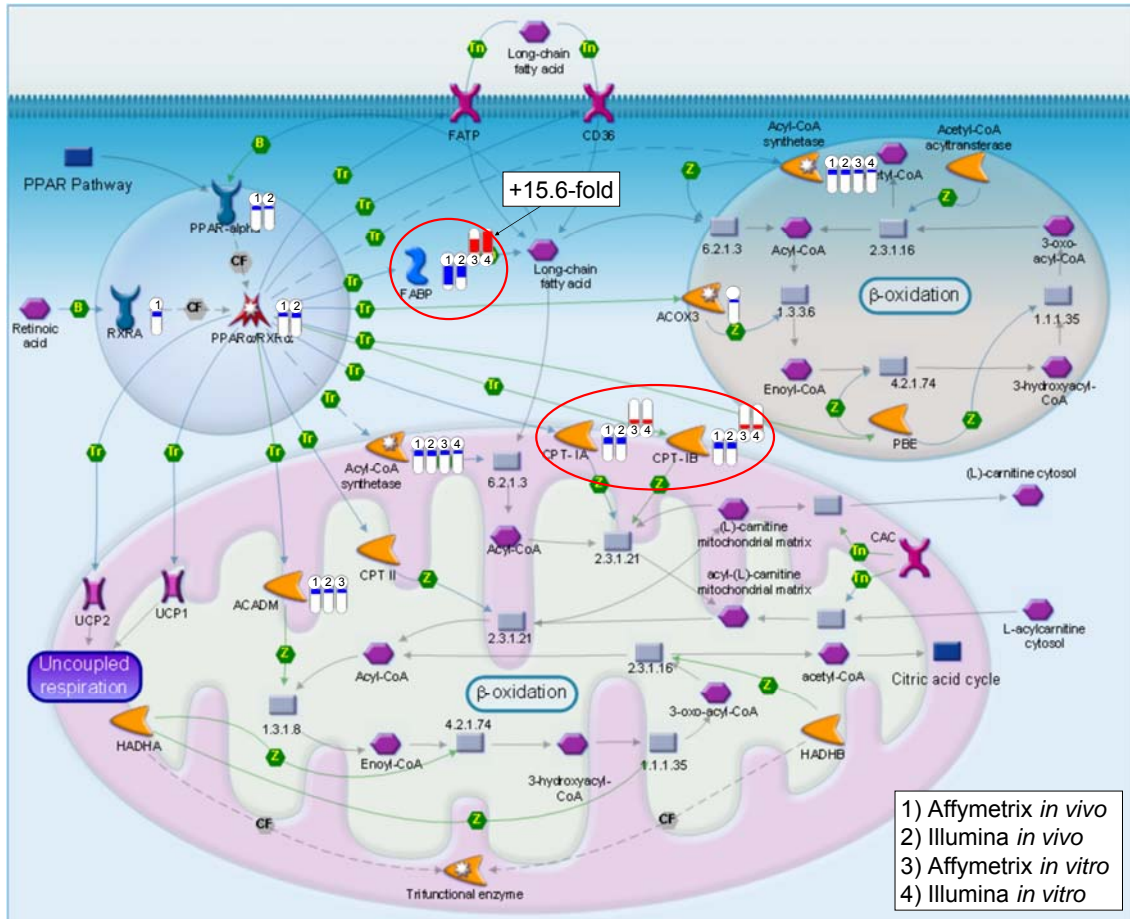


Figure 36: Transcriptional regulation of lipid metabolism by PPAR α . The expression of several genes involved in this pathway was repressed. Deregulation is indicated by either blue (up) or red (down) bars. The relative height resembles the extent of deregulation (modified from Metacore, GeneGO).

Perturbations in intracellular signalling are also connected with microvesicular steatosis. One of the top ranked pathways found to be affected was the Janus kinase-signal transducers and activators of transcription (JAK-STAT) signalling pathway. It plays an important role in the regulation of cellular development, growth and homeostasis and enables the cell to detect extracellular signals like cytokines, hormones, transporting them into the nucleus, consequently modulating gene expression by directly binding to promoter regions of genes. Waxman and his coworkers showed that cytochrome P450 enzymes, mainly Cyp2c11, are transcriptionally regulated by inhibition of this pathway (Waxman, 1999). Both, the

deregulation of the JAK-STAT pathway, as well as the inhibition of xenobiotic metabolism, could be shown in this study with both microarray platforms.

Another consequence of activating the JAK-STAT cascade is the initiation of inflammatory processes and proliferation of the hepatocytes. Downstream genes of JAK-STAT signalling are important transcription factors, like c-Myc and NF- κ B, which were also found to be activated by Tet treatment. c-Myc is, amongst many other functions, capable of driving cell proliferation by activating the expression of cyclins and inhibiting p21 expression. Gamma amino butyric acid (GABA), a neurotransmitter which also plays an important role in the regulation and inhibition of hepatocyte proliferation, was found to be consistently down regulated. Inflammatory processes were, analogous to the previous results, mainly seen 6 h after treatment and predominantly *in vivo*.

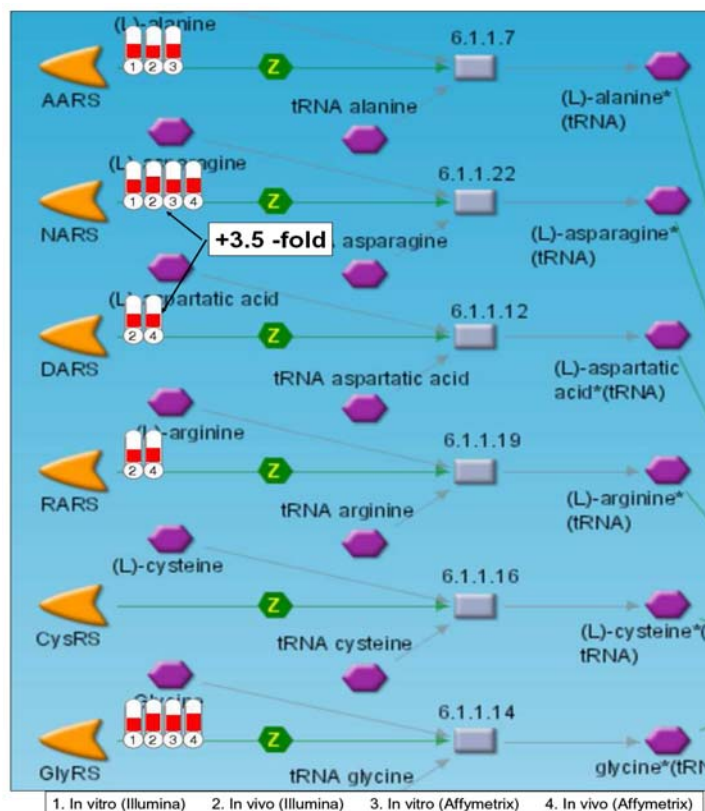


Figure 37: Induction of several aminoacyl-t-RNA synthetases (modified from Metacore, GeneGO).

STAT has a very important role in cellular growth and differentiation mechanisms and is responsible for the up regulation of ribosomal RNA synthesis. Tet preferentially binds to 70S ribosomes of bacteria inhibiting protein synthesis, but, with a lower affinity, they also inhibit the functionality of the 80S ribosome of eukaryotic cells (Ogata et al., 2000). In fact, a massive change in protein synthesis and related processes was detected. Several aminoacyl-t-RNA synthetases, responsible for the generation of aminoacyl-t-RNA, were induced, both *in vivo* and *in vitro* (Figure 37).

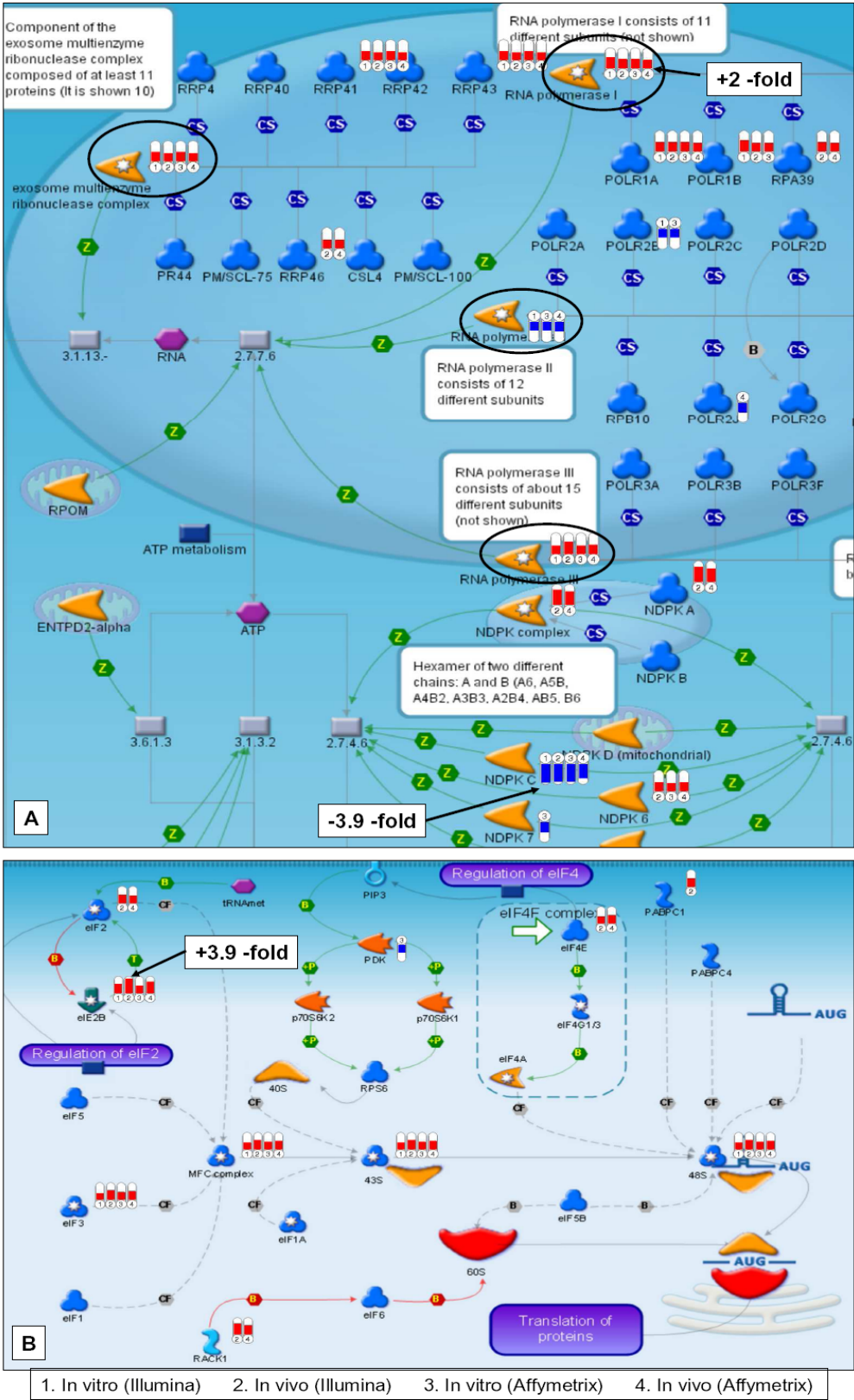


Figure 38: Perturbations in RNA metabolism. A) Details of the RNA and nucleotide homeostasis in cells. The RNA-polymerase I and the exosome were heavily induced (Red circles) whereas the RNA polymerase II was repressed (blue circle). B) Translation initiation, deregulation is indicated by either blue (up) or red (down) bars. The relative height resembles the extent of deregulation (modified from Metacore, GeneGO).

Additionally, the induction of rRNA producing enzymes was observed, e.g. the induction of Polymerase I. tRNA synthetic processes and the generation of nucleoside triphosphates by the nucleoside diphosphate kinase (NDPK) (Figure 38A). At the same time, polymerase II, responsible for the transcription of mRNA, was repressed and genes belonging to the exosome complex, which is the key player in RNA degradation, were induced. Also downstream events of RNA-metabolic processes were affected. Furthermore, the initiation of translation- and elongation factors, such as eIF3 or eIF2B, was clearly induced. Rack1, eIF2 and eIF4E were only detected as significantly deregulated *in vivo* (Figure 38B). All these changes lead to an imbalance in RNA homeostasis and can be interpreted as a compensatory reaction of the cells to overcome the reduction of protein synthesis by the binding of Tet.

All the effects described above were detected as deregulated *in vivo* as well as *in vitro*. Both platforms yielded comparable results, with regard to the number of deregulated genes, the dimension of deregulation and therefore the biological interpretation was identical.

Besides the common effects of Tet on hepatocytes *in vivo* and *in vitro*, differences in cellular reactions were detected. The changes in gene expression 24 h after treatment were analyzed for mechanisms specifically affected only *in vitro* or only *in vivo*. Using the network building capability of MetaCore™, several networks, enriched with genes specific to either one of the two experiments, were generated and ranked by pValue (Table 12).

Unique for Tet <i>in vitro</i>		Unique for Tet <i>in vivo</i>	
Network	pValue	Network	pValue
protein transport (21.4%), establishment of protein localization (21.4%), regulation of JAK-STAT cascade (7.1%)	3.41E-79	DNA repair (25.0%), response to DNA damage stimulus (27.5%), DNA metabolic process (32.5%)	1.69E-45
cell cycle process (48.7%), cell cycle (48.7%), regulation of progression through cell cycle (41.0%)	2.32E-33	cell cycle phase (39.0%), cell cycle process (48.8%), mitotic cell cycle (36.6%)	9.27E-22
vitamin metabolic process (36.8%), ventricular cardiac muscle cell differentiation (28.9%), cardiac muscle cell differentiation (28.9%)	1.87E-24	intracellular signalling cascade (65.9%), protein kinase cascade (47.7%), signal transduction (79.5%)	1.21E-11

Table 12: Top ranked networks based on genes detected only *in vivo* or *in vitro*.

Networks built from genes affected only *in vitro* were involved in the transport of proteins, parts of the JAK-STAT pathway, progression through cell cycle and induction of mitosis. Also mechanisms of cell adhesion and cellular reorganization were more pronounced than *in vivo*. On the other hand, mechanisms only affected *in vivo* were involved in DNA repair, inflammatory response and intra cellular signalling. The fact that both lists contained networks concerning cell cycle progression and other overlapping mechanisms indicate that the same underlying mechanisms were induced by Tet and that there might be different possibilities for the cell to fine-tune the exact regulation of gene expression.

3.1.2 Conclusions of the platform comparison study

Eventhough major difference exists between the paltforms, a high degree of similarity and comparability of the results was found. In this study, two large datasets were analyzed to elucidate the intra- and inter-platform comparability of two commercially available global gene expression platforms, the RatRef-12 Expression BeadChip (Illumina) and the Gene Chip[®] Rat Genome 230 2.0 Array (Affymetrix). Both platforms have fundamental differences in design and layout. They are based on different versions of the RefSeq sequence database and use different algorithms to design their probes. A mapping of the probe sequences of both platforms to the actual RefSeq Release 19 allowed the comparison of genes perfectly matched by both platforms. This mapping reduced the number of valid genes to 7,271 which were used in subsequent studies. The substantial size of the study provided the possibility to assess the characteristics of intra- and inter-platform differences with great statistical significance and to analyze the dataset in several different ways.

The technical variation of the data, shown by the CV values, was lower than 10% showing a good repeatability of both techniques. The interplatform comparison was more susceptible to variances. Due to the complexity of producing these types of platforms, concentration variations of reagents during reverse transcription, the effect of time and performance and the personal factor contribute to this variability. One should be aware that only a few of these basic causes can be eliminated. Microarray techniques are very sensitive to deviations and need a high level of standardization to minimize extraneous influences

The titration experiment demonstrated the sensitivity of both platforms. The measurement of a linear increase of intensity values was possible for medium expressed genes, whereas saturation effects for highly expressed genes were visible. However, a set of genes showed no correlation between the platforms. Due to the

identical samples measured on both platforms, there are mechanisms which may be causative for this observation. Most importantly, the location of the probe (-set) on the target cRNA sequence contributes to the variability of expression results. Stafford and Brun (2007) showed a correlation between the probe distance and measured results. Additionally, longer probe sequences, as used by Illumina (50mers), are less sensitive to degraded cRNA and possess different binding efficiencies. Differences in condensing algorithms, the data extraction and the multiple possibilities to analyze of the data also had great influence on the platform performance. Finally, a greater amount of genes showed no linear dependency if measured with Illumina suggesting saturation effects for the high expressed genes.

Ranking genes by fold change gave more reliable results than pValue ranked lists. Fold changes were calculated by comparing the measured intensity values directly whereas the pValue incorporates the signal to noise ratio. Combining the fold change based approach with the statistical significance (pValue) additionally increased the overlap.

The robustness of both microarray platforms was tested by applying a “real life” toxicogenomic test study. The implementation of biological replicates increased the variance in gene expression. Nevertheless, the concordance of ranked gene lists generated by pValue or fold change showed a large overlap. The size of this overlap was heavily dependent on the biological context of the samples and increased together with the number of genes deregulated by compound treatment. The data from the *in vitro* experiments seem to be more variable, the medians of the CVs tended to be higher than from the *in vivo* experiments. One possible explanation for this is the cellular stress caused by the perfusion and subsequent cell culture. Many changes in gene expression are caused during the perfusion procedure and related to the switching of hepatocytes from G₀-phase of the cell cycle back into G₁-phase (Papeleu et al., 2006). Additionally, it is also associated with various other effects like cytoskeletal perturbation (Baker et al., 2001; Chapman et al., 1973), dedifferentiation (Bayad et al., 1991), activation of immune response (Li et al., 2001), induction of apoptosis (Zvibel, Smets & Soriano, 2002; Czaja, 2002), the loss of polarization (LeCluyse, Audus & Hochman, 1994; Luttringer et al., 2002) and the activation of several intracellular signalling pathways (De Smet et al., 1998; Elaut et al., 2006a; 2006b; Boess et al., 2003).

A strong effect of time in culture on the variability between biological replicates may help explain the increased CV. However, this was not observed and it can be assumed that the effects of isolating the cells and culturing them in sandwich culture are only a minor reason for the increased CV. The fact that for the *in vivo* study a different rat

strain (Sprague-Dawley) was used than for the *in vitro* study (Wistar) may be a significant cause for the variance observed.

This conformity of detection was also seen in the Tet toxicogenomic study. The data from both platforms, analyzed separately, led to the same biological conclusions. Although there might be a bias introduced by probe mapping and selection in terms of biological content, both platforms clearly showed the proposed mechanisms of action of Tet. Inhibition of the mitochondrial β -oxidation together with impaired intracellular RNA and protein homeostasis are mechanisms leading to the accumulation of lipids and triglycerides in the cells, which *in vivo* leads to the toxic endpoint, microvesicular steatosis. Contributing to this toxicity might be the increased protein catabolism causing the liberation of nitrogen, which is normally removed from the cell through urea production or is reused through the citric acid cycle. Both pathways were also affected by treatment with Tet and are therefore contributing to its mechanism of toxicity.

The results of this study clearly show that both global gene expression techniques can be considered equally qualified and can be used for further toxicogenomic studies. Additionally, new details of the mechanisms of action of Tet were elucidated. Interestingly, these mechanisms were detected with high concordance not only *in vivo*, but also *in vitro*. The combination of an *in vitro* cell culture model with global gene expression approaches will facilitate the process of investigating mechanisms of action and in the prediction of possible toxic risk factors earlier than currently possible.

3.2 Establishment of a longer term cell culture of primary rat and human hepatocytes

A recent report on the root causes of failed drugs over the last 10 years stated that hepatotoxicity and cardiovascular toxicity are the main reasons (Schuster, Laggner & Langer, 2005). Hepatotoxicity in humans has the poorest correlation to regulatory animal testing with only half of the cases of human hepatotoxicity found in clinical trials being confirmed with concordant signals in animal toxicity studies (Olson et al., 2000). The development of new, more predictive models for hepatotoxicity screening is therefore crucial for the improvement of the drug developmental process. The replacement of animal tests by *in vitro* methods allows the combination of early screening and mechanistic studies and the realisation of the 3R principle. Currently, there are several *in vitro* models used for screening for hepatotoxicity, each of these models with its own advantages and drawbacks with regards to availability, throughput, viability of the cells over time and the opportunity to analyse multiple of parameters (chapter 1.5). The process of dedifferentiation of hepatocytes leading to a loss of liver specific functions, as well as the complexity of other models that do not allow their use in a higher throughput, are two of the main limitations restricting hepatocyte use in toxicological screening or basic research. At the same time, the possibility to perform experiments under strictly controlled and standardized laboratory conditions is favourable. The refinement of the existing primary hepatocyte cultures, allowing their use for longer term toxicity testing, will be a step towards the acceptance of these techniques as standard screening methods and will help to reduce animal testing. The opportunity to increase incubation times allows one to study long-term effects and also to apply pharmacologically relevant concentrations of the test compound. Since the number of cells needed for the analysis of a specific parameter is usually low, multiple experiments can be conducted with one batch of cells at the same time, making it possible to obtain various data from the same source.

The careful selection of endpoints, with respect to the relevance to the *in vivo* systems, is of great importance. One has to be aware that cells are always in contact with their surrounding tissue, other cell types and receive multiple signals from the entire organism under *in vivo* conditions and that these complex networks are not present *in vitro*. All results from isolated hepatocytes, as a mono-factorial model, have to be analyzed against this background.

Hepatocytes cultured in monolayer (ML) not only lose 75% of their total CYP450 during the first 24h after isolation, but also other liver specific functions and

differentiation markers (Gómez-Lechón et al., 2004; Davila & Morris, 1999; Farkas & Tannenbaum, 2005a). Several attempts to optimize the culture conditions have been reported, including the use of extracellular matrix (ECM) material, such as matrigel overlay (Schuetz et al., 1988) or collagen in a sandwich conformation (LeCluyse et al., 1994), the use of optimized culture medium (Enat et al., 1984), medium supplements (Sidhu & Omiecinski, 1995) and co-culture with other cell types (epithelial cells, sinusoidal cells or Kupffer cells) (Begue et al., 1994; Donato, Castell & Gómez-Lechón, 1994). These improvements allow the hepatocytes to regain cellular morphology, polarisation and to maintain physiological rates of albumin secretion (Dunn et al., 1991). Whereas the classically used monolayer culture is not suited for longer time culture of hepatocytes, the sandwich culture has proven to maintain some liver specific features for longer times, at levels comparable to *in vivo* conditions (Kern et al., 1997; Dunn et al., 1989) and to slow down the process of dedifferentiation (Tuschl & Müller, 2006).

3.2.1 Morphological and functional characterization of primary rat hepatocytes

Hepatocytes were isolated from male Wistar rats using a modification of the two-step perfusion method described by Seglen (Seglen, 1976). Cell viability was assessed by trypan blue dye exclusion and hepatocytes with >85% viability were plated as described previously. After seeding, cells appeared rounded and distinct from each other. In our laboratory, the SW culture was established using collagen I as an extracellular matrix environment, a serum free, amino-acid rich media composition (DMEM-F12) and dexamethasone and ITS as supplements (chapter 2.2.1). This culture was compared to rat hepatocytes cultured in ML culture with and without the addition of serum and SW culture with the addition of serum.

3.2.1.1 Morphological examinations

Cells were examined for morphological changes after seeding every day for up to two weeks. Already 4h after seeding, when media was changed from seeding media to culture media, a morphological distinction was seen between ML and SW cultures. Cells in ML had already regained their polygonal shape and started to establish extensive cell-cell contacts, whereas SW-cultured cells remained spherical and isolated for a longer period of time, probably resulting from the cells' immersion in the three dimensional ECM environment of the collagen gel (Figure 39). Cells in monolayer

spread out and had a more flattened morphology, mainly due to their attempt to establish contact with the ECM, whereas cells cultured in SW, after an initial delay, remained polygonal in shape. Initially, the cytoplasm appeared clear and membranes were smooth in both culture systems.

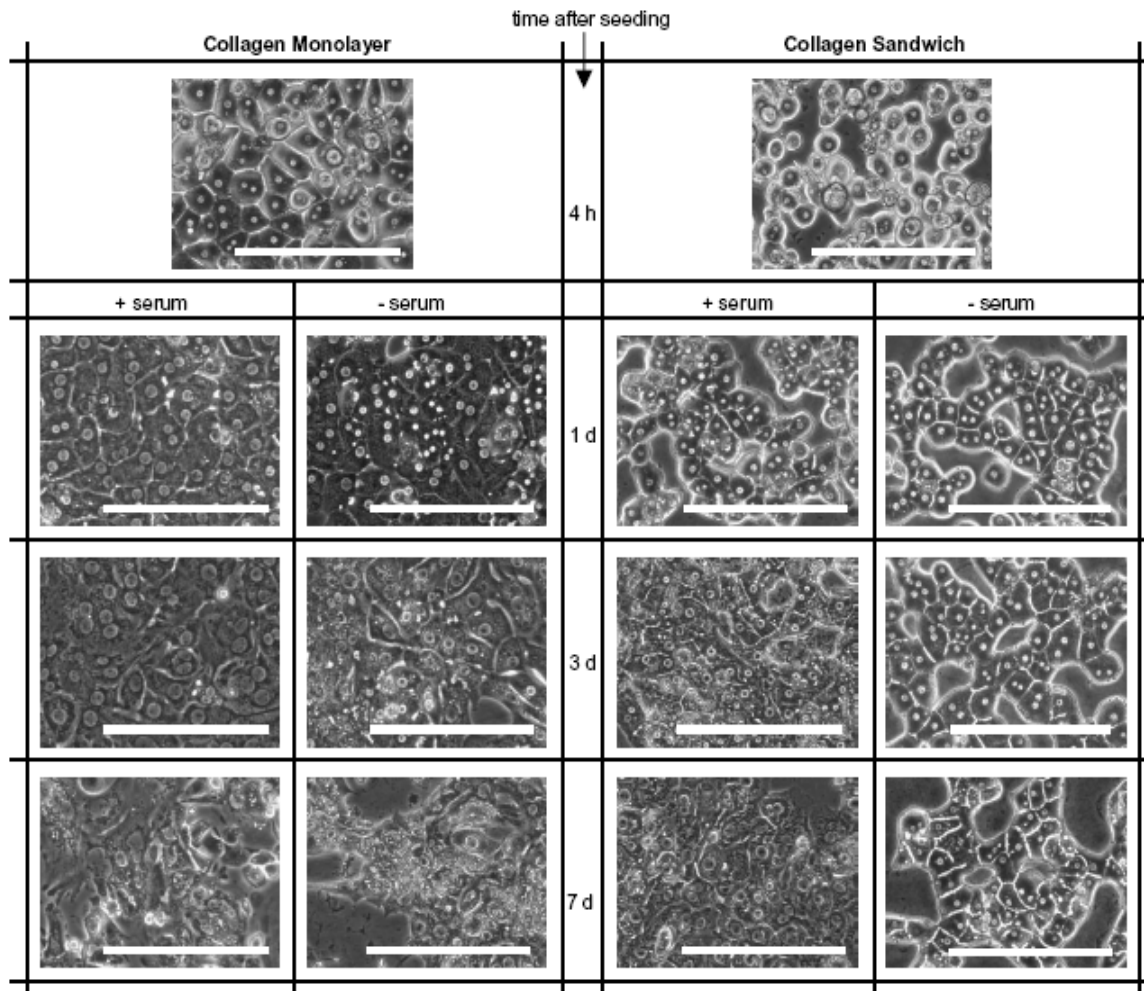


Figure 39: Effect of ECM environment and media formulation on morphological development and structural integrity of primary rat hepatocyte cultures. Cells were cultured for the indicated times on collagen monolayer or in a collagen gel sandwich with serum-free or serum-containing medium. Arrows indicate bile canaliculi-like structures. The white scale bar in the bottom right of each image corresponds to 200 μm .

One day after seeding, cells in all types of culture had made contact with each other and started to build structures which are described as bile canaliculi (Gautam, Ng & Boyer; 1987; LeCluyse et al., 1994). The number and distinctiveness of these structures increased in cells cultured without serum, which is consistent with the findings of Terry and Gallin, who reported an inhibitory effect of serum on the formation of bile canaliculi (Terry & Gallin, 1994). Over time, cells in monolayer spread out until

confluency and therefore had a flattened appearance, accompanied by an increase in the size of the nucleus. There were no longer well-delineated plasma membrane borders and bile canaliculi-like structures disappeared almost entirely. They moved towards each other and built clusters of cells. This was accompanied by the a more fibroblast-like morphology. Together, this depicts the dedifferentiation process in ML with and without serum. The cytoplasm of cells cultured with serum appeared granulated and inclusion bodies were first detected on day 3. In contrast to this, cells cultured in SW without serum displayed a stabile polygonal morphology with extensive bile canaliculi networks and a clear cytoplasm. This was true up to 14 days of culture. Cellular mobility and re-entry into the cell cycle was observed for cells cultured with serum and cells cultured in ML which started detaching from the culture plate surface. All these findings are in accordance with previously reported effects of serum, the overlay of cells with ECM-material and media supplementation (Dunn et al. 1989; Musat et al., 1993; LeCluyse et al., 1994; Tuschl & Müller, 2006).

It has been reported that changes induced by perfusion, morphological changes and intracellular energy and redox homeostasis are related to the dedifferentiation processes of hepatocytes (Greetje et al., 2006). However, the restoration of cell polarity combined with the regeneration of bile canaliculi and gap junctions leads to an increased expression of liver specific genes and a preservation of liver functions (Wilkinson & Dickson, 2001; Hamilton, Westmorel & George, 2001; LeCluyse et al., 1994). Since hepatocyte differentiation, drug metabolism and toxicity are inherently linked, the liver specific metabolic capability should ideally be maintained on *in vivo* level for as long as possible.

To acquire deeper insights into the functionality of the cultured hepatocytes, several cell type specific functions were examined. One of the most important features of hepatocytes is their ability to metabolise xenobiotics (chapter 1.3). The concentration of the specific CYP isoforms, regulated in multiple ways, has a major impact on the cells metabolic activity. Several transcription factors are responsible for the differential expression (Table 13), but a high degree of cross talk and interactive regulation has been reported (Yan & Caldwell, 2001; Guengerich, 2003; Dickins, 2004).

Enzyme	Transcription factor	Inducer	Substrates	Percentage of total CYP-enzyme in liver
CYP 1A1	AhR	BNF	Polycyclic aromatic hydrocarbons	1.2
CYP 2b	CAR	PB	Cyclophosphamide, Nicotine	1.9
CYP 2C	GH/CAR/PXR	PB	Retinoids	65
CYP 3A	PXR/CAR/GR	Dex	various substrates	14.6

Table 13: List of CYP isoforms tested in this study with appropriate transcription factors, potent inducers, typical substrates and their overall abundance in liver.

3.2.1.2 CYP inducibility

During this study, the inducibility of the CYP 1A, 2B, 2C and 3A isoforms was used as a sign of cell viability and differentiation status. Cells were cultured in ML and SW culture as previously described and dosed at 0 h, 3 d and 9 d with the appropriate inducer for 48 h. CYP 1A1 was induced with β -naphthoflavone (BNF; 10 μ M), CYP 2B and 2C with phenobarbital (PB; 500 μ M) and CYP 3A with dexamethasone (Dex; 50 μ M). The expression of specific CYP mRNAs was determined by TaqMan-PCR and the relative enzyme activity was measured using specific spectrophotometric methods (results were generated as part of a joint work with Gregor Tuschl, PhD-student).

Figure 40 shows that at early time points, the cells were still responsive to CYP induction. CYP 1A was heavily induced on the mRNA level in ML (160-fold) whereas in SW-culture the induction was only about 55-fold. Interestingly, on the enzyme activity level the activity of CYP 1A in SW culture superimposed the activity in ML. On the mRNA level, the inducibility of CYP 1A was consistent over time. In contrast, the induction of enzyme activity decreased over time in both culture systems. After 3 days, the activity of CYP 1A was 6 fold higher than the controls in ML and still 32-fold higher in SW. After 9 d in culture, CYP 1A could no longer be induced in ML but still reached 18-fold induction in SW culture. In general, cells remained much more responsive to CYP 1A induction in SW culture, where after 9 d in culture marked increase of enzyme activity was still detected.

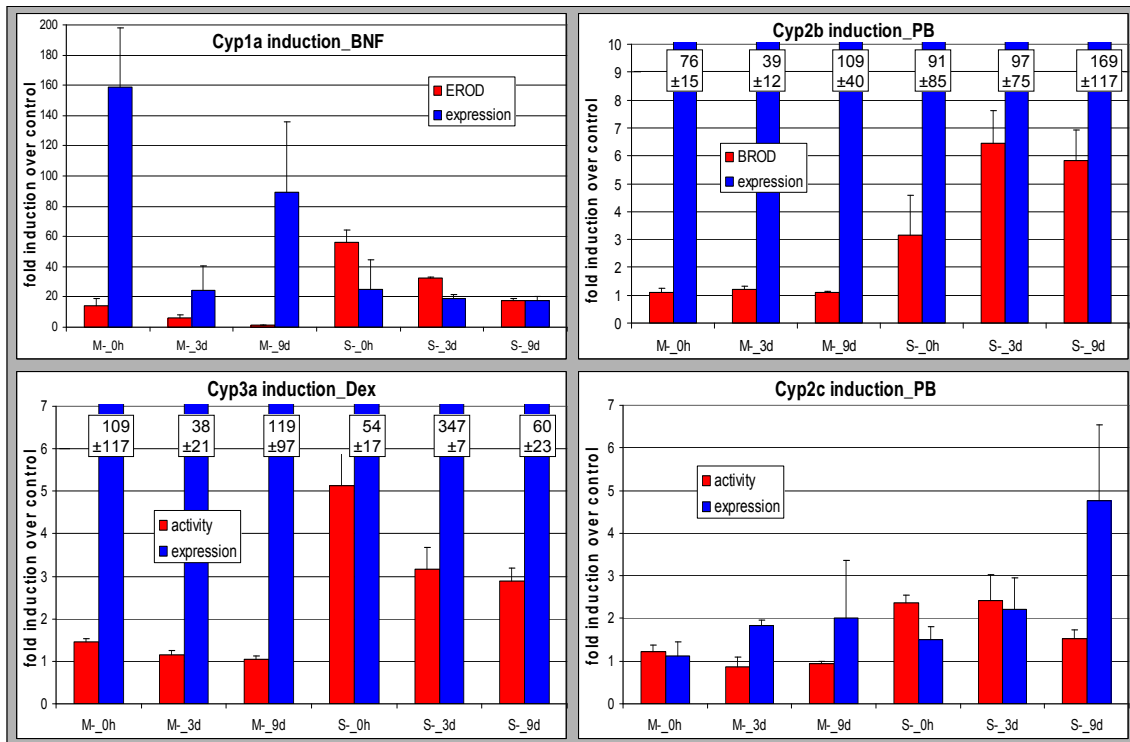


Figure 40: Relative induction of enzyme activity and mRNA expression for CYP1A, 2B, 3A and 2C. Depicted are the results of two cell cultures, ML and SW without serum. Cells were induced with either 10 μ M BNF, 50 μ M PB or 500 μ M Dex on days 0, 3 or 9 of culture and samples were taken 48h after induction. Bars illustrate changes in enzyme activity (red bars) or mRNA expression (blue bars) relative to time matched vehicle controls. Bars illustrate mean values of fold induction from triplicate measurements with standard deviation.

The responsiveness of cells to PB and Dex mediated CYP 2B and CYP 3A induction was stable over time in both types of culture. The mRNA levels of CYP 2B and CYP 3A were about 50-100 times higher than in the uninduced control. Differences between both culture conditions were again detected on the enzyme activity level. Whereas no induction in enzyme activity was detected for ML culture, both enzymes were induced in SW culture at all time points. The activity level was 3-7 times above the control level and inducibility was retained BNF until the end of the culture period.

Unlike the other CYPs, CYP 2C was neither inducible on the mRNA nor on the enzyme activity level in ML culture at the 0 h time point. Over time no increase was detected on the activity level, but mRNA expression was two fold induced at later time points. In SW culture, a small increase (about 2-fold) was initially detected for activity and expression. The inducibility of CYP 2C mRNA expression increased over time up to 5 fold after nine days of culture. In contrast the enzyme activity inducibility remained stable over time. Additional western blot analyses showed good correlations with the previous results of gene expression and protein activity tests. Isolated protein was separated by SDS-

PAGE, proteins were blotted and subsequently CYP isoforms were detected with specific antibodies. Figure 41 shows examples of the results for CYP 1A1, 2B and 3A1. The determined signals were detected at a molecular weight between 50 – 60 kDa and are therefore in good agreement with the calculated molecular weights of the CYP isoforms at 59 kDa, 56 kDa and 57 kDa, respectively.

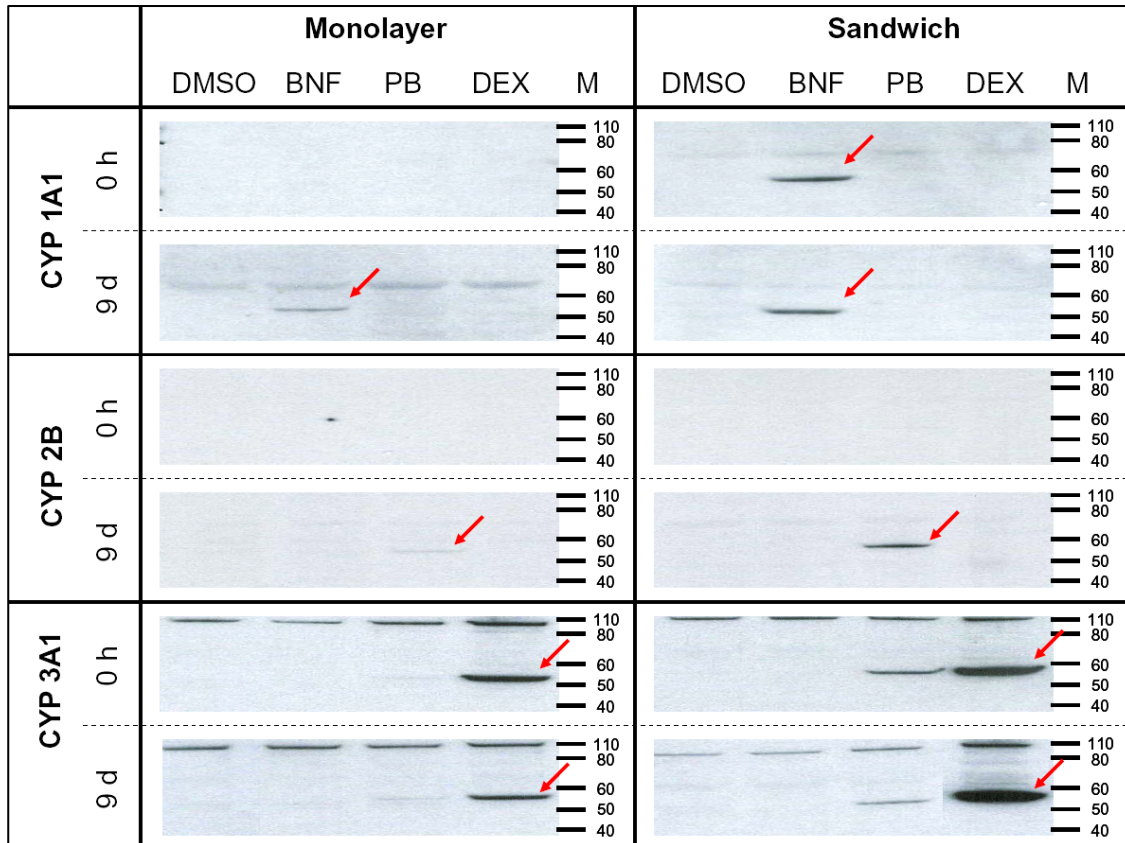


Figure 41: Protein extracts of induced hepatocytes were separated by SDS-PAGE and CYP isoforms were subsequently detected by western blot analysis as described. The red arrow highlights the induced CYP-isoforms.

CYP 1A1 was unchanged at 0 h but was weakly induced on protein level after 9 d in ML-FCS culture by BNF. In contrast to this, CYP 1A1 already was induced at the early time point in SW-FCS culture and inducibility endured over the time of culturing. The CYP 2B isoform could not be induced at the starting point in either culture but after 9 d, PB caused a slight increase in both cultures which was more pronounced in SW-FCS culture. The CYP 3A1 isoform was induced in both types of cell culture at all time points by DEX. Whereas the decreasing signal intensity over time for ML-FCS cultured cells implicates a decreasing inducibility, SW-FCS cultured cells showed exactly the opposite effect. Additionally, cells cultured in SW-FCS exhibited an increased level of

CYP 3A1 after treatment with PB, which could also be seen on the activity level (data not shown) and which was not true for cells cultured in ML-FCS conformation.

In general, the enzyme activity and the inducibility on mRNA and protein level of the CYP isoforms tested was higher and more stable over time in SW culture. This is an indication of a higher capability and a more differentiated status of these cells.

3.2.1.3 Canalicular transport

The reestablishment of cell-polarity, the formation of bile canaliculi together with the expression of genes encoding for the transport of xenobiotics are a prerequisite for functional transport processes in cultured hepatocytes. It was previously demonstrated that SW-cultured hepatocytes re-established functional polarity and form bile canaliculi at their contact sites (LeCluyse et al., 1994; Talamini, Kappus & Hubbard, 1997). The ATP-dependent canalicular anion transporter Mrp2 (Multidrug resistance-associated protein 2) is responsible for the transport of multivalent organic anions, including glutathione and glucuronide conjugates (Akerboom et al., 1991; Elferink et al., 1995). As canalicular efflux may be the rate limiting step in biliary excretion of xenobiotics, the influence of culture conditions on the functionality of according transporters was examined. Cells were incubated with carboxy-DCFDA, a fluorescent substrate for Mrp2, and therefore the dye efflux from hepatocytes cultured in either ML or SW culture into the bile canaliculi was determined over time.

At the beginning of the culture, on day 0, no canalicular structures were seen and consequently, no transport was detected. Together with the reestablishment of cellular polarity, canalicular structures developed at the contact site of cells with longer times. As previously stated, these structures were more pronounced in cells cultured without the addition of serum and were more stable in SW culture. The fluorescent substrate accumulated in cells without contact to other cells. It was transported out of the cells only if the canalicular structures in between the cells were established (Figure 42).

After 3 days in culture, only cells cultured in SW culture without serum showed pronounced canalicular networks which remained active until the end of culture on day 9. As expected, other culture methods were unable to obtain transport activity of the substrate. After 3 days in ML culture, some cells appeared to have integrated the fluorescent substrate into granular structures of the cell (Figure 42, arrow 1). This could be caused by Mrp2 molecules being accumulated in intra-hepatocytic vesicles. Previous studies showed the storage of hepatic transporters inside the cell where they are delivered to the canalicular domain following increased physiological demand (Wakabayashi, Kipp & Arias, 2006; Kipp & Arias, 2002). The lack of cellular polarization and canalicular structures may cause an accumulation of these vesicles.

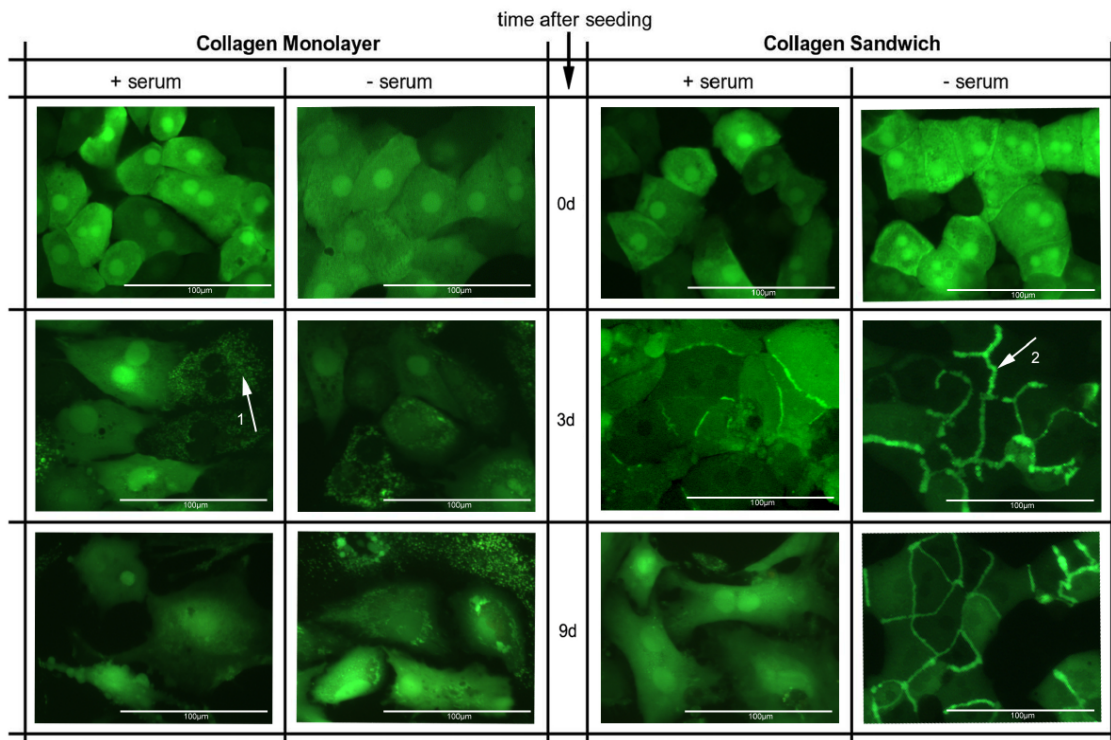


Figure 42: Microscopic pictures of hepatocytes cultured in ML and SW with and without serum. To visualize canalicular transport processes, they were incubated with carboxy-DCFDA and cells were cultured for up to 9 d. Arrows indicate 1) the accumulation of the dye in granular structures and 2) the accumulation of the dye in canalicular structures.

3.2.1.4 Conclusions of the morphological and functional data

Primary hepatocytes are a widely used model to study acute toxic effects or drug metabolism. Primary cultures of isolated hepatocytes, as a mono-factorial model, display most of the metabolic liver functions and are therefore well suited for this purpose.

The use of strict standardization, higher throughput and consistent capabilities of primary cells for toxicological issues are major advantages of *in vitro* systems. A lot of work has been undertaken to establish and optimize a culture method for primary hepatocytes that overcomes the disadvantages of dedifferentiation. The study described above showed clearly that the environment of an *in vitro* culture has a critical impact on liver specific functionality of primary hepatocytes, including morphology, gene and protein expression, as well as the loss of other cell type specific attributes. The beneficial effects of ECM overlay in SW culture showed an ability to retain a differentiated status and some important liver specific functions, like albumin secretion, biliary transport processes or metabolism (Dunn et al., 1989; LeCluyse et al., 2000;

LeCluyse et al., 1994). The time of culture could thus be prolonged up to several weeks without severe morphological changes (suggesting reduced dedifferentiation). By optimizing the media composition and a careful selection of media supplementation, the formation of functionally active bile canaliculi was promoted. In this chapter, the beneficial effects of ECM overlay on the survival rate, on cell morphology and several essential functional aspects of hepatocytes were clearly shown. Already the morphological examination of primary hepatocytes over time showed distinct differences in cellular behavior in different cell cultures. Cells cultured in SW-FCS were organized in acinar structures characteristic of the tissue of origin (Farkas & Tannenbaum, 2005b; LeCluyse et al., 2000). Further details of improved structural components have been previously described by Davila (Davila & Morris, 1999).

In addition to the polygonal shape, the three dimensional environment has positive effects on gene expression. The SW-FCS culture showed not only the preservation of morphological properties but also an increased inducibility of several CYP isoenzymes, both on the level of gene, on protein expression and on the enzymatic activity. These results are in agreement with other researchers, who also reported improved viability and phase 1 metabolism (LeCluyse et al., 1994; Dunn et al. 1989; Tuschl & Müller, 2006; Gebhardt et al., 2003; Hamilton et al., 2001), even when other media compositions or Matrigel was used. The key signal for this improvement therefore seems to be the introduction of a third dimension by plating the cells into a gel and giving them the possibility to retain their physiological form instead of a flattened morphology as for ML cultures.

These results support the applicability of long-term hepatocyte cultures for CYP-induction studies. It has even been suggested that serum-free collagen sandwich cultures can be used to examine CYP induction of several test compounds consecutively in one culture with recovery phases between treatment stages (PRIMACYT Cell Culture Technology GmbH, personal communication). This would be a step towards higher throughput and also help to further reduce animal usage in preclinical drug development. A recently published report explicitly promoted the addition of several CYP inducers into the culture media to keep the cells induced and to maintain elevated levels of metabolic enzymes throughout the culture (Kienhuis et al., 2007). The ability of this system to obtain results physiologically relevant results has still to be proven.

The reorganization of canalicular structures could be enhanced by serum free media and the addition of Dex. These structures were stable and functionally active over the whole time of SW culture, shown by the transport experiments with carboxy-DCFDA. The lack of transport activity at early time points of culture may be caused by

endocytotic processes removing Mrp2 from the cell surface during the process of perfusion, which is only reversed by the reestablishment of cellular polarity (Graf & Boyer, 1990). The fact that canaliculi-like structures are stable over time makes these cultures especially valuable for transport studies. An additional effect of Dex is the inhibition of spontaneous apoptosis by inhibiting caspase-8 activation and increasing anti-apoptotic signals like Bcl-2 and Bcl-x_L (Bailly-Maitre et al., 2002).

Altogether, these results show that hepatocytes cultured in serum-free collagen sandwich conformation partly recover from stress during liver perfusion, adapt to the cell culture conditions and stay morphologically unchanged for several weeks. They regain their functionally important cell polarity, rebuild cell borders (tight junctions, bile canaliculi) and retain several aspects of their functionality over time in culture offering the ability to investigate alterations in cellular structures induced by chemical treatment with classic light microscopy. Furthermore, the increased use of human cells will add additional value to the results.

3.3 Global expression studies with different human and rat cell culture systems

The utility of *in vitro* cultured hepatocytes for toxicological studies is highly dependent on the preservation of biochemical and metabolic functionalities.

The application of novel “-omics” techniques allows the design of new strategies and is expected to be applicable in early screening and mechanism-based risk assessment in toxicology (Stubberfield & Page, 1999; Suter, Babiss & Wheeldon, 2004; Pennie et al., 2000). Recent studies showed the principal applicability of *in vitro* systems in combination with “-omics” technologies to generate valid and useful data concerning hepatotoxicity (Farkas & Tannenbaum, 2005b; Groneberg et al., 2002). However, there is still a need for improving the culturing conditions to increase predictivity and significance of these *in vitro* models (Beigel et al., 2008). The possibility of getting insight into the mechanisms affected by a compound after treatment has to be analyzed against the background of basal gene expression. Additionally, the knowledge of the underlying mechanisms of toxicity is expected to facilitate species extrapolation and to help predict possible risk factors.

Currently, rodent *in vivo* systems are the experimental models of choice, but *in vitro* systems such as primary hepatocytes in SW culture, are now being established and used as replacement or at least as an early screening. For the application of *in vitro* toxicity studies and the interpretation of data generated by toxicogenomic studies *in*

vitro, new aspects have to be considered. As cells are cultured in an artificial environment, it is crucial to be familiar with the basal gene expression for each culture method. Several factors have been suggested to contribute to the phenotype of mature hepatocytes *in vivo*. The concentration gradient of a large number of hormones and other signals, like metabolites and oxygen, transported with the blood flow, allow the cells to detect and respond to the actual physiological status of the body (Sell, 2001; Püschel & Jungermann, 1994). In addition, the tissue architecture and composition (Bedossa & Paradis, 2003; Reid et al., 1992), paracrine signalling and the direct communication with other cell types of the liver (González et al., 2002) affect the metabolic state of hepatocytes. The temporal loss of liver specific functions, the main obstacle of using primary hepatocytes, could be due to the loss of external signals.

In the case of longer-term culture of hepatocytes, the adaptation to the cell culture conditions and the change of gene expression over time has to be carefully considered before starting toxicological studies. The procedure of isolating the hepatocytes has an influence on cellular gene expression and induces inflammatory and dedifferentiation processes (De Smet et al., 1998; Bayad et al., 1991). Further alterations may be introduced by adaptation processes to the culture conditions and by the duration of culture and are highly dependent on the type of culture. Morphological changes over time in culture, as observed in ML culture, are inherently connected to fundamental changes in gene expression.

This study was conducted to gain a better understanding of how varying culture conditions affect gene expression in primary human and rat hepatocytes, to examine the principal applicability for toxicological studies and to select a system of choice for subsequent studies. Functional differences between the different cell cultures relative to the liver were revealed as important for data interpretation. Special emphasis was put on initial changes introduced by the preparation and plating of the cells, the changes over the time in culture and the influence of the overlay with collagen to generate a three dimensional ECM environment. Generally, two types of cell culture, short-term cultures and longer-term cultures, have to be discriminated (Figure 43, Details see Chapter 1.5). Culture methods used for short-term toxicity testing were liver slices and cell suspensions. Whereas the latter is used for metabolic studies for only a few hours (Gebhardt et al., 2003; Cross & Bayliss, 2000), liver slices have been characterized for up to 48h in culture (Lupp, Danz & Müller, 2001). In contrast to isolated hepatocytes, liver slices contain all cell types of the liver and therefore gene expression data will be different to hepatocytes alone. To account for this factor, the whole liver was used as the reference system for liver slices.

Hepatocytes in ML culture and in SW culture were cultured for up to 9 d as already described. In the rat experiments, cells were incubated with (ML+/SW+), or without (ML-/SW-) the addition of serum, human hepatocytes were only cultured without serum. Additionally, the gene expression of an established cell line (for rat FaO cells, for human HepG2 cells) was analyzed. As a new and promising approach, the HepaRG cell line was analyzed. For all isolated cell culture methods, freshly isolated hepatocytes were used as a reference for the change of gene expression over time. Samples were taken and hybridized to either an Illumina RatRef-8 or a HumanRef-6 BeadChip array. All culture conditions and time points were measured in biological triplicates. Data was uploaded into Expressionist[®]Analyst (Genedata), normalized with the LOESS algorithm and analyzed for each culture type separately. Results of the subsequent pathway analyses in MetaCore[™] (GeneGo) were compared across different cultures and time points. Gene expression changes of 45 genes were confirmed with TaqMan RT-PCR.

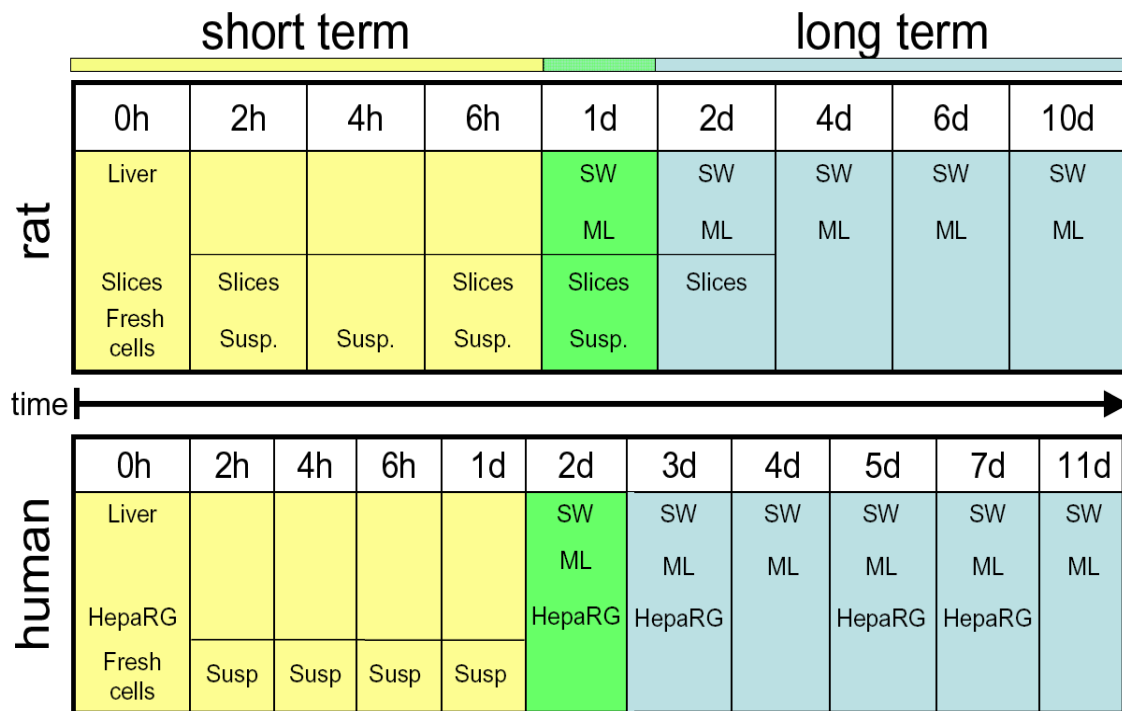


Figure 43: Overview of the different cell culture models used in this study. The time intervals where samples have been taken are specified.

The main goal of all clustering algorithms is to order experiments according to their inter-cluster difference and thereby gaining a logical overview of their relationship to each other. Figure 44 shows a hierarchical clustering of the different culture types conducted with rat and human hepatocytes. It is clear that the gene expression profiles

3 RESULTS AND DISCUSSION

of short term cultures (liver slices and suspension culture) are relatively similar to the liver and freshly isolated cells (blue cluster). Interestingly, the liver slices separated from this cluster already after 6 h. For the long-term rat hepatocyte cultures, a separate cluster was built, which split into three sub-clusters. The first one (green) contains early time points of ML as well as SW cultures. The later time points (4 d until the end of culture) built the second sub-tree of this cluster which in turn can also be subdivided into SW and ML cultures cultured without serum. The third sub-cluster, clearly separated from the other two, was built up from cells cultured with the addition of serum. Two small groups completely separated from all other experiments, cells cultured in ML with serum and the hepatoma cell line (FaO).

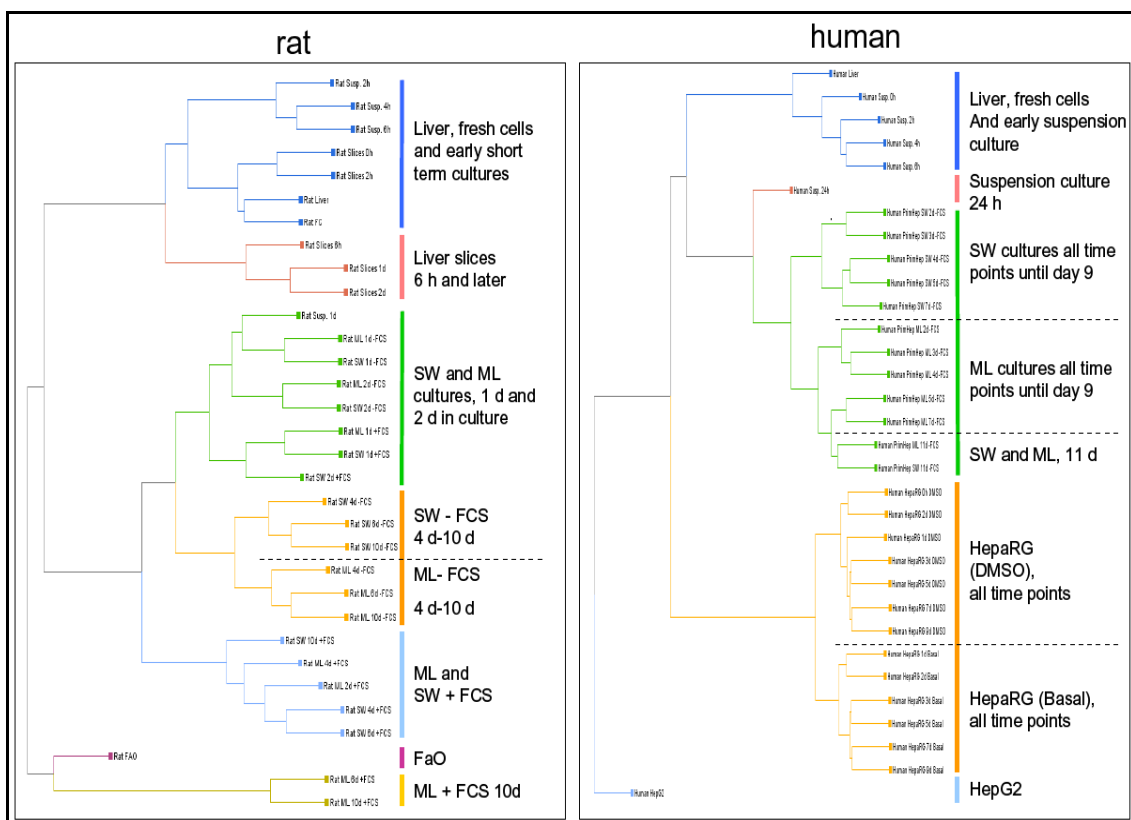


Figure 44: Hierarchical cluster analysis of the different culture types conducted with rat and human hepatocytes. Groups of experiments for each time point and culture type were pooled and are shown here as one data point. The cluster height reflects the inter-cluster difference, the colour of the tree-segments indicate groups of experiments with high concordance in gene expression.

The cluster analysis of human gene expression resulted in slightly different results from the rat analysis. Short-term experiments clustered together with the FC and liver for the initial period of culture and separated after one day in culture (green and red). The ML and SW cultures separated from the other conditions, but as two distinct sub-clusters.

As human hepatocytes showed better stability in gene expression, all time points were grouped together, even after 11 d in culture. The outlier group (light blue) was built from data of the HepG2 cell line. All time points and both culture conditions of HepaRG cells formed one large cluster with two separated sub-clusters, which was much closer to primary hepatocytes than to the other cell line used in these experiments (HepG2).

Given the immense amount of data and the large number of genes found to be deregulated in all of the cell cultures, only general trends are discussed in this chapter. Gene expression changes caused by the different types of cell culture, mechanisms and pathways important for toxicological studies and the liver specific character of hepatocytes will be highlighted.

3.3.1 Initial changes introduced by the process of perfusion

3.3.1.1 Primary rat hepatocytes

Changes in gene expression related to the perfusion itself were analysed by a comparison of freshly isolated hepatocytes (FC) with the liver. 535 Genes were found to be significantly ($p\text{Value} < 0.01$) deregulated more than two-fold, 403 of these were decreased and the expression of the other 132 genes was increased (Appendix 7 and Appendix 8). The higher number of genes being reduced is already an indication for the causative process, as the change of mRNA abundance may reflect more the lack of other cell types with different gene expression than a change of gene expression in hepatocytes themselves. To confirm this hypothesis, these two groups of genes, and the affected pathways and processes, were analyzed (Table 14). Genes found to be down regulated were involved in inflammatory processes, like antigen presentation or interferon signalling, cell-matrix interactions, blood coagulation or angiogenesis. These mechanisms are, at least partially, the task of the other cell types in the liver.

Kupffer cells are resident tissue macrophages, which play a key role in inflammatory processes in the liver. They are able to produce a variety of cytokines, which act in a paracrine manner on hepatocytes (Ramadori & Armbrust, 2001) by binding to highly specific cell-surface receptors. This binding may activate a vast number of intracellular signalling cascades, with clear changes on gene expression. Interleukin 18 (IL18), for example, which was found to be decreased after perfusion, has the potential to activate inflammatory responses and to activate the release of atopic effector molecules, such as histamine, in mast cells and basophiles. IL-18 and IL-12 act synergistically to stimulate natural killer cells to produce IFN-gamma, an immunomodulatory cytokine (Gracie, Robertson & McInnes, 2003). Therefore, endogenous IL-18 plays a major role

in induction of some types of liver injuries in mice and human (Tsutsui et al., 2003). Other inflammation related genes and genes involved in antigen presentation and leukocyte trans-endothelial migration were found to be less abundant after perfusion, indicating the loss of Kupffer cells. Endothelial cells are reported to be actively involved in inflammatory processes (antigen presentation), which was also found to be reduced. The ECM environment of the liver is important not only for cellular attachment but also for intra- and intercellular signalling. *In vivo*, signalling occurs via several molecules produced by the different cell types. Decorin is a small proteoglycan that is able to regulate cell proliferation, migration and different growth factors' activities. It has been reported to be produced by Ito and endothelial cells, but not in hepatocytes and Kupffer cells and to be induced during acute liver damage (Gallai et al., 1996). Here, it was found to be less abundant after perfusion (-7.8-fold). Additionally Type I, Type III and Type IV procollagen expression was found to be reduced, which normally takes place predominantly in nonparenchymal cells (Milani et al., 1989), indicating the absence of cell types producing these collagens.

Down regulated	Up regulated
Cell adhesion; Cell-matrix interactions	Cell cycle; G1-S Interleukin regulation
Proteolysis; ECM remodelling	Reproduction; FSH-beta signalling pathway
Blood coagulation	Signal transduction; ERBB-family signalling
Proteolysis; Connective tissue degradation	Cell cycle; G1-S Growth factor regulation
Cell adhesion; Platelet-endothelium-leucocyte interactions	Signal transduction; Leptin signalling
Development; Blood vessel morphogenesis	Reproduction; GnRH signalling pathway
Apoptosis; Apoptosis mediated by external signals	Inflammation; IL-6 signalling
Proliferation; Negative regulation of cell proliferation	DNA damage-Checkpoint
Inflammation; Interferon signalling	Signal transduction; ESR1-nuclear pathway
Development; Regulation of angiogenesis	Inflammation; Histamine signalling

Table 14: Top 10 ranked GO processes found to be deregulated in relation to the liver after isolation of rat hepatocytes.

Nevertheless, processes such as cell cycle, intracellular signalling pathways or inflammatory processes (e.g. IL-6 and histamine signalling) were found to be induced (Table 14). It is known that hepatocytes are primed for proliferation during isolation (Etienne et al., 1988; Loyer et al., 1996), which could clearly be reflected in this data. Although IL6 was not directly deregulated, pathways and processes induced by IL6 were observed to be induced. IL6 together with IL1 activate the MAPK (mitogen-activated protein kinase) cascades and the JAK/STAT pathway (Heinrich et al., 2003). The activated MAPK pathway is linked to cell cycle progression. Activating the JAK/STAT pathway results in multiple changes in gene expression, as it is involved in the immune response, principal cell fate decisions, regulating the processes of cell proliferation, differentiation and apoptosis.

Altogether, these results show the effective elimination of nonparenchymal cell types. It is important to note that inflammatory processes mediated by these cells will only take place in a limited manner in culture. Although the time from perfusion to sampling was relatively short for rat, some early inflammatory processes could already be detected. This may have been initialized during the perfusion of the liver (via signalling of the still existing nonparenchymal cells). Intracellular signalling pathways connected to inflammation and cell cycle processes were activated in FC, indicated by the up-regulation c-Jun, ATF and Gadd45 d. Changes in cytoskeletal structure and processes concerning ECM remodelling are inherent to the perfusion procedure and can not be overcome.

Liver slices, which were not perfused, retain their original architectural structure and the inherent liver cell heterogeneity with their cell-cell interactions, were directly compared to the liver. At the beginning of culturing (0 h) 1,074 genes were found to be deregulated, 452 were up, 622 down regulated. These genes represented inflammatory responses, response to wounding and several intracellular signalling pathways. Noticeable was the induction of translational processes, but also genes correlated to DNA-damage and signal transduction (related to stress response) were up regulated.

3.3.1.2 Primary human hepatocytes

It is well known that species-specific differences in gene expression and metabolic activity can cause completely different behaviour of the cells in culture (Hengstler et al., 2000; O'Brien, Chan & Silber, 2004; Richert et al., 2002). For a direct comparison, human hepatocytes were observed under the same conditions so that results of global gene expression data were analyzed with regard to similarities and differences to the processes taking place in rat hepatocytes.

Primary human hepatocytes were prepared from pieces of liver obtained from partial lobectomy. The time from operative intervention in the hospital to isolation of the hepatocytes was longer than the “in lab” procedure of rat liver perfusion. Kupffer cells secrete signalling molecules, like TNF α and other cytokines, thereby activating an inflammatory response in hepatocytes. This fact was reflected by additional differences in gene expression.

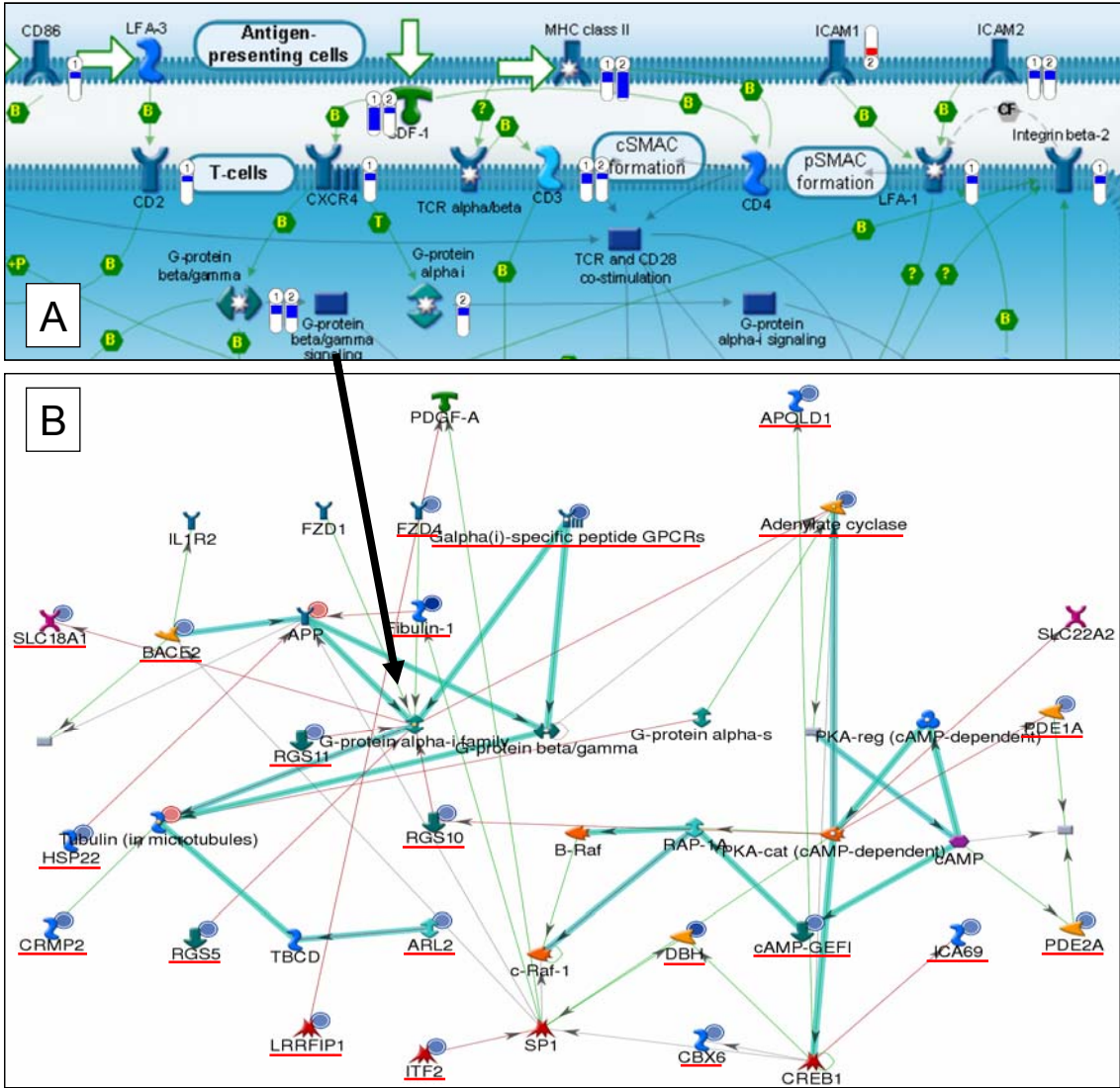


Figure 45: Cellular surface receptors and their connection to cellular signalling. A) Cell-surface related genes and their expression values in freshly isolated hepatocytes in relation to the liver. The fold change is shown as bars (1= rat orthologue; 2= human), blue means down regulated, red means up regulated. B) Network of G protein signalling and cAMP associated genes deregulated after perfusion of liver. The genes underlined in red were found to be reduced in freshly isolated cells.

As expected, the major changes in gene expression between liver and FC resulted from the removal of other hepatic cell types. In particular adhesion molecules, like integrins and cell surface markers, or ECM related genes were found to be significantly reduced. T-cells, for example make brief contact with antigen-presenting cells (APCs) facilitated by chemokines and adhesion molecules, including integrins. The TCR-CD3 (T-cell receptor complex) recognizes the peptide-major histocompatibility complex MHC class II. Integrins like *Itgb2* (Integrin beta2) are then dynamically redistributed to the site of contact. *Cd2*, a cell surface antigen involved in T lymphocyte activation and proliferation was reduced, as was *Cxcr4*, a G_i protein-coupled receptor for the chemokine Sdf-1 (stromal cell-derived factor-1) (Wettschureck & Offermanns, 2005) (Figure 45). Downstream processes of these G_i proteins are coupled via phosphoinositide-specific phospholipase C (PLC-gamma1) (Illenberger et al., 2003) and PI3K (Brock et al., 2003) to intracellular second messenger mechanisms, mediating the immune response and a variety of other intra cellular processes. As an example, a network was built from the down regulated genes, integrating G-protein signalling, cAMP-mediated signalling and the regulation of adenylate cyclase activity, which in turn regulates multiple processes.

Many genes involved in the functional reorganization and biogenesis of the cytoskeleton and ECM remodelling processes were lost. Genes involved in xenobiotic metabolism related processes were also affected.

In contrast to the rat hepatocytes, cell cycle related processes were not found to be induced to a large extent, indicating that no proliferative mechanisms were taking place at this early time point in human hepatocytes. Additionally, stress induced processes were detected resulting in a rise of genes involved in the inflammatory response (Complement system of inflammation). Another difference to the situation in rat was that many genes involved in translational and transcriptional processes were induced, reflecting the reaction of human hepatocytes to an increased need to produce proteins and maybe the longer time to react to the external signals caused by the extended time from dissection to cell isolation. In rats, these processes were found to be deregulated only to a minor degree. Correspondingly, there was an induction of several enzymes responsible for amino acid and energy metabolism, indicating a raised need for energy in the cells.

Interestingly, several major hepatic pathways were induced, including steroid inactivation, the hydroxylation by CYP enzymes and conjugation with glucuronide and sulphate. The induction of steroid biotransformation enzymes is partly mediated as a feedback loop through a group of nuclear receptors, including the glucocorticoid receptor (GR), the constitutive androstane receptor (CAR), the pregnane X receptor

(PXR), and the peroxisome proliferator activated receptors (PPARs) (You, 2004). These transcription factors also have important roles in regulation of liver specific gene expression and xenobiotic metabolism. Additionally, GR activation has immunosuppressive abilities by preventing the transcription of immune related genes and leads to increased plasma amino acids (Hayashi et al., 2004).

Down regulated	Up regulated
Cell adhesion; Cell-matrix interactions	Translation initiation
Cell adhesion; Platelet-endothelium-leucocyte interactions	Proteolysis; Ubiquitin-proteosomal proteolysis
Cytoskeleton; Actin filaments	Response to hypoxia and oxidative stress
Cytoskeleton; Regulation of rearrangement	Proteolysis in cell cycle and apoptosis
Development; Neurogenesis: Axonal guidance	Translation in mitochondria
Proteolysis; ECM remodelling	Inflammation; Complement system
Proteolysis; Connective tissue degradation	Translation; Elongation-termination
Cell adhesion; Leucocyte chemotaxis	Transcription; mRNA processing
Inflammation; Histamine signalling	Transport; Iron transport
Cell adhesion; Integrin-mediated cell-matrix adhesion	Transport; Manganese transport

Table 15: Top 10 ranked GO processes found to be deregulated in relation to the liver after isolation of human hepatocytes

3.3.2 Temporal changes in global gene expression

For a full characterization of the impact of culture conditions on the behavior and functionality of hepatocytes over time, transcriptional changes were analyzed globally across the complete dataset. Therefore, fold-changes and statistical significance were calculated in relation to the particular starting points of the culture, which was defined as the reference sample (Appendix 3 and Appendix 4). For the short term culture methods, such as liver slices and suspension cultures, reference samples were defined as the 0 h time point after isolation, which means freshly cut liver slices or freshly isolated hepatocytes, respectively. The latter was used to eliminate the background of gene expression changes due to the lack of other cell types.

As previously described, the process of isolating hepatocytes caused a large number of gene expression changes which, at least in part, can be considered as common and therefore are present in all types of cultures. Consequently, the 1 d time point after plating was defined as the starting point for the longer term culture methods. The initial

changes were thereby excluded from the analysis and evaluated separately. Due to the fact that the human hepatocytes were prepared and plated in France, the first time point analyzed, 2 d after perfusion, was used as the reference sample.

Short term cultures generally showed a high correlation to their reference experiments (Figure 46). This is true not only for the liver slices, which still contain all liver-typical cells, but also for the hepatocyte suspension cultures. Major effects were first detected after 6 h for liver slices and suspension cultures and after 1 day in culture, clear differences were seen. After one day, the gene expression in both cultures was measurably different to controls correlating with the decline in viability observed for these cells.

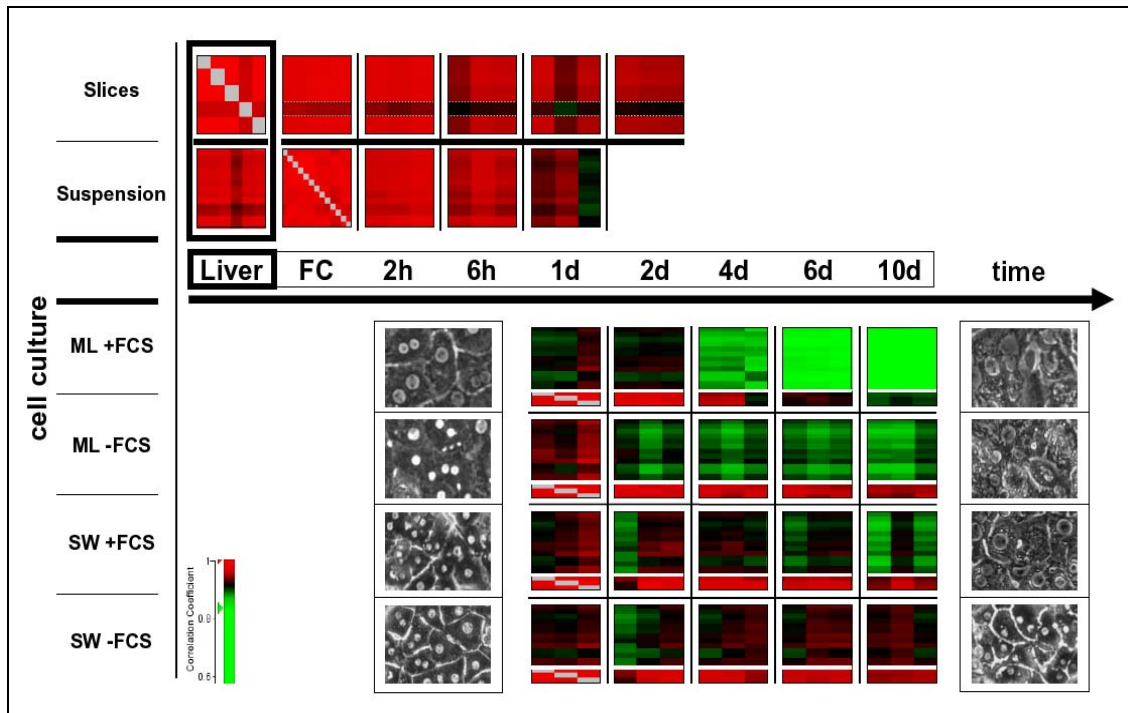


Figure 46: Heat maps of the correlation coefficients of rat cell culture experiments compared to the reference system over time. Each square in a column or line represents the gene expression correlation of a given sample at a certain time point (arrow) relative to the reference experiments. The intensity-changes in global gene expression were used as the basis for the calculation of the correlation. Long-term experiments were split: the upper part of the square shows the correlation of the experiments to freshly isolated cells, the lower part indicates the correlation to the 1 d sample, which was defined as the reference experiment for later analyses. Red squares indicate high correlation (>0.9), whereas green indicates a low correlation. The pictures show cells of each longer-term culture at day one (left) and day 10 (right) of culture.

The longer term cultures were compared to FC as well as to cells in culture for one day. Shown in the lower part of Figure 46 are the heat maps visualizing the correlations between each time point and FC (above white line in each square) and day one of culture (below white line in each square). A reduction of the correlation coefficient, visualized by a shift from red to black to green, indicates significant changes in global gene expression in comparison to the references. For all cultures, by day one a reduced correlation was seen, although it was most pronounced in ML+FCS. As shown in the previous chapter, the initial changes introduced by the elimination of other cell types and the initial adaptation processes are likely to cause similar changes in all types of cultures.

The correlation coefficient of ML+FCS cultured cells decreased over time when compared with gene expression in FC and with cells one day in culture, reflecting the advancing dedifferentiation processes. This result perfectly correlates to the morphological analyzes described before with no stabilization of gene expression detected.

The removal of FCS from the culture media and the addition of Dex improved the correlations. The extent of initial changes was reduced and processes moving the cells away from hepatocyte-like gene expression were significantly slowed down, at least globally, after two days in culture. Until the end of culture, the gene expression of these cells showed more stability. As the aim of toxicogenomics is the detection of gene expression changes caused by compound treatment, it is important, especially *for in vitro* models, to reduce the background of genes changing due to other factors, such as the culturing, to a minimum.

Cells cultured in SW in the presence of serum showed the initial changes which were less pronounced compared to ML+FCS. Globally, the cells remained in this state until day four. Afterwards, a reduction of the gene expression correlation coefficient was detected. This process was intensified at later time points indicating the onset of dedifferentiation in these cells.

In SW culture without serum the addition of Dex had additionally positive effects on global gene expression. The gene expression changes due to the isolation process and adaptation to the culture environment, although still quite high, were least pronounced and global gene expression over time was most stable of all cultures tested. From two days in culture until the end of the culture, an increase in correlation to FC was observed suggesting some regenerative processes were taking place in these cells.

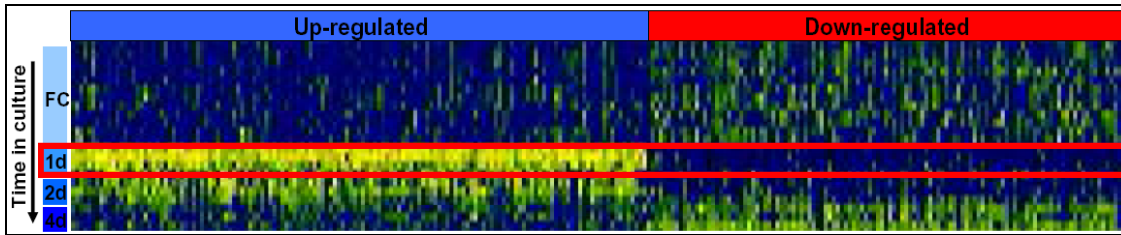


Figure 47: Heat map of genes transiently deregulated one day after perfusion in sandwich culture without serum.

Genes found to be transiently deregulated after one day in culture and returning to their original expression level (Figure 47) were mainly genes known to be involved in early stress response, inflammatory mechanisms and intracellular signalling. Networks built from these specifically deregulated genes (confidence of 95% to be only deregulated at 1 d in SW-FCS) confirmed these findings but also showed a link to the regulation of fatty acid biosynthetic processes (Table 16). The expression of the PPARs was reduced 1.8-fold. This transcription factor is known for its ability to induce gluconeogenesis and to reduce fatty acid β -oxidation.

Processes	Size	Target	p-Value
immune system process (40.0%), V(D)J recombination (7.5%), nitric oxide transport (5.0%)	50	10	1.05e-21
protein kinase cascade (44.0%), stress-activated protein kinase signaling pathway (26.0%), protein amino acid phosphorylation (44.0%)	50	10	1.64e-21
fatty acid biosynthetic process (23.1%), carboxylic acid biosynthetic process (23.1%), organic acid biosynthetic process (23.1%)	50	8	8.45e-18
regulation of biosynthetic process (20.6%), regulation of cellular biosynthetic process (20.6%), biological regulation (79.4%)	50	9	2.35e-19
response to stress (65.1%), positive regulation of cellular metabolic process (46.5%), positive regulation of metabolic process (46.5%)	50	8	7.23e-17

Table 16: Top five networks highly enriched with genes found to be deregulated only at day one in SW-FCS cultured hepatocytes. “Size” refers to the number of network objects contained and “Target” is the number of affected objects contained in these networks.

Figure 48 shows the correlation of global gene expression for the different human cell cultures tested. Again, the short term suspension culture retained liver specific gene expression only for a short time. After 6 h, global gene expression was still hepatocyte-like, but after this time point a rapid change was detected.

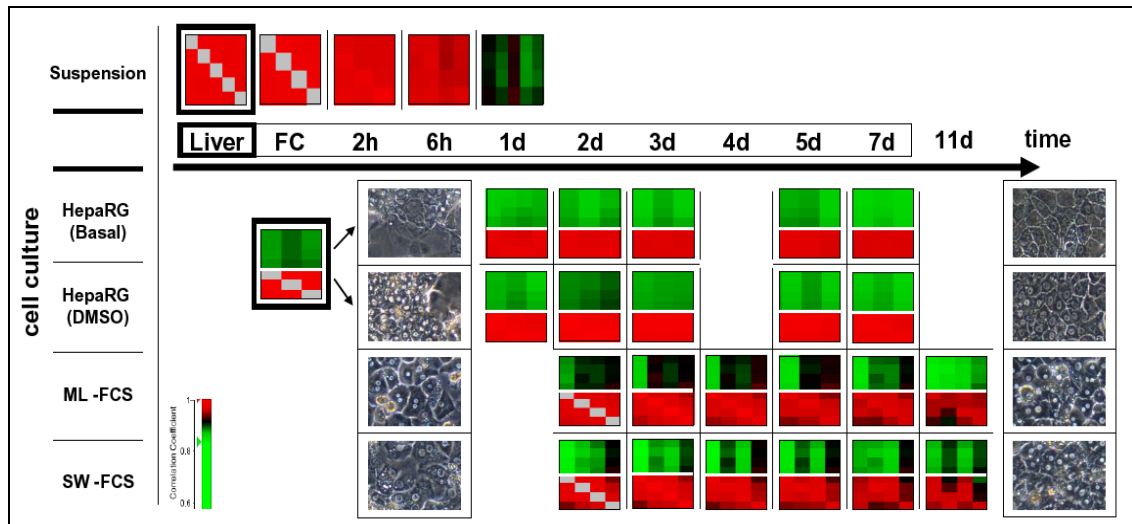


Figure 48: Heat maps of the correlation coefficients of human cell culture experiments to their reference systems over time. Experiments were ordered according to the time scale (big arrow) and separated into short- and long-term experiments. The intensity-changes in global gene expression were used as the basis for the calculation of the correlation. Long-term experiments are split up; the upper part of the square shows the correlation of the experiments to freshly isolated cells, the lower part indicates the correlation to the status 1 d after plating which was defined as the reference experiment for later analyses. Red squares indicate high correlation, green indicate low correlation. The pictures show cells of each longer-term culture at day one (left) and day 10 (right) of culture.

The results of the long term cultures displayed differences from the results gained with rat hepatocytes. Due to technical reasons, the 2 d time point was the first sample to be taken and therefore this was defined as a second reference, together with FC. For ML and SW cultures, a distinctly worse correlation was detected at the initial time points. This change of gene expression was less pronounced in ML culture indicating a greater stability of these cells. Over time, both cultures demonstrated only minor changes pointing to a generally better stability of gene expression in human cells compared with the situation in rat. Another source of variance when working with primary human cells is the large inter-individual donor difference. Both the basal gene expression and the individual reactions of the cells can be remarkably different. This was confirmed by our data. Four different donors were clearly differentiated, based on their gene expression and the extent of gene expression changes over time (Figure 48 ML and SW). The correlation “in-between” donors at a certain time point was 0.97 for primary cultured human hepatocytes. For the suspension culture, the level of correlation between different time points was in the same range (0.95). Therefore, genes found to be differentially deregulated may be influenced more by donor specificity than by time in culture.

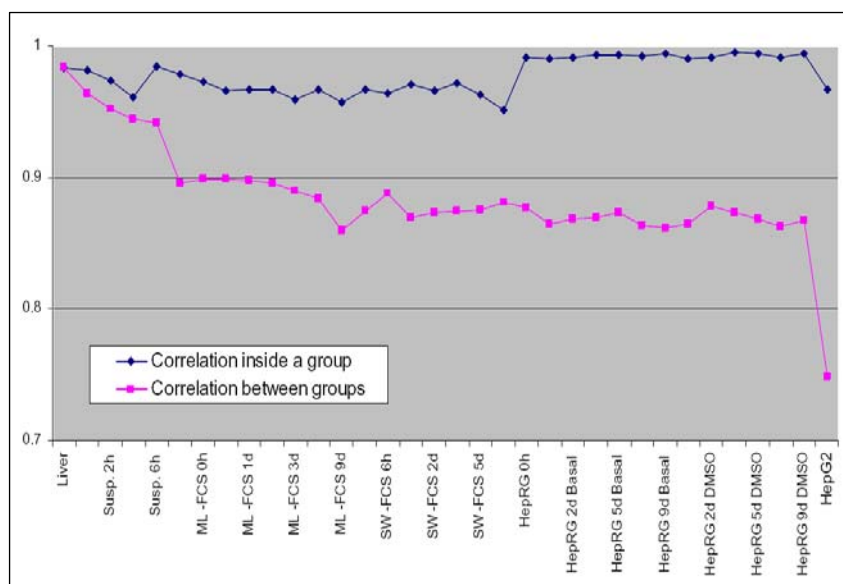


Figure 49: Plot of intra group and inter group correlation coefficients of human hepatocyte cultures.

Experiments with primary human hepatocytes should be carefully analyzed with respect to donor specific gene expression. If possible, more than three biological replicates should be included to ensure that general biological trends are visible above any individual variances.

For both rat and human, the established cell lines (FaO and HepG2, respectively) were found to vary greatly from primary cells, showing many differences in global gene expression. Another cell line, the recently established HepaRG, showed a high stability of gene expression over time. Additionally, the gene expression was closer to that of primary human hepatocytes than that of HepG2 cells. Large differences were detected compared to FC, maybe due to the lack of inter-individual differences and the increased stability of gene expression over time in culture. These cells may therefore be a suitable experimental system for toxicogenomics studies. Further analyses have to be conducted, including the monitoring of the existence of certain metabolic enzymes, which allows liver-like metabolism in these cells (chapter 3.3.6.4).

3.3.3 Analysis of protein expression with SELDI-TOF

Proteins, as the effector-molecules in cells, are dependent not only on the amount of transcribed mRNA but also on multiple post-transcriptional and translational mechanisms. It is well known that the amount of a protein is not necessarily correlated with the gene expression (Gygi et al., 1999; Chen et al., 2002). To study if gene expression changes during culture of primary hepatocytes translated into differences in protein expression studies were conducted using the SELDI technology. The abundance of certain protein masses in ML-FCS and SW-FCS cultured primary rat hepatocytes were measured and analyzed (Figure 50).

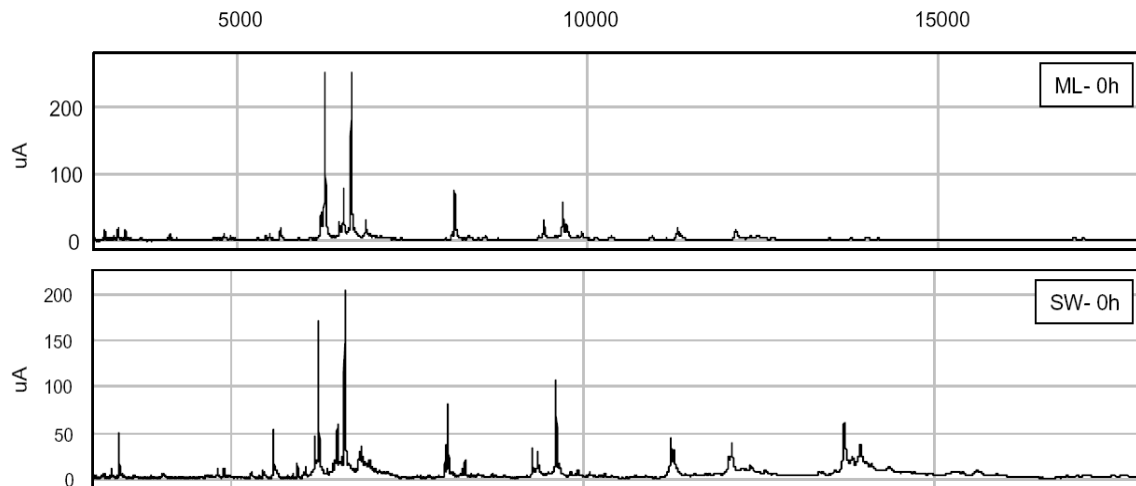


Figure 50: Representative SELDI-spectra detected by analysis of protein samples of either ML-FCS (upper spectrum) or SW-FCS (lower spectrum) cultured rat hepatocytes. Four biological replicates were measured per time point and culture condition and subsequently analyzed for changes over time.

The ProteinChip CM10 array was used to bind and detect positively charged proteins. A hierarchical clustering based on significant mass-ion-peaks detected within the spectra showed a clear separation of early (0 h – 1 d) and late (3 d – 9 d) time points for both culture types. Inside both clusters, individual time points were partially separated. To improve discrimination, only mass-ion-peaks which were significant in all spectra of all animals were identified and chosen as the basis for further analysis. This resulted in 33 mass-ion-peaks for ML-FCS cultured cells, and 26 for SW-FCS. Time points were analyzed for changes in peak intensity separately and compared to the protein profile of freshly isolated cells. Although the resulting heat map representing the correlation of the protein expression to the reference (Figure 51 A) shows no clear separation of ML-FCS and SW-FCS, more severe changes in protein expression were detected in ML-FCS indicated by the stronger colours representing positive or negative changes in correlation.

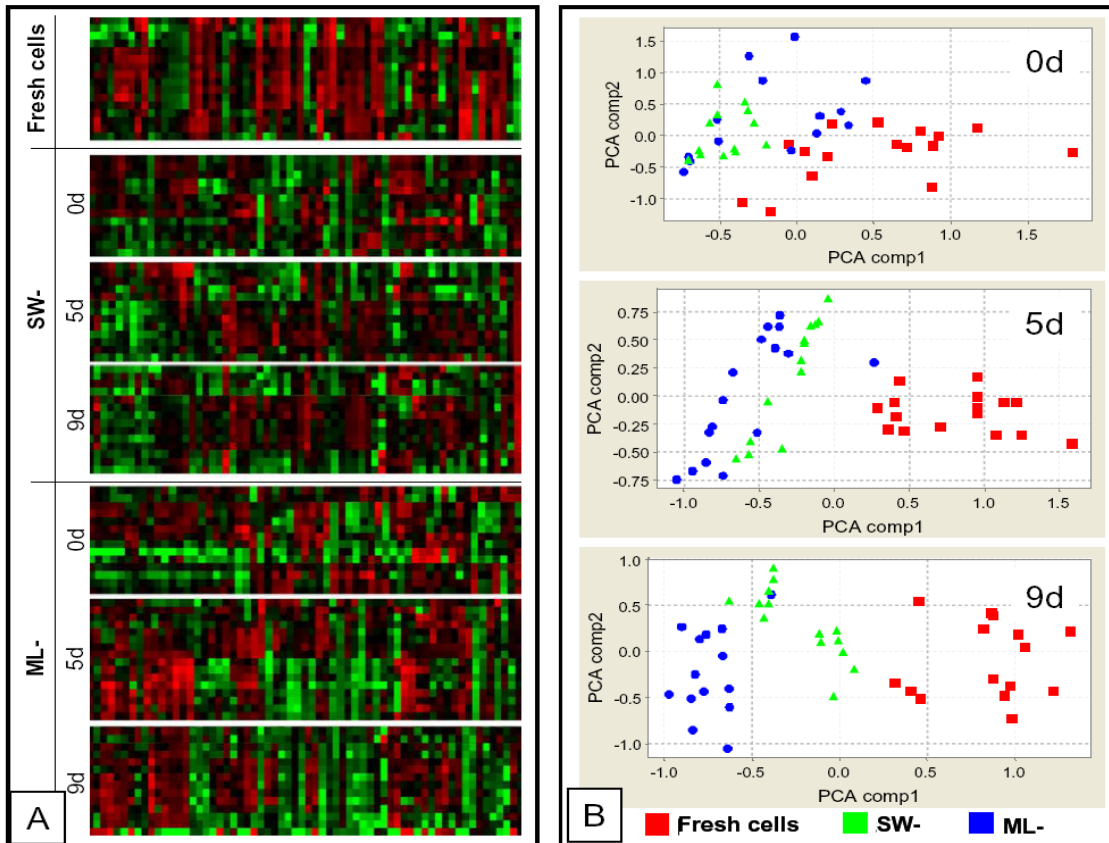


Figure 51: A) Correlation map of 59 mass-ion-peaks detected in samples of ML-FCS and SW-FCS cultured cells. Green resembles a low and red a high correlation to the reference spectrum. B) Two-dimensional PCAs computed by using the SELDI-Spectra analysis of technical replicate measurements of four biological replicates.

Shown in Figure 51B are two-dimensional PCAs, demonstrating the spread of the data within each experiment. At early time points, differences between cell cultures and freshly isolated cells were less pronounced and therefore the data clouds overlapped. FC were only slightly separated and ML-FCS cultures tended to be located closer to FC than SW-FCS cultures, although this result was not statistically significant. At later time points, clouds separated as individual groups. After 5 d in culture, the protein expression of SW-FCS cultured cells was closer to FC than ML-FCS cultured cells. This effect was enforced after 9 d in culture, protein expression of SW-FCS cultured cells was detected to be less changed and therefore to be more hepatocyte like than the continuously changing protein expression of ML-FCS cultured cells.

Although protein profiling does not allow an exact identification of the proteins underlying the 59 mass-ion-peaks, these results fit well with the results of gene expression, which indicated changes at early time points in culture and a greater stability of SW-FCS cultured cells. Improvements of the SELDI technology, to allow identification of single peaks and to improve the sensitivity of peak detection, will

further enhance the usability and utility of this technique for identifying protein patterns. By combining both genomic and proteomic approaches, possibilities to further elucidate mechanisms of toxicity using cultured primary hepatocytes will be improved.

3.3.4 Gene expression in established cell lines used as reference

The gene expression in established cell lines was compared to FC. FaO is a rat hepatoma cell line with a hepatocyte like phenotype. Some liver-specific enzymes and liver-enriched transcription factors were found to be expressed, although in lower abundance (Clayton, Weiss & Darnell, 1985) than *in vivo*. It has been used for mechanistic analyses for PPARalpha target genes and the induction of apoptosis (König & Eder, 2006; Coyle et al., 2003), lipid metabolism (Latruffe et al., 2000) or CYP expression studies (Hakkola, Hu & Sundberg, 2003).

In comparison to FC, substantial differences in gene expression were detected, 4952 genes were differentially expressed in this cell line. Of the 2951 down regulated genes, many were involved in the regulation of lipid metabolism, MAPK signalling, metabolism of xenobiotics by cytochrome P450 and several important metabolic pathways. Additionally, cellular adhesion was found to be impaired, implying that the cells are less responsive to extracellular stimuli. It's not surprising that many of the higher expressed genes were involved in cell cycle progression and DNA replication, but also several intracellular signalling cascades, like the ERK, Wnt, Insulin and ErbB pathways, showed increased expression.

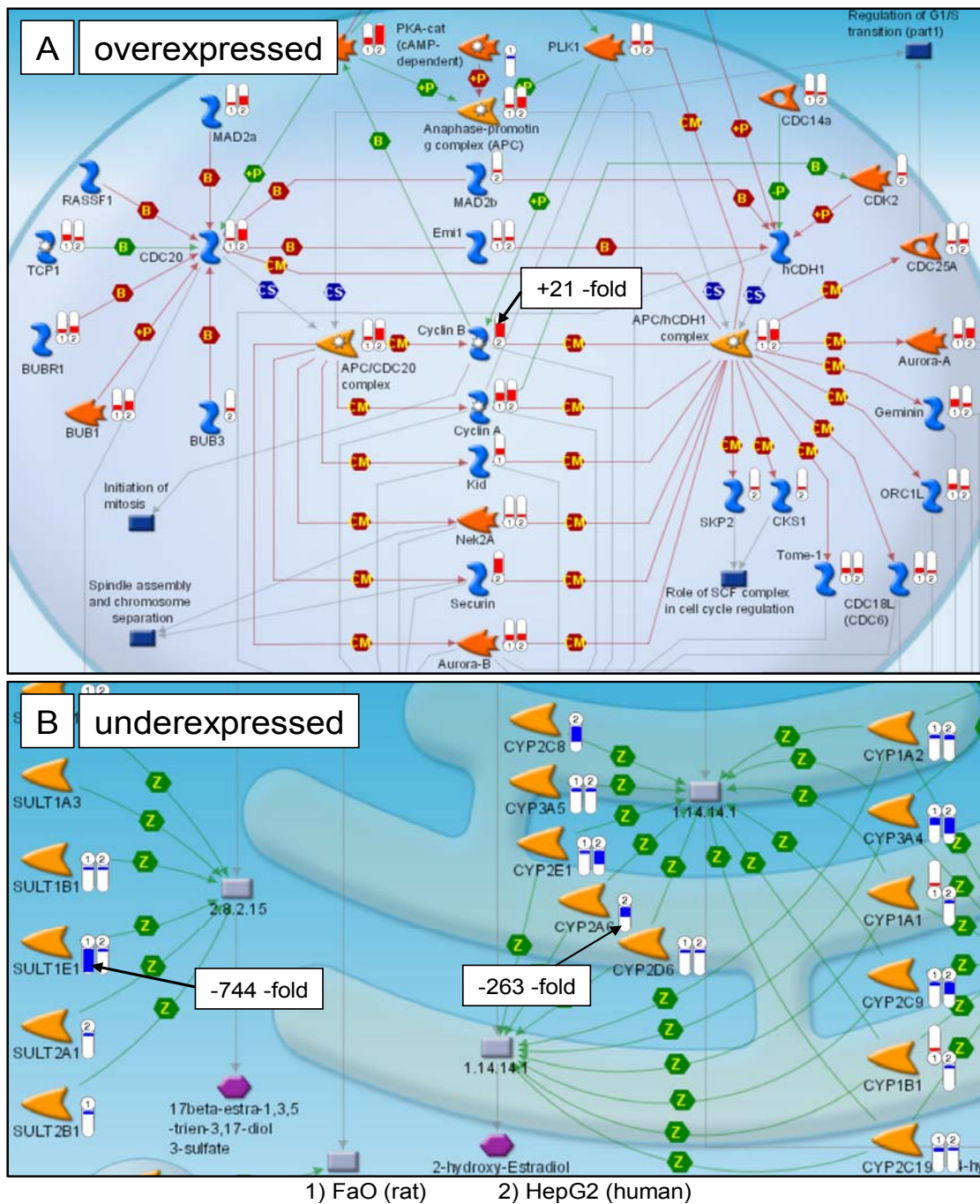


Figure 52: Example of canonical pathway maps showing over and underexpressed genes in the stable cell lines FaO (rat) or HepG2 (human). A) Detail of the anaphase promoting complex (APC). B) Detail of the estradiol metabolism pathway (modified from Metacore, GeneGO).

The human hepatoma derived HepG2 cell line, analogous to the FaO cells, is often used for mechanistic studies, although there is only poor predictivity to the *in vivo* situation (Brandon et al., 2003; Knasmüller et al., 2004). Some differences in gene expression to FaO cells (rat) were detected, however the predominant tendencies were

found to be similar. Cell cycle related genes and adhesion molecules were overexpressed and genes involved in cellular differentiation, especially intracellular signalling and xenobiotic metabolism, were deregulated.

Figure 52A shows the anaphase promoting complex (APC), which is an important regulator of cell cycle progression, which targets the mitotic cyclins for degradation. This, and several other cell cycle related proteins, was found to be overexpressed in both cell types. Figure 52B depicts the estrogen metabolism pathway including many repressed genes, which also play important roles in xenobiotic metabolism.

Taken together, pronounced differences in many of the cellular mechanisms were detected in both established cell lines. It must be assumed that these changes have severe consequences on cellular mechanisms and therefore also on liver specific functionality. Toxicity experiments conducted in either one of these cell lines should therefore be carefully planned and the data generated treated with caution. Additionally, there is a need for knowledge about the metabolism of any test compound. Extrapolation to the *in vivo* situation has to be performed very carefully to circumvent misinterpretation. These cell lines should be used only for special toxicological questions and results should be interpreted against the background of reduced metabolic activity and altered intracellular signalling leading to non-physiological reactions.

3.3.5 Changes of gene expression early in culture - Cellular adaptation processes in primary hepatocytes

It has been shown that the most dramatic change in gene expression occurs during the first day of culturing (our data, Beigel et al., 2008). To review this processes taking place in cultured hepatocytes, the initial changes of gene expression on the first day after plating were studied separately. The gene expression of freshly isolated cells was compared to the gene expression of cells cultured for one day in either SW or ML culture with or without the addition of serum. To obtain relevant results, commonly affected genes were selected and processes taking place in all types of culture were analyzed.

As can be seen in Table 17, more than 50% (1,838) of genes were commonly deregulated in all four types of cell culture. This remarkably high percentage indicates common processes which are ongoing and are probably due to the isolation of cells and general adaptation processes to the new environment. Many of these processes are of course independent from the culture conditions.

Culture system	Overall	Down regulated	Up regulated
ML culture + FCS	3780	1681	2099
ML culture - FCS	3025	1612	1413
SW culture + FCS	3112	1650	1462
SW culture - FCS	3621	1920	1701

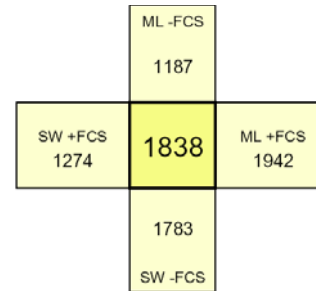


Table 17: Number of genes deregulated after one day in culture. The Venn-diagram on the right side shows the overlap of the overall-gene lists. 1,838 Genes were commonly deregulated and used for further analyses.

To further analyze these common mechanisms and highlight any differences in the adaptation processes between different culture conditions, genes differentially expressed compared to FC in any of the cultures were chosen. Table 18 shows the top 10 canonical pathways affected by the adaptation process.

Among the most affected pathways, amino acid and energy metabolism were ranked at the top, indicating a reduction of amino acid synthesis. Two processes may contribute to this effect. First, hepatocytes are very metabolically active cells *in vivo*, with a large number of proteins produced and secreted into the system. The lack of external signalling may lead to a reduction in these processes, thereby slowing down the synthesis rate and therefore the high need for the production of amino acids is reduced. Second, at least parts of these pathways were induced by the perfusion process and their reduction after 1 d in culture can therefore be seen as a recovery process by returning to their original (lower) expression levels.

The top ranked down-regulated pathway was the regulation of lipid metabolism via several transcription factors. This is of importance because the lipid metabolism is not only closely related to xenobiotic metabolism, but also these transcription factors are responsible for the induction of several enzymes involved in metabolism, cell cycle and inhibition of apoptosis (Latruffe et al., 2000; Kersten et al., 2001; Kliewer et al., 1999). Additionally, fatty acids themselves have the ability to bind to transcription factors and therefore influence the overall gene expression of the cells (Wolfrum & Spener, 2000; Wolfrum et al., 2001; Sampath & Ntambi, 2004). Other processes found to be negatively affected were inflammation-related, such as parts of the complement system, the kallikrein-kinin system, both of which depend on blood circulating proteins and therefore were expected to be reduced.

Down regulated	Up regulated
Regulation of lipid metabolism via PPAR, RXR and VDR	Cytoskeleton remodelling
Glycine, serine, cysteine and threonine metabolism	Cell adhesion; Integrin mediated cell adhesion
Leucine, isoleucine and valine metabolism	Role of tetraspanins in the integrin-mediated cell adhesion
Alanine, cysteine and L-methionine metabolism	TGF, Wnt and cytoskeletal remodelling
Oxidative phosphorylation	Endothelial cell contacts by non junctional mechanisms
Peroxisomal branched chain fatty acid metabolism	Signal transduction; Akt signalling
Propionate metabolism	Regulation of actin cytoskeleton by Rho GTPases
Tryptophan metabolism	Transcription; Role of Akt in hypoxia induced HIF1 activation
Mitochondrial ketone bodies biosynthesis and metabolism	Fibronectin-binding integrins in cell motility
Immune response; Lectin induced complement pathway	Translation; Insulin regulation of protein synthesis

Table 18: Top 10 canonical pathways affected by genes commonly deregulated as part of the adaptation process to cell culture.

The pathways found to be heavily induced were involved in cellular adhesion, cytoskeletal remodelling and the corresponding intracellular signalling dependent on these processes. After perfusion, the cells have to adhere to the surface of the culture dishes and to rebuild cellular contacts. Along with this, the reestablishment of their polarization and their polygonal shape is going on. All these processes require cytoskeletal remodelling and are known to influence gene expression, especially integrins. These transmembrane molecules are not only connected to the cytoskeleton but also to intracellular signalling mechanisms, again directly influencing gene expression (Stupack, 2007; Giancotti & Ruoslahti, 1999; Giancotti & Tarone, 2003; Häussinger, Reinehr & Schliess 2006). AKT signalling, for example, is downstream of integrin mediated signalling and influences cell adhesion and intracellular structural protein formation. Figure 53 shows the induction of several genes involved in this pathway.

Interestingly, several inflammatory pathways were induced indicating that hepatocytes themselves are partially capable of initiating an inflammatory response alone. The Jak-

Stat pathway is known to be initiated through certain cytokines, like IL-6, which is one of the most important mediators of the acute phase response. Although the initial signal, IL-6, is secreted by macrophages; downstream receptor mediated events take place in other cell types.

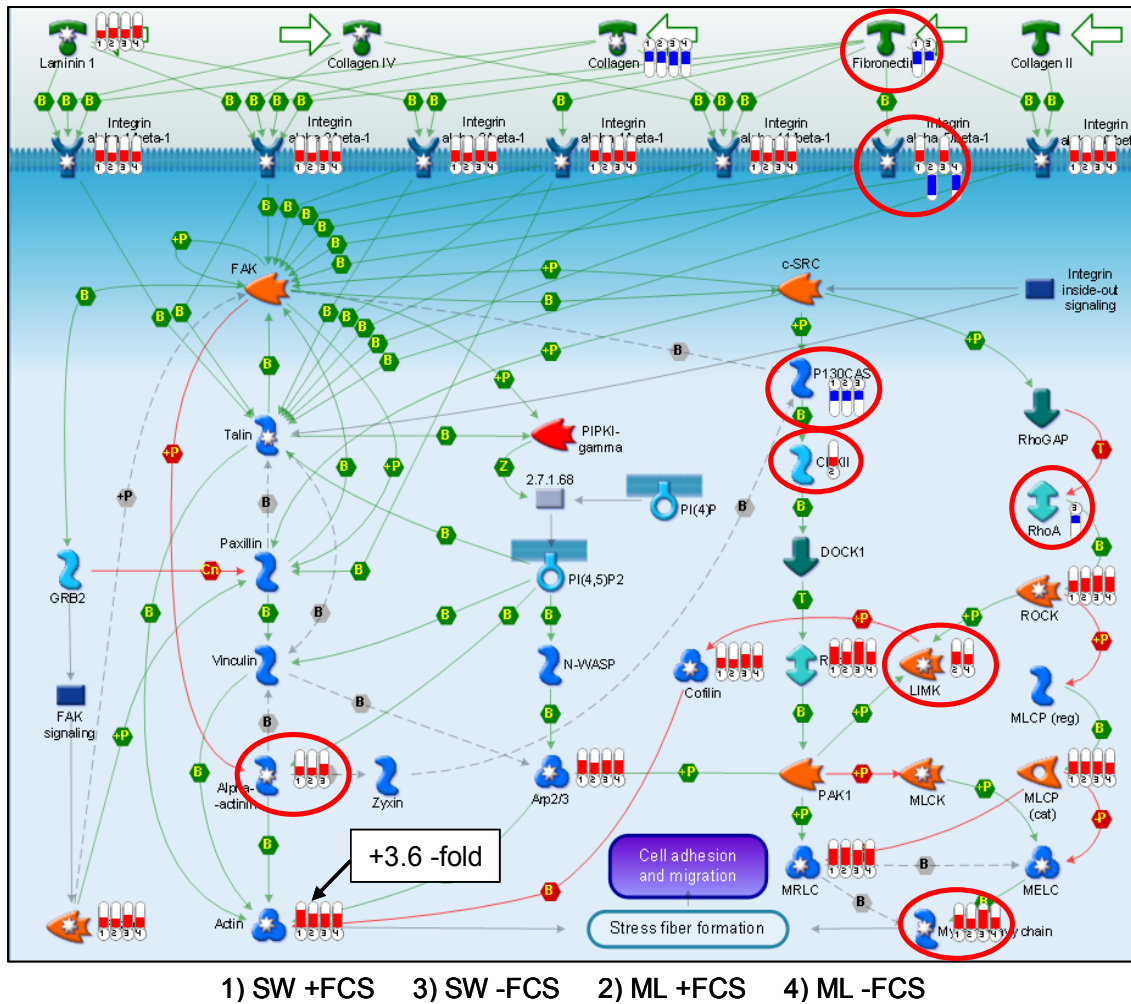


Figure 53: Canonical pathway map showing the changes in the expression of genes involved in signal transduction by AKT signalling. Red bars indicate induction, blue bars the repression of gene expression. Red circles indicate genes found to vary in expression between the different types of culturing on day one (modified from Metacore, GeneGO).

The previous results reported in this work showed that the SW culture without the addition of serum both, morphologically and in terms of global gene expression, conserved best the *in vivo* situation of the liver. At this early time point (1 d), the differences between the cell cultures were only minor with none of the top ranked pathways or processes being affected in one and not in the other cell cultures. The differences were restricted to the degree of expression changes of a gene between the cultures and to single genes found in only one sample. This may be explained by the

cut-off values selected, which filtered genes expressed just below in one sample whereas they pass in other samples. Therefore, the initial processes can be considered as common to all cultures, only the extent can be influenced by the type of cell culture. About 46% of genes found to be more than 1.5 fold deregulated in either ML-FCS or SW-FCS cultures, (pValue <0.05) were found to be deregulated just below this level in the other cultures (Table 19). These results illustrate a central problem in the analysis of global gene expression. The setting of cut-off values is always correlated with a loss of information, which in turn may be biologically important. Different approaches have been proposed to overcome this drawback (Guo et al., 2006; Chen et al., 2007).

These specifically filtered genes play important roles in cellular fate. Mbtps1, a serine protease that cleaves ER membrane-bound sterol regulatory element-binding proteins (SREBPs), plays a central role in the regulation of lipid metabolism. This transcriptionally active fragment of SREBP is released from the membrane for translocation to the nucleus. Hsbp1 may be involved in the stabilization or repair of cytoskeletal elements and Bcl2l11 and Bcl2l2 both belong to the BCL-2 protein family, the first promoting and the latter inhibiting apoptosis.

Name	Description	pValue SW-FCS	Fold-Change SW-FCS	pValue ML-FCS	Fold-Change ML-FCS
Mbtps1	Membrane-bound transcription factor protease	3.84E-04	-2.19	4.64E-02	-1.47
Ca3	Carbonic anhydrase 3	2.52E-02	-1.34	8.16E-04	-1.61
Ilkap	Integrin-linked kinase-associated serine/threonine phosphatase 2C	9.73E-05	-1.51	1.24E-03	-1.33
Hsbp1	Heat shock factor binding protein 1	7.86E-07	-1.86	5.48E-04	-1.39
Mt3	Metallothionein 3	3.81E-06	1.63	1.57E-03	1.42
lkbkap	Inhibitor of kappa light polypeptide enhancer in B-cells, kinase complex-associated protein	6.55E-03	1.39	9.51E-05	1.74
Arnt	Aryl hydrocarbon receptor nuclear translocator	6.17E-06	2.38	4.73E-03	1.34
Tsg101	Tumor susceptibility gene 101	2.59E-03	1.42	1.55E-04	1.60
Edn1	Endothelin 1	2.57E-03	1.30	6.18E-05	1.57
Creb1	cAMP responsive element binding protein 1	6.15E-05	1.48	3.23E-06	1.61
Bcl2l11	BCL2-like 11 (apoptosis facilitator)	5.52E-07	1.59	8.07E-09	1.48
Bcl2l2	Bcl2-like 2	2.75E-07	1.75	2.42E-03	1.47

Table 19: Selection of genes found to be filtered out in either SW –FCS or ML –FCS due to just one value not fulfilling the cut off values.

3.3.5.1 Liver slices

When analyzing the gene expression changes over time in relation to the reference experiment, the 6 h time point showed especially striking results in liver slices. Whereas in all other culture systems the number of deregulated genes increased continuously over time, the maximum of 1824 genes was deregulated at 6 h in liver slices (Figure 54). After this peak, the number of deregulated genes significantly declined, implicating a transient mechanism only active for the first few hours in culture. The 790 genes affected only at this certain time point (Figure 54) were filtered out and analyzed for mechanistic function.

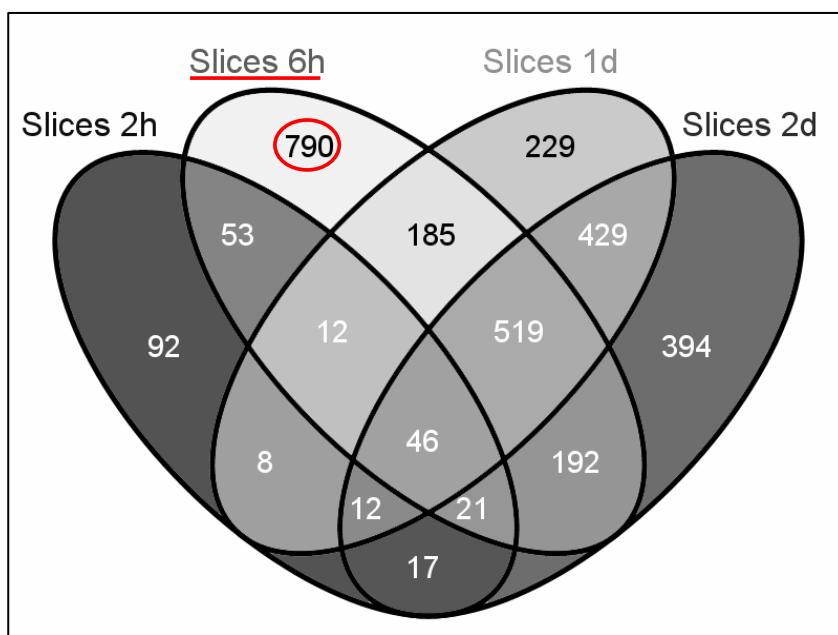


Figure 54: Venn-diagram of deregulated genes at certain time points. The number of genes in each overlapping segment indicates genes commonly deregulated in these experiments. The red circle indicates the number of genes only deregulated 6 h after culturing.

Many of the genes induced were involved in chemotaxis, inflammatory response, cell adhesion and downstream signalling. These are processes which normally take place because of wounding, cellular stress or other pro-inflammatory stimuli activating cytokine signalling. Indeed, several cytokines were found to be heavily up regulated indicating a strong influence of activated Kupffer cells on gene expression.

Table 20 shows the top ranked networks built with genes commonly deregulated in liver slices with the percentage of certain cellular processes indicated in parentheses. Networks showing mostly down-regulated genes showed affects on several mechanisms concerning cellular biosynthetic processes, metabolism and replication. Interestingly, an apoptotic mechanism, the activation of caspase via cytochrome c, was reduced which contradicts the general trend of induced cellular stress. This indicates the delicate balance of regulation of apoptotic processes in cells with several pro- and anti-apoptotic mechanisms taking place simultaneously.

common down regulated	p-Value	common up regulated	p-Value
neurotransmitter metabolic process (13.6%), nitrogen compound metabolic process (27.3%), ketone body biosynthetic process (4.5%)	2.54E-32	small GTPase mediated signal transduction (29.5%), cell morphogenesis (40.9%), cellular structure morphogenesis (40.9%)	6.65E-08
response to chemical stimulus (36.8%), protein export from nucleus (10.5%), male somatic sex determination (5.3%)	9.87E-26	cell-matrix adhesion (18.4%), cell-substrate adhesion (18.4%), cell adhesion (28.9%)	8.7E-30
caspase activation via cytochrome c (13.3%), apoptotic program (23.3%), complement activation (16.7%)	1.15E-26	response to stress (44.7%), biological regulation (74.5%), response to external stimulus (29.8%)	2.64E-26
phosphoinositide-mediated signalling (25.0%), G-protein signalling, coupled to IP3 second messenger (phospholipase C activating) (21.4%), positive regulation of protein kinase activity (25.0%)	5.6E-18	wound healing (20.5%), blood coagulation (15.9%), coagulation (15.9%)	2.49E-22
chromatin silencing at telomere (8.0%), telomeric heterochromatin formation (8.0%), chromatin silencing at rDNA (8.0%)	8.19E-20	chemotaxis (37.5%), taxis (37.5%), locomotory behavior (39.6%)	1.57E-14

Table 20: Cellular mechanisms affected by time induced gene expression changes in liver slices.

Building the networks based on the 790 genes specifically deregulated after 6 h principally confirmed the results of the time course analysis with the induction of inflammatory response, stress-activated protein kinase signalling and the induction of the cell cycle as a signal for the start of early regenerative processes taking place. Simultaneously, the expression of genes involved in nucleic and amino acid metabolism was clearly reduced which may be a consequence of oxidative stress. This is a major cause of liver damage that can be initiated by ischemia/reperfusion due to missing blood flow, thus generating an oxygen deficit in the inner layers of the slices. The main sources of reactive oxygen species (ROS) for hepatocytes are internal CYPs, Kupffer cells and neutrophils, with the latter two being missing in isolated hepatocyte cultures. It has been shown that an imbalance between the generation of ROS and the antioxidant defence capacity of the cell affects major cellular mechanisms, including the metabolism of lipids, proteins and DNA (Cesaratto et al., 2004). ROS can also influence gene expression profiles by affecting intracellular signal transduction pathways (Cesaratto et al., 2004). Signalling by activated Kupffer cells, involving TGF beta and other cytokines, leads to stimulated proteoglycan synthesis, proliferation, and transformation into myofibroblast-like cells.

Several chemo-attractant genes, like cytokines, were up regulated indicating an activation of hepatic macrophages and an ongoing immune response were de-

regulated (Figure 55). At the same time, anti-inflammatory processes were induced, indicated by thioredoxin reductase 1 (Txnrd1), which was 3-fold induced exclusively at 6 h and is a critical antioxidant enzyme for the protection against oxidative stress. Stefin A2 (Stfa2), the expression of which was induced 17.8-fold, acts as a cysteine protease inhibitor, amongst which the caspases are an important group.

Unique for down regulated Slices 0 h/6 h	p-Value	Unique for up regulated Slices 0 h/6 h	p-Value
amino acid transport (12.0%), L-amino acid transport (8.0%), amine transport (12.0%)	2.63E-60	intracellular signalling cascade (46.7%), cell development (55.6%), cellular component organization and biogenesis (62.2%)	9.16E-11
DNA metabolic process (50.0%), DNA repair (33.3%), response to DNA damage stimulus (35.7%)	1.8E-28	response to stimulus (62.8%), response to stress (44.2%), stress-activated protein kinase signalling pathway (14.0%)	8.42E-17
transcription from RNA polymerase II promoter (41.7%), macromolecule metabolic process (80.6%), cellular metabolic process (86.1%)	1.76E-24	regulation of progression through cell cycle (31.2%), regulation of cell cycle (31.2%), insulin receptor signalling pathway (12.5%)	4.29E-15

Table 21: Cellular mechanisms affected by gene expression changes exclusively in liver slices after 6 h in culture

The changes in gene expression in liver slices in general were characterized by a very intense immune response at all time points. This is potentially a large disadvantage and thus it has to be questioned whether their use in global gene expression studies makes sense against the advantage of retaining the liver specific architecture, cellular composition and therefore liver specific responses. The immune cells of the liver are already activated by the process of generating the slices. Additionally, the lack of blood flow drives the hypoxia in the inner layers of the slice leading to multiple reactions and increased effects on gene expression in these cells. These processes lead to a transient induction of inflammatory processes in slices after 6 h in culture (Table 21 and Figure 55). These processes may potentially overlay any additional effects caused by compound treatment. However, for the analysis of direct toxicity that affects non-parenchymal cells, liver slices are one of the few *in vitro* system options available.

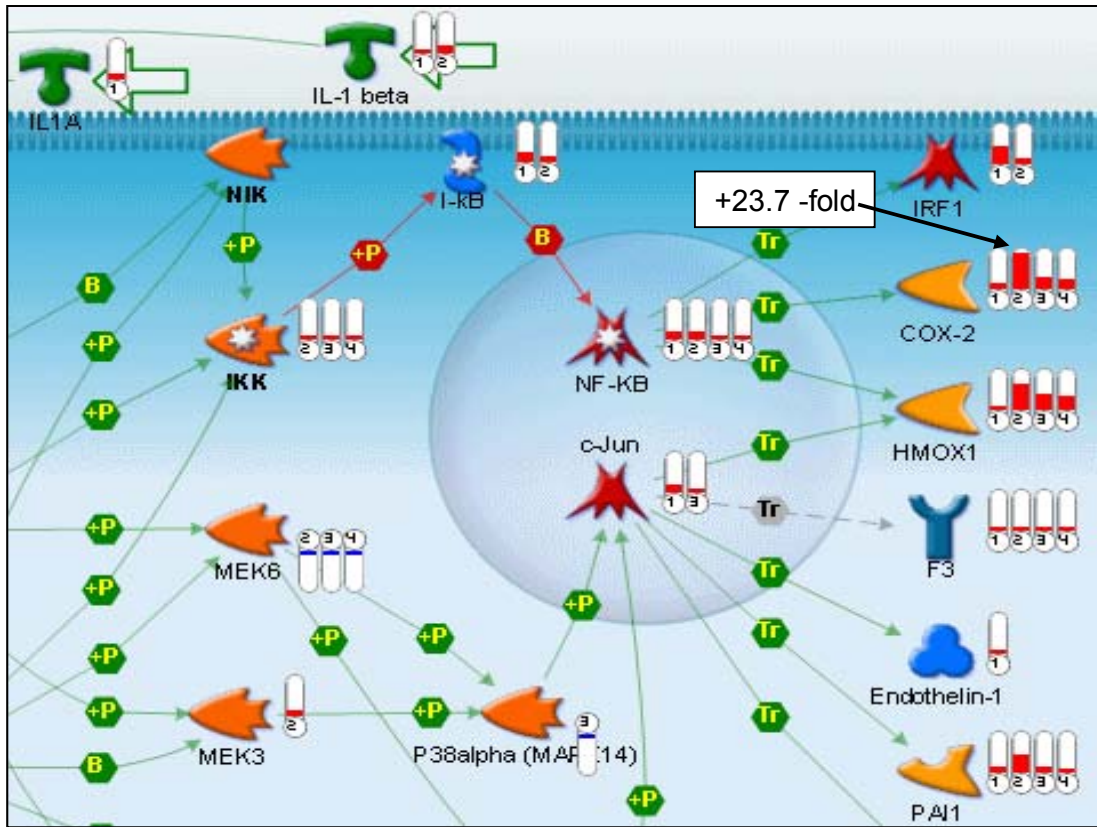


Figure 55: Time course of gene expression changes in liver slices. Shown is a part of the IL1 signalling pathway indicating a strong activation at early time points with the return to moderate expression levels by day 2. Red bars indicate induction, blue bars the repression of gene expression (modified from Metacore, GeneGO).

3.3.6 Molecular mechanisms affected over time in culture

3.3.6.1 Overview of the affected mechanisms in rat hepatocytes

In order to investigate the differences in gene expression taking place during culturing, with a special emphasis on the differences in the experimental systems used, genes were grouped according to gene ontology in several functional categories and further analyzed (Figure 56). This approach was chosen to reduce the number of genes, which introduced a high background noise into the data when taken as a whole. Additionally, it has the advantage of filtering the data while minimizing the loss of important and specific information.

The gene expression of short-term cultures (liver slices and suspension culture) shared a high correlation to the reference (freshly isolated hepatocytes) indicating the advantage of short term culturing. As early as 6 h after the isolation of the cells, larger changes in gene expression were seen, which increased over time.

The long-term cultures all failed to preserve this high level of correlation to fresh hepatocytes over time. Generally, hepatocytes cultured with the addition of FCS tended to show changes in gene expression after 2 – 5 d, in all gene groups, indicating a strong dedifferentiation processes. The same effect was seen in cells cultured in ML culture, where initial gene expression changed rapidly, followed by a more gradual change over time. The gene expression of cells cultured in SW culture without FCS was more stable over time. In this culture system initial changes did take place indicating an adaptation process to the culture conditions. For the later time points, the gene expression stabilized or even recovered, indicated by an increasing correlation, for example for protein metabolism, mRNA processing or lipid metabolism when compared to the starting point of the culture.

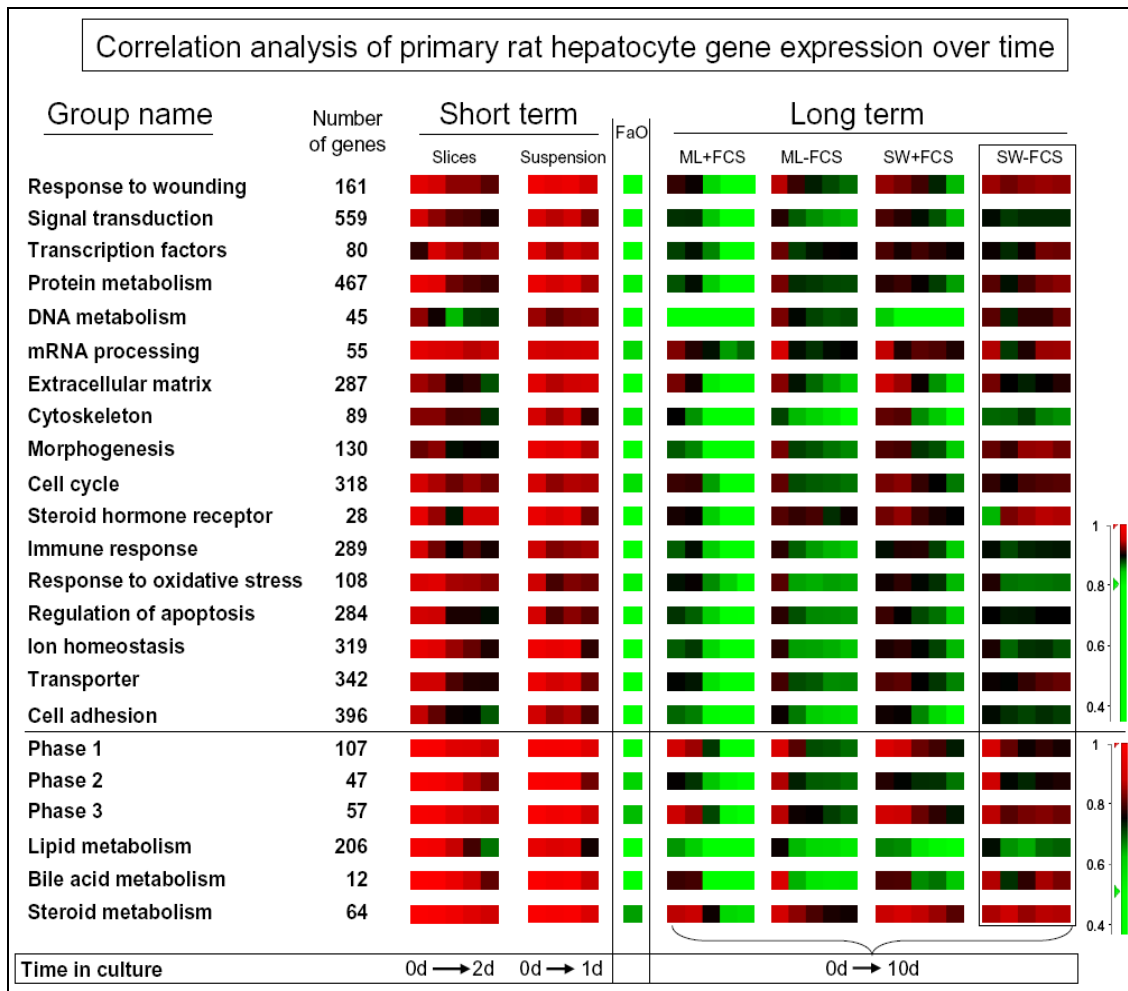


Figure 56: Temporal correlation plots of functional gene groups representing important cellular and liver specific mechanisms for different primary rat hepatocyte culture methods. Changes in the correlation of gene expression in comparison to the reference experiments (FC) are indicated by a change of colour. The calibration bars on the right side indicate the colour scheme which was chosen for an optimal visualization.

The functional classification of genes revealed the involvement of several biological processes as well as clear differences between the culture systems used. It is not intended here to describe all changes in gene expression taking place during culturing, instead, by discussing few, discriminating genes, the differences between the culture systems are discussed and general tendencies of gene expression changes elucidated.

3.3.6.2 Response to wounding, oxidative stress and immune response

Genes which are known to code for markers of hepatotoxicity or cellular stress, such as heme oxygenase1 (Hmox1), paraoxonase1 (Pon1) and several cytokines, were amongst the genes found to be differentially deregulated between the cultures (Table 22). Hmox1 is an essential enzyme in heme catabolism which has also a protective role against cellular stress, especially during inflammatory processes and oxidative stress (Wunder & Potter, 2003). It is induced by cytokines, hypoxia or ROS and is hypothesized to contribute to the decrease of CYP activity in culture (Kutty et al., 1988). This gene was induced initially in all cultures but reduced in expression over time in FCS-free long term cultures.

Already in short-term cultures a transient induction of cytokines and pro-inflammatory genes was detected. The chemokine ligand 1 (Cxcl1) acts as a neutrophil chemoattractant and was heavily induced during early stages of culture. In longer time cultures, especially in SW-, the expression of Cxcl1 was reduced again to an expression close to the control. Other cytokines, like Interleukin1 (Il1a), which is involved in various immune responses and inflammatory processes, are normally expressed in macrophages and monocytes and are therefore likely to be reduced in hepatocyte cultures. The alpha-2-macroglobulin (A2m), a protease inhibitor and cytokine transporter is a classic marker for activated immune responses in the liver (Kurokawa et al., 1987). It was induced during suspension culture, in ML-FCS culture and in early stages of SW-FCS.

The inflammatory process of hydrolyzing oxidized phospholipids to generate free oxidized fatty acids is mediated by platelet-activating factor acetylhydrolase (Pla2g7), which was induced in suspension and long term cultures with FCS. Hydroxysteroid (11-beta) dehydroxigenase1 (Hsd11b1) was reduced in all long term cultures with the exception of SW-FCS. This enzyme catalyzes the conversion of the stress hormone cortisol to the inactive metabolite cortisone.

Another gene indicating an increase of oxidative stress was the reduction of thioredoxin (Txn) expression in ML cultures. Txn is a small, di-thiol containing protein and a key

3 RESULTS AND DISCUSSION

player in maintaining cellular redox status and redox-controlled cell functions by transferring reducing-equivalents to disulfide groups (Burke-Gaffney, Callister & Nakamura, 2005). Besides this, several transcription factors, like p53, NF κ B, AP1 and the glucocorticoid receptor, are known to possess thiol groups and to be partly regulated by Txn, thereby altering various essential cellular processes.

Symbol	Accession-Nr.	Susp	Slice	ML+FCS			ML-FCS			SW+FCS			SW-FCS		
		1 d	1 d	1 d	6 d	10 d	1 d	6 d	10 d	1 d	6 d	10 d	1 d	6 d	10 d
A2m	NM_012488	3.8				2.5	43.8	9.9	12.3			2.9	51.4		
Ccnd1	NM_171992		-3.0		2.6	5.4	-8.8	-2.3				2.6	-10.3	-4.8	-4.1
Cpb2	NM_053617		-2.4		-6.1	-11.1		-3.3	-3.4	-2.1				-2.8	-2.4
Crp	NM_017096	-5.3	-4.2	-40.9	-31.4		-5.2	-3.2		-3.4	-3.5				
Cxcl1	NM_030845	22.9	15.1	39.3	15.1	13.5	13.7	6.5	6.2	46.1	15.2	15.6	12.8	3.4	2.7
Cxcl2	NM_053647	4.1	3.3	22.6	8.5	3.9	4.7	4.4	4.2	18.6		2.2	6.8		
F10	NM_017143	-3.6	-2.4	-3.1	-36.9	-46.7	-2.3	-9.3	-10.4		-4.0	-3.7		-3.6	-2.6
Hmox1	NM_012580	8.4	4.8	11.3	4.3	7.0	7.3			22.9	4.1	7.9	17.0		
Hrmt1l2	NM_024363	4.0	2.5	2.2	4.5	4.2		2.0	2.3	2.0	2.4	2.5			
Hsd11b1	NM_017080			-47.2	-24.8		-2.5	-2.5		-8.5	-7.6				
Il1a	NM_017019	-4.1	-2.7			-4.6	-6.7	-5.5	-2.9			-5.3	-5.2	-5.6	-5.7
Il1b	NM_031512					-2.3	-3.0	-3.0				-2.3	-2.4	-2.5	-2.8
Ndst1	NM_024361				-3.4	-4.1		-2.79	-3.2		-2.0	-2.5			
Pla2g7	NM_001009353	3.5			2.3	9.8						3.0			
Pon1	NM_032077			-97.6	-110.5		-13.4	-14.7		-3.4	-5.4		-4.1	-3.9	-8.5
Proc	NM_012803			-4.5	-20.0	-25.1	-2.4	-8.0	-6.5	-2.6	-5.5	-5.3	-2.2	-3.5	-2.5
Saa4	NM_001009478		-2.2	-105.3	-59.1		-2.6	-2.5		-2.2	-2.2				
Serpind1	NM_024382	-3.9	-13.3	-14.7	-220.9	-226.4	-12.3	-110.9	-125.2	-13.7	-8.7	-9.8	-10.2	-69.1	-97.8
Txn2	NM_053331			-2.2	-2.7	-2.6		-2.0	-2.2						
Tp53	NM_030989	2.4	2.6	4.0			2.3	2.3	2.5	2.7	2.4				

Table 22: Fold change values of several genes concerning the response to wounding, oxidative stress and the immune response. Genes selected were at least 2-fold deregulated at multiple time points and had a significance level of lower than 0.05 in at least one of the cultures.

It is known that hepatocytes are primed to re-enter the cell cycle during hepatocyte isolation, a process known to be triggered by inflammation and to underlie the dedifferentiation process of cultured hepatocytes (Papeleu et al., 2006). For cell cycle progression, additional growth factors, like EGF (Epidermal Growth Factor) or HGF (Hepatocyte Growth Factor) are required. The expression of Cyclin D1 (Ccnd1), found to be induced in hepatocytes cultured with FCS, separates the cells from these signals and initiates the proliferation.

Another process affected was the regulation of blood coagulation. Under normal conditions, hepatocytes are triggered to increase the synthesis of coagulant and complement factors and protease inhibitors by proinflammatory cytokines, as a response to wounding (Dhainaut et al., 2001). In culture, the expression of serpin peptidase inhibitor (Serpind1), which rapidly inhibits thrombin, carboxypeptidase B2

(Cpb2), which down regulates fibrinolysis, and protein C (Proc), a zymogen that catalyzes the inactivation of blood coagulation cofactors like coagulation factor X (F10), are clearly repressed in all types of culture. This can be seen as a physiological response to wounding and induction of wound healing processes due to the isolation procedure itself.

3.3.6.3 ECM, cytoskeleton and tissue remodelling

Large differences were also detected in the gene expression of ECM components, cell adhesion and cytoskeletal related genes (Table 23). The cellular morphology and formation of cell-to-cell and cell-to-matrix- contacts have proven to be of essential importance for cellular survival and functionality (Dunn et al. 1989; Richert et al., 2002; Hamilton et al., 2001) and are one of the key differences distinguishing the cell cultures from each other.

Collagens are the main constituent of the ECM. Collagen 1a1 and 3a1 (Col1a2 and Col3a1) were heavily down regulated during the perfusion, indicating the loss of several collagen expressing cell types. Especially Col3a1 is known to be expressed in connective tissues and blood vessels. Whereas the collagen expression in cultures without FCS remained stable, although at a low level in freshly isolated hepatocytes, the expression rose again over time when cultured with FCS. This may be a sign of the progressive dedifferentiation of hepatocytes towards a fibroblast like cell type and the induction of proliferation.

Symbol	Accession-Nr.	Susp	Slice	ML+FCS			ML-FCS			SW+FCS			SW-FCS		
		1 d	1 d	1 d	6 d	10 d	1 d	6 d	10 d	1 d	6 d	10 d	1 d	6 d	10 d
Actb	NM_031144			3.0	2.8	3.0	2.8	2.7	2.7	3.7			2.8		
Actn1	NM_031005			2.2	4.9	5.1		4.0	4.3		2.8	2.1			
Cf1	NM_017147			2.5	2.6	2.5	2.3	2.6	2.5		2.2	2.2			
Col1a2	NM_053356	-2.1	-15.5	-37.9		4.3	-33.6	-15.0	-3.0	-27.0		5.0	-31.6	-28.1	-9.9
Col3a1	NM_032085.1	-2.7	-11.2	-14.4	-8.0		-14.1	-13.5	-9.0	-13.9	-9.0		-14.6	-14.5	-13.6
Defb1	NM_031810			6.3			28.9	17.7	11.4	2.3			23.8	32.2	20.9
Gja1	NM_012567		-4.5	-10.1	11.5	12.2	-10.8	-9.2	-3.9	-9.0		6.6	-12.5	-11.9	-5.8
Lamc1	XM_341133		2.4		2.2	2.5	2.8	2.7	3.1				2.3		
Mgp	NM_012862		-8.5	-12.9	-3.2		-12.5	-12.3	-5.8	-9.9	-2.3		-12.6	-12.4	-9.7
Mmp12	NM_053963	24.5			116.1	226.1					43.5	104.1			
Msn	NM_030863				5.6	14.8		3.6	4.6		3.1	3.9			
Myh10	NM_031520			3.1	5.2	5.2		2.5	2.9	2.2	3.0	3.0			
Nexn	NM_139231				4.6	3.5		2.4	2.6						
Pfn2	NM_030873				4.3	4.9		2.7	3.8		2.3	2.5			2.2
Spp1	NM_012881	18.6			100.6	199.4					22.6	78.7			
Timp1	NM_053819	7.5	-2.96	2.3	11.2	13.4			2.6		4.9	7.3		-2.4	-2.4
Tpm1	NM_019131				6.3	5.8		2.3	2.2		3.2	3.0			

Table 23: ECM, adhesion or cytoskeletal related genes distinguishing the different cell cultures from each other.

The influence of FCS on inflammatory processes in isolated primary hepatocytes is demonstrated by matrix metalloproteinase12 (Mmp12), which is also called macrophage elastase and is involved in the breakdown of extracellular matrix in physiological as well as inflammatory processes (Mohammed et al., 2005). This enzyme is normally found in epithelial tissue and contributes to wound healing, but is also found in hepatoma cells triggering neovascularisation (Lyu & Joo, 2005). Mmp12 was found to be induced only in suspension and in late time points of ML and SW culture when cultured with FCS. The endogenous metalloproteinase inhibitor (Timp-1) was induced in all cultures except for SW-FCS, indicating changes in the reorganisation of the ECM environment as a reaction to cellular damage and inflammation or growth which may help explaining the change in cell morphology.

The cytoskeleton and their contact to the ECM by cell adhesion molecules and external signalling are connected to intracellular signalling cascades and mediate specific and important cellular processes. The reestablishment of these contacts, together with the re-establishment of cellular polarity and the stability of the actin cytoskeleton, are crucial requirements for hepatotypic functionality and for reducing the cellular stress (Page et al., 2007). The Gap junction protein alpha (Gja1) was reduced at early time points in culture but induced later on, except for SW- cultured cells. Gja1 is associated with endothelial cells and immature hepatocytes, again indicating the dedifferentiation processes in culture after addition of FCS (large induction ML+FCS 124-fold induced and SW+, 59-fold) (González et al., 2002).

The contact between ECM and the reorganisation of the actin cytoskeleton in response to external signals is mediated by profilins (Pfn 2), tropomyosin 1 (Tpm1) and moiesin (Msn), which were all induced in long term cultures, except for SW-. Actin itself (Actb) was mainly induced in ML cultured cells reflecting the need to reorganize the cytoskeleton due to their flattened shape. Finally, myosin heavy polypeptide 10 (Myh10) and secreted phosphoprotein 1 are physiologically expressed in immature smooth muscle cells and endothelial cells (Hiroi et al., 1996) and were induced by ML culturing and after the addition of FCS.

3.3.6.4 Metabolic competence

The metabolic competence of hepatocytes is one of the key elements defining their usability for toxicological studies. Besides the inducibility of CYP enzymes, which has been discussed extensively in chapter 3.2, there are several other genes involved in phase 1, phase 2 and phase 3 metabolisms. Previous studies have demonstrated predominantly a down regulation of phase 1 metabolism in cultures already over night as well as in later stages of culture (Baker et al., 2001; Lupp et al., 2001; Richert et al.,

2002). These findings were generally corroborated by our studies, but in SW-FCS cultured cells the decrease was less pronounced and they displayed a more stable gene expression over time.

Symbol	Accession-Nr.	Susp	Slice	ML+FCS			ML-FCS			SW+FCS			SW-FCS		
		1 d	1 d	1 d	6 d	10 d	1 d	6 d	10 d	1 d	6 d	10 d	1 d	6 d	10 d
Adh1	NM_019286			-18.8	-67.4	-46.9		-2.5	-2.9	-7.7					
Adh4	NM_017270			-3.0	-5.5	-6.1	-2.5	-2.6	-2.8	-3.1	-3.0	-3.4	-2.9		
Adhfe1_predicted	XM_342794	-17.1	-8.6	-6.5	-123.3	-104.0	-4.0	-33.3	-22.6	-6.5	-25.0	-40.0	-3.9	-4.7	-2.6
Cyp1a1	NM_012540				3.1	3.8		2.6	5.1					4.0	11.9
Cyp1a2	NM_012541			-5.4	-138.7	-100.4	-3.5	-103.5	-70.8	-8.4	-92.6	-83.9	-4.3	-64.7	-69.2
Cyp2a1	NM_012692	-8.0	-5.1	-8.9	-55.7	-50.6	-4.6	-18.8	-18.3	-4.3	-4.0	-4.2	-3.9	-3.0	-2.4
Cyp2c	NM_019184	-3.7	-4.7	-2.6	-276.3	-188.6	-2.5	-4.7	-7.0	-2.8	-36.8	-119.5	-2.4	-3.0	-2.4
Cyp2e1	NM_031543	-2.5	-3.6		-360.9	-336.4		-216.4	-262.4		-170.1	-267.7		-100.1	-91.5
Cyp3a1	NM_173144	-2.9	-2.7	-2.1	-403.2	-397.8		-2.0	-2.0	-2.2	-42.6	-100.0			
Cyp3a3	NM_013105	-5.4	-3.7	-2.4	-278.7	-233.4				-2.4	-47.1	-78.9			
Cyp8b1	NM_031241	-43.4	-9.1	-66.0	-222.0	-171.4	-46.2	-46.8	-20.8	-39.7	-56.4	-13.9	-39.8	-4.6	-2.3
Fmo1	NM_012792	-22.2	-19.1	-4.3	-59.1	-57.3	-16.7	-31.2	-40.7	-4.7	-50.3	-55.1	-14.7	-23.1	-15.5

Table 24: Phase 1 metabolism genes found to be differentially regulated. (Fold change>2 and pV<0.05).

Table 24 shows genes involved in phase 1 metabolism, which were differentially deregulated in primary rat hepatocyte cultures. The gene expression of several CYP isoforms was strongly repressed, however the extent of deregulation differed greatly. For example Cyp8b1 was repressed in all cultures, but whereas the expression was reduced up to 171-fold in ML+FCS, 21-fold in ML-FCS and 14-fold in SW+FCS on day 10 in culture, it was reduced only 2.3-fold in SW-FCS cultures. Other CYPs, like Cyp2c and Cyp3a1, were inhibited by the addition of FCS to the culture media but not in DEX containing, FCS free cultures. The three dimensional environment of SW culture had a positive effect on Cyp2a1 expression, Cyp1a2 however was unaffected and its expression was reduced equally in all cultures.

UDP glucuronosyltransferases (Ugt) have a broad substrate specificity and mediate the glucoronidation of intermediate metabolites. Although DEX was previously shown to induce UGT transcription *in vitro* (Jemnitz et al., 2000), these results could only be confirmed for Ugt1a7 during this study. The other isoforms remained unaffected in SW-FCS culture and were reduced in expression in short term and in ML cultures.

Also of importance for xenobiotic detoxification is the transfer of sulfonate groups from 3'-phosphoadenosine 5'-phosphosulfate (PAPS) to target nucleophilic metabolites, which is mediated by sulfotransferases (Sult). These enzymes have overlapping substrate specificities with Ugts, but higher affinity and lower activity. The expression of the different isoenzymes differed from each other as well as between the different

cultures. In short-term cultures and in cells cultured with FCS, all sulfotransferases were reduced whereas in FCS free cultures Sult1a1 and Sult1b1 were not affected.

Symbol	Accession-Nr.	Susp	Slice	ML+FCS			ML-FCS			SW+FCS			SW-FCS		
		1 d	1 d	1 d	6 d	10 d	1 d	6 d	10 d	1 d	6 d	10 d	1 d	6 d	10 d
Gss	NM_012962		3.5	4.4	2.2		2.4	2.5	2.5	3.8	2.8	2.5		2.2	2.8
Gsta2	NM_017013	-7.4			-17.8	-15.2	-2.3	-11.4	-10.0				-2.6	-4.3	-5.5
Gstm3	NM_031154	-9.1	-3.2	-8.3	-24.0	-21.4	-6.5	-16.9	-15.8	-7.8	-19.1	-18.2	-5.9	-7.8	-3.8
Gstp1	XM_579338		21.5	23.6	51.6	55.3	4.4	20.0	32.0	19.5	63.2	63.7		12.6	11.2
Sult1a1	NM_031834	-3.5	-12.0	-26.8	-108.2	-104.6				-19.3	-8.2	-12.3			
Sult1b1	NM_022513	-3.1	-2.3	-10.3	-29.2	-37.0				-9.7	-2.6	-3.0			
Sult1c1	NM_031732	-51.7	-41.9	-24.9	-352.9	-326.9	-22.7	-237.0	-296.6	-27.0	-10.0	-31.5	-18.0	-140.9	-139.5
Sult1c2	NM_133547	-10.3	-3.8	-11.2	-17.2	-17.4	-9.3	-13.6	-11.9	-10.3	-12.7	-13.4	-5.2	-9.3	-12.5
Ugt1a7	NM_130407						6.8	5.6	6.1				5.7	6.6	5.5
Ugt2b	NM_031533	-3.2			-5.8	-9.3						-2.2			
Ugt2b10	XM_223299	-5.6	-5.9	-6.9	-16.9	-8.7	-3.1	-3.4	-2.9	-5.8	-3.0	-3.1	-3.0		
Ugt2b3	NM_153314	-3.0			-4.4	-7.2		-2.1				-2.1			
Ugt2b4	NM_001004271	-3.1			-4.8	-4.3		-2.0				-2.5			
Ugt2b4	XM_579544	-2.3			-2.7	-2.3		-2.2							
Ugt2b5	NM_001007264	-3.1	-2.4		-10.4	-17.3		-3.1	-2.7		-2.3	-2.9			

Table 25: Genes of the phase 2 metabolism found to be differentially regulated (fold change>2 and pV<0.05).

Glutathione is essential, not only for phase 2 metabolism, but also for intracellular redox homeostasis. Glutathione synthase (Gss) expression was induced in all types of culture, whereas the expression of several Glutathione S-transferases (Gst) was reduced. Gsts are a large group of enzymes responsible for detoxification by conjugating several electrophilic intermediates to glutathione. They are encoded by at least five gene families (alpha, mu, pi, sigma, and theta) and are an essential component of cellular antioxidant defence mechanisms. The placental Gstp1, known for its specific expression during rat hepatocarcinogenesis, is a well defined dedifferentiation marker (Vanhaecke, Elaut & Rogiers, 2001) and also used as a tumour marker (Sakai & Muramatsu, 2007). It was induced in long term cultures, especially in the presence of FCS, and minimally in SW-FCS. Gsta2, the most abundantly expressed Gst in liver, was reduced, but was more stable in SW cultured cells.

3.3.6.5 Intracellular signalling and transcription factors

As mentioned earlier, ligand activated transcription factors coordinately regulate the expression of a vast number of genes involved in detoxification and many other cellular processes. They often form obligate heterodimers with the retinoid X receptor (RXR) and hence, the importance of keeping the expression levels of these genes as similar

to fresh liver as possible, to preserve liver-like detoxification function, is essential. Other transcription factors are important for cellular differentiation and the regulation of genes involved in cell cycle, inflammatory processes or energy metabolism.

Hepatocyte nuclear factor 4 α (Hnf4a) plays a critical role in the maintenance of hepatocyte phenotype, lipid and bile acid metabolism (Sladek, 1994). Moreover, the expression of other transcription factors, like pregnane X receptor (PXR) and liver X receptor (LXR), and of several CYP isoforms require HNF4a activity (Tirona & Kim, 2005). In culture, FCS reduced the expression of this important TF whereas it was unchanged in serum free cultures (Table 26). Many ligand activated receptors, like RXR, PXR, CAR or Ahr, were repressed in liver slices and long-term cultures, except for SW-FCS cultures. This culture system seems to retain liver specific transcription of these important genes at physiological levels over longer times.

Epidermal growth factor (EGF) and connective tissue growth factor (Ctgf) both showed no difference in expression between the different cell cultures. Whereas EGF, important for liver regeneration and the reentry into the cell cycle after lesions, was continuously reduced in all types of culture, Ctgf was strongly induced in all but suspension cultures. Ctgf promotes cell adhesion and cell motility in nonparenchymal liver cells and therefore cell activation during liver regeneration following injury (Pi et al., 2008).

Symbol	Accession-Nr.	Susp	Slice	ML+FCS			ML-FCS			SW+FCS			SW-FCS		
		1 d	1 d	1 d	6 d	10 d	1 d	6 d	10 d	1 d	6 d	10 d	1 d	6 d	10 d
Ahr	XM_579375	-6.2	-2.6	-2.7			-2.1			-3.8			-2.3		
Aif1	NM_017196	-2.2	-20.0	-36.9	-3.7		-31.6	-56.8	-53.0	-23.3	-2.9		-31.3	-49.1	-45.0
Arntl	NM_024362				-2.6	-3.0		-2.2	-2.1		-3.4	-2.8			
Cd53	NM_012523		-4.5	-3.7	2.6	5.7	-4.1	-5.2	-4.9	-4.0		2.4	-4.1	-5.2	-4.8
Ctgf	NM_022266		3.7		30.4	31.3	30.1	28.4	26.9	-2.3	33.5	32.0	21.3	35.4	33.3
Egf	NM_012842	-5.1	-4.2	-4.1	-7.5	-9.7	-2.7	-6.4	-7.0	-3.5	-3.9	-5.3	-2.2	-3.1	-2.9
Hnf4a	NM_022180				-4.3	-3.8					-2.4	-2.2			
Khdrbs1	NM_130405				3.0	3.0		2.1	2.1		2.4	2.3			
Nr1h3/LXR	NM_031627		-2.3	-3.3	-5.7	-5.4	-2.2	-3.2	-3.1	-2.7	-3.6	-3.2	-3.6		-2.0
Nr1h4/FXR	NM_021745		-3.1	-4.0	-10.6	-13.5	-2.5	-4.4	-4.6	-3.3	-2.0	-2.5	-4.7		-2.0
Nr1i2/PXR	NM_052980	-2.3	-3.8	-4.0	-5.7	-5.7				-2.9	-2.7	-2.7			
Nr1i3/CAR	NM_022941		-5.2	-5.7	-13.1	-13.1	-2.5	-6.6	-4.8	-4.7	-8.2	-8.0	-4.6		
Nrp1	NM_145098	-2.1	-5.2	-5.5			-5.7	-5.3	-4.3	-5.7	-3.9		-5.8	-5.9	-5.7
Pdzk1	NM_031712	-2.4	-4.7	-4.0	-12.4	-15.5	-3.5	-4.8	-5.7	-2.3			-3.0	-2.7	-2.6
Rgs2	NM_053453	2.2			31.8	34.9	-2.6		3.8		15.9	23.2	-2.4		3.9
Rgs3	NM_019340					2.3		-3.9	-2.7		2.3	2.7		-3.9	-3.7
Rxra	NM_012805	-2.3		-2.5	-3.5	-3.4		-2.6	-2.9		-2.1	-2.1			
Tcf4	NM_053369		-2.2				-2.2		-2.1	-2.1	-2.2		-2.1	-2.4	-2.3
Thrb	NM_012672	-3.2		-2.3	-4.0	-5.2		-2.7	-3.3	-2.4					
Tnfsf13	NM_001009623			-3.1			-3.7	-2.3	-2.4	-2.4			-4.0	-3.8	-3.6
Vldlr	NM_013155			6.7	5.0	5.4	4.4			5.3	4.3	4.6	8.5		

Table 26: Gene expression changes of liver enriched transcription factors (fold change>2 and pV<0.05).

The expression of CD53, initially repressed in all cultures, was increased over time in FCS containing cultures. CD53 is a transmembrane protein mediating signal transduction events that plays a role in the regulation of cell development, growth regulation and motility by forming complexes with integrins.

3.3.6.6 Affected mechanisms in human hepatocytes

In contrast to rat hepatocytes, the human orthologue genes, again clustered together to functional groups, were much more stable over time (Figure 57). In most of the groups no clear differences in the dedifferentiation processes were detected over time and gene expression changes in ML and in SW cultures were comparable. Interestingly, the liver progenitor cell line HepaRG showed partly specific hepatotypic gene expression and displayed stable expression over time. Clear differences were found in the expression of genes involved in cellular signalling, mRNA-processing, ECM-proteins, cell adhesion and metabolism.

Table 27 shows genes which displayed differences in expression in some major functional categories. Most important for toxicology, the deregulation of xenobiotic metabolism was less severe than in rat hepatocytes with some of the main enzymes mediating phase 1 metabolism (Cyp1a1 and 2E1) being down regulated. The glutathione system, which is encoded in distinct genomic clusters and represented here by Gstm3 and Gsp1, was less expressed in HepaRG cells, whereas Gsta was inversely regulated. Gsta's are the main enzymes for the detoxification of lipid peroxidation products whereas the other isoforms are mainly responsible for the detoxification of other electrophilic metabolites (Pham, Barber & Gallagher, 2004).

Some of the differences found between HepaRG cells and primary human hepatocytes can be explained by the lower expression of certain transcription factors. The activating transcription factor 3 (ATF3), CCAAT/enhancer binding protein α (CEBPA) and the glucocorticoid receptor (Nr3c1) were found to be lower expressed in HepaRG cells than in liver. This glucocorticoid receptor can act as both a transcription factor and as a regulator of other transcription factors. ATF3 is a member of the activation transcription factor/cAMP responsive element-binding (CREB) protein family and binds to certain promoter and enhancer sequences. In addition to the positive or negative regulation of transcription, CEBPA is known to inhibit cyclin dependent kinases (CDK2 and CDK4), thereby causing growth arrest in cultured cells.

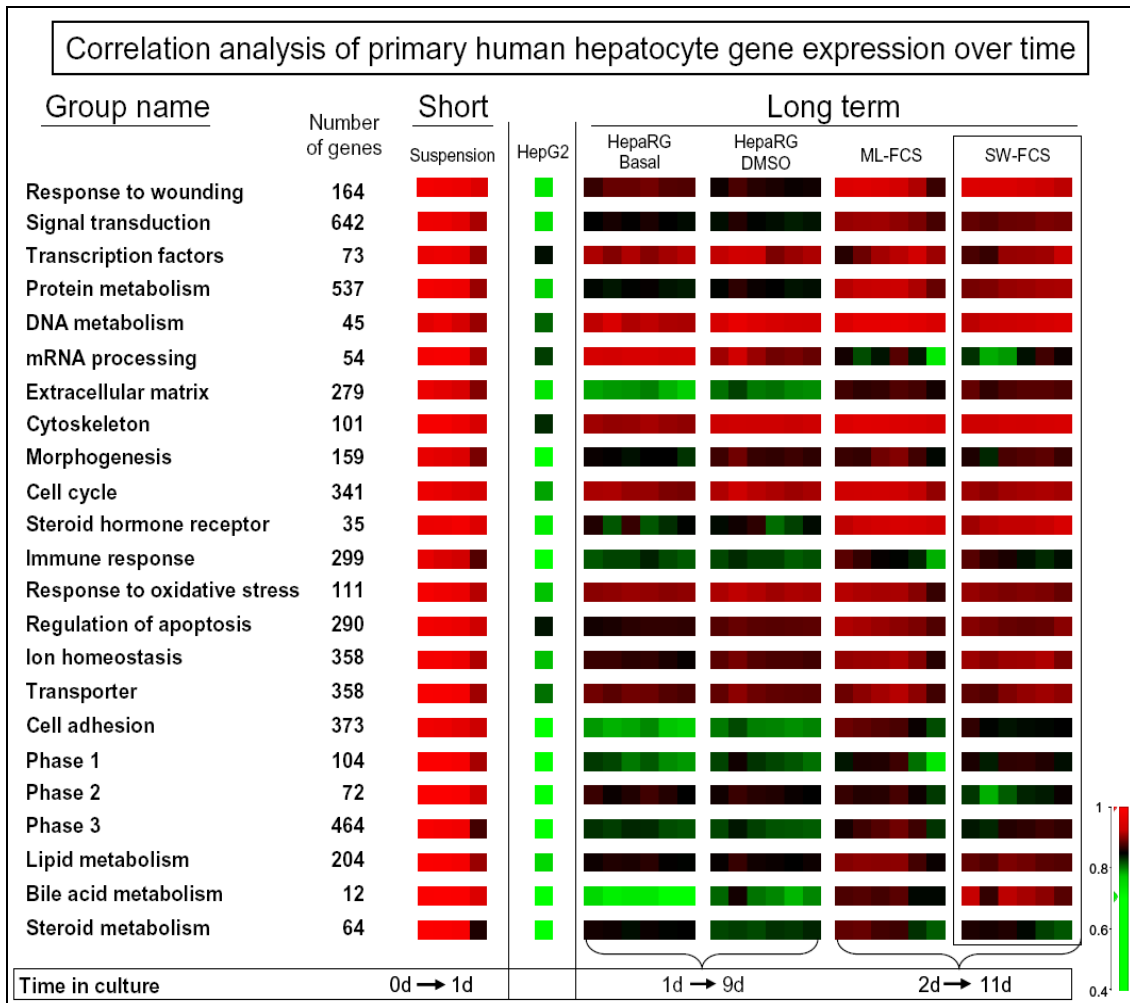


Figure 57: Group wise correlation analysis of the gene expression of primary human hepatocytes. The correlation plots represent important cellular and liver specific mechanisms for different primary rat hepatocyte culture methods. Changes in the correlation of gene expression in comparison to the reference experiments (FC) are indicated by a change of colour. The calibration bar on the right side indicates the colour scheme which was chosen for an optimal visualization.

The expression levels of several genes correlating with inflammatory response and cytoskeletal and ECM rearrangement, like the formiminotransferase cyclodeaminase (Ftcd), which binds vimentin intermediate filaments, thereby regulating cytoskeletal rearrangement, were found to differ from the levels in liver, implicating the onset of restructuring in primary hepatocytes which in general was different in HepaRG cells.

Symbol	Accession-Nr.	Susp	HepaRG (Basal)			HepaRG (DMSO)			ML-FCS			SW-FCS		
		1 d	1 d	6 d	10 d	1 d	6 d	10 d	1 d	6 d	10 d	1 d	6 d	10 d
ALDH3A1	ILMN_6390		17.6	18.4	23.7	26.1	19.1	31.1			2.6	2.5	2.8	3.0
APOA2	ILMN_18670		-2.8		-2.7	-11.3	-8.0	-13.2						
ATF3	ILMN_6468		-4.5	-2.8	-4.0	-4.4	-3.9	-3.5			2.2			
CD44	ILMN_7737		2.9	3.5	3.4			2.2	-2.1	-2.7		-2.1	-3.2	
CEBPA	ILMN_27029		-3.6		-2.3	-3.0	-2.1	-2.9	-3.4					
CTGF	ILMN_3374		2.5	2.4	2.9				-6.0	-2.6	-3.7	-8.8	-4.3	-3.3
CYP1A2	ILMN_19528	-8.0	-49.3	-62.8	-54.5	-47.5	-37.0	-39.5	-13.1	-2.4	-3.0	-7.0		-3.2
CYP2E1	ILMN_27893		-31.1	-11.3	-14.8	-9.0	-4.7	-12.1	-2.4	-20.1	-34.5		-10.0	-8.3
CYP4B1	ILMN_25411		24.7	27.5	33.6	29.5	32.7	26.0						
EGFR	ILMN_15615		-3.2	-2.6	-2.5	-2.4	-2.4	-2.0					-2.0	
FABP1	ILMN_11988	-3.6	-2.3		-2.6	-3.0		-6.5	-24.7	-7.6	-9.2	-15.2	-3.0	-5.1
FBP1	ILMN_16804	-5.5	-250.3	-275.3	-268.2	-273.0	-220.1	-234.5	-14.3	-11.1	-13.3	-7.1	-6.1	-7.6
FTCD	ILMN_8918	-3.8	-193.6	-210.3	-193.2	-192.4	-158.3	-179.2	-4.3	-4.9	-4.8	-3.2	-2.9	-3.3
GSTA1	ILMN_30031							-2.6	-3.4	-5.1	-5.0	-4.4	-4.9	-3.3
GSTM3	ILMN_2804		-3.0	-3.0	-3.1	-3.0	-2.7	-2.9						
GSTP1	ILMN_10475	-2.8	-11.0	-13.2	-13.7	-11.2	-10.1	-10.1		-2.1				
HMOX1	ILMN_25059	2.6	-4.0	-4.9	-5.5	-3.3	-3.3	-2.4						
ISL1	ILMN_25965		3.7	3.7	4.6	5.6	5.0	5.4						
LPL	ILMN_2233		10.5	10.6	7.5	16.0	12.6	9.2						
MAOA	ILMN_11566		2.1	2.1	2.0	2.5	2.2	2.2				-2.5		
MMP7	ILMN_9188		7.0	11.3	17.0	4.0	3.7	4.4						
NQO1	ILMN_27575								2.2	4.4	7.8	2.0	5.7	8.1
NR3C1	ILMN_21266		-2.7	-3.4	-3.2	-2.8	-2.4	-2.9						
PON1	ILMN_24208	-7.4	-3.3	-3.5	-4.5	-5.6	-4.4	-6.9	-14.7	-8.3	-14.2	-11.8	-6.3	-8.1
PPARGC1A	ILMN_16547	-6.2	-4.7	-3.7	-4.3	-4.1	-4.3	-5.4	-9.2	-8.4	-9.5	-10.6	-16.7	-14.4
S100A6	ILMN_13161		-6.1	-8.2	-7.4	-7.9	-6.9	-7.6	2.2	14.1	24.5	2.0	14.1	15.2
S100A8	ILMN_13072	-2.5	4.0	2.4		2.3	2.4	2.1	-4.9	-13.3	-12.4	-2.8	-9.7	-7.2
SGK	ILMN_2451		-2.5	-4.4	-3.1	-4.3	-5.0	-4.9	-8.4	-18.9	-18.7	-6.1	-21.2	-16.2
SLC7A7	ILMN_16478		10.4	11.5	12.9	8.4	7.2	7.5		-2.1	-2.0			-2.2
SPP1	ILMN_9394		9.7	8.7	4.6	2.4	2.2		-2.1	-2.1	-2.0	-2.2	-2.0	
SULT2A1	ILMN_16119	-13.7	-2.8	-2.4	-2.1				-8.9	-9.6	-7.2	-14.1	-9.8	-7.9
TIMP1	ILMN_3162		3.6	2.9	3.3	3.3	3.8	4.1						
TNFRSF11B	ILMN_6495		22.9	24.0	9.6	8.5	7.0	6.5						

Table 27: Subset of genes differentially expressed in human primary hepatocytes and HepaRG cells. factors (fold change>2 and pV<0.05).

3.3.7 Confirmation of the microarray results with TaqMan PCR

Over all, more than 4000 genes were found to be differentially regulated between the different cell cultures and the liver or freshly isolated hepatocytes. The genes were selected by statistical significance (pValue<0.01) and fold change (either 1.5-fold or 2-fold). Even though the technique used (Illumina BeadChip arrays) is highly standardized, there is still a possibility to obtain false positive results.

The data obtained by microarray experiment were confirmed by two different ways. First, the comparison to previously published gene expression data, which partly covered the experiments described here (Groneberg et al. 2002; Holme, 1985; Baker et al., 2001; Boess et al., 2003; Tuschl & Müller, 2006; Beigel et al., 2008) revealed every close resemblance in the general tendencies and pathways affected. In Addition, TaqMan PCR was used to verify the results of the global gene expression measurements. Therefore, TLDA cards were designed for high, moderate and low expressed rat and human genes of toxicological importance which were found to be significantly deregulated in culture. Experiments were conducted as stated in chapter 2.2.4.3, using the same RNA as starting material which previously was used for the microarray experiments (results were generated as part of a joint work with Gregor Tuschl, PhD-student).

TaqMan PCR was conducted with samples of 15 rat cell culture conditions (FaO cells, liver slices and suspension culture after 1 d in culture, ML+/-FCS and SW+/-FCS after 1 d, 6 d and 10 d in culture) and with 43 genes of toxicological relevance resulting in an overall number of 645 genes tested in biological triplicates (Appendix 3 and Appendix 4). 530 Of these genes fulfilled the quality cut-off values of being either >2-fold deregulated in the TaqMan experiments or being >2-fold deregulated with a pValue below 0.05 in the microarray experiment. From these 530 genes, 89% (471) were accordingly detected as deregulated with both techniques. None of these 471 genes differed in terms of direction of deregulation resulting in 100% consistent results with the selected parameters for the rat experiments.

The results of human TaqMan analysis revealed slightly different results. In this case, 34 genes were tested in 13 cell culture conditions (Suspension culture after 1 d, HepaRG cells in Basal/DMSO-media, at 1 d, 2 d, and 9 d, ML-FCS and SW-FCS at 2 d, 7 d and 11 d) resulting in an overall number of 442 genes tested in biological triplicates (Appendix 5 and Appendix 6). Of these genes tested only 285 items were significantly deregulated. From these 285, only 37% (105) were commonly detected as deregulated with both techniques, but none of these items were detected to be inversely deregulated. The significantly lower rate of detection can be explained by the large human donor variation (Figure 49). The individual differences in gene expression lowered the number of genes matching the significance level cut off and therefore the overall detection rate. Nevertheless, the cut of values chosen guaranteed high quality and trustworthy results in both species. The TaqMan confirmation of some toxicologically important genes validated the results from the microarrays.

Further analysis of the entire data set might give more details of the general adaptation processes taking place after perfusion and the differences between the different culture

systems. A very interesting aspect for future studies is the implementation of HepaRG as a new cell line displaying partly distinct, liver specific and stable gene expression.

3.3.8 Conclusions from the characterization of primary hepatocytes in culture

The application of toxicogenomic methods in combination with longer term cultured hepatocytes is a promising, but currently an error prone, approach. As gene expression is a highly dynamic and complex process, an optimization and standardization of the liver perfusion and culture conditions is crucial to maintain liver specific properties and gene expression and to generate reproducible and reliable results. Generally, the application of global gene expression serves two main goals. Firstly, it allows an exact characterization of the processes going on in the primary hepatocytes after perfusion and therefore leads to a greater understanding of these underlying processes and regulatory mechanisms controlling gene expression. Secondly, it is an essential prerequisite for each experimental model, especially for new and alternative *in vitro* models, to exactly characterize all relevant features and to estimate the capabilities and the value with respect of the expected results.

Although previous studies showed the existence of various posttranscriptional and posttranslational modifications influencing the correlation between mRNA and proteins, the relatively small dataset shown here, four CYP-isoforms measured on mRNA, protein and activity level, showed comparable results. Additionally, the results from global gene expression analysis are supported by proteomic profiling. Even though fewer mass peaks were significantly detected in comparison to the gene expression, these profiles were sufficient to support previous results. The peak patterns clearly clustered according to time in culture and separated the different culture systems suggesting that SW-FCS is the most “liver-like” long term culture system. The major disadvantage of SELDI technology is that it is not clear which proteins were present.

Changes in gene expression were detected already directly after the perfusion. These initial changes can be seen as a result of fundamental changes of cellular morphology and tissue disruption, as a result of stress during perfusion, the lack of signalling by other cell types and hormones and finally as an adaptation processes to the new *in vitro* environment. Some of these changes are inherent to the procedure of perfusion and were therefore expected. They can be minimized with the help of the serum composition. For example the lack of hormonal stimulation was balanced by the addition of Dex, a glucocorticoid analogue known to preserve metabolic activity and differentiation status in hepatocytes. Other processes are harder to avoid. The oxygen

gradient between perivenous and periportal hepatocytes and Wnt signalling by endothelial cells are known for their contribution to functional liver zonation (Braeuning et al., 2006; Kienhuis et al., 2007), but are obviously missing from all culture systems.

The results of the global gene expression and from proteomic SELDI analysis clearly show the importance of an exactly defined and standardized cell culture. As the regulation of gene expression is a dynamic process, the degree of change is highly dependent on the type of culture and the time points chosen. To gain further insights into the processes taking place and to link their importance and relevance to toxicology, pathway analysis was conducted with genes found to be significantly deregulated.

Over all, more than 4000 genes were found to be differentially expressed in all of the cell cultures compared to the liver or freshly isolated hepatocytes over time. It is obvious that the multiple effects and consequences can only be partially discussed here and so the study focused on changes accumulated over time in different cultures on a global level, as well as on specific toxicologically important and functionally related sets of genes. Special emphasis was put on a key function of these cells, i.e., their metabolic competence.

Previous studies showed that most of the changes in culture are taking place during the first 24 to 48 h after plating (Beigel et al., 2008). These results were confirmed by this study. Additionally, the results of the global gene expression allowed a detailed view on the processes taking place during this time. The perfusion itself caused many changes in gene expression. Inflammatory responses and adaptation processes to the cell culture environment were characterized by the induction of many pro-inflammatory early response genes, like cytokines. In turn, this was accompanied by ECM reorganization, changes in intracellular signalling and the previously mentioned proliferative effects. Interestingly, many genes regulating blood flow and blood vessel buildup were induced, emphasizing the importance of the liver for these processes.

Previous studies suggest that phase 2 metabolism is better preserved by cells in culture than phase 1 enzymes (Kern et al., 1997; Rogiers & Vercruysse, 1998). Our data contradicted this and revealed the deviations in expression levels of these enzymes when compared to the liver. Also here the SW-FCS culture delivered the most "liver-like" gene expression over a longer time for both phase 1 and phase 2 enzymes.

The addition of Dex not only improved the morphological appearance but also significantly increased the levels of metabolic enzymes such as CYP isoforms, several phase 2 isoenzymes and cellular transporters. Dex is known to induce a variety of enzymes including phase 2 enzymes by binding to hormonal activated transcription

factors (Waxman, 1999; Jemnitz et al., 2000). Figure 7 shows the main transcription factors and their complex interactions which can influence several important cellular processes. It is obvious to see that changes in transcription factors can lead to multiple modifications in cellular physiology. We showed here that the long-term culture system preserved best many transcription factors and several of the downstream processes.

The short term cultures tested (liver slices and suspension culture) both showed a rapid decline in viability and gene expression. They are used for CYP-induction, biotransformation and cell viability studies. All of these studies rely on the proteins that are still present while in the liver and therefore deliver reliable results. Because of the rapid loss of hepatotypic functionality and gene expression, gene expression analyses have to be questioned, due to their poor reliability and correlation to the *in vivo* situation. Additionally, in liver slices, an overwhelming inflammatory response was seen with extensive signalling between the cell types (especially Kupffer cells, endothelial cells and hepatocytes) leading to the generation of nitric oxide (NO), oxidative stress and therefore increasing cellular stress. In addition, liver slices are thought to represent the *in vivo* situation better by the retention of the original ECM and cellular composition, this might mask many additional changes introduced by compound treatment making this culture system only suited for special applications such as a model for non-parenchymal mediated hepatotoxicity, cell-interaction studies or for canalicular transport studies.

Primary human hepatocytes generally showed much more stable gene expression than rat hepatocytes in ML as well as in SW culture. In contrast to rat, based on the gene expression, no clear difference between ML and SW cultures was detected. Classical dedifferentiation markers like *Gstp1* were not affected in either culture and the enzymes driving metabolism were mostly stable and closer to the liver expression than in rat. For example, the CYP isoforms 1A2 and 2E1, which were heavily reduced in rat hepatocytes at later time points were much less deregulated in human hepatocytes and showed no difference between ML and SW. The massive immune response seen in rat hepatocytes was not observed in human cells to the same extent. This might be due to the fact that the experiments started one day later after perfusion. The correlation analysis of the gene expression data suggests less oxidative stress, less perturbations in the cellular cytoskeleton and a more liver like expression of the cellular transcription factors (Figure 56 and Figure 57).

Despite the fact that primary human hepatocytes are much more difficult to obtain and much more expensive, their excellent stability makes them an ideal experimental system for toxicogenomics. Previous studies by Richert and her co-workers identified the use of cryopreserved hepatocytes as an alternative making this test system

independent from surgery, time and place (Richert et al., 2006; Alexandre et al., 2002). The studies conducted were short term (24 h), therefore the possibility to prolong the time in culture with cryopreserved human hepatocytes without additional loss of specific functionality has to be proven.

When conducting studies with human hepatocytes, there are other major obstacles to be aware of. Human donors show great variability. First of all, genetic variability plays a significant role. The medical history and the moral conduct of the individuals has also a big influence, all together resulting in much larger inter-individual differences and making it harder to reach statistical cut-off values. Additionally, the genetic polymorphisms present in phase 1, phase 2 and phase 3 enzymes in some individuals, making them exceedingly fast or slow metabolizers, influences the results of the toxicological studies. Therefore, a special emphasis has to be put on the statistical analysis of the individual human donors.

Established cell lines, both rat and human, differed significantly from all other cultures. Dramatically lower expression of many metabolically important enzymes and the lack of inducibility might result in an underestimation or even complete lack of compound toxicity. Previous studies have reported an identification rate for cytotoxicity of only 70% when compared with known toxicity in either *in vitro* assays in primary hepatocytes, in *in vivo* assays in rats, or in pre-clinical development (Westerink & Schoonen, 2007). Despite these disadvantages, hepatoma cell lines still have significant benefits as an easy-to-handle and stable test system for special applications. An exception was the human hepatoma cell line HepaRG. This relatively new established cell line has, compared to the other cell lines used, significantly elevated levels of metabolic enzymes as well as many other typical hepatocyte features (Parent et al., 2004). Previous findings from Kanebratt (Kanebratt & Andersson, 2008) were corroborated and even expanded upon these studies. They reported that the expression of CYP enzymes, transporter proteins, and transcription factors was stable in differentiated HepaRG cells over a period of 6 weeks. Most CYPs were lower but still stably expressed compared to primary hepatocytes, except for CYP3A4 and CYP7A1 (Kanebratt & Andersson, 2008). In these studies, the expression level of CYP4B1 was about 30 fold higher in HepaRG cells than in hepatocytes. This enzyme is suspected to activate certain carcinogenic compounds and thereby contribute to cellular damage. The expression of CYPs generally decreased slightly when cells were cultured in basal media without DMSO, whereas phase 2 enzymes and phase 3 transporters and other liver-specific factors were unaffected. Transporter studies showed the existence of active transporters at the contact surfaces of these cells (data not shown). Additionally, the global gene expression showed a higher

correlation of these cells to primary hepatocytes than to HepG2 cells, indicating at least partially differentiated cells.

Taken together, the above described results of the morphological analyses, the functional tests, proteomic and global gene expression analysis clearly showed an advantage of the SW-FCS culture over the other cell cultures of primary rat hepatocytes. Alterations in xenobiotic metabolism and other hepatocyte-specific cellular functionalities, while still changing, were least pronounced. SW-FCS cultured cells showed the highest sensitivity to CYP inducers as well as being functionally active for over two weeks. Another important fact is the increased stability of gene expression from two days in culture up to two weeks. In some cases, even an increase in correlation to FC was observed suggesting some regenerative processes were taking place in SW-FCS.

All together, these results make SW-FCS the culture system best suited for toxicogenomic studies for the generation of high-quality quantitative data under standardised cell culture conditions.

3.4 Development of an *in vitro* liver toxicity prediction model based on longer term primary hepatocyte culture

3.4.1 Introduction to the *in vitro* prediction model

The comparison of gene expression profiles from animals exposed to compounds belonging to the same class has been reported to result in a relatively high correlation, including the comparisons between different species treated with the same compound (Amin et al., 2002; Hamadeh et al., 2002a; 2002b). The assumption that compounds causing the same toxic endpoints also generate a unique gene expression signature has led to attempts to classify compounds according to their genomic profile. Up to now, several studies e.g. by Zidek et al. (2007) and Ellinger-Ziegelbauer et al. (2008), have shown the possibility to use this approach for the successful classification of unknown compounds. However, there are still many drawbacks, which have to be resolved. All the studies reported so far were conducted *in vivo* and therefore, they do not help for early screening in drug development. The fact that huge reference databases are required to generate classification results of high quality and predictivity shows that further progress in the development of these techniques is required. Meanwhile there are commercial service providers with large databases (mainly based on *in vivo* experiments) and automated profile analysis, but they are very expensive. *In vitro* data is highly dependent of the culture system used which, as already mentioned, is not standardized yet and therefore the data generated is not totally trustworthy.

To test whether we can overcome the ethical, time and financial bottleneck of animal usage, our *in vitro* system was tested with 15 well known model compounds, as a proof of concept study. Subsequently, a blinded control study was conducted to validate the test system. Based on the results described in chapter 3.2, the SW-FCS conformation was defined as best cell system suited for further toxicogenomic studies. The aim of this study was therefore to generate a robust dataset, which could be used to generate a computational model for the classification of hepatotoxic compounds and negative controls samples *in vitro*.

3.4.2 Short description of the test compounds

The compounds used in this study are classic model compounds for hepatotoxicity and they were selected according to previous in-house data and published *in vivo* studies (Zidek et al., 2007). For all of the hepatotoxic compounds (Figure 58), there is already

information available about their mechanism of action, or at least of their adverse effects *in vivo*. Additionally, a former drug candidate from Merck KGaA, which was stopped during development due to hepatotoxicity, was employed as a blinded control sample for the verification of the test system.

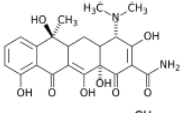
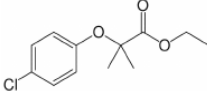
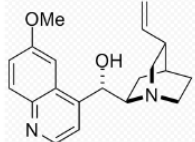
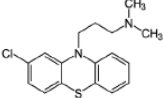
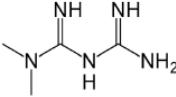
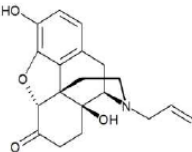
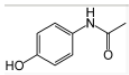
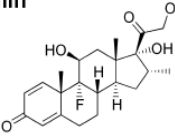
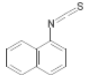
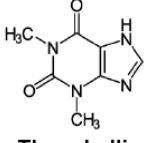
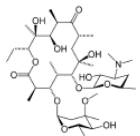
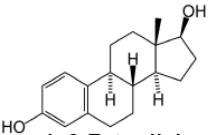
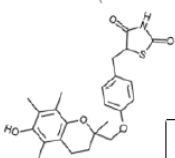
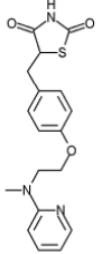
Toxic compounds	Structures	Effect	Non-toxic compounds and their structures
Tetracycline		Microvesicular steatosis	Clofibrate  Quinidine 
Chlorpromazine		Cholestasis	Metformin  Naloxone 
Acetaminophen*		Centrilobular necrosis*	Dexamethasone 
ANIT		Cholestasis	Theophylline 
Erythromycin-Estolate		Cholestasis	17β-Estradiol 
Troglitazone		Fulminant hepatic failure (Idiosyncratic)	Rosiglitazone 
	Blinded compound EMD X		DMSO-control

Figure 58: Molecular structures of the toxic and non-toxic compounds used in the classification model. *Acetaminophen, was not included in the model because of a lack of toxicity in the *in vitro* model (details see Figure 59)

Tetracycline is a bacteriostatic antibiotic widely used in daily practice and therefore of importance to toxicological research. Dose dependently, it causes microvesicular steatosis. The mechanism of action was discussed in detail in chapter 3.1.

Chlorpromazine (Cp) is an aliphatic phenothiazine which is used therapeutically as an anti-psychotic drug. The mechanism of action is still poorly understood, but liver injury and a periportal inflammatory reaction causes cholestasis, as well as a significant elevation of serum alanine aminotransferase (ALT).

The toxicity of *Erythromycin-Estolate* (EE), a macrolid bacteriostatic antibiotic, is clinically similar to Cp. However, the progression to chronic liver damage from this drug

has not been clearly established. There is evidence that the effects of EE result from both metabolite-dependent and hypersensitivity-mediated processes (Westphal et al., 1994). EE was also reported to cause reductions of bile flow and bile acid excretion in a dose dependent manner (Gaeta et al., 1985; de Longueville et al., 2003).

In 1968, Desmet et al. reported the ability of α -naphthyl-isothiocyanate (ANIT) to directly cause hepatobiliary cholestasis in the rat. It was used as a classic model compound to study the mechanisms of intrahepatic cholestasis. Although not finally clarified, it is proposed that ANIT causes liver injury in a dose dependent way by a reduction of the hepatic antioxidant defence system mediated by SOD and catalase, which in turn could contribute to the development of hepatic lipid peroxidation (Ohta et al., 1999). Additionally, the unstable thiocarbamoyl-GSH conjugate (GS-ANIT) is exported in the bile canaliculi and, after dissociation, ANIT accumulates, thereby leading to damage of biliary endothelial cells (Jean & Roth, 1995).

The toxicity of Acetaminophen (AAP), a commonly used analgesic, is the most common cause of acute liver failure in man (Larson et al., 2005). It is catalyzed by CYP enzymes, mainly by CYP2E1 and CYP1A2, to a toxic intermediate which in turn is deactivated by building adducts with glutathione (Mutschler et al., 2008). Excessive amounts of the metabolite leads to a depletion of glutathione resulting in adduct formation and to increased susceptibility to oxidative stress. It was reported that an inhibition of metabolism led to a resistance against AAP (Zaher et al., 1998).

Troglitazone (Tro) is an anti-diabetic and anti-inflammatory drug which was withdrawn from the market in 2000 due to idiosyncratic reaction leading to drug-induced hepatitis. It belongs to the class of thiazolidinediones, the same class as Rosiglitazone (Rosi). The mechanism of action is proposed to act via activation of peroxisome proliferator-activated receptors (PPARs), mainly the γ -Type. The anti-inflammatory effects are correlated with a reduction of *nuclear factor kappa-B* (NF κ B) accompanied by an increase in its inhibitor (I κ B) (Aljada et al., 2001). *In vitro* studies of Tro and Rosi cytotoxicity in human hepatocytes revealed differences in the toxicity of Tro and Rosi whereby Tro appeared to be more toxic than Rosi, by all endpoints (Lloyd et al., 2002).

Another PPAR activator is one of the non-toxic compounds used in this study, Clofibrate (Clo). By activating PPAR α , it causes a lowering of triglyceride-levels in the blood and activates the lipoprotein lipase (Lpl) (Mutschler et al., 2008). As with all

PPAR activators, this compound may have carcinogenic potential in long-term experiments, but it causes no acute liver damage.

Metformin (Met), analogous to the thiazolidinediones Tro and Rosi, lowers glucose production in the liver and is therefore used as an oral antihyperglycemic drug in the management of type 2 diabetes. In contrast to Tro and Rosi, Met acts primarily by decreasing endogenous gluconeogenesis, whereas Tro acts by increasing the rate of insulin mediated peripheral glucose disposal (Inzucchi et al., 1998). Even so, this drug has been in clinical use for up to 40 years now and detailed molecular mechanisms remain unclear. Recent gene expression studies found several genes deregulated linked to metabolic pathways involved in gluconeogenesis and lipid metabolism (Heishi et al., 2006).

Theophylline (Theo) is a caffeine related xanthine derivative, an alkaloid which is used for the treatment of respiratory diseases. It acts by inhibition of phosphodiesterase activity and has additionally anti-inflammatory effects. It is metabolized extensively in the liver (up to 70%) and undergoes N-demethylation via cytochrome P450 1A2 (Mutschler et al., 2008). This compound is not known to cause liver damage, but nevertheless, due to its several other side effects, it is only used as a second- or even third-line clinical solution (Boswell-Smith, Cazzola & Page, 2006)

17 β -Estradiol (17bEs) is an important naturally occurring steroid hormone. It acts as a female sex hormone and causes prostate enlargement in males (Mutschler et al., 2008). It was shown that in chronic studies that this compound increased the incidence of tumours in several organs (Shull et al., 1997), but no direct adverse effects on the liver are known.

The synthetic glucocorticoid Dexamethasone (DEX) has an immunosuppressive activity and also inhibits inflammatory processes. Due to these effects, it is used in clinics as an antagonist for liver damage caused by inflammation. Additionally, by binding to intracellular receptors, the transcription of multiple genes, e.g., metabolic enzymes, is modulated.

Naloxone (Nal) antagonizes opioid effects by competing for the same receptor sites. It is therefore a pure narcotic antagonist without the side effects of respiratory depression, psychotomimetical effects or pupillary constriction, it exhibits essentially no

pharmacological activity (Sadée et al., 2005). It is metabolized in the liver, primarily by glucuronide conjugation and excreted in urine.

Quinidine (Q) is an antiarrhythmic agent. Additionally, it is used as an antimalarial schizonticide. It acts by inhibiting mainly the fast inward sodium transporter of neurons (I_{Na}). It also inhibits the CYP2D6 which can cause increased blood levels of the drug. By inhibition of transporter proteins, it can cause some peripherally acting drugs to have CNS side effects, such as respiratory depression, if the two drugs are co-administered (Sadeque et al., 2000). Quinidine is metabolized by CYP3A4 and there are several different hydroxylated metabolites, some of which have antiarrhythmic activity (Nielsen et al., 1999).

The new compound EMD X is an internal Merck Serono compound. It was accepted to be used for the verification of the classification model but detailed background information, as well as the molecular structure, are proprietary.

3.4.3 Experimental setup and dose finding

The culture of primary rat hepatocytes was conducted in SW-FCS conformation. After plating, cells were incubated for three days to adapt to the cell culture environment. Previous results showed that most changes in gene expression occur in the first two days after perfusion and that, in SW-FCS culture, gene expression stabilized afterwards (chapter 3.3). This time of pre-culturing was chosen to avoid a high level of false positive genes which may mask any compound specific effects.

For dose finding, two different cytotoxicity tests were conducted with membrane integrity (LDH-test) and cell viability (ATP-test) as the endpoints. For each compound, a series of multiple concentrations was run at least in biological triplicates for all time points tested to ensure statistical validity of the results. EC_{20} values were calculated for both cytotoxicity tests at all time points. The EC_{20} is the concentration of drug/xenobiotic required to induce a 20% loss of membrane integrity (LDH-test) or a 20% reduction in ATP content (ATP-test).

The final test concentrations for each compound were selected by combining the results from the LDH- and ATP-tests. One fifth of the EC_{20} value was taken as a second concentration. This non-cytotoxic dose is still expected to have effects on gene expression.

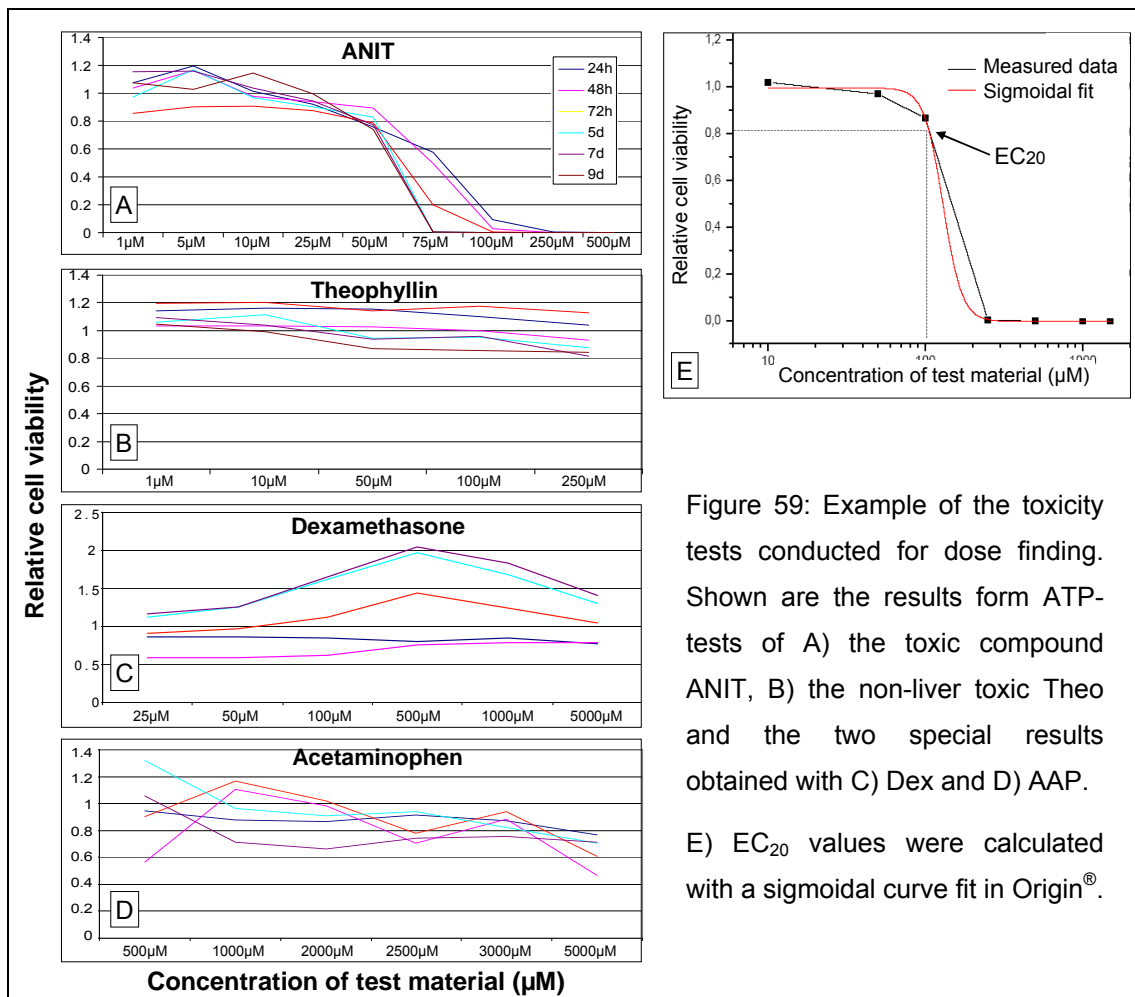


Figure 59: Example of the toxicity tests conducted for dose finding. Shown are the results from ATP-tests of A) the toxic compound ANIT, B) the non-liver toxic Theo and the two special results obtained with C) Dex and D) AAP.

E) EC₂₀ values were calculated with a sigmoidal curve fit in Origin®.

ANIT, as a positive compound showed a clear dose and time dependency in its cytotoxic effects, with a suggested threshold of about 50 μM. For Theo, a non-liver toxic compound, no effects were detected up to the limit of solubility. In this case, the highest soluble concentration was defined as the high dose and one fifth as the low dose. Dex showed a very unusual dose response. No toxicity was detected, but instead, an increase of cellular viability at a medium concentration of 500 μM was seen (Figure 59C). As discussed previously, Dex has a positive effect on liver gene expression and stabilizes cell viability and gene expression in culture. Nevertheless, at high doses, other mechanisms seem to be having a negative effect on cell viability. Additionally, morphological changes were observed at all doses (Figure 60). The number and diameter of the bile canaliculi was significantly increased. Up to the medium dose, this was accompanied by an increase of canalicular transport, demonstrated by an accumulation of a fluorescent substrate in the canaliculi. However, at high doses of Dex, even though the bile canaliculi were again increased in diameter, this transport mechanism was inhibited and biliary transport was reduced (data not shown). To allow for these findings, three doses were used for Dex.

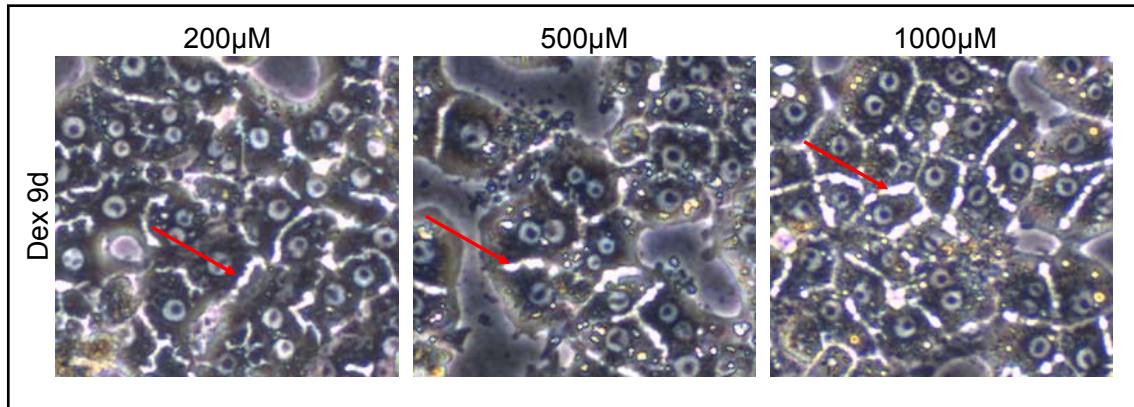


Figure 60: Primary rat hepatocytes in SW-FCS 9 d after dosing with three concentrations of Dex. The red arrows indicate the bile canaliculi.

AAP, a classic liver toxic compound, did not show any toxicity in SW-FCS cultured hepatocytes. This is in contrast to previously reported studies, which clearly showed a toxic effect (Thedinga et al., 2007; Mingoia et al., 2007; Suzuki et al., 2008; Ullrich et al., 2007). A major difference between previous studies and this approach is the time in culture and the time of dosing. Whereas other studies were mainly short term with the compound treatment 4 h or 24 h, cells were treated in this study after 3 days. Looking at the mechanism of action, it becomes clear that AAP is not toxic itself but is metabolized to toxic intermediates by CYP isoforms, mainly CYP2E1. By looking at the gene expression data of rat hepatocytes in culture (Table 24), a strong reduction in CYP2E1 expression was seen. Jemnitz and his co-workers showed a clear dependency of AAP toxicity and time point of dosing with a greatly increased resistance to toxicity at later time points, in different species. Interestingly, they found no clear correlation of AAP toxicity to CYP2E1 activity (Jemnitz et al., 2008). These results show the importance of a detailed knowledge of the test system and ideally of the mechanism of action and metabolism of the compound tested. Due to these results, AAP was removed from the dataset and was not used for the calculation of the prediction model.

As a result of the toxicity tests, the concentrations noted in Table 28 were used as the final concentrations used in the gene expression profiling experiments. For clarification, the higher concentration will be named “high” and the lower concentration will be named “low”.

Compound	Low Dose [μ M]	High Dose [μ M]	Compound	Low Dose [μ M]	High Dose [μ M]
Tet	40	200	Cp	4	20
Clo	200	1000	Q	20	100
Theo	50	250	DEX	200/500	1000
ANIT	9	45	Rosi	16	80
Nal	12	60	Tro	14	70
EE	17	85	Met	300	1500
17bEs	0.05	0.25	EMD 335825	200	1000
AAP	1000	5000			

Table 28: Concentrations of the test compounds used. The high concentration resembles the approximation of the EC₂₀ of both cytotoxicity tests conducted (LDH- and ATP-test), the low concentration is one fifth of this value. Dex, as a special case, has a third concentration due to the fact that at this concentration a positive effect on cell viability was detected.

Cells were exposed to the test compounds continuously for 9 d with media change every second day and observed for morphological changes (Figure 61). To exclude any solvent effects which may have influenced gene expression, compounds were concordantly dissolved in DMSO as a 200x stock resulting in an end concentration of 0.5% of DMSO in the media. In the case of Met, which itself is not soluble in organic solvents, the DMSO was added directly to the media to guarantee standardized conditions. Therefore, time matched vehicle controls were treated with 0.5% DMSO.

Samples were taken at 2 h, 1 d, 3 d, 5 d, 7 d, and on day 9 after the first dosing. RNA was reverse transcribed, labelled and hybridized on Illumina RatRef-12 BeadChips. Data analysis was conducted in BeadStudio (Illumina Inc.) and Expressionist Analyst (Genedata). Data was normalized with the LOESS algorithm in order to compare multiple arrays. Fold changes and statistical analysis were calculated in regard to the time matched vehicle controls.

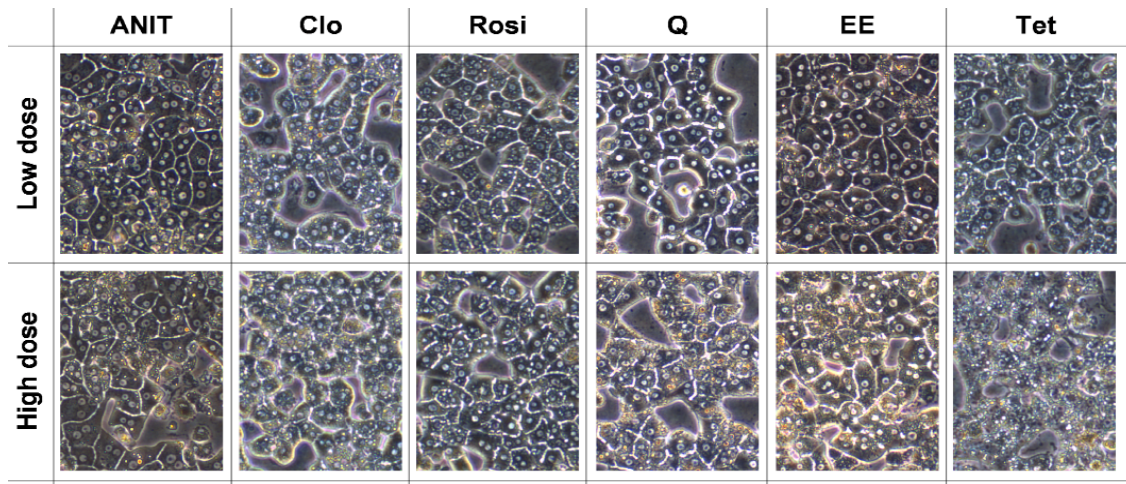


Figure 61: Cells dosed with either the high or low dose of ANIT, Clo, Rosi, Q, EE or Tet on day nine of treatment. Interestingly, not only the hepatotoxic but also non-hepatotoxic compounds caused morphological changes, including the accumulation of lipid droplets (Clo, Q). On the other hand, ANIT did not significantly alter the morphology of the hepatocytes. Most severe changes were detected in cells dosed with high concentrations of Tet. These results fit to previously published *in vivo* data (Zidek et al., 2007).

3.4.4 Data Analysis and establishment of an *in vitro* prediction model for hepatotoxicity

As a first overview of the data a hierarchical clustering was performed with all time points tested (2 h, 6 h, 1 d, 3 d, 5 d, and 9 d after dosing). As shown in Figure 62, no clear separation was achieved at any of these time points. On days one and five, Rosi and Clo separated from the other experiments, but on day one also the liver toxic compound Tet grouped together with them. All other experiments were organized in two large groups but clearly not based on toxicity. At later time points, cells treated with all three doses of Dex separated from the other experiments and built their own cluster. These findings were also shown by other clustering methods, such as PCA (Figure 63). These results re-enforce the difficulty in establishing a model based on global gene expression. Also toxic compounds have specific mechanisms of action with specific gene expression changes, and these differences can be hidden by the large number of unaffected genes. To establish a model capable of discriminating between the two defined groups, other techniques are needed.

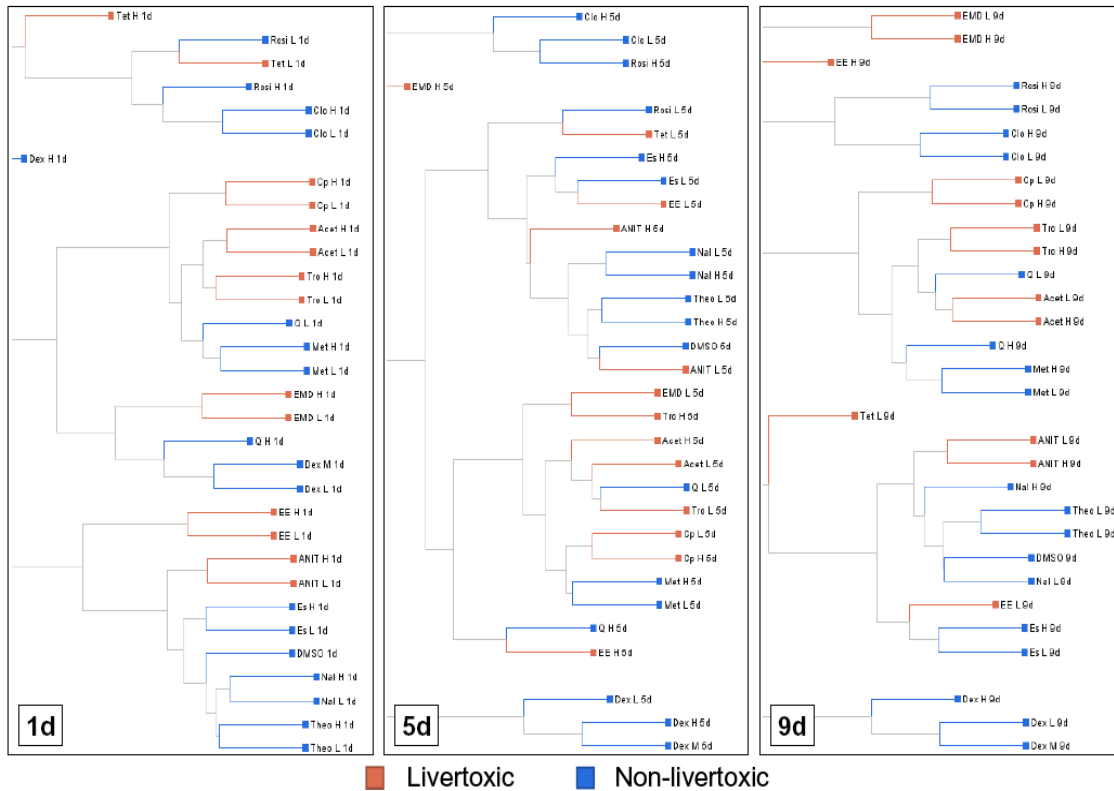


Figure 62: Hierarchical clustering from global gene expression data from compound treated primary rat hepatocytes. Shown are the results from cells dosed for 1 d, 5 d and 9 d with the previously described model compounds. No obvious separation of toxic and non-toxic compounds was achieved at any time point.

The normalized data was grouped by compound, time point, and dose. Finally two groups, toxic and non-toxic, were defined according to the previously defined toxicity (see Figure 58). First, the possibility to create a functional classification model was

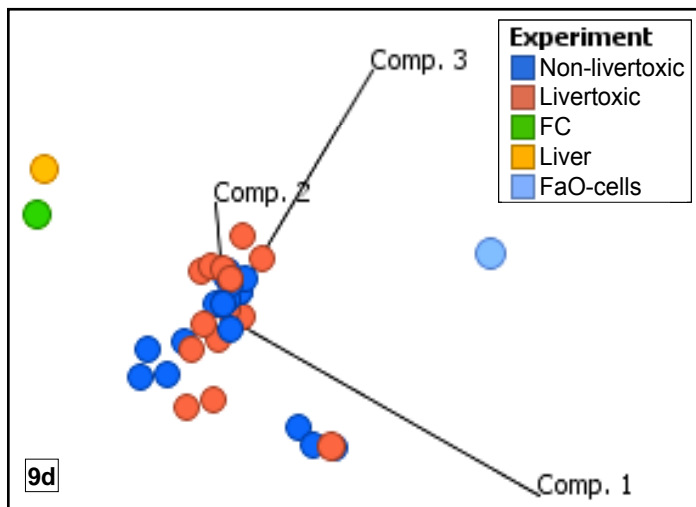


Figure 63: PCA with global gene expression data from cells treated for 9 d with previously described model compounds.

tested. Therefore, trainings sets were created for all time points and for the high and low doses separately as well as for both together. The classification was conducted with four different classification algorithms to account for any potential “peculiarities” in the dataset. The support vector machine algorithm (SVM), the sparse linear discriminant analysis, the fisher linear discriminant

analysis and the K-nearest neighbour analysis, all of which are supervised learning methods, were used. They were applied on the same dataset that was used for the training, but in this case, the leave-one-out cross-validation method was applied. This means that the training set was applied 1,000 times on the whole dataset, but in every run, 15% of the dataset were removed and the remaining data was classified. This classification method was checked for its accuracy afterwards and misclassification rates for each of these algorithms were calculated. This number defines the percentage by which the samples were allocated to the wrong group. At the same time, genes were ranked according to their importance for this discrimination and the number of genes needed for best results were calculated. Results are shown in Figure 64.

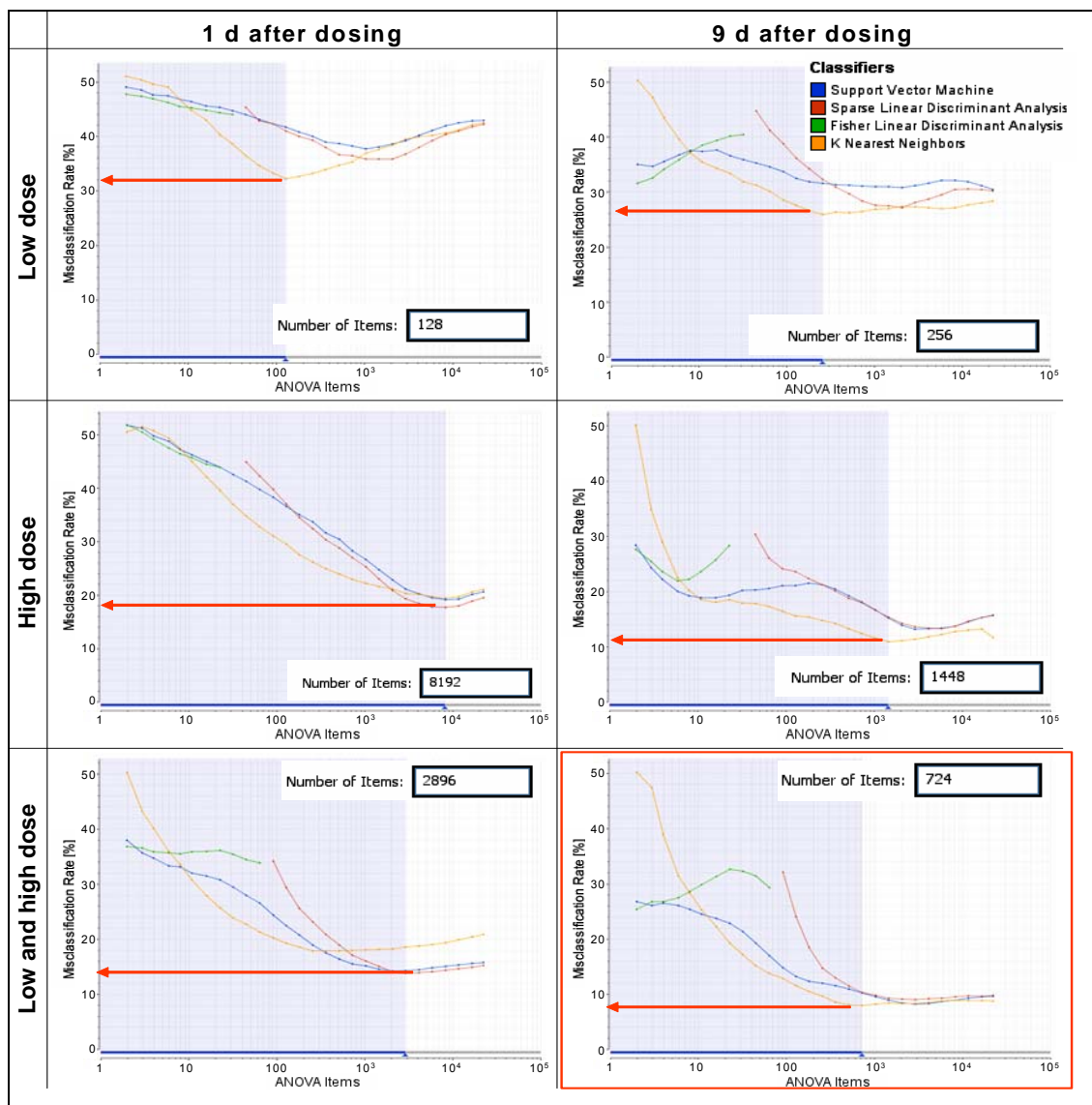


Figure 64: Construction of the classification models and gene rankings. Four different algorithms were applied to discriminate between two previously defined groups (toxic and non-toxic). For each algorithm, the misclassification rate and the number of genes needed for best results were calculated.

In most cases, the classification algorithm of K nearest neighbour resulted in the best predictions. Generally, the misclassification rates were lower for the samples treated for 9 d than for samples treated for shorter times. By analysing only the low dose samples, a misclassification rate of approximately 32% was detected one day after dosing. This result was only slightly, but not significantly, improved at later time points. Taking only the high dose groups into the model resulted in a misclassification rate of 19% after one day of dosing and 11% after 9 d. Best results were obtained with samples dosed for 9 d in culture taking both doses together into the model. In this case, the misclassification rate was reduced to 7.5%. To reach this rate, only 724 genes were needed and were sufficient.

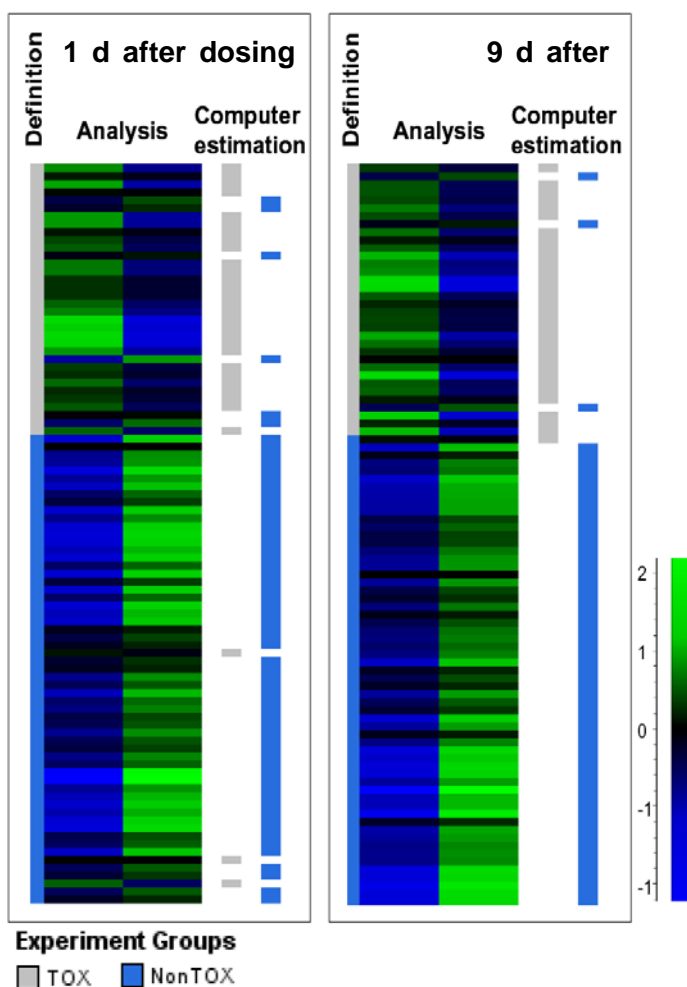


Figure 65: Visualization of the “leave one out” cross validation showing the defined groups (left side) as basis for the calculation. The calculated significance is indicated by green as toxic and blue as non toxic (see side bar). The computer estimation for the whole dataset is shown on the right side of the figures. Shown are the results (both doses) on day 1 and 9 after dosing.

Figure 65 shows examples of the results of the cross validations, 1 d and 9 d after dosing. It is clear to see the reduction of misclassified samples for the later time point. Whereas in the early samples the computer estimated both false positive and false negative samples, at later time points there were no falsely positive predicted samples. Only three samples were misclassified, all of which were low dose samples. One biological replicate of each, Tro, Tet and ANIT was wrongly predicted to be non-toxic. However, the whole group was still classified as toxic. All three groups had a classifier output of below 0.5, which means that they were relatively close to the imaginary midline between both groups and do not significantly differ. All together, this shows the need for replicate experiments

to increase robustness of the model by tolerating single experiments to be misclassified but retaining the overall correct result.

The main objective of this study was to determine whether it would be possible to distinguish between hepatotoxic and non-hepatotoxic compounds with the help of an *in vitro* system and global gene expression analysis. The clustering analysis of the global gene expression data alone did not allow such discrimination. By using the support vector machine algorithm together with a cross-validation, it was possible to obtain a subset of genes that allowed the discrimination, with a false discovery rate of only 7.5%. These results clearly show the advantage of longer term dosing for the establishment of gene expression changes, which clearly contribute to the discrimination of the two groups. Short term experiments only show the acute effects of a compound, like inflammatory or immune responses. This is not sufficient in *in vitro* experiments, because of the lack of certain cell types and therefore specific mechanisms may be missing. Dosing for longer times has the advantage of increasing compound specific gene expression changes and therefore enables the discrimination algorithms to find basic differences between toxic and non-toxic compounds in the dataset.

At the same time, the combination of two different dosing schemes also contributed to a better model. This could be simply due to the fact that more data was available for the algorithm, making the comparison more valid. Additionally, by combining high and low doses, further information hidden in the global gene expression data set may be accessible to the algorithm. It is noticeable that the low dose treated samples alone were poorly distinguishable by the algorithms but improved the result of the whole dataset. This shows that this effect is not just additive but that there is really additional information introduced into the calculation by the low dose samples. For future applications these results imply that large datasets and, if possible, two (or more) doses are required for these kind of calculations.

As detailed above, the aim of such prediction models is the classification of new data from novel compounds. This would not be possible by simple clustering methods but by ranking genes according to their contribution to the discrimination of the predefined groups and generation classifiers, this goal was achieved.

For the verification of this prediction model, the potential hepatotoxicity of EMD X was predicted. Dosing and data acquisition for this compound was conducted exactly as described for the model compounds. Additionally, the same classifier was applied to the whole dataset, including the data from AAP and the model compounds used for the calculation of this model as a retrospective verification of the previously analyzed data.

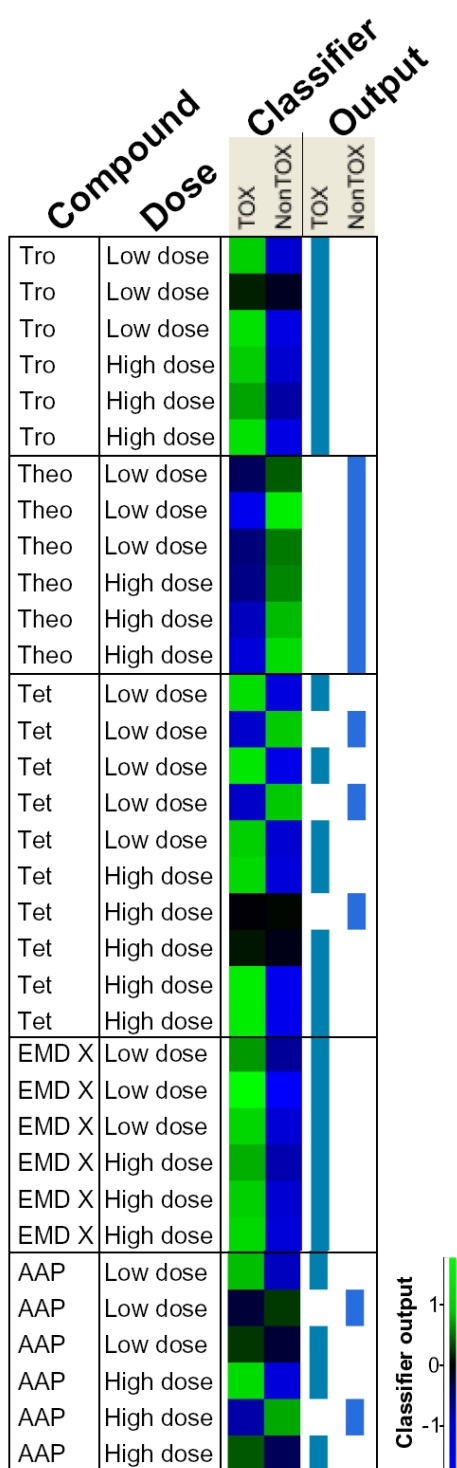


Figure 66: Result of the classification of data gained from primary rat hepatocytes treated for 9 d with Tro, Theo, Tet, EMD X and AAP. Shown are the concordances to the classifier, where green means high and blue means low concordance, and the final estimation of the algorithm.

With altogether 120 experiments, the calculated misclassification rate of 7.5% would allow nine experiments to be wrongly classified (partly shown in Figure 66). Overall, only eight experiments were misclassified. In most cases, all experiments were classified correctly, independent of the dose. For Tet, two out of five low dosed and one of the high dosed experiments were misclassified. Even so, because of the five biological replicates, the majority of these experiments were still correctly classified resulting in an overall correct classification for Tet. The new compound EMD X, was classified as hepatotoxic. All experiments were clearly allocated to this group resulting in a robust classification. This result corroborated perfectly with previously obtained results from other in house studies (data not shown).

Another interesting result was obtained by the classification of AAP. Even so no toxicity was detected in the cytotoxicity tests (LDH and ATP test), the compound was still classified as hepatotoxic in both high and low dose treatment groups based on the global gene expression. A closer look on the single experiments revealed that in both doses, one experiment was classified as non toxic and two as toxic. The classifier output in most cases was unequivocal suggesting borderline classification. This means that the classification of this compound is less robust than for EMD X. Nevertheless, the classification showed an effect which could not be detected by cytotoxicity tests, but is well known *in vivo*.

3.4.5 Analysis of the top ranked genes of the prediction model

During the process of calculating the prediction model, the genes were ranked by importance for the discrimination process. This ranking was achieved by ANOVA, a variance analysis method. The results showed 724 genes to be essential for the best classification of the experiments at 9 d (Appendix 13). These genes were analyzed for their molecular function and their involvement in toxicologically important cellular processes.

The dataset, although quite large, is certainly not sufficient to discriminate between different types of hepatotoxicity. There are multiple pathways leading to toxicity, with complex and intersecting mechanisms. The aim of this work was to evaluate the possibility to detect and predict general hepatotoxicity.

It is important to mention that the algorithm used for gene ranking is not selecting the genes according to their fold change, their statistical significance or their biological functions but according to their contribution to the classification. Nevertheless, it might be helpful to have a closer look at the genes that differentiated between hepatotoxic and non-hepatotoxic compounds.

Figure 67 shows the result of a k-means clustering, which grouped the genes according to their gene expression profile in all samples. It can be seen that none of the clusters were discriminative on their own. But taken together, the information contained in these profiles is the basis for the discrimination model generated.

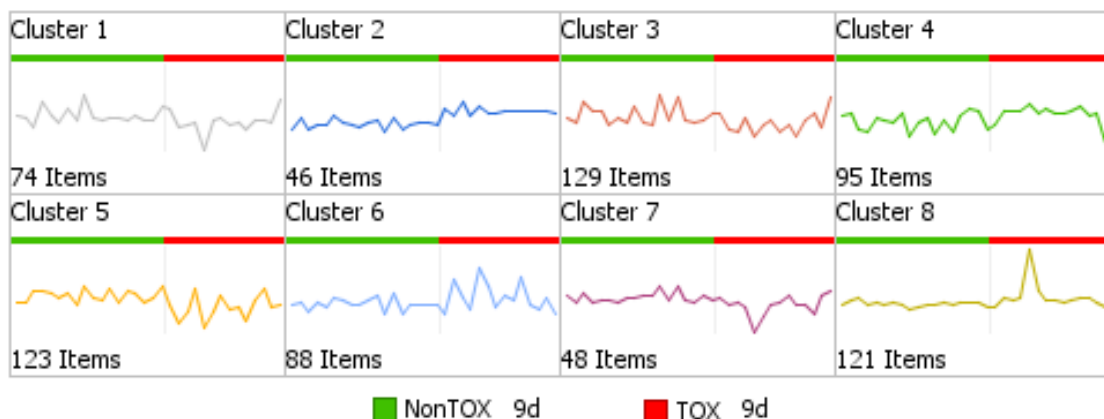


Figure 67: Results of a k-means clustering with all samples used for classifying and the 724 top ranked genes at day 9 of treatment. Genes were grouped according to their gene expression profile.

The PCA in Figure 68 was calculated with the 724 top ranked genes. In comparison to the PCA shown in Figure 63, which was calculated with the whole dataset, both groups

have now separated at least to a certain degree, although still no complete separation was seen. Thus, these genes clearly have inherent information that enables the separation of these groups, but at the same time, they are not sufficient for a 100% separation, explaining the false classification rate of 7.5%.

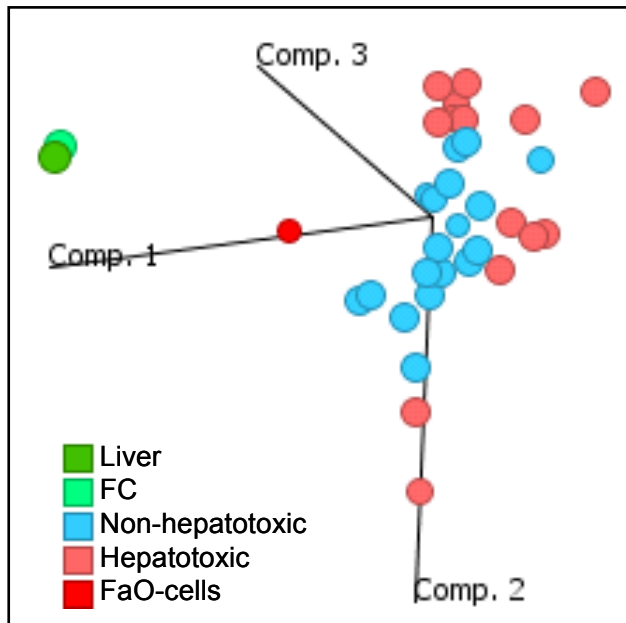


Figure 68: PCA with the 724 top ranked genes from the model previously described.

The top “hit” when a Fisher’s Exact Test analysis was performed was proteasome complex and protein degradation. In total, 17 protein subunits of the proteasome were important for discrimination. The proteasome is a multiprotein complex which has an important function in protein degradation in an ATP/ubiquitin-dependent process, in a non-lysosomal related fashion. A modified proteasome, the immuno-proteasome, is responsible for the processing of class I MHC peptides and is therefore involved in immunogenic responses. Another function of the proteasome is the directionality of the cell cycle by degrading the polyubiquitinated cyclins. Changes in cell cycle are often the result of cell damage or the recovery process following, for example, a necrotic event. The impairment of the cell cycle is also documented by cyclin-dependent kinases (Cdk7) or s-phase related proteins, which were also part of this gene selection. Several genes, Myc, Egf, the MAP kinase activated protein kinase2 (Mapkapk2), Tgf β 2 and the inhibitor of kappaB kinase (Ikbkb), play important roles in intracellular signalling and thereby influence cellular fate, growth, cell cycle or metabolism. Other signals may drive the cell in the direction of apoptosis or survival as a reaction to oxidative stress or cell damage.

The involvement of energy metabolism in liver toxicity was highlighted by lactate dehydrogenase B (Ldhd), triosephosphate isomerase (Tim) and Enolase. Also directly

linked to ATP production are genes such as ATP synthase C1 and d subunits, cytochrome c reductases NADH dehydrogenases. Other genes function as part of cellular adhesion complexes, for example the junctional adhesion molecule 3 (Jam3) and claudin 10, which are part of the tight junction complex and integrin-mediated cell adhesion. Both proteins are important for canalicular functionality.

Xenobiotic metabolism genes were also contained in the selection. CYPs 1A1 and 2E1 have important functions in the detoxification of a large number of compounds and therefore it is not surprising to find them included. Microsomal Gst 2 is an important phase 2 enzyme for drug detoxification and is involved in the production of leukotrienes and prostaglandin E, which are important mediators of inflammation.

Taken together it is clear that many of the discriminative genes ranked are linked to mechanisms known to be related to toxicity or cellular damage. Again, it is important to note that the compounds used for this model work via a variety of mechanisms, which is shown by many genes affecting multiple important pathways.

3.5 Insights into the mechanisms of action for selected compounds

From the beginning, the aim of this study was the establishment of a model that can predict general hepatotoxicity in an *in vitro* system. Nevertheless, the amount of data collected during our study allows to perform additional mechanistic analyses. The comparison of the data generated from an *in vitro* toxicogenomics study with Tet showed high correlation to the results of an *in vivo* study with the same compound (chapter 3.1.1.4). Of course, not all the compounds can be conferred here in this detail, but some interesting new findings are discussed. Details of the mechanism of action of EMD X, which clearly showed toxicity in cell culture and was classified as toxic by the predictive model is be discussed in this chapter. Additionally, AAP is discussed, because the result from the predictive model (supported by *in vivo* data) differs from the results gained with standard *in vitro* cell viability testing. To show that genomic profiling can have conflicting results, too, some effects of Dex will be discussed in the context of cell morphology.

3.5.1 EMD X

The proprietary Merck compound EMD X, was used for validation of the model because of the availability of extensive in-house data. In fact, while being blinded for the model testing, it is known to cause hypertrophy of hepatocytes and, in high doses,

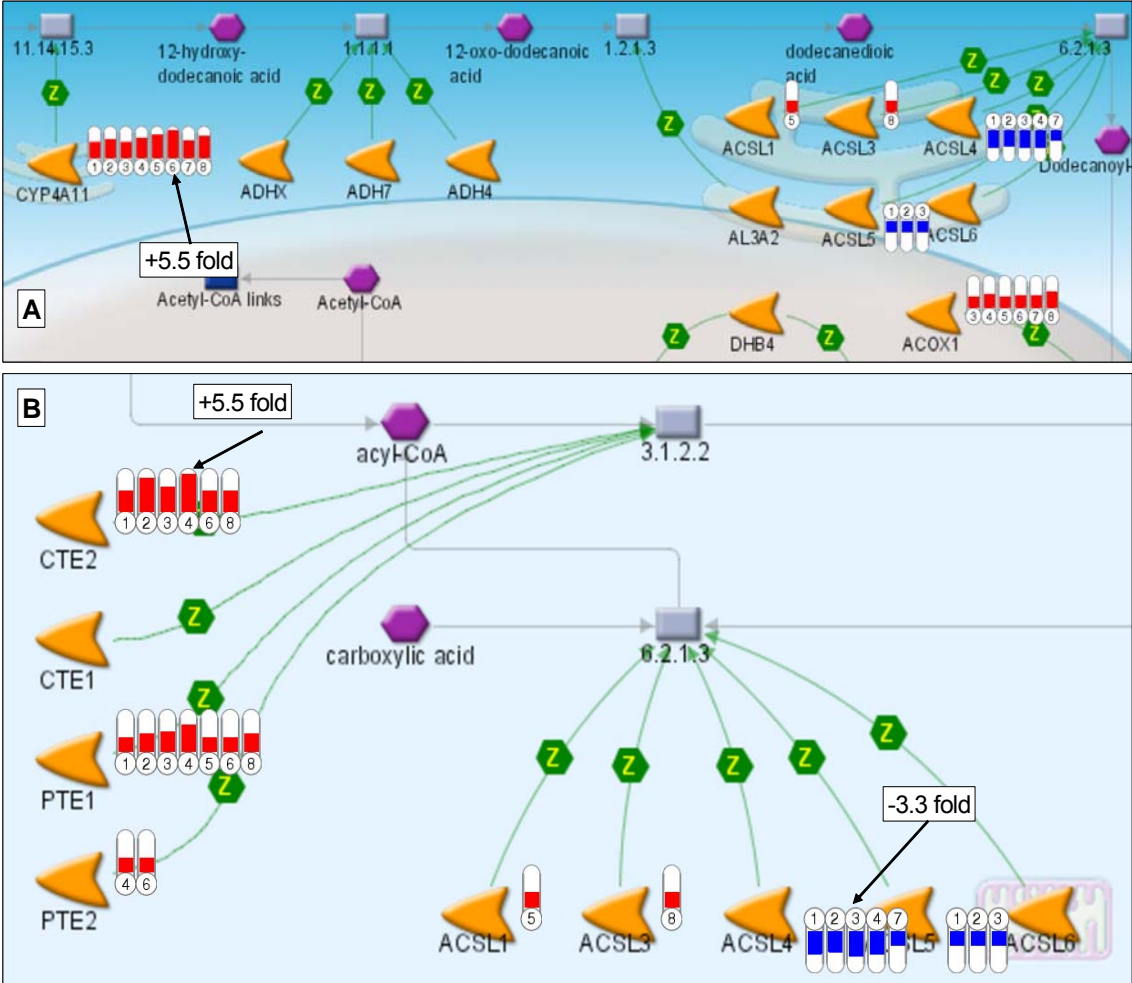
bile duct inflammation, hyperplasia and liver cell necrosis. At least some of these hepatotoxic effects seem to be present *in vitro* as well, leading to a clear classification of EMD X as hepatotoxic.

Looking at the induced genes and mechanisms, it is obvious that this compound affected fatty acid and energy metabolism. The top ranked mechanisms there included the activation of fatty acid synthase activity, regulation of lipid metabolism via LXR, NF- κ B and SREBP. Also fatty acid oxidation and PPAR α dependent genes, like Acox1, Cpt1 α and β , Cte1 and CYP4A, were induced (Figure 69). Acyl-CoA thioesterases (Cte), which generates carboxylic acid and free Coenzyme A, were induced, whereas the generation of acetyl-CoA by acyl-CoA synthetases (ACSL) was reduced simultaneously. A metabolic activation was found to result as a response to an external stimulus, probably to EMD X treatment. Although the PPAR α activation is not directly proven, these results show a high correlation to the results of the *in vivo* in-house data and exhibit clear characteristics of PPAR-dependent gene expression changes.

CYP4A11 catalyzes the omega-hydroxylation of various fatty acids and was consistently induced, as was carnitine palmitoyltransferase (Cpt1a), the enzyme that catalyses the transfer of long chain fatty acids to carnitine for translocation across the mitochondrial inner membrane. These changes imply an increased need for energy of the cells after compound treatment. Whether this is a direct effect of EMD X treatment or a secondary effect due to the recovery after cellular damage can not be concluded from this data and needs to be further studied.

The strong induction of several Gst enzymes indicates a reaction to oxidative stress within the cells. This might be caused by an increased metabolism resulting in increased amounts of ROS generated or by inflammatory processes. In support of the latter is the activation of AKT kinase (mediating survival to oxidative stress) at early time points and the finding that apoptosis related mechanisms being activated including the transcriptional up-regulation of caspases.

Several genes involved in cellular adhesion, fibronectin, actin and other genes, were found to be reduced, implying cytoskeletal remodelling and a reduction of cellular anchoring, which may have been caused by the increase in cell volume, shown by histopathological investigations. Additionally, E-cadherin, which is used as a prognostic marker for hepatocellular cancer (Iso et al., 2005) was reduced at all time points and all doses.



- | | | | |
|----------------|----------------|----------------|----------------|
| 1. EMD 1d Low | 3. EMD 3d Low | 5. EMD 5d Low | 7. EMD 9d Low |
| 2. EMD 1d High | 4. EMD 3d High | 6. EMD 5d High | 8. EMD 9d High |

Figure 69: Details of the omega-oxidation pathway of fatty acids (A) and the CoA biosynthesis pathway (B). Both pathways were found to be induced by EMD X treatment (modified from Metacore, GeneGO).

Noticeable was the strong reduction of the complement pathway at all time points at both doses (Figure 70). This pathway, consisting of more than 30 proteins mainly synthesized in the liver (more than 90%), is part of the innate immune system and works by proteosomal activation after stimulation. The complement cascade leads to massive amplification of the response and to activation of the cell-killing membrane attack complex, thereby functioning as a pathogenic defense mechanism (Mayer, 1984). Other functions include the attracting of immune cells, increasing the permeability of vascular walls and the initiation of inflammation. Earlier studies showed that transcription is induced during acute phase response following liver injury (Prada, Zahedi & Davis, 1998; Stapp et al., 2005).

The expression of complement factors is thought to be transcriptionally controlled by several liver specific transcription factors (TFs) (such as HNF's and C/EBP's) (Pontoglio et al., 2001; Garnier, Circolo & Colten, 1996). Interestingly, these factors were only slightly affected. The effect that EMD X has on these TFs, and the resulting strong inhibition of the complement pathway, is important and still needs to be confirmed.

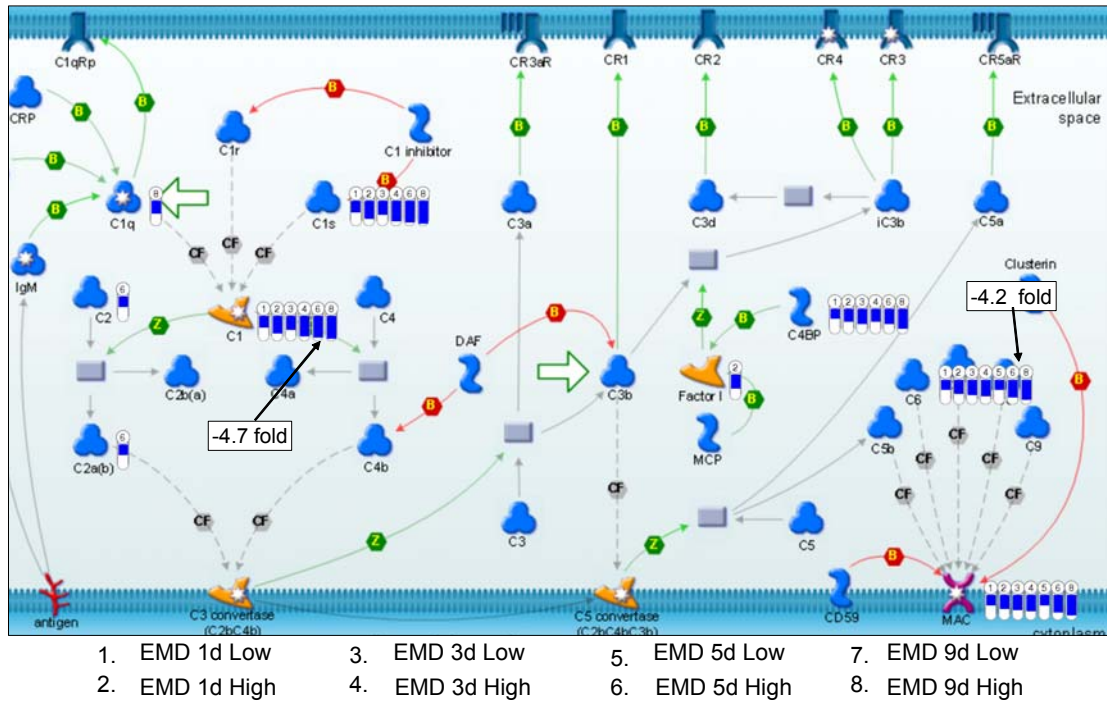


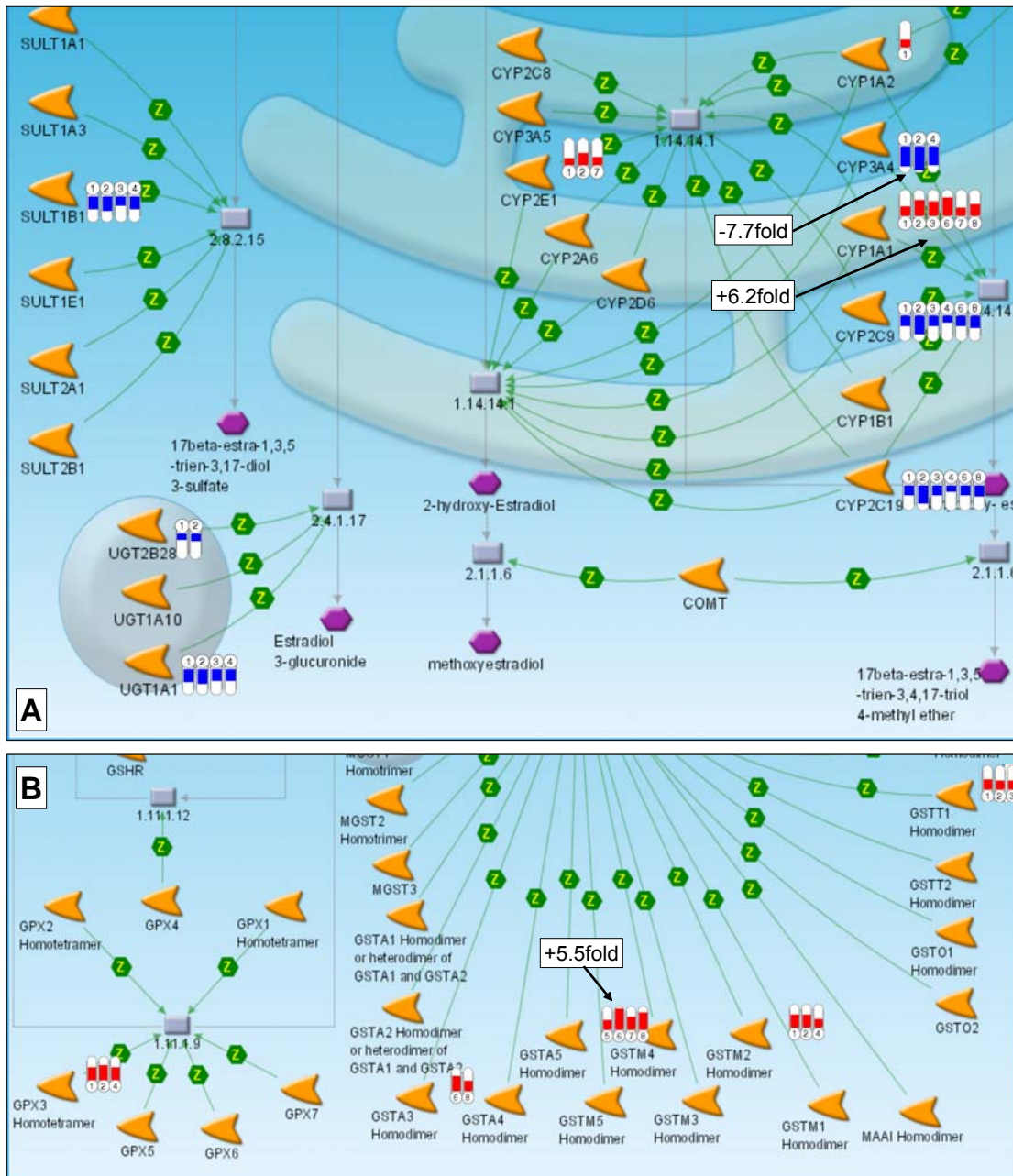
Figure 70: Genes of the classical complement pathway were found to be heavily reduced after EMD X treatment, independent of time and dose (modified from Metacore, GeneGO).

These results are in good concordance with in house *in vivo* data, where in rats treated with EMD X a reduction of C1s and C6 was detected. However, C4bp, reduced *in vitro*, was nearly unaffected *in vivo*. A loss of complement activity results in diminished liver regeneration, accompanied by transient or fatal liver failure after partial hepatectomy (Strey et al., 2003). It may therefore be concluded that an impaired recovery after cellular damage may contribute to the hepatocyte necrosis seen in the histopathology after treatment.

3.5.2 AAP

AAP is one of the best studied compounds in respect to liver toxicity, because of two reasons. It was previously shown that primary hepatocytes lose their sensitivity to AAP and become resistant over time in culture (Jemnitz et al., 2008). These results

were confirmed by our negative cytotoxicity tests. If dosed 4 h or 1 d after plating, cells clearly showed reduced viability and increased LDH release (data not shown). Treatment 3 d after plating had no effect on ATP content or membrane integrity. Nevertheless, AAP was classified as hepatotoxic by our prediction model. The mechanistic gene expression analysis revealed clear adverse effects, but also showed a reduction of these effects over time.



- | | | | |
|---------------------|---------------------|---------------------|---------------------|
| 1. AAP 1d Low Dose | 3. AAP 3d Low Dose | 5. AAP 5d Low Dose | 7. AAP 9d Low Dose |
| 2. AAP 1d High Dose | 4. AAP 3d High Dose | 6. AAP 5d High Dose | 8. AAP 9d High Dose |

Figure 71: Genes of the phase 1 and phase 2 metabolism deregulated by AAP treatment in culture. Red bars indicate induction, blue bars the repression of gene expression (modified from Metacore, GeneGO).

AAP causes centrilobular hepatic necroses, via the CYP-generated reactive electrophilic metabolite N-acetyl-p-benzoquinone (NAPQI) (Tonge et al., 1998). The main players are the CYP-isoforms 1A2, 2E1 and 3A4. Normally, NAPQI is detoxified by an addition-reaction to GSH. This causes a depletion of GSH at higher doses and leads to covalently bound protein adducts, which finally cause the toxic effect (James, Mayeux & Hinson, 2003; Mitchell et al., 1973).

Overall, the deregulations observed were more intense at the beginning of treatment, with return to the baseline expression than at later time points of culture. CYP 1A2 and 2E1 were found to be significantly down regulated over time in cultures suggesting this as the reason for the increasing immunity of cells in culture. However, the same isoforms were found to be induced by AAP, making it possible that small amounts of the toxic metabolite may have been produced. Other isoforms, such as CYP 3A4 or 2C19, were heavily down regulated by AAP (Figure 71).

Generally, a reduction of phase 1 xenobiotic metabolism was observed whereas phase 2 metabolism showed an inconsistent picture. Sult1B1 and UGT isoforms were reduced, and several Gst isoforms were induced. UGTs were previously shown to be less expressed during liver regeneration after AAP treatment (Tian et al., 2005). Together, these results can be interpreted as a cellular mechanism for the protection of the cell against oxidative stress and the increased need for antioxidants, like GSH, to overcome the toxicity caused by AAP treatment. Deregulations in the AKT kinase pathway (Figure 72A) were time dependent. At early time points, HSP90, a molecular chaperone involved in ATP-dependent folding of proteins and in sequestering damaged proteins, was strongly reduced. Deregulations of genes downstream of AKT kinase imply a toxic mechanism early after dosing. MDM2 is a protein which affects the cell cycle, apoptosis and carcinogenesis by inactivating p53 and by interacting with other proteins (Bose & Ghosh, 2007). While this antagonist is repressed, p53 as well as caspase 9 and NF κ B were induced, driving the cells towards apoptosis.

Figure 72B and C show the reduction of other important cellular mechanisms. CDK7 is, as a complex with cyclin H and MAT1, an essential component of the transcription factor TFIIH, which is involved in transcriptional initiation and DNA repair. All three genes were reduced initially by AAP treatment. Additionally, the initialisation of translation was reduced. Together with the building of protein adducts by NAPQI, this reduction of correctly folded proteins may contribute to the toxicity of AAP.

All these effects may be the consequence of cellular stress caused by AAP and may be the reason that our model classified AAP into the category hepatotoxic. This result suggests the possibility to detect underlying toxic mechanisms that cannot be detected with other, established *in vitro* methods. The fact that most effects detected were only

transiently visible and no effects could be detected by cell viability tests may be an initial step to further studies, which are needed to uncover the mechanism of the increasing lack of response of primary hepatocytes in culture.

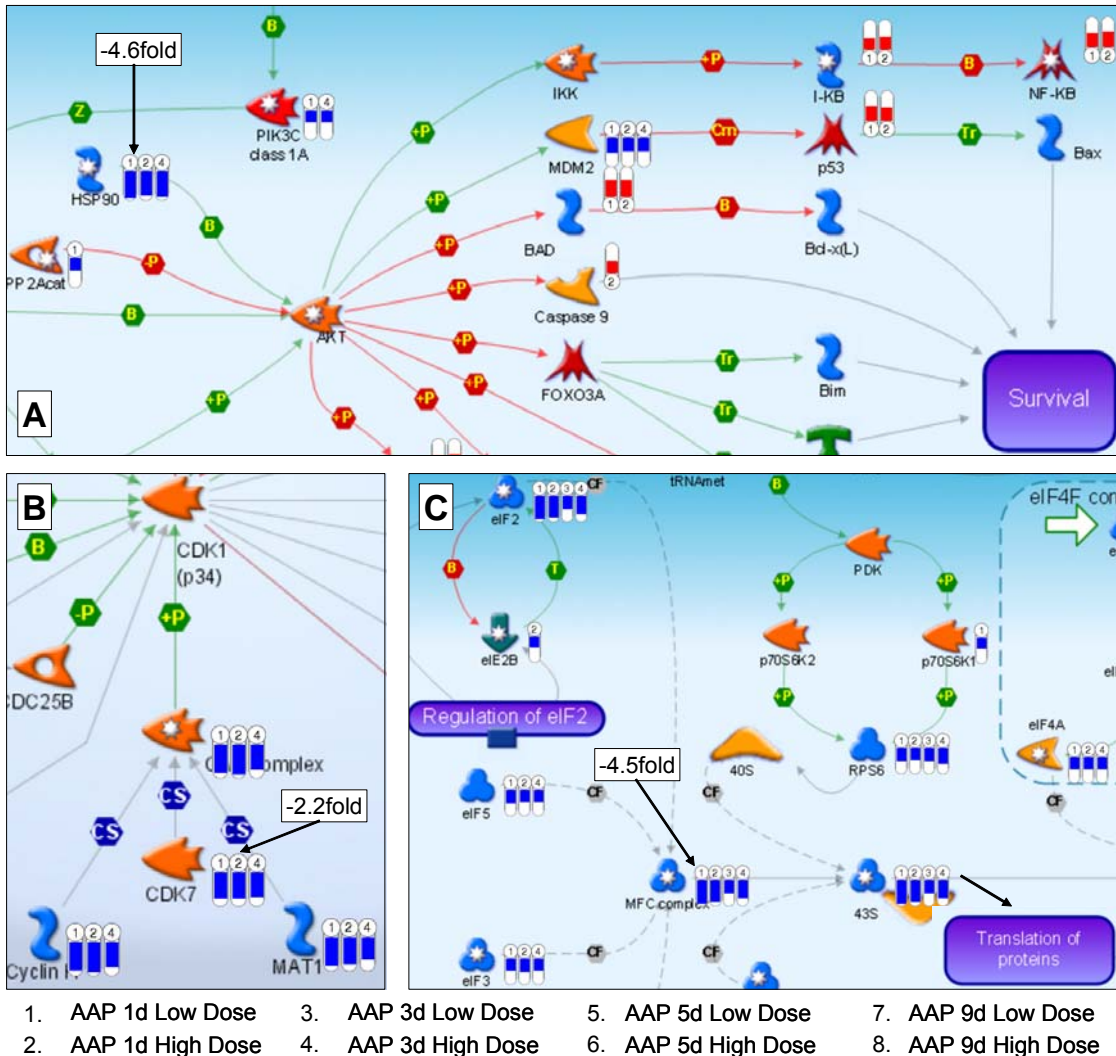


Figure 72: Deregulations caused by AAP treatment. A) AKT-kinase pathway, B) section of the cell cycle, C) translation initiation. Red bars indicate induction, blue bars the repression of gene expression (modified from Metacore, GeneGO).

3.5.3 Dex

As previously noted, Dex had a positive effect on cell viability and biliary transport, but only at the medium dose (500µM) group. It is known from previous studies that Dex inhibits hepatocellular proliferation at high doses by inhibiting tumor necrosis factor (TNF) and IL-6 (Nagy et al. 2003). The analysis of the gene expression data revealed an induction of nucleotide metabolism and transcription by RNA polymerase II, only at the medium dose. In contrast to this, there seems to be less oxidative stress, indicated

by an induction of oxidative stress related genes only in low and high dosed cells, but not in the medium dose. In contrast to this, pyruvate metabolism and insulin dependent signaling were reduced. The insulin pathway is critical for the regulation of intracellular glucose levels. The activated nucleotide production and the increased mRNA production are both energy consuming processes. At the same time, the energy producing pathways were reduced. These changes in gene expression are direct effect of Dex as a glucocorticoid and basal to the morphological and functional changes observed still needs to be analyzed. A real understanding of the underlying mechanisms taking place at the different concentrations could not be elucidated with this data.

The different compounds showed relatively large overlaps in gene expression changes. At the same time, all had some unique gene expression profiles (as discussed here). In cases where the same mechanism of action is involved, (e.g. Tro and Clo as PPAR α activators), known target genes like CYP4A and Cte were induced, but also clear differences were detected. For other compounds, unknown target genes and pathways were uncovered, which may give the beginning for future mechanistic investigations.

In contrast to previously conducted *in vivo* studies, no universal gene regulations were detected confined to in one of the both predefined compound-groups (Zidek et al., 2007). None of the genes were deregulated in one direction by all hepatotoxic compounds. Instead, sets of genes involved in the same cellular mechanism were detected, together building a network of regulatory processes and cellular reactions after compound treatment. Sometimes it is not easy to discriminate direct effects from secondary effects. For example, the induction of cell cycle related genes could be indicative for a mitogenic effect of a compound, or the initiation of the cell cycle could be a reaction to generated cellular damage. It is known that regenerative processes occur after liver necrosis and include proliferation (Viebahn & Yeoh, 2008).

Often energy metabolism was affected, including changes in fatty acid oxidation, glycogenolysis and acetyl-CoA synthesis. This was also true for compounds which are non hepatotoxic. In general, all cellular reactions need or deliver energy equivalents, so it is not surprising to find changes in gene expression as a reaction to the cellular need. As a normal reaction, the cells are capable of handling these changes and to produce enough energy to sustain their metabolism. If energy consumption is too high or the production falls below the minimum needed for proper function, additional mechanisms are activated causing cell damage or driving the cell into necrosis or apoptosis (Nieminen, 2003).

4 CONCLUDING REMARKS AND FUTURE PERSPECTIVES

In this work, new *in vitro* and molecular techniques were applied to establish a new, early test system for toxicological research. A wide range of alternative approaches are currently being developed to gain mechanistic information, to speed up the process of early screening in drug development, to improve the toxicological testing procedure itself and, of course, to reduce the number of animals used for toxicity testing. At the same time, new technical developments and options are being adopted into toxicology laboratories and tested for their suitability and robustness. One promising approach is the analysis of gene expression changes by microarrays (Amin et al., 2002). The combination of both of these basic approaches, *in vitro* experiments and modern technology, will help to answer some of the key questions faced by toxicology.

Primarily, the applicability of two commercially available gene expression platforms was examined by a thorough comparative study of data gained from *in vitro* as well as *in vivo* experiments. Our results demonstrated that the high quality and correlation of generated data on a technical level lead to a high concordance in terms of the biological interpretations, making both platforms applicable for use in toxicological studies. This result was supported by the high correlation with TaqMan gene expression data. Recently, the FDA initiated a microarray “control” study (MAQC), which clearly showed the intra- and interlaboratory comparability of microarray results as well as the consistent results obtained from different microarray platforms (Guo et al., 2006; Shi et al., 2006).

The comparison of several *in vitro* culture systems, each with their own advantages and disadvantages in terms of throughput, viability and metabolic activity (Table 2), on both morphological and functional levels, as well as the global gene expression level permitted insights into basal mechanisms which take place during cell culture. The combination of both global gene expression and primary hepatocytes has been performed before in smaller studies covering only limited, more specific questions, when compared to the data presented here in this thesis (Baker et al., 2001; Boess et al., 2003; Braeuning et al., 2006). This PhD work was an important step towards the understanding of how varying culture conditions affect hepatocellular differentiation and function. At the same time, this comparison and subsequent optimizations lead to the establishment of a standardized and robust long-term hepatocyte culture system with clearly characterized morphological, functional and gene expression functions.

4 CONCLUDING REMARKS AND FUTURE PERSPECTIVES

All of this data was necessary to allow for good data interpretation based on the background level of gene expression during culturing and to define the horizon of expectation to ensure the reliability of this test system.

The main problem of all primary hepatocyte cultures is the reduction of metabolic activity over time in culture. While this is true for short term cultures like suspension cultures, liver slices and ML cultures, our data showed a deceleration of this process by culturing the hepatocytes in the SW conformation without FCS. Not only the basal gene expression of several CYPs was found to be higher in SW- cultures, but also the treatment with well known inducers resulted in an improved inducibility of the four CYPs tested. These findings are supported by published data on both the functional level as well as in terms of gene expression (Elaut et al., 2006a; LeCluyse et al., 2000; Richert et al., 2002; Rogiers & Vercruysse, 1998; Coecke et al., 2005).

These results provided us with confidence to go forward with this in vitro culture system for a toxicogenomics study using several well known hepatotoxicants to show compound dependent gene expression changes and to compare different mechanisms of action. This data was not only used for mechanistic analyses but also to successfully develop a computer based discrimination model for hepatotoxicity. Up to now, studies employing such predictive models are based on in vivo data and are mainly focused on acute toxicity (Hamadeh et al., 2002b; Zidek et al., 2007; Ellinger-Ziegelbauer et al., 2008; Ruepp et al., 2005). This model is the first study combining in vitro toxicology and toxicogenomics to test the possibility of using primary hepatocytes dosed for 9 d to depict sub-chronic toxicity.

Surprisingly, even though a relatively small database was used, the classification of the compounds used was successful, with a misclassification rate of only 7.5% after 9 days. Knowing the fact that multiple gene expression changes are caused by the perfusion itself and the adaption to the culture conditions, this is a high-quality result and reflects the robustness of this in vitro system to predict the in vivo outcome.

The resulting discrimination model was challenged with two blinded compounds to prove its ability to detect hepatotoxicity based on global gene expression. EMD X is a former Merck compound which was stopped in development and is known to be hepatotoxic. Using our model it was clearly predicted to be hepatotoxic. AAP has been reported to lose toxic potency in primary hepatocytes over time in culture (Jemnitz et al., 2008), which was also seen in our dose finding experiments. Nevertheless, it was predicted to be a hepatotoxin based on gene expression changes indicating that, although not visibly damaging the cells, AAP still caused changes at the gene level which would lead to hepatotoxicity. Further studies are needed to better understand the

4 CONCLUDING REMARKS AND FUTURE PERSPECTIVES

mechanistic processes taking place in culture and the insensitivity of primary hepatocytes to AAP toxicity.

In the last few decades, a new paradigm has emerged based on the assumption that knowing the mechanism of action of a toxic compound would enable the development of predictive models which would help new, safer compounds to be brought quicker onto the market. The search for adaptive changes in gene expression has resulted in many genes being proposed as predictive biomarkers, although only a few of them have been shown to be really decisive. Currently, new techniques in bioinformatic analysis has lead to the identification of gene signatures and networks which seem to contain more information and therefore to be more reliable than single gene biomarkers (Khor et al., 2006).

The ultimate goal of these in vitro toxicogenomic studies is the establishment of a predictive screening model which is easy to use and which delivers reliable, high quality results. The results presented here are very promising, but this study is just the starting point for a more thorough classification process. As mentioned before, the size of the database used for classification is crucial for the validity of the system. This is highlighted by the fact that the best results were obtained with the whole dataset (low and high dose together). Is it really beneficial to combine two dosing schemes, or is the improvement due to the increasing size of the dataset? The high dose was chosen due to the reduction of cell viability, but changes in gene expression resulting from low dose treatment were seen as well. These low-dose effects may also contain important information for the prediction model.

Another important point to consider is the dosing-scheme itself. Always controversially discussed (Monro, 1990; Campbell & Ings, 1988) and of central importance to the outcome of any in vitro experiment, there are currently no specific guidelines available. To avoid false positive or negative results, a list of general criteria would be helpful to exclude unsuitable samples due to incorrect dosing or differences in the culturing conditions. In toxicology testing, doses greatly in excess of pharmacologically active doses are used to induce adverse effects, therefore there might be effects obtained also for (in vivo) non toxic compounds, leading to false results. On the other hand, if a threshold value is not achieved, even toxic compounds may be classified as non toxic. A potential solution would be the application of a minimum number of deregulated genes according to t-test statistic and/or fold-change. A minimum set of deregulated genes might be adequate for discrimination. Whereas for non toxic compounds the genes affected should either be involved in non-damaging processes or random, toxic compounds should generate gene profiles clearly connected to adverse cellular fate

4 CONCLUDING REMARKS AND FUTURE PERSPECTIVES

and viability. The conduction of these tests with multiple doses, which is enabled by in vitro experiments, is also a possibility to increase data quality.

The compound selection allowed a proof of concept for the constructed prediction model, although it was too small to cover all of the various potential mechanisms of hepatotoxicity. The gene set of 724 genes was capable of discriminating the compounds used to build the model, as well as to correctly classify newly added compounds with a misclassification rate of 7.5%. These results need to be further validated and refined, by including more compounds with specific modes of action or to focus a certain compound classes. This will increase the robustness of the predictive system and facilitate improved data interpretation.

Finally, the insecurity of extrapolating the results in between species, especially to men, may be overcome by the possibility to conduct these experiments with human hepatocytes. Also human hepatocytes can be successfully cultured in either ML- or SW-conformation, there is still the need to optimize the culture conditions. Because of the difficulties and the costs of getting high quality human hepatocytes in a sufficient amount, there might also be other options like the new HepaRG cell line which may be considered. Yet, the data obtained during this work is promising but not sufficient to attest the qualification of either possibility.

To conclude, screening tests alone do not allow for a final estimation of the hazard and risk of a compound, but molecular toxicology can contribute by improving the mechanistic understanding, refining the predictivity of toxicological outcomes and to significantly reduce animal usage in toxicology and, more generally, in drug discovery. We have now a robust, semi-validated long-term cell culture system that can be used in drug discovery for predicting hepatotoxicity as well as helping the toxicologist to understand a compounds mechanism of action. Therefore, the development of this predictive in vitro test system can be seen as a contribution to the efforts to implement the principles of 3R into the daily toxicological work.

5 REFERENCES

- Aardema, M. J. & MacGregor, J. T. (2002). Toxicology and genetic toxicology in the new era of "toxicogenomics": impact of "-omics" technologies. *Mutat Res*, 499(1), 13-25.
- Akerboom, T. P., Narayanaswami, V., Kunst, M. & Sies, H. (1991). ATP-dependent S-(2,4-dinitrophenyl)glutathione transport in canalicular plasma membrane vesicles from rat liver. *J Biol Chem*, 266(20), 13147-52.
- Alexandre, E., Viollon-Abadie, C., David, P., Gandillet, A., Coassolo, P., Heyd, B., Heyd, B., Manton, G., Wolf, P., Bachellier, P., Jaeck, D. & Richert, L. (2002). Cryopreservation of adult human hepatocytes obtained from resected liver biopsies. *Cryobiology*, 44(2), 103-13.
- Aljada, A., Garg, R., Ghanim, H., Mohanty, P., Hamouda, W., Assian, E. & Dandona, P. (2001). Nuclear factor-kappaB suppressive and inhibitor-kappaB stimulatory effects of troglitazone in obese patients with type 2 diabetes: evidence of an antiinflammatory action? *J Clin Endocrinol Metab*, 86(7), 3250-6.
- Ames, B. N., Lee, F. D. & Durston, W. E. (1973). An improved bacterial test system for the detection and classification of mutagens and carcinogens. *Proc Natl Acad Sci U S A.*, 70(3), 782-6.
- Amin, R. P., Hamadeh, H. K., Bushel, P. R., Bennett, L., Afshari, C. A. & Paules, R. S. (2002). Genomic interrogation of mechanism(s) underlying cellular responses to toxicants. *Toxicology*, 181-182, 555-63.
- Anderson, N. L. & Anderson, N. G. (2002). The human plasma proteome: history, character, and diagnostic prospects. *Mol Cell Proteomics*, 1(11), 845-67.
- Andrade, R. J., Camargo, R., Lucena, M. I. & González-Grande, R. (2004). Causality assessment in drug-induced hepatotoxicity. *Expert Opin Drug Drug Saf*, 3(4), 329-44.
- Bader, A., Frühauf, N., Zech, K., Haverich, A. & Borlak, J. T. (1998). Development of a small-scale bioreactor for drug metabolism studies maintaining hepatospecific functions. *Xenobiotica*, 28(9), 815-25.
- Bailly-Maitre, B., de Sousa, G., Zucchini, N., Gugenheim, J., Boulukos, K. E. & Rahmani, R. (2002). Spontaneous apoptosis in primary cultures of human and rat hepatocytes: molecular mechanisms and regulation by dexamethasone. *Cell Death Differ*, 9(9), 945-55.
- Baker, T. K., Carfagna, M. A., Gao, H., Dow, E. R., Li, Q., Searfoss, G. H. & Ryan, T. P. (2001). Temporal gene expression analysis of monolayer cultured rat hepatocytes. *Chem Res Toxicol*, 14(9), 1218-31.
- Ballet, F. (1997). Hepatotoxicity in drug development: detection, significance and solutions. *J Hepatol*, 26 Suppl 2, 26-36.
- Bandara, L. R. & Kennedy, S. (2002). Toxicoproteomics - a new preclinical tool. *Drug Discov Today*, 7(7), 411-8.
- Bayad, J., Sabolovic, N., Bagrel, D., Magdalou, J. & Siest, G. (1991). Influence of the isolation method on the stability of differentiated phenotype in cultured rat hepatocytes. *J Pharmacol Methods*, 25(1), 85-94.
- Bedossa, P. & Paradis, V. (2003). Liver extracellular matrix in health and disease. *J Pathol*, 200(4), 504-15.
- Begue, J. M., Guguen-Guillouzo, C., Padeloup, N. & Guillouzo A. (1994). Prolonged maintenance of active cytochrome P-450 in adult rat hepatocytes co-cultured with another liver cell type. *Hepatology*, 4(5), 839-42.
- Beigel, J., Fella, K., Kramer, P., Kroeger, M. & Hewitt, P. (2008). Genomics and proteomics analysis of cultured primary rat hepatocytes. *Toxicol in vitro*, 22(1), 171-81.
- Benoit, G., Cooney, A., Giguere, V., Ingraham, H., Lazar, M., Muscat, G., Perlmann, T., Renaud, J. P., Schwabe, J., Sladek, F., Tsai, M. J. & Laudet, V. (2006).

- International Union of Pharmacology. LXVI. Orphan nuclear receptors. *Pharmacol Rev*, 58(4), 798-836.
- Berridge, M. V., Herst, P. M. & Tan, A. S. (2005). Tetrazolium dyes as tools in cell biology: new insights into their cellular reduction. *Biotechnol Annu Rev*, 11, 127-52.
- Berthiaume, F., Moghe, P. V., Toner, M. & Yarmush, M. L. (1996). Effect of extracellular matrix topology on cell structure, function, and physiological responsiveness: hepatocytes cultured in a sandwich configuration. *FASEB J*, 10(13), 1471-84.
- Besaratinia, A. & Pfeifer, G. P. (2005). DNA adduction and mutagenic properties of acrylamide. *Mutat Res*, 580(1-2), 31-40.
- Blouin, A., Bolender, R. P. & Weibel, E. R. (1977). Distribution of organelles and membranes between hepatocytes and nonhepatocytes in the rat liver parenchyma. A stereological study. *J Cell Biol*, 72(2), 441-55.
- Boelsterli, U. A. (2003). Disease-related determinants of susceptibility to drug-induced idiosyncratic hepatotoxicity. *Curr Opin Drug Discov Devel*, 6(1), 81-91.
- Boess, F., Kamber, M., Romer, S., Gasser, R., Muller, D., Albertini, S. & Suter, L. (2003). Gene expression in two hepatic cell lines, cultured primary hepatocytes, and liver slices compared to the in vivo liver gene expression in rats: possible implications for toxicogenomics use of in vitro systems. *Toxicol Sci*, 73(2), 386-402.
- Bose, I. & Ghosh, B. (2007). The p53-MDM2 network: from oscillations to apoptosis. *J of BioSci*, 32(5), 991-7.
- Boswell-Smith, V., Cazzola, M. & Page, C. P. (2006). Are phosphodiesterase 4 inhibitors just more theophylline? *J Allergy Clin Immunol*, 117(6), 1237-43.
- Braeuning, A., Itrich, C., Köhle, C., Hailfinger, S., Bonin, M., Buchmann, A. & Schwarz, M. (2006). Differential gene expression in periportal and perivenous mouse hepatocytes. *FEBS J*, 273(22), 5051-61.
- Brandon, E. F. A., Raap, C. D., Meijerman, I., Beijnen, J. H. & Schellens, J. H. M. (2003). An update on in vitro test methods in human hepatic drug biotransformation research: pros and cons. *Toxicol Appl Pharmacol*, 189(3), 233-46.
- Brock, C., Schaefer, M., Reusch, H. P., Czupalla, C., Michalke, M., Spicher, K., Schultz, G. & Nürnberg, B. (2003). Roles of G beta gamma in membrane recruitment and activation of p110 gamma/p101 phosphoinositide 3-kinase gamma. *J Cell Biol*, 160(1), 89-99.
- Brown, P. O. & Botstein, D. (1999). Exploring the new world of the genome with DNA microarrays. *Nat Genet*, 21(1 Suppl), 33-7.
- Bulera, S. J., Eddy, S. M., Ferguson, E., Jatkoa, T. A., Reindel, J. F., Bleavins, M. R. & De La Iglesia, F. A. (2001). RNA expression in the early characterization of hepatotoxicants in Wistar rats by high-density DNA microarrays. *Hepatology*, 33(5), 1239-58.
- Burchiel, S. W., Knall, C. M., Davis, J. W., Paules, R. S., Boggs, S. E. & Afshari, C. A. (2001). Analysis of genetic and epigenetic mechanisms of toxicity: potential roles of toxicogenomics and proteomics in toxicology. *Toxicol Sci*, 59(2), 193-5.
- Burke, M. D., Thompson, S., Elcombe, C. R., Halpert, J., Haaparanta, T. & Mayer, R. T. (1985). Ethoxy-, pentoxy- and benzyloxyphenoxazones and homologues: a series of substrates to distinguish between different induced cytochromes P-450. *Biochem Pharmacol*, 34(18), 3337-45.
- Burke-Gaffney, A., Callister, M. E. J. & Nakamura, H. (2005). Thioredoxin: friend or foe in human disease? *Trends Pharmacol Sci*, 26(8), 398-404.
- Butte, A. (2002). The use and analysis of microarray data. *Nat Rev Drug Discov*, 1(12), 951-60.
- Callander, R. D., Mackay, J. M., Clay, P., Elcombe, C. R. & Elliott, B. M. (1995). Evaluation of phenobarbital/beta-naphthoflavone as an alternative S9-induction

- regime to Aroclor 1254 in the rat for use in in vitro genotoxicity assays. *Mutagenesis*, 10(6), 517-22.
- Campbell, D. B. & Ings, R. M. (1988). New approaches to the use of pharmacokinetics in toxicology and drug development. *Hum Toxicol*, 7(5), 469-79.
- Cesaratto, L., Vascotto, C., Calligaris, S. & Tell, G. (2004). The importance of redox state in liver damage. *Ann Hepatol*, 3(3), 86-92.
- Chapman, G. S., Jones, A. L., Meyer, U. A. & Montgomery Bissell, D. (1973). Parenchymal cells from adult rat liver in nonproliverating monolayer culture: II. Ultrastructural studies. *J Cell Biol*, 59(3), 735-47.
- Chen, G., Gharib, T. G., Huang, C., Taylor, J. M. G., Misek, D. E., Kardia, S. L., Giordano, T. J., Iannettoni, M. D., Orringer, M. B., Hanash, S. M. & Beer, D. G. (2002). Discordant protein and mRNA expression in lung adenocarcinomas. *Mol Cell Proteomics*, 1(4), 304-13.
- Chen, J. J., Hsueh, H., Delongchamp, R. R., Lin, C. & Tsai, C. (2007). Reproducibility of microarray data: a further analysis of microarray quality control (MAQC) data. *BMC Bioinformatics*, 8, 412.
- Chin, K. & Kong, A. N. T. (2002). Application of DNA microarrays in pharmacogenomics and toxicogenomics. *Pharm Res*, 19(12), 1773-8.
- Ching, K. Z., Tenney, K. A., Chen, J. & Morgan, E. T. (1996). Suppression of constitutive cytochrome P450 gene expression by epidermal growth factor receptor ligands in cultured rat hepatocytes. *Drug Metab Dispos*, 24(5), 542-6.
- Clayton, D. F., Weiss, M. & Darnell, J. E. (1985). Liver-specific RNA metabolism in hepatoma cells: variations in transcription rates and mRNA levels. *Mol Cell Biol*, 5(10), 2633-41.
- Coecke, S., Blaauboer, B. J., Elaut, G., Freeman, S., Freidig, A., Gensmantel, N., Hoet, P., Kapoulas, V. M., Ladstetter, B., Langley, G. Leahy, D., Mannens, G., Meneguz, A., Monshouwer, M., Nemery, B., Pelkonen, O., Pfaller, W., Prieto, P., Proctor, N., Rogiers, V., Rostami-Hodjegan, A., Sabbioni, E., Steiling, W. & van de Sandt, J. J. (2005). Toxicokinetics and metabolism. *Altern Lab Anim*, 33 Suppl 1, 147-75.
- Coyle, B., Freathy, C., Gant, T. W., Roberts, R. A. & Cain, K. (2003). Characterization of the transforming growth factor-beta 1-induced apoptotic transcriptome in FaO hepatoma cells. *J Biol Chem*, 278(8), 5920-8.
- Cross, D. M. & Bayliss, M. K. (2000). A commentary on the use of hepatocytes in drug metabolism studies during drug discovery and development. *Drug Metab Rev*, 32(2), 219-40.
- Czaja, M. J. (2002). Induction and regulation of hepatocyte apoptosis by oxidative stress. *Antioxid Redox Signal*, 4(5), 759-67.
- Davila, J. C. & Morris, D. L. (1999). Analysis of cytochrome P450 and phase 2 conjugating enzyme expression in adult male rat hepatocytes. *In Vitro Cell Dev Biol Anim*, 35(3), 120-30.
- De Smet, K., Beken, S., Vanhaecke, T., Pauwels, M., Vercruyssen, A. & Rogiers, V. (1998). Isolation of rat hepatocytes. *Methods Mol Biol*, 107, 295-301.
- Desmet, V. J., Krstulović, B. & Damme, B. V. (1968). Histochemical study of rat liver in alpha-naphthyl isothiocyanate (ANIT) induced cholestasis. *Methods Mol Biol*, 52(2), 401-421.
- Dhainaut, J. F., Marin, N., Mignon, A. & Vinsonneau, C. (2001). Hepatic response to sepsis: interaction between coagulation and inflammatory processes. *Crit Care Med*, 29(7 Suppl), S42-7.
- Dickins, M. (2004). Induction of cytochromes P450. *Curr Top Med Chem*, 4(16), 1745-66.
- Dix, D. J., Gallagher, K., Benson, W. H., Groskinsky, B. L., McClintock, J. T., Dearfield, K. L. & Farland, W. H. (2006). A framework for the use of genomics data at the EPA. *Nat Biotechnol*, 24(9), 1108-11.

- Donato, M. T., Castell, J. V. & Gómez-Lechón, M. J. (1994). Cytochrome P450 activities in pure and co-cultured rat hepatocytes. Effects of model inducers. *In Vitro Cell Dev Biol Anim*, 30A(12), 825-32.
- Dunn, J. C., Tompkins, R. G. & Yarmush, M. L. (1991). Long-term in vitro function of adult hepatocytes in a collagen sandwich configuration. *Biotechnol Prog*, 7(3), 237-45.
- Dunn, J. C., Yarmush, M. L., Koebe, H. G. & Tompkins, R. G. (1989). Hepatocyte function and extracellular matrix geometry: long-term culture in a sandwich configuration. *FASEB J*, 3(2), 174-7.
- Ekins, S., Murray, G. I., Burke, M. D., Williams, J. A., Marchant, N. C. & Hawksworth, G. M. (1995). Quantitative differences in phase I and II metabolism between rat precision-cut liver slices and isolated hepatocytes. *Drug Metab Dispos*, 23(11), 1274-9.
- Elaut, G., Henkens, T., Papeleu, P., Snykers, S., Vinken, M., Vanhaecke, T. & Rogiers, V. (2006). Molecular mechanisms underlying the dedifferentiation process of isolated hepatocytes and their cultures. *Curr Drug Metab*, 7(6), 629-60.
- Elaut, G., Papeleu, P., Vinken, M., Henkens, T., Snykers, S., Vanhaecke, T. & Rogiers, V. (2006). Hepatocytes in suspension. *Methods Mol Biol*, 320, 255-63.
- El-Bahay, C., Gerber, E., Horbach, M., Tran-Thi, Q. H., Röhrdanz, E. & Kahl, R. (1999). Influence of tumor necrosis factor-alpha and silibin on the cytotoxic action of alpha-amanitin in rat hepatocyte culture. *Toxicol Appl Pharmacol*, 158(3), 253-60.
- Elias, E. & Mills, C. O. (2007). Coordinated defence and the liver. *Clin Med*, 7(2), 180-4.
- Ellinger-Ziegelbauer, H., Gmuender, H., Bandenburg, A. & Ahr, H. J. (2008). Prediction of a carcinogenic potential of rat hepatocarcinogens using toxicogenomics analysis of short-term in vivo studies. *Mutat Res*, 637(1-2), 23-39.
- Ellinger-Ziegelbauer, H., Stuart, B., Wahle, B., Bomann, W. & Ahr, H. (2004). Characteristic expression profiles induced by genotoxic carcinogens in rat liver. *Toxicol Sci*, 77(1), 19-34.
- Enat, R., Jefferson, D. M., Ruiz-Opazo, N., Gatmaitan, Z., Leinwand, L. A. & Reid, L. M. (1984). Hepatocyte proliferation in vitro: its dependence on the use of serum-free hormonally defined medium and substrata of extracellular matrix. *Proc Natl Acad Sci U S A*, 81(5), 1411-5.
- Enomoto, K., Nishikawa, Y., Omori, Y., Tokairin, T., Yoshida, M., Ohi, N., Nishimura, T., Yamamoto, Y. & Li, Q. (2004). Cell biology and pathology of liver sinusoidal endothelial cells. *Med Electron Microsc*, 37(4), 208-15.
- Etienne, P. L., Baffet, G., Desvergne, B., Boissard-Rissel, M., Glaise, D. & Guguen-Guillouzo, C. (1988). Transient expression of c-fos and constant expression of c-myc in freshly isolated and cultured normal adult rat hepatocytes. *Oncogene Res*, 3(3), 255-62.
- Evans, W. E. & Relling, M. V. (1999). Pharmacogenomics: translating functional genomics into rational therapeutics. *Science*, 286(5439), 487-91.
- Farkas, D. & Tannenbaum, S. R. (2005a). In vitro methods to study chemically-induced hepatotoxicity: a literature review. *Curr Drug Metab*, 6(2), 111-25.
- Farkas, D. & Tannenbaum, S. R. (2005b). Characterization of chemically induced hepatotoxicity in collagen sandwiches of rat hepatocytes. *Toxicol Sci*, 85(2), 927-34.
- Fella, K., Glückmann, M., Hellmann, J., Karas, M., Kramer, P. & Kröger, M. (2005). Use of two-dimensional gel electrophoresis in predictive toxicology: identification of potential early protein biomarkers in chemically induced hepatocarcinogenesis. *Proteomics*, 5(7), 1914-27.
- Fielden, M. R. & Zacharewski, T. R. (2001). Challenges and limitations of gene expression profiling in mechanistic and predictive toxicology. *Toxicol Sci*, 60(1), 6-10.

- Förster, T. (1948). Zwischenmolekulare Energiewanderung und Fluoreszenz. *Annalen der Physik*, 437(1-2), 55-75.
- Fréneaux, E., Labbe, G., Letteron, P., The Le Dinh, Degott, C., Genève, J., Larrey, D. & Pessayre, D. (1988). Inhibition of the mitochondrial oxidation of fatty acids by tetracycline in mice and in man: possible role in microvesicular steatosis induced by this antibiotic. *Hepatology*, 8(5), 1056-62.
- Friedman, S. L. (1997). Molecular mechanisms of hepatic fibrosis and principles of therapy. *J Gastroenterol*, 32(3), 424-30.
- Gabler, W. L. & Creamer, H. R. (1991). Suppression of human neutrophil functions by tetracyclines. *J Periodontal Res*, 26(1), 52-8.
- Gaeta, G. B., Utili, R., Adinolfi, L. E., Abernathy, C. O. & Giusti, G. (1985). Characterization of the effects of erythromycin estolate and erythromycin base on the excretory function of the isolated rat liver. *Toxicol Appl Pharmacol*, 80(2), 185-92.
- Gallai, M., Kovalszky, I., Knittel, T., Neubauer, K., Armbrust, T. & Ramadori, G. (1996). Expression of extracellular matrix proteoglycans perlecan and decorin in carbon-tetrachloride-injured rat liver and in isolated liver cells. *Methods Mol Biol*, 148(5), 1463-71.
- Garnier, G., Circolo, A. & Colten, H. R. (1996). Constitutive expression of murine complement factor B gene is regulated by the interaction of its upstream promoter with hepatocyte nuclear factor 4. *J Biol Chem*, 271(47), 30205-11.
- Gatzidou, E. T., Zira, A. N. & Theocharis, S. E. (2007). Toxicogenomics: a pivotal piece in the puzzle of toxicological research. *J Appl Toxicol*, 27(4), 302-9.
- Gautam, A., Ng, O. C. & Boyer, J. L. (1987). Isolated rat hepatocyte couplets in short-term culture: structural characteristics and plasma membrane reorganization. *Hepatology*, 7(2), 216-23.
- Gebhardt R, Hengstler JG, Müller D, Glöckner R, Buenning P, Laube B, Schmelzer E, Ullrich M, Utesch D, Hewitt N, Ringel M, Hilz BR, Bader A, Langsch A, Koose T, Burger HJ, Maas J & Oesch F. (2003). New hepatocyte in vitro systems for drug metabolism: metabolic capacity and recommendations for application in basic research and drug development, standard operation procedures. *Drug Metab Rev*, 35(2-3), 145-213.
- Giancotti, F. G. & Ruoslahti, E. (1999). Integrin signaling. *Science*, 285(5430), 1028-32.
- Giancotti, F. G. & Tarone, G. (2003). Positional control of cell fate through joint integrin/receptor protein kinase signaling. *Annu Rev Cell Dev Biol*, 19, 173-206.
- Gómez-Lechón, M. J., Donato, T., Ponsoda, X. & Castell, J. V. (2003). Human hepatic cell cultures: in vitro and in vivo drug metabolism. *Altern Lab Anim*, 31(3), 257-65.
- Gómez-Lechón, M. J., Ponsoda, X., Bort, R. & Castell, J. V. (2004). The use of cultured hepatocytes to investigate the metabolism of drugs and mechanisms of drug hepatotoxicity. *Altern Lab Anim*, 29(3), 225-31.
- González, H. E., Eugeni, E. A., Garcés, G., Solís, N., Pizarro, M., Accatino, L. & Sáez, J. C. (2002). Regulation of hepatic connexins in cholestasis: possible involvement of Kupffer cells and inflammatory mediators. *Am J Physiol Gastrointest Liver*, 282(6), G991-G1001.
- Goodman, L. S., Limbird, L. E., Milinoff, P. B., Ruddon, R. W. & Gilman, A. G. (1996). *Goodman and Gilman's: The Pharmacological Basis of Therapeutics* (9th ed., p. 1905). McGraw-Hill, Columbus.
- Gordon, E. M., Douglas, M. C., Jablonski, P., Owen, J. A., Sali, A. & Watts, J. M. (1972). Gastrointestinal hormones and bile-secretion studies in the isolated perfused pig liver. *Surgery*, 72(5), 708-21.
- Gracie, J. A., Robertson, S. E. & McInnes, I. B. (2003). Interleukin-18. *J Leukoc Biol*, 73(2), 213-24.
- Graf, J. & Boyer, J. L. (1990). The use of isolated rat hepatocyte couplets in hepatobiliary physiology. *J Hepatol*, 10(3), 387-94.

- Gripon, P., Rumin, S., Urban, S., Le Seyec, J., Glaise, D., Cannie, I., Guyomard, C., Lucas, J., Trepo, C. & Guguen-Guillouzo, C. (2002). Infection of a human hepatoma cell line by hepatitis B virus. *Proc Natl Acad Sci U S A*, 99(24), 15655-60.
- Groneberg, D. A., Grosse-Siestrup, C. & Fischer, A. (2002). In vitro models to study hepatotoxicity. *Toxicol Pathol*, 30(3), 394-9.
- Guengerich, F. P. (2003). Cytochromes P450, drugs, and diseases. *Mol. Interv*, 3(4), 194-204.
- Guigoz, Y., Werffeli, P., Favre, D., Juillerat, M., Wellinger, R. & Honegger, P. (1987). Aggregate cultures of foetal rat liver cells: development and maintenance of liver gene expression. *Biol Cell*, 60(3), 163-71.
- Gunderson, K. L., Kruglyak, S., Graige, M. S., Garcia, F., Kermani, B. G., Zhao, C., Che, D., Dickinson, T., Wickham, E., Bierle, J., Doucet, D., Milewski, M., Yang, R., Siegmund, C., Haas, J., Zhou, L., Oliphant, A., Fan, J. B., Barnard, S. & Chee, M. S. (2004). Decoding randomly ordered DNA arrays. *Genome Res*, 14(5), 870-7.
- Guo, L., Lobenhofer, E. K., Wang, C., Shippy, R., Harris, S. C., Zhang, L., Mei, N., Chen, T., Herman, D., Goodsaid, F. M., Hurban, P., Phillips, K. L., Xu, J., Deng, X., Sun, Y. A., Tong, W., Dragan, Y. P. & Shi, L. (2006). Rat toxicogenomic study reveals analytical consistency across microarray platforms. *Nat Biotechnol*, 24(9), 1162-9.
- Gygi, S. P., Rochon, Y., Franza, B. R. & Aebersold, R. (1999). Correlation between protein and mRNA abundance in yeast. *Mol Cell Biol*, 19(3), 1720-30.
- Hakkola, J., Hu, Y. & Ingelman-Sundberg, M. (2003). Mechanisms of down-regulation of CYP2E1 expression by inflammatory cytokines in rat hepatoma cells. *J Pharmacol Exp Ther*, 304(3), 1048-54.
- Hamadeh, H.K., Bushel, P.R., Jayadev, S., DiSorbo, O., Bennett, L., Li, L., Tennant, R., Stoll, R., Barrett, J.C., Paules, R.S., Blanchard, K. & Afshari, C.A. (2002). Prediction of compound signature using high density gene expression profiling. *Toxicol Sci*, 67(2), 232-40.
- Hamadeh, H.K., Bushel, P.R., Jayadev, S., Martin, K., DiSorbo, O., Sieber, S., Bennett, L., Tennant, R., Stoll, R., Barrett, J.C., Blanchard, K., Paules, R.S. & Afshari, C.A. (2002). Gene expression analysis reveals chemical-specific profiles. *Toxicol Sci*, 67(2), 219-31.
- Hamilton, G. A., Jolley, S. L., Gilbert, D., Coon, D. J., Barros, S. & LeCluyse, E. L. (2001). Regulation of cell morphology and cytochrome P450 expression in human hepatocytes by extracellular matrix and cell-cell interactions. *Cell Tissue Res*, 306(1), 85-99.
- Hamilton, G. A., Westmorel, C. & George, A. E. (2001). Effects of medium composition on the morphology and function of rat hepatocytes cultured as spheroids and monolayers. *In Vitro Cell Dev Biol Anim*, 37(10), 656-67.
- Häussinger, D., Reinehr, R. & Schliess, F. (2006). The hepatocyte integrin system and cell volume sensing. *Acta physiologica (Oxford, England)*, 187(1-2), 249-55.
- Hayashi, R., Wada, H., Ito, K. & Adcock, I. M. (2004). Effects of glucocorticoids on gene transcription. *Eur J Clin Pharmacol*, 500(1-3), 51-62.
- Heinrich, P. C., Behrmann, I., Haan, S., Hermanns, H. M., Müller-Newen, G. & Schaper, F. (2003). Principles of interleukin (IL)-6-type cytokine signalling and its regulation. *Biochem J*, 374(Pt 1), 1-20.
- Heishi, M., Ichihara, J., Teramoto, R., Itakura, Y., Hayashi, K., Ishikawa, H., Gomi, H., Sakai, J., Kanaoka, M., Taiji, M. & Kimura, T. (2006). Global gene expression analysis in liver of obese diabetic db/db mice treated with metformin. *Diabetologia*, 49(7), 1647-55.
- Hengstler, J. G., Utesch, D., Steinberg, P., Platt, K. L., Diener, B., Ringel, M., Swales, N., Fischer, T., Biefang, K., Gerl, M., Böttger, T. & Oesch, F. (2000). Cryopreserved primary hepatocytes as a constantly available in vitro model for

- the evaluation of human and animal drug metabolism and enzyme induction. *Drug Metab Rev*, 32(1), 81-118.
- Heredi-Szabo, K., Kis, E., Molnar, E., Gyorfi, A. & Krajcsi, P. (2008). Characterization of 5(6)-Carboxy-2,'7'-Dichlorofluorescein Transport by MRP2 and Utilization of this Substrate as a Fluorescent Surrogate for LTC4. *J Biomol Screen*, 13(4), 295-301.
- Hewitt, N. J. & Hewitt, P. (2004). Phase 1 and II enzyme characterization of two sources of HepG2 cell lines. *Xenobiotica*, 34(3), 243-56.
- Hiroi, J., Kimura, K., Aikawa, M., Tojo, A., Suzuki, Y., Nagamatsu, T., Omata, M., Yazaki, Y. & Nagai, R. (1996). Expression of a nonmuscle myosin heavy chain in glomerular cells differentiates various types of glomerular disease in rats. *Kidney Int*, 49(5), 1231-41.
- Holme, J. A. (1985). Xenobiotic metabolism and toxicity in primary monolayer cultures of hepatocytes. *NIPH Ann*, 8(2), 49-63.
- Howard, R. B., Christensen, A. K., Gibbs, F. A. & Pesch, L. A. (1967). The enzymatic preparation of isolated intact parenchymal cells from rat liver. *J Cell Biol*, 35(3), 675-84.
- Hutchens, T. W. & Yip, T. (1993). New desorption strategies for the mass spectrometric analysis of macromolecules. *Rapid Commun Mass Spectrom*, 7(7), 576-580.
- Illenberger, D., Walliser, C., Nurnberg, B., Diaz Lorente, M. & Gierschik, P. (2003). Specificity and structural requirements of phospholipase C-beta stimulation by Rho GTPases versus G protein beta gamma dimers. *J Biol Chem*, 278(5), 3006-14.
- Imai, T., Jiang, M., Kastner, P., Chambon, P. & Metzger, D. (2001). Selective ablation of retinoid X receptor alpha in hepatocytes impairs their lifespan and regenerative capacity. *Proc Natl Acad Sci U S A*, 98(8), 4581-6.
- Ingelman-Sundberg, M., Ronis, M. J., Lindros, K. O., Eliasson, E. & Zhukov, A. (1994). Ethanol-inducible cytochrome P4502E1: regulation, enzymology and molecular biology. *Alcohol, Supplement*, 2, 131-9.
- Inzucchi, S. E., Maggs, D. G., Spollett, G. R., Page, S. L., Rife, F. S., Walton, V. & Shulman, G. I. (1998). Efficacy and metabolic effects of metformin and troglitazone in type II diabetes mellitus. *N Engl J Med*, 338(13), 867-72.
- Irigaray, P., Newby, J. A., Clapp, R., Hardell, L., Howard, V., Montagnier, L., Epstein S. & Belpomme D. (2007). Lifestyle-related factors and environmental agents causing cancer: an overview. *Biomedicine & pharmacother*, 61(10), 640-58.
- Irizarry, R. A., Hobbs, B., Collin, F., Beazer-Barclay, Y. D., Antonellis, K. J., Scherf, U. & Speed T. P. (2003). Exploration, normalization, and summaries of high density oligonucleotide array probe level data. *Biostatistics*, 4(2), 249-64.
- Iso, Y., Sawada, T., Okada, T. & Kubota, K. (2005). Loss of E-cadherin mRNA and gain of osteopontin mRNA are useful markers for detecting early recurrence of HCV-related hepatocellular carcinoma. *Eur J Surg Oncol*, 92(4), 304-11.
- Jaeschke, H., Gores, G. J., Cederbaum, A. I., Hinson, J. A., Pessayre, D. & Lemasters, J. J. (2002). Mechanisms of hepatotoxicity. *Toxicol Sci*, 65(2), 166-76.
- James, L. P., Mayeux, P. R. & Hinson, J. A. (2003). Acetaminophen-induced hepatotoxicity. *Drug Metab Dispos*, 31(12), 1499-506.
- Jean, P. A. & Roth, R. A. (1995). Naphthylisothiocyanate disposition in bile and its relationship to liver glutathione and toxicity. *Biochem Pharmacol*, 50(9), 1469-74.
- Jemnitz, K., Veres, Z., Monostory, K. & Vereczkey, L. (2000). Glucuronidation of thyroxine in primary monolayer cultures of rat hepatocytes: in vitro induction of UDP-glucuronosyltransferases by methylcholanthrene, clofibrate, and dexamethasone alone and in combination. *Drug Metab Dispos*, 28(1), 34-7.
- Jemnitz, K., Veres, Z., Monostory, K., Kóbori, L. & Vereczkey, L. (2008). Interspecies differences in acetaminophen sensitivity of human, rat, and mouse primary hepatocytes. *Toxicol In Vitro*, 22(4), 961-7.

- Kanebratt, K. P. & Andersson, T. B. (2008). Evaluation of HepaRG cells as an in vitro model for human drug metabolism studies. *Drug Metab Dispos*, 36(7), 1444-52.
- Kaplowitz, N. (2001). Drug-induced liver disorders: implications for drug development and regulation. *Drug Drug Saf*, 24(7), 483-90.
- Kern, A., Bader, A., Pichlmayr, R. & Sewing, K. F. (1997). Drug metabolism in hepatocyte sandwich cultures of rats and humans. *Biochem Pharmacol*, 54(7), 761-72.
- Kersten, S., Mandard, S., Escher, P., Gonzalez, F. J., Tafuri, S., Desvergne, B. & Wahli, W. (2001). The peroxisome proliferator-activated receptor alpha regulates amino acid metabolism. *FASEB J*, 15(11), 1971-8.
- Kessova, I. & Cederbaum, A. I. (2003). CYP2E1: biochemistry, toxicology, regulation and function in ethanol-induced liver injury. *Curr Mol Med*, 3(6), 509-18.
- Kevresan, S., Kuhajda, K., Kandrak, J., Fawcett, J. P. & Mikov, M. (2007). Biosynthesis of bile acids in mammalian liver. *Eur J Drug Metab Pharmacokinet*, 31(3), 145-56.
- Khor, T. O., Ibrahim, S. & Kong, A. T. (2006). Toxicogenomics in drug discovery and drug development: potential applications and future challenges. *Pharm Res*, 23(8), 1659-64.
- Kienhuis, A. S., Wortelboer, H. M., Maas, W. J., van Herwijnen, M., Kleinjans, J. C. S., van Delft, J. H. M. & Stierum, R. H. (2007). A sandwich-cultured rat hepatocyte system with increased metabolic competence evaluated by gene expression profiling. *Toxicol In Vitro*, 21(5), 892-901.
- Kipp, H. & Arias, I. M. (2002). Trafficking of canalicular ABC transporters in hepatocytes. *Annu Rev Physiol*, 64, 595-608.
- Klebanov, L. & Yakovlev, A. (2007). How high is the level of technical noise in microarray data? *Biol Direct*, 2, 9.
- Kliwer, S. A., Lehmann, J. M., Milburn, M. V. & Willson, T. M. (1999). The PPARs and PXR: nuclear xenobiotic receptors that define novel hormone signaling pathways. *Recent Prog Horm Res*, 54, 345-67; discussion 367-8.
- Kmieć, Z. (2001). Cooperation of liver cells in health and disease. *Adv Anat Embryol Cell Biol*, 161, III-XIII, 1-151.
- Knasmüller, S., Mersch-Sundermann, V., Kevekordes, S., Darroudi, F., Huber, W. W., Hoelzl, C., Bichler, J. & Majer, B. J. (2004). Use of human-derived liver cell lines for the detection of environmental and dietary genotoxicants; current state of knowledge. *Toxicology*, 198(1-3), 315-28.
- Kohonen, T., (1997). *Self-organizing maps*. Springer-Verlag New York, Inc., Secaucus, NJ.
- König, B. & Eder, K. (2006). Differential action of 13-HODE on PPARalpha downstream genes in rat Fao and human HepG2 hepatoma cell lines. *J Nutr Biochem*, 17(6), 410-8.
- Kostrubsky, V. E., Strom, S. C., Hanson, J., Urda, E., Rose, K., Burliegh, J., Zocharski, P., Cai, H., Sinclair, J. F. & Sahi, J. (2003). Evaluation of hepatotoxic potential of drugs by inhibition of bile-acid transport in cultured primary human hepatocytes and intact rats. *Toxicol Sci*, 76(1), 220-8.
- Kroeger, M. (2006). How omics technologies can contribute to the '3R' principles by introducing new strategies in animal testing. *Trends Biotechnol*, 24(8), 343-6.
- Krumdieck, C. L., dos Santos, J. E. & Ho, K. J. (1980). A new instrument for the rapid preparation of tissue slices. *Anal Biochem*, 104(1), 118-23.
- Kuo, W. P., Liu, F., Trimarchi, J., Punzo, C., Lombardi, M., Sarang, J., Whipple, M. E., Maysuria, M., Serikawa, K., Lee, S. Y., McCrann, D., Kang, J., Shearstone, J. R., Burke, J., Park, D. J., Wang, X., Rector, T. L., Ricciardi-Castagnoli, P., Perrin, S., Choi, S., Bumgarner, R., Kim, J. H., Short, G. F. 3rd, Freeman, M. W., Seed, B., Jensen, R., Church, G. M., Hovig, E., Cepko, C. L., Park, P., Ohno-Machado, L. & Jenssen, T. K. (2006). A sequence-oriented comparison of gene expression measurements across different hybridization-based technologies. *Nat Biotechnol*, 24(7), 832-40.

- Kurokawa, S., Ishibashi, H., Hayashida, K., Tsuchiya, Y., Hirata, Y., Sakaki, Y., Okubo, H. & Niho, Y. (1987). Kupffer cell stimulation of alpha 2-macroglobulin synthesis in rat hepatocytes and the role of glucocorticoid. *Cell Struct Funct*, 12(1), 35-42.
- Kutty, R. K., Daniel, R. F., Ryan, D. E., Levin, W. & Maines, M. D. (1988). Rat liver cytochrome P-450b, P-420b, and P-420c are degraded to biliverdin by heme oxygenase. *Arch Biochem Biophys*, 260(2), 638-44.
- LaBrecque, D. (1994). Liver regeneration: a picture emerges from the puzzle. *The American J Gastroenterol*, 89(8 Suppl), S86-96.
- Laishes, B. A. & Williams, G. M. (1976). Conditions affecting primary cell cultures of functional adult rat hepatocytes. 1. The effect of insulin. *In Vitro*, 12(7), 521-32.
- Landry, J., Bernier, D., Ouellet, C., Goyette, R. & Marceau, N. (1985). Spheroidal aggregate culture of rat liver cells: histotypic reorganization, biomatrix deposition, and maintenance of functional activities. *J Cell Biol*, 101(3), 914-23.
- Larson, A. M., Polson, J., Fontana, R. J., Davern, T. J., Lalani, E., Hynan, L. S., Reisch, J. S., Schiødt, F. V., Ostapowicz, G., Shakil, A. O., Lee, W. M.; Acute Liver Failure Study Group., (2005). Acetaminophen-induced acute liver failure: results of a United States multicenter, prospective study. *Hepatology*. 2005 Dec;42(6):1364-72.
- Latruffe, N., Passilly, P., Jannin, B., Motojima, K., Cherkaoui Malki, M., Schohn, H., Clemencet, M. C., Boscoboinik, D. & Dauça, M. (2000). Relationship between signal transduction and PPAR alpha-regulated genes of lipid metabolism in rat hepatic-derived Fao cells. *Cell Biochem Biophys*, 32 (Spring), 213-20.
- Lawyer, F. C., Stoffel, S., Saiki, R. K., Chang, S. Y., Landre, P. A., Abramson, R. D. & Gelfand, D. H. (1993). High-level expression, purification, and enzymatic characterization of full-length *Thermus aquaticus* DNA polymerase and a truncated form deficient in 5' to 3' exonuclease activity. *PCR Methods Appl*, 2(4), 275-87.
- LeCluyse, E. L., Ahlgren-Beckendorf, J. A., Carroll, K., Parkinson, A. & Johnson, J. (2000). Regulation of glutathione S-transferase enzymes in primary cultures of rat hepatocytes maintained under various matrix configurations. *Toxicol in vitro*, 14(2), 101-15.
- LeCluyse, E. L., Audus, K. L. & Hochman, J. H. (1994). Formation of extensive canalicular networks by rat hepatocytes cultured in collagen-sandwich configuration. *Am J Physiol*, 266(6 Pt 1), C1764-74.
- LeCluyse, E. L., Fix, J. A., Audus, K. L. & Hochman, J. H. (2000). Regeneration and maintenance of bile canalicular networks in collagen-sandwiched hepatocytes. *Toxicol in vitro*, 14(2), 117-32.
- LeCluyse, E., Madan, A., Hamilton, G., Carroll, K., DeHaan, R. & Parkinson, A. (2000). Expression and regulation of cytochrome P450 enzymes in primary cultures of human hepatocytes. *J Biochem Mol Toxicol*, 14(4), 177-88.
- LeCluyse, E. L., Alexandre, E., Hamilton, G. A., Viollon-Abadie, C., Coon, D. J., Jolley, S. & Richert, L. (2005). Isolation and culture of primary human hepatocytes. *Methods Mol Biol*, 290, 207-29.
- LeCluyse, E., Bullock, P., Madan, A., Carroll, K. & Parkinson, A. (1999). Influence of extracellular matrix overlay and medium formulation on the induction of cytochrome P-450 2B enzymes in primary cultures of rat hepatocytes. *Drug Metab Dispos*, 27(8), 909-15.
- Lee, W. M. (2003). Drug-induced hepatotoxicity. *N Engl J Med*, 349(5), 474-85.
- Lerche-Langr, C. & Toutain, H. J. (2000). Precision-cut liver slices: characteristics and use for in vitro pharmaco-toxicology. *Toxicology*, 153(1-3), 221-253.
- Lesko, L. J. & Woodcock, J. (2004). Translation of pharmacogenomics and pharmacogenetics: a regulatory perspective. *Nat Rev Drug Discov*, 3(9), 763-9.
- Lettieri, T. (2006). Recent applications of DNA microarray technology to toxicology and ecotoxicology. *Environ Health Perspect*, 114(1), 4-9.
- Lewis, J. H. (2002). Drug-induced liver disease. *Curr Opin Gastroenterol* 18(3), 307-13.

- Li, J., Pankratz, M. & Johnson, J. A. (2002). Differential gene expression patterns revealed by oligonucleotide versus long cDNA arrays. *Toxicol Sci*, 69(2), 383-90.
- Li, W., Liang, X., Leu, J. I., Kovalovich, K., Ciliberto, G. & Taub, R. (2001). Global changes in interleukin-6-dependent gene expression patterns in mouse livers after partial hepatectomy. *Hepatology*, 33(6), 1377-86.
- Linke, K., Schanz, J., Hansmann, J., Walles, T., Brunner, H. & Mertsching, H. (2007). Engineered liver-like tissue on a capillarized matrix for applied research. *Tissue Eng*, 13(11), 2699-707.
- Liu, X., Brouwer, K. L., Gan, L. S., Brouwer, K. R., Stieger, B., Meier, P. J., Audus, K. L. & LeCluyse, E. L. (1998). Partial maintenance of taurocholate uptake by adult rat hepatocytes cultured in a collagen sandwich configuration. *Pharm Res*, 15(10), 1533-9.
- Liu, X., Chism, J. P., LeCluyse, E. L., Brouwer, K. R. & Brouwer, K. L. (1999). Correlation of biliary excretion in sandwich-cultured rat hepatocytes and in vivo in rats. *Drug Metab Dispos*, 27(6), 637-44.
- Lloyd, S., Hayden, M. J., Sakai, Y., Fackett, A., Silber, P. M., Hewitt, N. J. & Li, A. P. (2002). Differential in vitro hepatotoxicity of troglitazone and rosiglitazone among cryopreserved human hepatocytes from 37 donors. *Chem Biol Interact*, 142(1-2), 57-71.
- Lottaz, C., Yang, X., Scheid, S. & Spang, R. (2006). OrderedList--a bioconductor package for detecting similarity in ordered gene lists. *Bioinformatics*, 22(18), 2315-6.
- de Longueville, F., Atienzar, F. A., Marcq, L., Dufrane, S., Evrard, S., Wouters, L., Leroux, F., Bertholet, V., Gerin, B., Whomsley, R., Arnould, T., Remacle, J. & Canning, M. (2003). Use of a low-density microarray for studying gene expression patterns induced by hepatotoxicants on primary cultures of rat hepatocytes. *Toxicol Sci*, 75(2), 378-92.
- Loyer, P., Ilyin, G., Cariou, S., Glaise, D., Corlu, A. & Guguen-Guillouzo, C. (1996). Progression through G1 and S phases of adult rat hepatocytes. *Prog Cell Cycle Res*, 2, 37-47.
- Lu, H., Chua, K., Zhang, P., Lim, W., Ramakrishna, S., Leong, K. W. & Mao, H. Q. (2005). Three-dimensional co-culture of rat hepatocyte spheroids and NIH/3T3 fibroblasts enhances hepatocyte functional maintenance. *Acta Biomater*, 1(4), 399-410.
- Lupp, A., Danz, M. & Müller, D. (2001). Morphology and cytochrome P450 isoforms expression in precision-cut rat liver slices. *Toxicology*, 161(1-2), 53-66.
- Luttringer, O., Theil, F. P., Lavé, T., Wernli-Kuratli, K., Guentert, T. W. & de Saizieu, A. (2002). Influence of isolation procedure, extracellular matrix and dexamethasone on the regulation of membrane transporters gene expression in rat hepatocytes. *Biochem Pharmacol*, 64(11), 1637-50.
- Lyu, J. & Joo, C. (2005). Wnt-7a up-regulates matrix metalloproteinase-12 expression and promotes cell proliferation in corneal epithelial cells during wound healing. *J Biol Chem*, 280(22), 21653-60.
- Mah, N., Thelin, A., Lu, T., Nikolaus, S., Kühbacher, T., Gurbuz, Y., Eickhoff, H., Klöppel, G., Lehrach, H., Mellgård, B., Costello, C. M. & Schreiber, S. (2004). A comparison of oligonucleotide and cDNA-based microarray systems. *Physiol Genomics*, 16(3), 361-70.
- Makowski, P. & Pińska, S. (1997). Participation of the multispecific organic anion transporter in hepatobiliary excretion of glutathione S-conjugates, drugs and other xenobiotics. *Pol J Pharmacol*, 49(6), 387-94.
- Marquardt, H. & Schäfer, S. G. (2004). *Lehrbuch der Toxikologie*. (2nd ed.). Wissenschaftliche Verlagsgesellschaft, Stuttgart.
- Marquardt, H., Schafer, S. G., McClellan, R. & Welch, F., (1999), Toxicology, Academic Press, NY.

- Matsumoto, T. & Kawakami, M. (1982). The unit-concept of hepatic parenchyma—a re-examination based on angioarchitectural studies. *Acta Pathol Jpn*, 32 Suppl 2, 285-314.
- Mattes, W. B., Pettit, S. D., Sansone, S., Bushel, P. R. & Waters, M. D. (2004). Database development in toxicogenomics: issues and efforts. *Environ Health Perspect*, 112(4), 495-505.
- Mayer, M. M. (1984). Complement. Historical perspectives and some current issues. *Complement*, 1(1), 2-26.
- McGall, G. H. & Fidanza, J. A. (2001). Photolithographic synthesis of high-density oligonucleotide arrays. *Methods Mol Biol*, 170, 71-101.
- McKee, E. E., Ferguson, M., Bentley, A. T. & Marks, T. A. (2006). Inhibition of Mammalian Mitochondrial Protein Synthesis by Oxazolidinones. *Antimicrob Agents Chemother*, 50(6), 2042–2049.
- Merrick, B. A. & Madenspacher, J. H. (2005). Complementary gene and protein expression studies and integrative approaches in toxicogenomics. *Toxicol Appl Pharmacol*, 207(2 Suppl), 189-94.
- Milani, S., Herbst, H., Schuppan, D., Hahn, E. G. & Stein, H. (1989). In situ hybridization for procollagen types I, III and IV mRNA in normal and fibrotic rat liver: evidence for predominant expression in nonparenchymal liver cells. *Hepatology*, 10(1), 84-92.
- Mingoia, R. T., Nabb, D. L., Yang, C. & Han, X. (2007). Primary culture of rat hepatocytes in 96-well plates: effects of extracellular matrix configuration on cytochrome P450 enzyme activity and inducibility, and its application in in vitro cytotoxicity screening. *Toxicol In Vitro*, 21(1), 165-73.
- Miranti, C. K. (2002). Application of cell adhesion to study signaling networks. *Methods Cell Biol*, 69, 359-83.
- Mitchell, J. R., Jollow, D. J., Gillette, J. R. & Brodie, B. B. (1973). Drug metabolism as a cause of drug toxicity. *Drug Metab Dispos*, 1(1), 418-23.
- Mohammed, F. F., Pennington, C. J., Kassiri, Z., Rubin, J. S., Soloway, P. D., Ruther, U., Edwards, D. R. & Khokha, R. (2005). Metalloproteinase inhibitor TIMP-1 affects hepatocyte cell cycle via HGF activation in murine liver regeneration. *Hepatology*, 41(4), 857-867.
- Monro, A. M. (1990). Interspecies comparisons in toxicology: the utility and futility of plasma concentrations of the test substance. *Regul Toxicol Pharmacol*, 12(2), 137-60.
- Montoudis, A., Seidman, E., Boudreau, F., Beaulieu, J., Menard, D., Elchebly, M., Mailhot, G., Sane, A. T., Lambert, M., Delvin, E. & Levy, E. (2008). Intestinal fatty acid binding protein regulates mitochondrion beta-oxidation and cholesterol uptake. *J Lipid Res*, 49(5), 961-72.
- Müller, D., Glöckner, R., Rost, M. & Steinmetzer, P. (1998). Monooxygenation, cytochrome P450-mRNA expression and other functions in precision-cut rat liver slices. *Exp Toxicol Pathol*, 50(4-6), 507-13.
- Müller, A. S. & Pallauf, J. (2003). Effect of increasing selenite concentrations, vitamin E supplementation and different fetal calf serum content on GPx1 activity in primary cultured rabbit hepatocytes. *J Trace Elem Med Biol*, 17(3), 183-92.
- Musat, A. I., Sattler, C. A., Sattler, G. L. & Pitot, H. C. (1993). Reestablishment of cell polarity of rat hepatocytes in primary culture. *Hepatology*, 18(1), 198-205.
- Mutschler, E., Geisslinger, G., Kroemer, H. K., Ruth, P. & Schäfer-Korting, M. (2008). *Arzneimittelwirkungen: Mit einführenden Kapiteln in die Anatomie, Physiologie und Pathophysiologie* (9th ed.). Wissenschaftliche Verlagsgesellschaft, Stuttgart.
- Nagy, P., Kiss, A., Schnur, J. & Thorgeirsson, S. S. (2003). Dexamethasone inhibits the proliferation of hepatocytes and oval cells but not bile duct cells in rat liver. *Hepatology*. 28(2):423-9.
- Nielsen, T. L., Rasmussen, B. B., Flinois, J., Beaune, P. & Brosen, K. (1999). In Vitro Metabolism of Quinidine: The (3S)-3-Hydroxylation of Quinidine Is a Specific

- Marker Reaction for Cytochrome P-4503A4 Activity in Human Liver Microsomes. *J Pharmacol Exp Ther*, 289(1), 31-37.
- Nieminen, A. (2003). Apoptosis and necrosis in health and disease: role of mitochondria. *Int Rev Cytol*, 224, 29-55.
- Nikkilä, J., Törönen, P., Kaski, S., Venna, J., Castrén, E. & Wong, G. (2002). Analysis and visualization of gene expression data using self-organizing maps. *Neural Netw*, 15(8-9), 953-66.
- Nuwaysir, E. F., Bittner, M., Trent, J., Barrett, J. C. & Afshari, C. A. (1999). Microarrays and toxicology: the advent of toxicogenomics. *Mol Carcinog*, 24(3), 153-9.
- O'Brien, P. J., Chan, K. & Silber, P. M. (2004). Human and animal hepatocytes in vitro with extrapolation in vivo. *Chem Biol Interact*, 150(1), 97-114.
- Ohta, Y., Kongo, M., Sasaki, E. & Harada, N. (1999). Change in hepatic antioxidant defense system with liver injury development in rats with a single naphthylisothiocyanate intoxication. *Toxicology*, 139(3), 265-75.
- Ogata, I., Mochida, S., Tomiya, T. & Fujiwara, K. (1991). Minor contribution of hepatocytes to collagen production in normal and early fibrotic rat livers. *Hepatology*, 14(2), 361-7.
- Ogata, K., Ohno, R., Terao, K., Iwasaki, K. & Endo, Y. (2000). Some properties and the possible role of intrinsic ATPase of rat liver 80S ribosomes in peptide bond elongation. *J Biochem*, 127(2), 221-31.
- Ohira, H., Abe, K., Yokokawa, J., Takiguchi, J., Rai, T., Shishido, S. & Sato, Y. (2003). Adhesion molecules and CXC chemokines in endotoxin-induced liver injury. *Fukushima J Med Sci*, 49(1), 1-13.
- Olson, H., Betton, G., Robinson, D., Thomas, K., Monro, A., Kolaja, G., Lilly, P., Sanders, J., Sipes, G., Bracken, W., Dorato, M., Van Deun, K., Smith, P., Berger, B. & Heller, A. (2000). Concordance of the toxicity of pharmaceuticals in humans and in animals. *Regul Toxicol Pharmacol*, 32(1), 56-67.
- Olson, H., Betton, G., Stritar, J. & Robinson, D. (1998). The predictivity of the toxicity of pharmaceuticals in humans from animal data- an interim assessment. *Toxicol Lett*, 102-103, 535-8.
- Orphanides, G. (2003). Toxicogenomics: challenges and opportunities. *Toxicol Lett*, 140-141, 145-8.
- Oude Elferink, R. P., Meijer, D. K., Kuipers, F., Jansen, P. L., Groen, A. K. & Groothuis, G. M. (1995). Hepatobiliary secretion of organic compounds; molecular mechanisms of membrane transport. *Biochim Biophys Acta*, 1241(2), 215-68.
- Page, J. L., Johnson, M. C., Olsavsky, K. M., Strom, S. C., Zarbl, H. & Omiecinski, C. J. (2007). Gene Expression Profiling of Extracellular Matrix as an Effector of Human Hepatocyte Phenotype in Primary Cell Culture. *Toxicol. Sci*, 97(2), 384-397.
- Paine, A. J. & Andreakos, E. (2004). Activation of signalling pathways during hepatocyte isolation: relevance to Toxicol in vitro. *Toxicol In Vitro*, 18(2), 187-93.
- Papeleu, P., Vanhaecke, T., Henkens, T., Elaut, G., Vinken, M., Snykers, S. & Rogiers, V. (2006). Isolation of rat hepatocytes. *Methods Mol Biol*, 320, 229-37.
- Parent, R. & Beretta, L. (2008). Translational control plays a prominent role in the hepatocytic differentiation of HepaRG liver progenitor cells. *Genome Biol*, 9(1), R19.
- Parent, R., Marion, M., Furio, L., Trépo, C. & Petit, M. (2004). Origin and characterization of a human bipotent liver progenitor cell line. *Gastroenterology*, 126(4), 1147-56.
- Parrish, M. L., Wei, N., Duenwald, S., Tokiwa, G. Y., Wang, Y., Holder, D., Dai, H., Zhang, X., Wright, C., Hodor, P., Cavet, G., Phillips, R. L., Sun, B. I. & Fare, T. L. (2004). A microarray platform comparison for neuroscience applications. *J Neurosci Methods*, 132(1), 57-68.
- Pascussi, J. M., Gerbal-Chaloin, S., Fabre, J. M., Maurel, P. & Vilarem, M. J. (2000). Dexamethasone enhances constitutive androstane receptor expression in

- human hepatocytes: consequences on cytochrome P450 gene regulation. *Mol Pharmacol*, 58(6), 1441-50.
- Pennie, W. D. (2000). Use of cDNA microarrays to probe and understand the toxicological consequences of altered gene expression. *Toxicol Lett*, 112-113, 473-7.
- Pennie, W. D., Tugwood, J. D., Oliver, G. J. & Kimber, I. (2000). The principles and practice of toxicogenomics: applications and opportunities. *Toxicol Sci*, 54(2), 277-83.
- Pfaffl, M. W. (2001). A new mathematical model for relative quantification in real-time RT-PCR. *Nucleic Acids Res*, 29(9), e45.
- Pham, R. T., Barber, D. S., & Gallagher, E. P., (2004). GSTA is a major glutathione S-transferase gene responsible for 4-hydroxynonenal conjugation in largemouth bass liver. *Mar Environ Res*, 58 (2-5), 485-488.
- Pi, L., Ding, X., Jorgensen, M., Pan, J., Oh, S., Pintilie, D., Brown, A., Song, W. Y. & Petersen, B. E. (2008). Connective tissue growth factor with a novel fibronectin binding site promotes cell adhesion and migration during rat oval cell activation. *Hepatology*, 47(3), 996-1004.
- Pontoglio, M., Pausa, M., Doyen, A., Viollet, B., Yaniv, M. & Tedesco, F. (2001). Hepatocyte nuclear factor 1alpha controls the expression of terminal complement genes. *J Exp Med*, 194(11), 1683-9.
- Powers, M. J., Domansky, K., Kaazempur-Mofrad, M. R., Kalezi, A., Capitano, A., Upadhyaya, A., Upadhyaya, A., Kurzawski, P., Wack, K. E., Stolz, D. B., Kamm, R. & Griffith, L. G. (2002). A microfabricated array bioreactor for perfused 3 d liver culture. *Biotechnol Bioeng*, 78(3), 257-69.
- Prada, A. E., Zahedi, K. & Davis, A. E. (1998). Regulation of C1 inhibitor synthesis. *Immunobiology*, 199(2), 377-88.
- Püschel, G. P. & Jungermann, K. (1994). Integration of function in the hepatic acinus: intercellular communication in neural and humoral control of liver metabolism. *Prog Liver Dis*, 12, 19-46.
- Pusztai, L. (2006). Chips to Bedside: Incorporation of Microarray Data into Clinical Practice. *Clin Cancer Res*, 12(24), 7209-7214.
- Radisavljevic, Z. M. & González-Flecha, B. (2004). TOR kinase and ran are downstream from PI3K/Akt in H₂O₂-induced mitosis. *J Cell Biochem*, 91(6), 1293-1300.
- Ramadori, G. & Armbrust, T. (2001). Cytokines in the liver. *Eur J Gastroenterol Hepatol*, 13(7), 777-84.
- Rannug, A., Alexandrie, A. K., Persson, I. & Ingelman-Sundberg, M. (1995). Genetic polymorphism of cytochromes P450 1A1, 2 d6 and 2E1: regulation and toxicological significance. *J occup environ med*, 37(1), 25-36.
- Raudys, S. (2000). How good are support vector machines? *Neural Netw*, 13(1), 17-9.
- Reid, L. M., Fiorino, A. S., Sigal, S. H., Brill, S. & Holst, P. A. (1992). Extracellular matrix gradients in the space of Disse: relevance to liver biology. *Hepatology*, 15(6), 1198-203.
- Rialland, L., Guyomard, C., Scotte, M., Chesné, C. & Guillouzo, A. (2000). Viability and drug metabolism capacity of alginate-entrapped hepatocytes after cryopreservation. *Cell Biol Toxicol*, 16(2), 105-16.
- Richert, L., Alexandre, E., Lloyd, T., Orr, S., Viollon-Abadie, C., Patel, R., Kingston, S., Berry, D., Dennison, A., Heyd, B., Manton, G. & Jaeck, D. (2004). Tissue collection, transport and isolation procedures required to optimize human hepatocyte isolation from waste liver surgical resections. A multilaboratory study. *Liver Int*, 24(4), 371-8.
- Richert, L., Binda, D., Hamilton, G., Viollon-Abadie, C., Alexandre, E., Bigot-Lasserre, D., Bars, R., Coassolo, P. & LeCluyse, E. (2002). Evaluation of the effect of culture configuration on morphology, survival time, antioxidant status and metabolic capacities of cultured rat hepatocytes. *Toxicol in vitro*, 16(1), 89-99.

- Richert, L., Liguori, M. J., Abadie, C., Heyd, B., Manton, G., Halkic, N. & Waring, J. F. (2006). Gene expression in human hepatocytes in suspension after isolation is similar to the liver of origin, is not affected by hepatocyte cold storage and cryopreservation, but is strongly changed after hepatocyte plating. *Drug Metab Dispos*, 34(5), 870-9.
- Rodríguez-Antona, C., Donato, M. T., Boobis, A., Edwards, R. J., Watts, P. S., Castell, J. V. & Gómez-Lechón, M. J. (2002). Cytochrome P450 expression in human hepatocytes and hepatoma cell lines: molecular mechanisms that determine lower expression in cultured cells. *Xenobiotica*, 32(6), 505-20.
- Rogiers, V. & Vercruyse, A. (1998). Hepatocyte cultures in drug metabolism and toxicological research and testing. *Methods Mol Biol*, 107, 279-94.
- Roter, A. H. (2005). Large-scale integrated databases supporting drug discovery. *Curr Opin Drug Discov Devel*, 8(3), 309-15.
- Ruepp, S., Boess, F., Suter, L., de Vera, M. C., Steiner, G., Steele, T., Weiser, T. & Albertini, S. (2005). Assessment of hepatotoxic liabilities by transcript profiling. *Toxicol Appl Pharmacol*, 207(2 Suppl), 161-70.
- Russell, W. & Burch, R. (1959). *The Principles of Humane Experimental Technique*. Methuen, London.
- Sadée, W., Wang, D. & Bilsky, E. J. (2005). Basal opioid receptor activity, neutral antagonists, and therapeutic opportunities. *Life Sci*, 76(13), 1427-1437.
- Sadeque, A. J., Wandel, C., He, H., Shah, S. & Wood, A. J. (2000). Increased drug delivery to the brain by P-glycoprotein inhibition. *Clin Pharmacol Ther*, 68(3), 231-7.
- Sahu, S. C. (2008). *Hepatotoxicity: From Genomics to in Vitro and in Vivo Models* (1st ed., p. 704). Wiley & Sons, West Sussex.
- Sakai, M. & Muramatsu, M. (2007). Regulation of GST-P gene expression during hepatocarcinogenesis. *Methods Enzymol*, 401, 42-61.
- Sampath, H. & Ntambi, J. M. (2004). Polyunsaturated fatty acid regulation of gene expression. *Nutr Rev*, 62(9), 333-9.
- Schena, M. (1996). Genome analysis with gene expression microarrays. *Bioessays*, 18(5), 427-31.
- Scholz, G., Pohl, I., Genschow, E., Klemm, M. & Spielmann, H. (1999). Embryotoxicity screening using embryonic stem cells in vitro: correlation to in vivo teratogenicity. *Cells Tissues Organs*, 165(3-4), 203-11.
- Schoonen, W. G. E. J., Westerink, W. M. A., de Roos, J. A. D. M. & Débiton, E. (2005). Cytotoxic effects of 100 reference compounds on Hep G2 and HeLa cells and of 60 compounds on ECC-1 and CHO cells I. Mechanistic assays on ROS, glutathione depletion and calcein uptake. *Toxicol in vitro*, 19(4), 505-16.
- Schuetz, E. G., Li, D., Omiecinski, C. J., Muller-Eberhard, U., Kleinman, H. K., Elswick, B. & Guzelian, P. S. (1988). Regulation of gene expression in adult rat hepatocytes cultured on a basement membrane matrix. *J Cell Physiol*, 134(3), 309-23.
- Schuster, D., Laggner, C. & Langer, T. (2005). Why drugs fail- a study on side effects in new chemical entities. *Curr Pharm Des*, 11(27), 3545-59.
- Scoazec, J. Y. & Feldmann, G. (1994). The cell adhesion molecules of hepatic sinusoidal endothelial cells. *J Hepatol*, 20(2), 296-300.
- Seglen, P. O. (1976). Preparation of isolated rat liver cells. *Methods Cell Biol*, 13, 29-83.
- Sell, S. (2001). The role of progenitor cells in repair of liver injury and in liver transplantation. *Wound Repair Regen*, 9(6), 467-82.
- Shi, L., Reid, L. H., Jones, W. D., Shippy, R., Warrington, J. A., Baker, S. C., Collins, P. J., de Longueville, F., Kawasaki, E. S., Lee, K. Y., Luo, Y., Sun, Y. A., Willey, J. C., Setterquist, R. A., Fischer, G. M., Tong, W., Dragan, Y. P., Dix, D. J., Frueh, F. W., Goodsaid, F. M., Herman, D., Jensen, R. V., Johnson, C. D., Lobenhofer, E. K., Puri, R. K., Schrf, U., Thierry-Mieg, J., Wang, C., Wilson, M., Wolber, P. K., Zhang, L., Amur, S., Bao, W., Barbacioru, C. C., Lucas, A. B.,

- Bertholet, V., Boysen, C., Bromley, B., Brown, D., Brunner, A., Canales, R., Cao, X. M., Cebula, T. A., Chen, J. J., Cheng, J., Chu, T. M., Chudin, E., Corson, J., Corton, J. C., Croner, L. J., Davies, C., Davison, T. S., Delenstarr, G., Deng, X., Dorris, D., Eklund, A. C., Fan, X. H., Fang, H., Fulmer-Smentek, S., Fuscoe, J. C., Gallagher, K., Ge, W., Guo, L., Guo, X., Hager, J., Haje, P. K., Han, J., Han, T., Harbottle, H. C., Harris, S. C., Hatchwell, E., Hauser, C. A., Hester, S., Hong, H., Hurban, P., Jackson, S. A., Ji, H., Knight, C. R., Kuo, W. P., LeClerc, J. E., Levy, S., Li, Q. Z., Liu, C., Liu, Y., Lombardi, M. J., Ma, Y., Magnuson, S. R., Maqsoodi, B., McDaniel, T., Mei, N., Myklebost, O., Ning, B., Novoradovskaya, N., Orr, M. S., Osborn, T. W., Papallo, A., Patterson, T. A., Perkins, R. G., Peters, E. H., Peterson, R., Philips, K. L., Pine, P. S., Pusztai, L., Qian, F., Ren, H., Rosen, M., Rosenzweig, B. A., Samaha, R. R., Schena, M., Schroth G. P., Shchegrova, S., Smith, D. D., Staedtler, F., Su, Z., Sun, H., Szallasi, Z., Tezak, Z., Thierry-Mieg, D., Thompson, K. L., Tikhonova, I., Turpaz, Y., Vallanat, B., Van, C., Walker, S. J., Wang, S. J., Wang, Y., Wolfinger, R., Wong, A., Wu, J., Xiao, C., Xie, Q., Xu, J., Yang, W., Zhang, L., Zhong, S., Zong, Y. & Slikker, W. Jr. (2006). The MicroArray Quality Control (MAQC) project shows inter- and intraplatform reproducibility of gene expression measurements. *Nat Biotechnol*, 24(9), 1151-61.
- Shull, J., Spady, T., Snyder, M., Johansson, S. & Pennington, K. (1997). Ovary-intact, but not ovariectomized female ACI rats treated with 17beta-estradiol rapidly develop mammary carcinoma. *Carcinogenesis*, 18(8), 1595-1601.
- Sidhu, J. S., Liu, F. & Omiecinski, C. J. (2004). Phenobarbital responsiveness as a uniquely sensitive indicator of hepatocyte differentiation status: requirement of dexamethasone and extracellular matrix in establishing the functional integrity of cultured primary rat hepatocytes. *Exp Cell Res*, 292(2), 252-64.
- Sidhu, J. S. & Omiecinski, C. J. (1995). Modulation of xenobiotic-inducible cytochrome P450 gene expression by dexamethasone in primary rat hepatocytes. *Pharmacogenetics*, 5(1), 24-36.
- Siegenthaler, Blum, (2006). *Klinische Pathophysiologie*. p. 860, Georg Thieme Verlag KG, Stuttgart.
- Sigal, S. H., Rajvanshi, P., Gorla, G. R., Sokhi, R. P., Saxena, R., Gebhard, D. R., Reid, L. M. & Gupta, S. (1999). Partial hepatectomy-induced polyploidy attenuates hepatocyte replication and activates cell aging events. *Am J Physiol*, 276(5 Pt 1), G1260-72.
- Simon, R., Radmacher, M. D., Dobbin, K. & McShane, L. M. (2003). Pitfalls in the use of DNA microarray data for diagnostic and prognostic classification. *J Natl Cancer Inst*, 95(1), 14-8.
- Sivaraman, A., Leach, J. K., Townsend, S., Iida, T., Hogan, B. J., Stolz, D. B., Fry, R., Samson, L. D., Tannenbaum, S. R. & Griffith, L. G. (2005). A microscale in vitro physiological model of the liver: predictive screens for drug metabolism and enzyme induction. *Curr Drug Metab*, 6(6), 569-91.
- Skett, P. & Bayliss, M. (1996). Time for a consistent approach to preparing and culturing hepatocytes? *Xenobiotica*, 26(1), 1-7.
- Sladek, F. M. (1994). Orphan receptor HNF-4 and liver-specific gene expression. *Receptor*, 4(1), 64.
- Slaughter, M. R., Thakkar, H. & O'Brien, P. J. (2002). Effect of diquat on the antioxidant system and cell growth in human neuroblastoma cells. *Toxicol Appl Pharmacol*, 178(2), 63-70.
- Smith, R. D. (2000). Probing proteomes--seeing the whole picture? *Nat Biotechnol*, 18(10), 1041-2.
- Southern, E. M. (1975). Detection of specific sequences among DNA fragments separated by gel electrophoresis. *J Mol Biol*, 98(3), 503-17.
- Stafford, P. & Brun, M. (2007). Three methods for optimization of cross-laboratory and cross-platform microarray expression data. *Nucleic Acids Res*, 35(10), e72.

- Stapp, J. M., Sjoelund, V., Lassiter, H. A., Feldhoff, R. C. & Feldhoff, P. W. (2005). Recombinant rat IL-1beta and IL-6 synergistically enhance C3 mRNA levels and complement component C3 secretion by H-35 rat hepatoma cells. *Cytokine*, 30(2), 78-85.
- Strey, C. W., Markiewski, M., Mastellos, D., Tudoran, R., Spruce, L. A., Greenbaum, L. E. & Lambris, J. D. (2003). The proinflammatory mediators C3a and C5a are essential for liver regeneration. *J Exp Med*, 198(6), 913-23.
- Stubberfield, C. R. & Page, M. J. (1999). Applying proteomics to drug discovery. *Expert Opin Investig Drugs*, 8(1), 65-70.
- Stupack, D. G. (2007). The biology of integrins. *Oncology (Williston Park)*, 21(9 Suppl 3), 6-12.
- Suter, L., Babiss, L. E. & Wheeldon, E. B. (2004). Toxicogenomics in predictive toxicology in drug development. *Chem Biol*, 11(2), 161-71.
- Suzuki, H., Inoue, T., Matsushita, T., Kobayashi, K., Horii, I., Hirabayashi, Y. & Inoue, T. (2008). In vitro gene expression analysis of hepatotoxic drugs in rat primary hepatocytes. *J Appl Toxicol*, 28(2), 227-36.
- Talamini, M. A., Kappus, B. & Hubbard, A. (1997). Repolarization of hepatocytes in culture. *Hepatology*, 25(1), 167-72.
- Terry, T. L. & Gallin, W. J. (1994). Effects of fetal calf serum and disruption of cadherin function on the formation of bile canaliculi between hepatocytes. *Exp Cell Res*, 214(2), 642-53.
- Thedinga, E., Ullrich, A., Drechsler, S., Niendorf, R., Kob, A., Runge, D., Keuer, A., Freund, I., Lehmann, M. & Ehret, R. (2007). In vitro system for the prediction of hepatotoxic effects in primary hepatocytes. *ALTEX*, 24(1), 22-34.
- Tian, H., Ou, J., Strom, S. C. & Venkataramanan, R. (2005). Activity and expression of various isoforms of uridine diphosphate glucuronosyltransferase are differentially regulated during hepatic regeneration in rats. *Pharm Res*, 22(12), 2007-15.
- Tirona, R. G. & Kim, R. B. (2005). Nuclear receptors and drug disposition gene regulation. *J Pharm Sci*, 94(6), 1169-1186.
- Tonge, R. P., Kelly, E. J., Bruschi, S. A., Kalthorn, T., Eaton, D. L., Nebert, D. W. & Nelson, S. D. (1998). Role of CYP1A2 in the hepatotoxicity of acetaminophen: investigations using Cyp1a2 null mice. *Toxicol Appl Pharmacol*, 153(1), 102-8.
- Tsutsui, H., Adachi, K., Seki, E. & Nakanishi, K. (2003). Cytokine-induced inflammatory liver injuries. *Curr Mol Med*, 3(6), 545-59.
- Turncliff, R. Z., Meier, P. J. & Brouwer, K. L. R. (2004). Effect of dexamethasone treatment on the expression and function of transport proteins in sandwich-cultured rat hepatocytes. *Drug Metab Dispos*, 32(8), 834-9.
- Turncliff, R. Z., Tian, X. & Brouwer, K. L. R. (2006). Effect of culture conditions on the expression and function of Bsep, Mrp2, and Mdr1a/b in sandwich-cultured rat hepatocytes. *Biochem Pharmacol*, 71(10), 1520-9.
- Tuschl, G. & Müller, S. O. (2006). Effects of cell culture conditions on primary rat hepatocytes-cell morphology and differential gene expression. *Toxicology*, 218(2-3), 205-15.
- Ulrich, R. G., Bacon, J. A., Cramer, C. T., Peng, G. W., Petrella, D. K., Stryd, R. P. & Sun, E. L. (1995). Cultured hepatocytes as investigational models for hepatic toxicity: practical applications in drug discovery and development. *Toxicol Lett*, 82-83, 107-15.
- Ulrich, R. G. (2003). The toxicogenomics of nuclear receptor agonists. *Curr Opin Chem Biol* 7, 505-10.
- Ullrich, A., Berg, C., Hengstler, J. G. & Runge, D. (2007). Use of a standardised and validated long-term human hepatocyte culture system for repetitive analyses of drugs: repeated administrations of acetaminophen reduces albumin and urea secretion. *ALTEX*, 24(1), 35-40.

- Vanhaecke, T., Elaut, G. & Rogiers, V. (2001). Effect of oxygen concentration on the expression of glutathione S-transferase activity in periportal and perivenous rat hepatocyte cultures. *Toxicol in vitro*, 15(4-5), 387-92.
- Veenstra, T. D. & Conrads, T. P. (2003). Serum protein fingerprinting. *Curr Opin Mol Ther*, 5(6), 584-93.
- Viebahn, C. S. & Yeoh, G. C. T. (2008). What fires prometheus? The link between inflammation and regeneration following chronic liver injury. *Int J Biochem Cell Biol*, 40(5), 855-73.
- Vinken, M., Elaut, G., Henkens, T., Papeleu, P., Snykers, S., Vanhaecke, T. & Rogiers, V. (2006). Rat hepatocyte cultures: collagen gel sandwich and immobilization cultures. *Methods Mol Biol*, 320, 247-54.
- Wakabayashi, Y., Kipp, H. & Arias, I. M. (2006). Transporters on demand: intracellular reservoirs and cycling of bile canalicular ABC transporters. *J Biol Chem*, 281(38), 27669-73.
- Warburg, O. (1923). Versuche an überlebendem Karzinomgewebe. *Biochem Z*, (142), 317-333.
- Waring, J. F., Jolly, R. A., Ciurlionis, R., Lum, P. Y., Praestgaard, J. T., Morfitt, D. C., Buratto, B., Roberts, C., Schadt, E. & Ulrich, R. G. (2001). Clustering of hepatotoxins based on mechanism of toxicity using gene expression profiles. *Toxicol Appl Pharmacol*, 175(1), 28-42.
- Waxman, D. J. (1999). P450 gene induction by structurally diverse xenochemicals: central role of nuclear receptors CAR, PXR, and PPAR. *Arch Biochem Biophys*, 369(1), 11-23.
- Westerink, W. M. A. & Schoonen, W. G. E. J. (2007). Cytochrome P450 enzyme levels in HepG2 cells and cryopreserved primary human hepatocytes and their induction in HepG2 cells. *Toxicol In Vitro*, 21(8), 1581-91.
- Westphal, J. F., Vetter, D. & Brogard, J. M. (1994). Hepatic side-effects of antibiotics. *J Antimicrob Chemother*, 33(3), 387-401.
- Wetmore, B. A. & Merrick, B. A. (2004). Toxicoproteomics: proteomics applied to toxicology and pathology. *Toxicol Pathol*, 32(6), 619-42.
- Wettschureck, N. & Offermanns, S. (2005). Mammalian G proteins and their cell type specific functions. *Physiol Rev*, 85(4), 1159-204.
- Widmann, J. J., Cotran, R. S. & Fahimi, H. D. (1972). Mononuclear phagocytes (Kupffer cells) and endothelial cells. Identification of two functional cell types in rat liver sinusoids by endogenous peroxidase activity. *J Cell Biol*, 52(1), 159-70.
- Wilkening, S., Stahl, F. & Bader, A. (2003). Comparison of primary human hepatocytes and hepatoma cell line Hepg2 with regard to their biotransformation properties. *Drug Metab Dispos*, 31(8), 1035-42.
- Wilkinson, R. C. & Dickson, A. J. (2001). Expression of CCAAT/enhancer binding protein family genes in monolayer and sandwich culture of hepatocytes: induction of stress-inducible GADD153. *Biochem Biophys Res Commun*, 289(5), 942-9.
- Williams, G. M., Bermudez, E. & Scaramuzzino, D. (1977). Rat hepatocyte primary cell cultures III. Improved dissociation and attachment techniques and the enhancement of survival by culture medium. *In vitro*, 13(12), 809-17.
- Winwood, P. J. & Arthur, M. J. (1993). Kupffer cells: their activation and role in animal models of liver injury and human liver disease. *Semin Liver Dis*, 13(1), 50-9.
- Wisse, E. (1977a). Ultrastructure and function of Kupffer cells and other sinusoidal cells in the liver. *Med Chir Dig*, 6(7), 409-18.
- Wisse, E. (1977b). On the endothelial cells of rat liver sinusoids. *Bibliotheca anatomica*, (16 Pt 2), 373-6.
- Wolfrum, C., Borrmann, C. M., Borchers, T. & Spener, F. (2001). Fatty acids and hypolipidemic drugs regulate peroxisome proliferator-activated receptors alpha - and gamma-mediated gene expression via liver fatty acid binding protein: a signaling path to the nucleus. *Proc Natl Acad Sci U S A*, 98(5), 2323-8.

- Wolfrum, C. & Spener, F. (2000). Fatty acids as regulators of lipid metabolism. *Eur J Lipid Sci Technol*, 102(12), 746-62.
- Woolfson, A. M. (1983). Amino acids--their role as an energy source. *Proc Nutr Soc*, 42(3), 489-95.
- Wrighton, S. A. & Stevens, J. C. (1992). The human hepatic cytochromes P450 involved in drug metabolism. *Crit Rev Toxicol*, 22(1), 1-21.
- Wunder, C. & Potter, R. F. (2003). The heme oxygenase system: its role in liver inflammation. *Curr Drug Targets Cardiovasc Haematol Disord*, 3(3), 199-208.
- Wysowski, D. K. & Swartz, L. (2005). Adverse Drug Event Surveillance and Drug Withdrawals in the United States, 1969-2002: The Importance of Reporting Suspected Reactions. *Arch Intern Med*, 165(12), 1363-69.
- Xu, C., Li, C. Y. & Kong, A. T. (2005). Induction of phase 1, II and III drug metabolism/transport by xenobiotics. *Arch Pharm Res*, 28(3), 249-68.
- Xu, J. J., Diaz, D. & O'Brien, P. J. (2004). Applications of cytotoxicity assays and pre-lethal mechanistic assays for assessment of human hepatotoxicity potential. *Chem Biol Interact*, 150(1), 115-28.
- Yamada, S., Otto, P. S., Kennedy, D. L. & Whayne, T. F. (1980). The effects of dexamethasone on metabolic activity of hepatocytes in primary monolayer culture. *In Vitro*, 16(7), 559-70.
- Yamazaki, M., Suzuki, H. & Sugiyama, Y. (1996). Recent advances in carrier-mediated hepatic uptake and biliary excretion of xenobiotics. *Pharm Res*, 13(4), 497-513.
- Yan, Z. & Caldwell, G. W. (2001). Metabolism profiling, and cytochrome P450 inhibition & induction in drug discovery. *Curr Top Med Chem*, 1(5), 403-25.
- Yeung, K. Y. & Ruzzo, W. L. (2001). Principal component analysis for clustering gene expression data. *Bioinformatics*, 17(9), 763-74.
- Yin, H., Kim, M., Kim, J., Kong, G., Lee, M., Kang, K., Yoon, B. I., Kim, H. L. & Lee, B. H. (2006). Hepatic Gene Expression Profiling and Lipid Homeostasis in Mice Exposed to Steatogenic Drug, Tetracycline. *Toxicol Sci*, 94, 206-16.
- You, L. (2004). Steroid hormone biotransformation and xenobiotic induction of hepatic steroid metabolizing enzymes. *Chem Biol Interact*, 147(3), 233-46.
- Zaher, H., Buters, J. T., Ward, J. M., Bruno, M. K., Lucas, A. M., Stern, S. T., Cohen, S. D. & Gonzalez, F. J. (1998). Protection against acetaminophen toxicity in CYP1A2 and CYP2E1 double-null mice. *Toxicol Appl Pharmacol*, 152(1), 193-9.
- Zidek, N., Hellmann, J., Kramer, P. & Hewitt, P. G. (2007). Acute hepatotoxicity: a predictive model based on focused illumina microarrays. *Toxicol Sci*, 99(1), 289-302.
- Zvibel, I., Smets, F. & Soriano, H. (2002). Anoikis: roadblock to cell transplantation? *Cell Transplant*, 11(7), 621-30.

APPENDIX

Appendix 1: Results of the one sided tests comparing gene lists ranked by p Value.

Settings

List comparison
 Assessing similarity of top ranks
 Length of lists 7263
 Quantile of invariant genes 0.5
 Number of random samples 1000

Affymetrix_In vivo, high dose_24h vs. Illumina_In vivo, high dose_24h

	Genes	Scores	p.values	Rev.Scores	Rev.p.values
0.115	100	3.396578	0.021	0.00E+00	0.942
0.077	150	12.872106	0	0.00E+00	0.999
0.058	200	29.560405	0	2.55E-04	1
0.038	300	87.649945	0	2.17E-02	1
0.029	400	183.980918	0	1.72E-01	1
0.023	500	324.038894	0	6.33E-01	1
0.015	750	891.757136	0	4.39E+00	1
0.012	1000	1806.952651	0	1.45E+01	1
0.008	1500	4819.958101	0	7.07E+01	1
0.006	2000	9604.577392	0	2.09E+02	1
0.005	2500	16356.67251	0	4.71E+02	1

Affymetrix_In vivo, high dose_6 h vs. Illumina_In vivo, high dose_6 h

	Genes	Scores	p.values	Rev.Scores	Rev.p.values
0.115	100	4.496039	0.012	0.00E+00	0.95
0.077	150	16.355067	0	0.00E+00	0.998
0.058	200	36.734735	0	0.00E+00	1
0.038	300	105.510524	0	5.53E-04	1
0.029	400	215.222581	0	1.41E-02	1
0.023	500	369.287354	0	9.00E-02	1
0.015	750	966.487184	0	1.39E+00	1
0.012	1000	1895.079548	0	7.04E+00	1
0.008	1500	4853.82513	0	5.12E+01	1
0.006	2000	9419.988236	0	1.76E+02	1
0.005	2500	15740.11764	0	4.28E+02	1

Affymetrix_In vivo, high dose_72 h vs. Illumina_In vivo, high dose_72 h

	Genes	Scores	p.values	Rev.Scores	Rev.p.values
0.115	100	0.0820066	0.394	0.00E+00	0.936
0.077	150	0.9049201	0.351	0.00E+00	0.998
0.058	200	3.5427757	0.288	1.45E-03	0.999
0.038	300	17.8166802	0.16	9.41E-02	1
0.029	400	48.203631	0.058	7.56E-01	1
0.023	500	97.9639087	0.02	2.88E+00	1
0.015	750	319.699483	0	2.12E+01	1
0.012	1000	697.2417988	0	6.92E+01	1
0.008	1500	1994.939427	0	3.06E+02	1
0.006	2000	4137.290714	0	8.25E+02	1
0.005	2500	7258.68298	0	1.75E+03	1

Affymetrix_In vivo, low dose_24h vs. Illumina_In vivo, low dose_24h

	Genes	Scores	p.values	Rev.Scores	Rev.p.values
0.115	100	1.991168	0.057	2.09E-04	0.888
0.077	150	6.969976	0.041	1.57E-02	0.902
0.058	200	15.638143	0.018	1.37E-01	0.91
0.038	300	45.759576	0	1.43E+00	0.919
0.029	400	95.184211	0	5.27E+00	0.946
0.023	500	166.214749	0	1.24E+01	0.976
0.015	750	451.538273	0	4.61E+01	0.999
0.012	1000	913.753175	0	1.06E+02	1
0.008	1500	2469.962063	0	3.34E+02	1
0.006	2000	5014.659594	0	7.77E+02	1
0.005	2500	8703.099602	0	1.52E+03	1

Affymetrix_In vivo, low dose_6 h vs. Illumina_In vivo, low dose_6 h

	Genes	Scores	p.values	Rev.Scores	Rev.p.values
0.115	100	7.283426	0.006	0	0.955
0.077	150	19.243393	0	0	1
0.058	200	36.969171	0	0.00001	1
0.038	300	92.427889	0	0.01222236	1
0.029	400	180.357296	0	0.12293679	1
0.023	500	306.936003	0	0.55805418	1
0.015	750	822.530248	0	5.62455642	1
0.012	1000	1662.852982	0	22.7816052	1
0.008	1500	4442.275855	0	126.114992	1
0.006	2000	8804.673908	0	371.034203	1
0.005	2500	14842.6007	0	814.456991	1

Affymetrix_In vivo, low dose_72 h vs. Illumina_In vivo, low dose_72 h

	Genes	Scores	p.values	Rev.Scores	Rev.p.values
0.115	100	0.6533219	0.148	1.02E-04	0.931
0.077	150	2.9582573	0.134	9.83E-03	0.945
0.058	200	6.9889852	0.122	8.04E-02	0.963
0.038	300	19.9385361	0.11	7.65E-01	0.977
0.029	400	40.3567281	0.106	2.73E+00	0.993
0.023	500	70.3485953	0.118	6.51E+00	1
0.015	750	201.443388	0.15	2.79E+01	1
0.012	1000	436.0229586	0.188	7.63E+01	1
0.008	1500	1310.829829	0.305	3.15E+02	1
0.006	2000	2856.292467	0.548	8.42E+02	1
0.005	2500	5208.756318	0.818	1.77E+03	1

Affymetrix_Tet_in vitro, 200µM_24h vs. Illumina_Tet_in vitro, 200µM_24h

	Genes	Scores	p.values	Rev.Scores	Rev.p.values
0.115	100	5.486148	0.009	0.00E+00	0.935
0.077	150	19.204741	0	0.00E+00	0.999
0.058	200	42.889678	0	2.55E-04	1
0.038	300	125.232997	0	2.22E-02	1
0.029	400	260.821096	0	1.85E-01	1
0.023	500	454.645129	0	7.13E-01	1
0.015	750	1213.559971	0	5.37E+00	1
0.012	1000	2392.390421	0	1.81E+01	1
0.008	1500	6122.928476	0	8.29E+01	1
0.006	2000	11833.59296	0	2.21E+02	1
0.005	2500	19662.67078	0	4.58E+02	1

Affymetrix_Tet_in vitro, 200µM_6 h vs. Illumina_Tet_in vitro, 200µM_6 h

	Genes	Scores	p.values	Rev.Scores	Rev.p.values
0.115	100	1.48309	0.069	0.00E+00	0.928
0.077	150	7.153101	0.032	1.47E-03	0.981
0.058	200	18.694907	0.006	2.48E-02	0.985
0.038	300	62.205048	0	4.50E-01	0.988
0.029	400	135.584691	0	2.20E+00	0.998
0.023	500	241.308089	0	6.24E+00	0.999
0.015	750	659.85671	0	3.12E+01	1
0.012	1000	1318.54695	0	8.42E+01	1
0.008	1500	3440.196261	0	3.09E+02	1
0.006	2000	6749.990373	0	7.60E+02	1
0.005	2500	11362.82429	0	1.54E+03	1

Affymetrix_Tet_in vitro, 200µM_72 h vs. Illumina_Tet_in vitro, 200µM_72 h

	Genes	Scores	p.values	Rev.Scores	Rev.p.values
0.115	100	0.00E+00	0.953	3.29E-04	0.899
0.077	150	1.32E-03	0.994	1.71E-02	0.922
0.058	200	2.81E-02	0.994	1.24E-01	0.944
0.038	300	6.53E-01	0.992	1.07E+00	0.974
0.029	400	3.87E+00	0.99	3.64E+00	0.991
0.023	500	1.28E+01	0.986	8.33E+00	0.999
0.015	750	8.52E+01	0.948	3.16E+01	1
0.012	1000	2.76E+02	0.856	7.53E+01	1
0.008	1500	1.21E+03	0.491	2.49E+02	1
0.006	2000	3.17E+03	0.179	5.90E+02	1
0.005	2500	6.42E+03	0.054	1.16E+03	1

Affymetrix_Tet_in vitro, 40µM_24h vs. Illumina_Tet_in vitro, 40µM_24h

	Genes	Scores	p.values	Rev.Scores	Rev.p.values
0.115	100	2.385667	0.054	4.10E-02	0.504
0.077	150	7.646565	0.027	3.67E-01	0.525
0.058	200	16.499255	0.008	1.20E+00	0.572
0.038	300	47.125522	0	4.46E+00	0.706
0.029	400	97.431035	0	9.62E+00	0.851
0.023	500	169.010198	0	1.66E+01	0.942
0.015	750	449.565631	0	4.36E+01	0.999
0.012	1000	897.035527	0	9.09E+01	1
0.008	1500	2417.73594	0	2.92E+02	1
0.006	2000	4950.564876	0	7.23E+02	1
0.005	2500	8652.718524	0	1.49E+03	1

Affymetrix_Tet_in vitro, 40µM_6 h vs. Illumina_Tet_in vitro, 40µM_6 h

	Genes	Scores	p.values	Rev.Scores	Rev.p.values
0.115	100	1.54447	0.07	1.64E-02	0.588
0.077	150	5.855951	0.052	2.09E-01	0.628
0.058	200	12.736524	0.035	8.40E-01	0.665
0.038	300	32.172252	0.02	4.06E+00	0.74
0.029	400	57.293263	0.031	1.04E+01	0.822
0.023	500	87.786004	0.049	2.05E+01	0.893
0.015	750	196.205276	0.163	6.66E+01	0.982
0.012	1000	375.311426	0.415	1.53E+02	1
0.008	1500	1069.383307	0.771	5.04E+02	1
0.006	2000	2385.423526	0.939	1.18E+03	1
0.005	2500	4494.577654	0.997	2.31E+03	1

Affymetrix_Tet_in vitro, 40µM_72 h vs. Illumina_Tet_in vitro, 40µM_72 h

	Genes	Scores	p.values	Rev.Scores	Rev.p.values
0.115	100	0.2532672	0.257	3.25E-02	0.527
0.077	150	1.4725369	0.249	3.15E-01	0.563
0.058	200	4.2493281	0.236	1.06E+00	0.609
0.038	300	16.3431309	0.184	4.06E+00	0.745
0.029	400	40.0437893	0.134	8.79E+00	0.866
0.023	500	78.6345881	0.089	1.52E+01	0.956
0.015	750	258.6040214	0.032	4.22E+01	1
0.012	1000	584.9951258	0.01	9.56E+01	1
0.008	1500	1780.971792	0.002	3.34E+02	1
0.006	2000	3846.553298	0.003	8.34E+02	1
0.005	2500	6931.927263	0.007	1.70E+03	1

Appendix 2: Results of the two sided tests comparing gene lists ranked by score.

Settings

List comparison

Assessing similarity of : top and bottom ranks

Length of lists : 7263

Quantile of invariant genes : 0.5

Number of random samples : 1000

Affymetrix_In vivo, high dose_24h vs. Illumina_In vivo, high dose_24h

	Genes	Scores	p.values	Rev.Scores	Rev.p.values
0.115	100	49.55621	0	0.00E+00	0.997
0.077	150	111.19045	0	0.00E+00	1
0.058	200	197.40218	0	0.00E+00	1
0.038	300	450.91057	0	1.65E-04	1
0.029	400	823.02235	0	8.51E-03	1
0.023	500	1322.53258	0	5.84E-02	1
0.015	750	3165.93227	0	8.55E-01	1
0.012	1000	5908.00598	0	3.74E+00	1
0.008	1500	14271.93084	0	2.11E+01	1
0.006	2000	26729.61978	0	6.50E+01	1
0.005	2500	43541.83669	0	1.59E+02	1

Affymetrix_In vivo, high dose_6 h vs. Illumina_In vivo, high dose_6 h

	Genes	Scores	p.values	Rev.Scores	Rev.p.values
0.115	100	54.99712	0	0.00E+00	0.996
0.077	150	129.93003	0	0.00E+00	1
0.058	200	236.95433	0	0.00E+00	1
0.038	300	547.40588	0	3.00E-03	1
0.029	400	989.25309	0	4.92E-02	1
0.023	500	1566.37151	0	2.62E-01	1
0.015	750	3621.70696	0	2.78E+00	1
0.012	1000	6586.25333	0	1.03E+01	1
0.008	1500	15395.64479	0	4.79E+01	1
0.006	2000	28266.90455	0	1.29E+02	1
0.005	2500	45425.74841	0	2.82E+02	1

Affymetrix_In vivo, high dose_72 h vs. Illumina_In vivo, high dose_72 h

	Genes	Scores	p.values	Rev.Scores	Rev.p.values
0.115	100	29.60283	0	0.00E+00	0.997
0.077	150	66.67136	0	5.59E-03	1
0.058	200	116.08303	0	7.25E-02	1
0.038	300	251.04498	0	1.14E+00	1
0.029	400	436.85835	0	5.47E+00	1
0.023	500	677.59694	0	1.59E+01	1
0.015	750	1542.033	0	8.53E+01	1
0.012	1000	2816.62934	0	2.41E+02	1
0.008	1500	6748.06413	0	8.96E+02	1
0.006	2000	12749.18053	0	2.13E+03	1
0.005	2500	21071.31965	0	4.07E+03	1

Affymetrix_In vivo, low dose_24h vs. Illumina_In vivo, low dose_24h

	Genes	Scores	p.values	Rev.Scores	Rev.p.values
0.115	100	38.01436	0	0.00E+00	0.997
0.077	150	82.74386	0	0.00E+00	1
0.058	200	145.71855	0	1.52E-03	1
0.038	300	328.20886	0	6.04E-02	1
0.029	400	588.14631	0	4.20E-01	1
0.023	500	928.80845	0	1.48E+00	1
0.015	750	2162.53377	0	9.97E+00	1
0.012	1000	3998.17757	0	3.17E+01	1
0.008	1500	9708.97803	0	1.43E+02	1
0.006	2000	18443.33018	0	4.10E+02	1
0.005	2500	30493.33326	0	9.33E+02	1

Affymetrix_In vivo, low dose_6 h vs. Illumina_In vivo, low dose_6 h

	Genes	Scores	p.values	Rev.Scores	Rev.p.values
0.115	100	35.45322	0	0.00E+00	0.997
0.077	150	79.64536	0	0.00E+00	1
0.058	200	147.2389	0	0.00E+00	1
0.038	300	363.52957	0	2.47E-03	1
0.029	400	696.20846	0	4.67E-02	1
0.023	500	1150.19933	0	2.74E-01	1
0.015	750	2835.18092	0	3.57E+00	1
0.012	1000	5332.80084	0	1.56E+01	1
0.008	1500	12882.55084	0	9.08E+01	1
0.006	2000	24036.39917	0	2.73E+02	1
0.005	2500	39035.32004	0	6.14E+02	1

Affymetrix_In vivo, low dose_72 h vs. Illumina_In vivo, low dose_72 h

	Genes	Scores	p.values	Rev.Scores	Rev.p.values
0.115	100	2.976163	0.055	0.00E+00	0.998
0.077	150	13.061734	0.007	2.96E-03	1
0.058	200	32.230139	0.001	4.58E-02	1
0.038	300	99.511169	0	7.66E-01	1
0.029	400	205.774151	0	3.63E+00	1
0.023	500	351.213881	0	1.02E+01	1
0.015	750	891.186768	0	5.26E+01	1
0.012	1000	1705.079388	0	1.49E+02	1
0.008	1500	4329.08781	0	6.02E+02	1
0.006	2000	8608.793868	0	1.58E+03	1
0.005	2500	14905.12842	0	3.31E+03	1

Affymetrix_Tet_in vitro, 200µM_24h vs. Illumina_Tet_in vitro, 200µM_24h

	Genes	Scores	p.values	Rev.Scores	Rev.p.values
0.115	100	22.58013	0	0.00E+00	0.996
0.077	150	60.57986	0	0.00E+00	1
0.058	200	120.59625	0	0.00E+00	1
0.038	300	314.46124	0	0.00E+00	1
0.029	400	616.46887	0	5.43E-04	1
0.023	500	1034.53955	0	1.10E-02	1
0.015	750	2619.72023	0	3.59E-01	1
0.012	1000	5028.59504	0	2.33E+00	1
0.008	1500	12577.73879	0	1.99E+01	1
0.006	2000	24149.41609	0	7.53E+01	1
0.005	2500	40096.48161	0	2.03E+02	1

Affymetrix_Tet_in vitro, 200µM_6 h vs. Illumina_Tet_in vitro, 200µM_6 h

	Genes	Scores	p.values	Rev.Scores	Rev.p.values
0.115	100	14.55154	0	0.4838354	0.315
0.077	150	35.10029	0	2.4942963	0.306
0.058	200	66.10476	0	6.397284	0.308
0.038	300	160.92214	0	19.4572677	0.387
0.029	400	302.45276	0	38.4889048	0.579
0.023	500	495.35045	0	62.8119617	0.798
0.015	750	1237.08209	0	146.950646	0.996
0.012	1000	2412.99373	0	269.555034	1
0.008	1500	6337.90474	0	670.206743	1
0.006	2000	12724.42496	0	1363.97036	1
0.005	2500	21927.40605	0	2470.59178	1

Affymetrix_Tet_in vitro, 200µM_72 h vs. Illumina_Tet_in vitro, 200µM_72 h

	Genes	Scores	p.values	Rev.Scores	Rev.p.values
0.115	100	16.85476	0	0.00E+00	0.998
0.077	150	46.75645	0	0.00E+00	1
0.058	200	95.6189	0	0.00E+00	1
0.038	300	253.80153	0	1.70E-03	1
0.029	400	498.04828	0	2.77E-02	1
0.023	500	835.2868	0	1.45E-01	1
0.015	750	2126.6926	0	1.47E+00	1
0.012	1000	4127.58671	0	5.50E+00	1
0.008	1500	10549.77083	0	3.23E+01	1
0.006	2000	20588.51822	0	1.22E+02	1
0.005	2500	34607.73555	0	3.43E+02	1

Affymetrix_Tet_in vitro, 40µM_24h vs. Illumina_Tet_in vitro, 40µM_24h

	Genes	Scores	p.values	Rev.Scores	Rev.p.values
0.115	100	1.016569	0.219	0.103141	0.617
0.077	150	5.186208	0.149	0.6876056	0.698
0.058	200	13.919643	0.085	1.983603	0.781
0.038	300	49.101183	0.021	7.0161555	0.924
0.029	400	114.181156	0.002	15.9344595	0.976
0.023	500	216.395932	0	29.8661677	0.997
0.015	750	677.855438	0	95.230228	1
0.012	1000	1506.573843	0	218.768469	1
0.008	1500	4573.798813	0	699.055785	1
0.006	2000	9930.830092	0	1584.58575	1
0.005	2500	17961.08234	0	3004.01755	1

Affymetrix_Tet_in vitro, 40µM_6 h vs. Illumina_Tet_in vitro, 40µM_6 h

	Genes	Scores	p.values	Rev.Scores	Rev.p.values
0.115	100	0.2559717	0.461	1.523661	0.148
0.077	150	1.6982916	0.443	5.871424	0.117
0.058	200	5.2381833	0.423	13.314133	0.089
0.038	300	21.1078175	0.385	36.409515	0.082
0.029	400	51.7865426	0.361	69.01333	0.118
0.023	500	100.3429219	0.357	111.300757	0.229
0.015	750	322.5465651	0.389	272.773391	0.659
0.012	1000	738.0425118	0.437	546.638554	0.934
0.008	1500	2368.086474	0.591	1589.41331	1
0.006	2000	5336.811315	0.838	3531.41974	1
0.005	2500	9905.492391	0.978	6631.43868	1

Affymetrix_Tet_in vitro, 40µM_72 h vs. Illumina_Tet_in vitro, 40µM_72 h

	Genes	Scores	p.values	Rev.Scores	Rev.p.values
0.115	100	8.16E-01	0.246	0.1634394	0.523
0.077	150	5.11E+00	0.132	0.9225119	0.584
0.058	200	1.56E+01	0.048	2.4006937	0.683
0.038	300	6.13E+01	0.004	7.3470961	0.881
0.029	400	1.47E+02	0	15.1555819	0.977
0.023	500	2.77E+02	0	26.5637358	0.997
0.015	750	8.23E+02	0	76.8447866	1
0.012	1000	1.73E+03	0	172.214448	1
0.008	1500	4.78E+03	0	588.618738	1
0.006	2000	9.79E+03	0	1472.45966	1
0.005	2500	1.71E+04	0	3013.93168	1

Appendix 3: Number of genes deregulated between different typers of primary rat hepatocyte culture. Shown are the results of an ANOVA concerning the effect of culture condition and the effect of time. Light grey means up regulated genes and the darker grey means down regulated genes.

Culture condition	Nr. of genes deregulated between culture conditions	Nr. of genes deregulated over time of culture
Liver/FC	336	
Liver/FaO	693	
Liver Slices	2178	
FC Susp.	1405	
FC/ML + FCS	123	922
FC/ML - FCS	178	610
FC/SW + FCS	253	924
FC/SW - FCS	267	1124
FC/ML + FCS	1320	463
FC/ML - FCS	992	383
FC/SW + FCS	864	260
FC/SW - FCS	722	204
FC/ML + FCS	910	235
FC/ML - FCS	826	98
FC/SW + FCS	1199	105
FC/SW - FCS	919	168

Appendix 4: Number of genes deregulated between time points of rat hepatocyte cultures were calculated with T-test statistics ($<pV$ 0.01; >1.5 fold). Light grey means up regulated genes and the darker grey means down regulated genes.

Short term cultures	Nr. of genes deregulated	ML cultures	Nr. of genes deregulated	SW cultures	Nr. of genes deregulated
Liver/FC	742	FC/ML +FCS 1 d	2099	FC/SW +FCS 1 d	1650
	868		1681		1462
Liver/FaO	2828	ML +FCS 1 d/2 d	143	SW +FCS 1 d/2 d	191
	2023		137		78
Liver Slices	452	ML +FCS 1 d/4 d	346	SW +FCS 1 d/4 d	396
	622		264		260
Slices 0 h/2 h	248	ML +FCS 1 d/6 d	990	SW +FCS 1 d/6 d	512
	54		836		328
Slices 0 h/6 h	885	ML +FCS 1 d/10 d	1218	SW +FCS 1 d/10 d	590
	939		1026		448
Slices 0 h/1 d	887	FC/ML -FCS 1 d	1612	FC/SW -FCS 1 d	1920
	661		1413		1701
Slices 0 h/2 d	988	ML -FCS 1 d/2 d	157	SW -FCS 1 d/2 d	242
	794		212		175
FC/Susp. 2 h	613	ML -FCS 1 d/4 d	362	SW -FCS 1 d/4 d	389
	778		371		275
FC/Susp. 4h	738	ML -FCS 1 d/6 d	546	SW -FCS 1 d/6 d	532
	819		485		356
FC/Susp. 6 h	898	ML -FCS 1 d/10 d	590	SW -FCS 1 d/10 d	684
	1063		457		373
FC/Susp. 1 d	1064				
	1385				

Appendix 5: List of rat genes measured with TaqMan PCR for the verification of the microarray experiments

Gene Symbol	Gene name	Accession Nr.	Gene Symbol	Gene name	Accession Nr.
Acox1	acyl-Coenzyme A oxidase 1, palmitoyl	NM_017340	Hnf4a	hepatocyte nuclear factor 4, alpha	NM_022180
Actn1	actinin, alpha 1	NM_031005	Hspa1b	heat shock 70kDa protein 1A	NM_212504
Adk	adenosine kinase	NM_012895	Jund	jun D proto-oncogene	XM_579658
Afp	alpha-fetoprotein	NM_012493	Abcb1	ATP-binding cassette, subfamily B (MDR/TAP), member 1	NM_012623
Nr1i3	nuclear receptor subfamily 1, group I, member 3	NM_022941	Abcb4	ATP-binding cassette, subfamily B (MDR/TAP), member 4	NM_012690
Cdh1	cadherin 1, type 1, E-cadherin (epithelial)	NM_031334	Abcc2	ATP-binding cassette, subfamily C (CFTR/MRP), member 2	XM_577883
Cebpa	CCAAT/enhancer binding protein (C/EBP), alpha	NM_012524	Abcc3	ATP-binding cassette, subfamily C (CFTR/MRP), member 3	NM_080581
Cebpb	CCAAT/enhancer binding protein (C/EBP), beta	NM_024125	Myc	v-myc myelocytomatosis viral oncogene homolog (avian)	NM_012603
Cpt1a	carnitine palmitoyltransferase 1A (liver)	NM_031559	Oatp1	Slco1a1 solute carrier organic anion transporter family, member 1a1	XM_579394
Ccnd1	cyclin D1	NM_171992	Cdkn1a	cyclin-dependent kinase inhibitor 1A (p21, Cip1)	NM_080782
Ccng1	cyclin G1	NM_012923	Pck1	Phosphoenolpyruvate carboxykinase	NM_198780
Cyp1a2	cytochrome P450, family 1, subfamily A, polypeptide 2	NM_012541	Alpi	alkaline phosphatase, liver/bone/kidney	NM_022665
Cyp2c	cytochrome P450, family 2, subfamily C, polypeptide 8	NM_019184	Nr1i2	nuclear receptor subfamily 1, group I, member 2	NM_052980
Cyp3a3	cytochrome P450, family 3, subfamily A, polypeptide 4	NM_013105	Rgn	regucalcin (senescence marker protein-30)	NM_031546
Fabp2	fatty acid binding protein 1, liver	NM_013068	Sod2	superoxide dismutase 2, mitochondrial	NM_017051
Fbp1	fructose-1,6-bisphosphatase 1	NM_012558	Tgfa	transforming growth factor, alpha	NM_012671
Gadd45a	growth arrest and DNA-damage-inducible, alpha	NM_024127	Tgfb1	transforming growth factor, beta 1 (Camurati-Engelmann disease)	NM_021578
Gsn	gelsolin (amyloidosis, Finnish type)	NM_001004080	Timp1	TIMP metalloproteinase inhibitor 1	NM_053819
Gsta3	glutathione S-transferase A1	NM_031509	Tnf	tumor necrosis factor (TNF superfamily, member 2)	NM_012675
Gstp2	glutathione S-transferase pi	NM_138974	Txn2	thioredoxin	NM_053331
Hmox1	heme oxygenase (decycling) 1	NM_012580	Ugt1a1	UDP glucuronosyltransferase 1 family, polypeptide A6	NM_012683
Tcf1	transcription factor 1, hepatic; LF-B1, hepatic nuclear factor (HNF1), albumin proximal factor	NM_012669			

Appendix 6: List of rat genes measured with TaqMan PCR for the verification of the microarray experiments

Gene Symbol	Gene name	Accession Nr.	Gene Symbol	Gene name	Accession Nr.
ACTN1	actinin, alpha 1	NM_001102	TCF1	transcription factor 1, hepatic; LF-B1, hepatic nuclear factor (HNF1), albumin proximal factor	NM_000545
ADK	adenosine kinase	NM_001123	HNF4A	hepatocyte nuclear factor 4, alpha	NM_000457
AFP	alpha-fetoprotein	NM_001134	JUND	jun D proto-oncogene	NM_005354
ALPI	alkaline phosphatase, liver/bone/kidney	NM_000478	ABCB1	ATP-binding cassette, sub-family B (MDR/TAP), member 1	NM_000927
CEBPA	CCAAT/enhancer binding protein (C/EBP), alpha	NM_004364	ABCB4	ATP-binding cassette, sub-family B (MDR/TAP), member 4	NM_000443
CEBPB	CCAAT/enhancer binding protein (C/EBP), beta	NM_005194	ABCC2	ATP-binding cassette, sub-family C (CFTR/MRP), member 2	NM_000392
CPT1A	carnitine palmitoyltransferase 1A (liver)	NM_00103184 7	ABCC3	ATP-binding cassette, sub-family C (CFTR/MRP), member 3	NM_003786
CCND1	cyclin D1	NM_053056	MYC	v-myc myelocytomatosis viral oncogene homolog (avian)	NM_002467
CCNG1	cyclin G1	NM_004060	CDKN1A	cyclin-dependent kinase inhibitor 1A (p21, Cip1)	NM_000389
CYP1A2	cytochrome P450, family 1, subfamily A, polypeptide 2	NM_000761	RGN	regucalcin (senescence marker protein-30)	NM_004683
CDH1	cadherin 1, type 1, E-cadherin (epithelial)	NM_004360	SOD2	superoxide dismutase 2, mitochondrial	NM_000636
FABP2	fatty acid binding protein 1, liver	NM_001443	TGFA	transforming growth factor, alpha	NM_003236
GADD45A	growth arrest and DNA-damage-inducible, alpha	NM_001924	TGFB1	transforming growth factor, beta 1 (Camurati-Engelmann disease)	NM_000660
FBP1	fructose-1,6-bisphosphatase 1	NM_000507	TXN2	thioredoxin	NM_003329, BC054866
GSN	gelsolin (amyloidosis, Finnish type)	NM_000177	TIMP1	TIMP metalloproteinase inhibitor 1	NM_003254
GSTA3	glutathione S-transferase A1	NM_145740	TNF	tumor necrosis factor (TNF superfamily, member 2)	NM_000594
HMOX1	heme oxygenase (decycling) 1	NM_002133	UGT1A1	UDP glucuronosyltransferase 1 family, polypeptide A6	NM_001072

Appendix 7: Genes induced in expression after the perfusion of rat liver. Listed are only genes more than 2-fold deregulated and with a $pV < 0.01$.

Symbol	Accession	Fold change	Symbol	Accession	Fold change	Symbol	Accession	Fold change
Acy1	XM_579142.1	2.0	LOC246266	NM_144750.1	2.0	Pmvk	NM_001008352	2.0
Adamts7_pred	XM_236471.3	2.5	LOC287419	XM_213367.3	2.0	Ppp1r10	XM_579471.1	2.1
Ankrd9_pred.	XM_576103.1	2.1	LOC287452	XM_213357.3	2.1	Ppp4c	XM_341929.2	2.1
Anpep	NM_031012.1	2.4	LOC288659	XM_213769.3	2.2	Prodh2_pred.	XM_341825.2	2.5
Apba3	NM_031781.1	2.1	LOC290500	XM_214256.3	2.6	Ptges2_pred.	XM_231144.3	2.1
Atf3	NM_012912.1	5.5	LOC291905	XM_214652.3	2.0	Ptov1	NM_001008304	2.2
Bat3	NM_053609.1	2.3	LOC293689	XM_215181.3	2.1	Rab11b	NM_032617.2	2.2
Besh3	XM_346854.2	2.2	LOC296733	XM_216063.3	2.1	RGD1305860_pred	XM_343183.2	2.3
Bhlhb2	NM_053328.1	6.1	LOC297388	XM_216181.2	2.2	RGD1311324_pred	XM_343028.2	2.3
Btd_pred.	XM_577477.1	2.1	LOC300043	XM_216963.3	2.0	Rgs3	NM_019340.1	2.2
Btg2	NM_017259.1	12.0	LOC303677	XM_221119.3	2.0	Rhob	NM_022542.1	2.3
Cbara1	NM_199412.1	2.1	LOC310395	XM_227134.3	2.7	Ring1	NM_212549.1	2.0
Ccs	NM_053425.1	2.0	LOC310585	XM_227366.3	2.0	Rps6ka1	NM_031107.1	2.0
Cd14	NM_021744.1	2.1	LOC360919	XM_341193.2	2.2	Scarb1	NM_031541.1	2.2
Cdc20	NM_171993.1	2.0	LOC361184	XM_341467.2	2.1	Scrn2_pred.	XM_573186.1	2.2
c-fos	XM_234422.3	5.0	LOC361523	XM_341808.2	2.7	Sds	NM_053962.2	2.4
Creb3l3_pred.	XM_576179.1	2.2	LOC362196	XM_342497.2	4.6	Sfrs9	NM_001009255.1	2.0
Creld1_pred.	XM_232270.3	2.1	LOC362287	XM_342601.2	2.0	Slc13a3	NM_022866.1	2.1
Cry1	NM_198750.1	2.4	LOC362840	XM_343168.2	2.4	Slc16a11_pred.	XM_213334.3	2.7
Cxzc5	NM_001007628	2.1	LOC362899	XM_343227.2	2.5	Slc16a13	NM_001005530.1	2.1
Cyp2t1	NM_134369.1	2.2	LOC362983	XM_343313.2	2.0	Slc25a25	NM_145677.1	2.8
Cyr61	NM_031327.2	3.1	LOC497733	XM_579432.1	2.5	Slc27a1	NM_053580.2	2.2
Ddx56	NM_001004211	2.3	LOC497875	XM_573059.1	2.4	Slc29a1	NM_031684.2	2.1
Dgkz	NM_031143.1	2.1	LOC498703	XM_573985.1	2.3	Slc39a3	NM_001008356.1	2.1
Dhcr24_pred.	XM_216452.3	2.5	LOC499072	XM_574354.1	2.2	Slc6a12	NM_017335.1	2.3
Dom3z	NM_212497.1	2.1	LOC499823	XM_575162.1	40.7	Snf1lk	NM_021693.1	3.6
Dp111_pred.	XM_343163.2	2.4	LOC499837	XM_580023.1	2.1	Soat2	NM_153728.2	2.0
Dusp1	NM_053769.2	3.3	LOC500019	XM_575373.1	3.3	Socs2	NM_058208.1	2.7
Dusp5	NM_133578.1	2.1	LOC502714	XM_578213.1	2.7	Srebfl	XM_213329.3	2.2
Egr1	NM_012551.1	11.1	LOC503325	XM_578859.1	4.1	Srm	NM_053464.1	2.3
Egr2	NM_053633.1	2.1	Mafb	NM_019316.1	2.4	Srms_pred.	XM_575301.1	2.0
Fam20a_pred.	XM_573215.1	2.1	Man2c1	NM_139256.1	2.1	Stard4_pred.	XM_214592.3	2.2
Fgf21	NM_130752.1	3.7	Mbd6_pred.	XM_343219.2	2.0	Stub1_pred.	XM_213270.3	2.1
Gadd45a	NM_024127.1	2.3	Mclc	NM_133414.1	2.4	Tieg	NM_031135.1	2.1
Gadd45g_pred	XM_237999.3	9.0	Minpp1	XM_342044.2	2.0	Tmem7_pred.	XM_236656.3	3.1
Gdf15	NM_019216.1	14.4	Mtch1_pred.	XM_215358.3	2.3	Tomm40	NM_212520.1	2.0
Gfra3	XM_341593.2	2.0	Myc	NM_012603.2	3.2	Tst	NM_012808.1	2.4
Gpaa1	NM_001004240	2.4	Myd116	NM_133546.1	4.6	Ube2m_pred.	XM_341790.2	2.4
Grina	NM_153308.1	2.0	Napa	NM_080585.1	2.1	Wbscr16_pred.	XM_341066.2	2.0
Hes1	NM_024360.2	2.7	Nat8	NM_022635.1	2.9	Zfp36	NM_133290.2	4.0
Hspbp1	NM_139261.1	2.0	Ndufv3l	NM_022607.1	2.0			
Ier2	NM_001009541	4.8	Nfil3	NM_053727.2	2.2			
Igfals	NM_053329.1	3.2	Oki38	NM_138504.2	2.6			
Igfbp1	NM_013144.1	5.3	Per2	NM_031678.1	2.1			
Jun	NM_021835.2	5.2	Pex14	NM_172063.1	2.2			
Junb	NM_021836.2	10.2	Phgdh	NM_031620.1	2.0			

Appendix 8: Genes reduced in expression after the perfusion of rat liver. Listed are only genes more than 2-fold deregulated and with a $pV < 0.01$.

Symbol	Accession	Fold change	Symbol	Accession	Fold change	Symbol	Accession	Fold change
Sept7	NM_022616	-2.4	Cmkor1	NM_053352	-2.1	Fcna	NM_031348	-3.9
1200013a08rik	NM_001007002	-2.1	Col14a1_pred	XM_235308	-8.1	Fli1_pred	XM_235979	-2.1
Acadsb	NM_013084	-2.7	Col1a2	NM_053356	-13.8	Folr2_pred	XM_215013	-2.1
Acsl4	NM_053623	-2.3	Col3a1	NM_032085	-8.4	Frg1_pred	XM_341442	-2.0
Adamts1	NM_024400	-3.4	Col4a1_pred	XM_214400	-2.4	Fstl1	NM_024369	-5.3
Adamts9_pred	XM_232202	-2.1	Col5a1	NM_134452	-2.6	Gbp2	NM_133624	-3.6
Adcy4	NM_019285	-2.1	Col5a2	XM_343564	-4.2	Ghr	NM_017094	-3.7
Adn	XM_343169	-4.9	Col6a3_pred	XM_346073	-2.0	Gja1	NM_012567	-6.8
Adora2a	NM_053294	-2.5	Col8a1_pred	XM_221536	-2.7	Gja4	NM_021654	-3.1
Adora3	NM_012896	-2.2	Coro1a	NM_130411	-3.3	Glipr1_pred	XM_576223	-2.2
Ahr	XM_579375	-2.6	Ctbp2	NM_053335	-2.1	Gmfg	NM_181091	-2.4
Aif1	NM_017196	-6.0	Ctgf	NM_022266	-5.2	Gna12	NM_031034	-2.1
Akr1b4	NM_012498	-3.7	Ctse	NM_012938	-2.2	Gnai2	NM_031035	-2.0
Alp1	NM_199097	-2.5	Ctss	NM_017320	-8.5	Gng11	NM_022396	-4.0
Anxa1	NM_012904	-5.3	Cxcl9	NM_145672	-2.0	Gpr105	NM_133577	-4.2
Anxa2	NM_019905	-2.2	Cyba	NM_024160	-4.5	Gpx3	NM_022525	-2.4
Anxa3	NM_012823	-8.8	Cybb	NM_023965	-2.6	Gstp1	XM_579338	-2.8
Anxa5	NM_013132	-2.0	Cyp2a1	NM_012692	-2.2	Gstp2	NM_138974	-4.3
Aox2	XM_579191	-2.3	Cyp3a3	NM_013105	-4.7	Gucy1b3	NM_012769	-3.5
App	NM_019288	-2.7	Cyp4b1	NM_016999	-3.4	Gzma	NM_153468	-3.1
Arhgdib	NM_001009600	-5.2	Dab2	NM_024159	-4.4	Hba-a1	NM_013096	-120.3
Asah3l_pred	XM_233138	-2.2	Dcir3	XM_579150	-3.3	Hbb	NM_033234	-106.2
Atp6v1a1_pred	XM_340987	-2.4	Dcn	NM_024129	-7.8	Hla-dmb	NM_198740	-2.4
B4galt6	XM_579528	-2.0	Ddah2	XM_579741	-2.0	Hod	NM_133621	-2.3
Bak1	NM_053812	-2.7	Ddx3x	XM_228701	-2.1	Ibtk_pred	XM_236481	-2.6
Bcl2a1	NM_133416	-2.6	Dnase1l3	NM_053907	-3.8	Icam2	NM_001007725	-2.7
Bcl6_pred	XM_221333	-3.4	Ecm1	NM_053882	-5.9	Ifi44_pred	XM_227821	-2.2
Bgn	NM_017087	-2.0	Ednrb	NM_017333	-4.5	Ifitm1_pred	XM_215117	-3.5
Bucs1_pred	XM_341917	-3.2	Ehd3	NM_138890	-2.1	Igfbp3	NM_012588	-8.6
C1qa	NM_001008515	-4.7	Eif1a_pred	NM_001008773	-2.9	Igfbp7_pred	XM_214014	-8.8
C1qb	NM_019262	-3.5	Eif3s6_pred	XM_576262	-2.0	Igj_pred	XM_341195	-3.6
C1qg	NM_001008524	-3.0	Eif4g2_pred	XM_341907	-3.7	Ik	NM_001005537	-2.0
C1qr1	NM_053383	-5.2	Eltf1	NM_022294	-2.5	Il1a	NM_017019	-2.6
Casp1	NM_012762	-4.4	Emcn	NM_001004228	-3.9	Il1b	NM_031512	-2.0
Ccl19_pred	XM_342824	-2.4	Emilin1_pred	XM_238447	-2.3	Itgb2_pred	XM_228072	-2.2
Ccl5	NM_031116	-5.5	Emp1	NM_012843	-2.3	Krt1-19	NM_199498	-2.4
Ccl6	NM_001004202	-4.4	Emp3	NM_030847	-2.4	Lamb1-1_pred	XM_216679	-3.4
Ccr5	NM_053960	-2.7	Emr1	XM_579174	-4.4	Laptm5	NM_053538	-2.5
Cd163_pred	XM_232342	-3.3	Esam	NM_001004245	-2.2	Lcp1_pred	XM_573816	-4.0
Cd36	NM_031561	-2.7	Ets1	NM_012555	-2.7	Ldb2_pred	XM_214054	-2.4
Cd48	NM_139103	-4.6	Evl	XM_579484	-2.3	Lgals1	NM_019904	-2.0
Cd53	NM_012523	-4.3	F2r	NM_012950	-3.2	Lgals3	NM_031832	-4.0
Cd68_pred	XM_213372	-3.1	F9	XM_346365	-6.4	Lgmn	NM_022226	-2.3
Cd74	NM_013069	-2.6	Fbln5	NM_019153	-3.1	LOC259245	NM_147213	-2.7
Cd83_pred	XM_341509	-3.4	Fcgr1_pred	XM_215643	-3.0	LOC287029	XM_212651	-2.0
Ceacam10	NM_173339	-2.2	Fcgr2b	NM_175756	-4.6	LOC287167	XM_213262	-4.0
Cklfs6_pred	XM_579183	-2.2	Fcgr3a	NM_207603	-2.3	LOC287899	XM_213548	-3.9

APPENDIX

LOC289384	XM_223076	-2.0	LOC362803	XM_343130	-2.0	LOC499615	XM_574941	-3.2
LOC289930	XM_223826	-2.0	LOC362934	XM_576293	-2.5	LOC499625	XM_574949	-2.2
LOC291936	XM_238042	-2.8	LOC363434	XM_343756	-2.1	LOC499638	XM_574960	-4.2
LOC293860	XM_238167	-4.1	LOC363767	XM_344015	-2.3	LOC499775	XM_580014	-2.0
LOC294337	XM_215375	-3.7	LOC365699	XM_345167	-2.5	LOC499984	XM_575338	-3.1
LOC294410	XM_228157	-2.1	LOC365814	XM_578024	-2.1	LOC499985	XM_575339	-2.9
LOC294744	XM_215486	-3.4	LOC366411	XM_575861	-2.2	LOC500015	XM_575369	-2.5
LOC294762	XM_215491	-2.1	LOC366588	XM_345652	-3.3	LOC500285	XM_575635	-2.9
LOC294942	XM_215541	-2.2	LOC367391	XM_346122	-2.2	LOC500336	XM_575687	-2.1
LOC295382	XM_227605	-2.0	LOC367846	XM_575151	-2.0	LOC500344	XM_575696	-2.4
LOC295660	XM_212955	-2.7	LOC497720	XM_579423	-2.1	LOC500373	XM_231625	-2.1
LOC295975	XM_215794	-2.2	LOC497757	XM_579393	-5.1	LOC500389	XM_575748	-2.2
LOC297504	XM_238366	-2.7	LOC497758	XM_579454	-4.8	LOC500398	XM_575757	-3.3
LOC300783	XM_217180	-2.3	LOC497767	XM_579388	-3.4	LOC500469	XM_575833	-2.4
LOC301276	XM_236965	-2.6	LOC497846	XM_579586	-3.3	LOC500488	XM_580072	-2.7
LOC302363	XM_217566	-3.4	LOC497936	XM_573123	-2.3	LOC500490	XM_575855	-2.0
LOC302671	XM_217618	-2.6	LOC497942	XM_573130	-2.1	LOC500495	XM_575859	-2.7
LOC303666	XM_221094	-2.4	LOC497987	XM_573183	-2.2	LOC500507	XM_575869	-2.5
LOC304138	XM_221702	-2.4	LOC498032	XM_573233	-2.5	LOC500586	XM_575955	-3.5
LOC306805	XM_225198	-2.0	LOC498076	XM_573278	-2.5	LOC500643	XM_576018	-2.4
LOC307907	XM_226529	-2.4	LOC498105	XM_573309	-4.2	LOC500695	XM_576077	-2.2
LOC308350	XM_218261	-4.4	LOC498162	XM_573377	-2.3	LOC500788	XM_576174	-2.3
LOC308654	XM_218706	-2.1	LOC498241	XM_573464	-2.6	LOC500829	XM_576219	-3.2
LOC310760	XM_227556	-2.8	LOC498245	XM_573468	-3.6	LOC500916	XM_576325	-2.4
LOC310926	XM_227769	-20.6	LOC498276	XM_573502	-3.7	LOC500941	XM_576351	-2.2
LOC312102	XM_231461	-5.9	LOC498277	XM_573503	-2.7	LOC500949	XM_576360	-2.2
LOC312924	XM_232634	-2.9	LOC498279	XM_573505	-4.6	LOC500988	XM_576400	-2.3
LOC313304	XM_233108	-2.3	LOC498371	XM_573606	-3.2	LOC501091	XM_576506	-2.1
LOC313308	XM_233081	-3.1	LOC498375	XM_573610	-3.2	LOC501187	XM_576615	-2.2
LOC313391	XM_233220	-2.0	LOC498378	XM_573613	-2.8	LOC501224	XM_576647	-2.2
LOC313445	XM_233297	-3.2	LOC498452	XM_573711	-2.1	LOC501245	XM_576664	-2.4
LOC313974	XM_233982	-2.1	LOC498557	XM_573833	-3.1	LOC501393	XM_576805	-2.4
LOC314075	XM_234092	-2.2	LOC498644	XM_573926	-3.1	LOC501396	XM_576808	-2.8
LOC315352	XM_235755	-2.2	LOC498669	XM_573952	-2.8	LOC501553	XM_576955	-2.7
LOC316186	XM_236876	-2.7	LOC498690	XM_573975	-4.3	LOC501562	XM_576967	-2.3
LOC316406	XM_237162	-2.5	LOC498799	XM_574084	-2.8	LOC501610	XM_577009	-2.5
LOC316481	XM_237252	-2.9	LOC498829	XM_574110	-2.4	LOC501619	XM_577018	-2.0
LOC317218	XM_228493	-2.8	LOC498973	XM_574260	-2.4	LOC502490	XM_577971	-3.9
LOC317312	XM_228667	-2.0	LOC498989	XM_574280	-2.8	LOC502953	XM_578458	-2.7
LOC317599	XM_229173	-2.3	LOC499300	XM_574598	-2.8	LOC502954	XM_578459	-2.0
LOC360602	XM_340880	-2.1	LOC499321	XM_574626	-2.9	LOC503409	XM_578948	-38.8
LOC360627	XM_340901	-2.1	LOC499481	XM_574804	-2.6	Loxl2_pred	XM_214225	-2.3
LOC360690	XM_340961	-2.6	LOC499526	XM_579974	-2.5	Lpl	NM_012598	-8.6
LOC361117	XM_341405	-4.0	LOC499531	XM_574855	-2.6	Lrrn3	NM_030856	-2.0
LOC361260	XM_341544	-2.5	LOC499554	XM_574879	-2.3	Ltbp1	NM_021587	-4.5
LOC361283	XM_341568	-2.3	LOC499560	XM_574884	-2.8	Lum	NM_031050	-2.0
LOC361885	XM_342182	-2.6	LOC499564	XM_574888	-2.6	Ly86_pred	XM_225636	-2.5
Mapre1	NM_138509	-2.5	Prss23	NM_001007691	-5.7	Tagln	XM_579512	-2.3
MGC105601	NM_001009620	-2.7	Psm1	NM_017278	-2.1	Tagln2_pred	XM_222906	-3.8
MGC72614	NM_199105	-2.6	Ptgs2	NM_031644	-2.8	Tax1bp1	NM_001004199	-2.1
MGC72973	NM_198776	-28.1	Pthr1	NM_020073	-3.9	Tcf21	XM_341737	-4.9

MGC94010	NM_001007732	-4.5	Ptprb_pred	XM_235156	-5.7	Tcf4	NM_053369	-2.2
MGC94782	NM_001004282	-2.2	Ptprc	NM_138507	-2.1	Tde2	NM_182951	-2.5
MGC95001	NM_001007619	-3.2	Ptpro	NM_017336	-2.8	Tek	XM_342863	-2.2
Mgp	NM_012862	-12.6	Ramp2	NM_031646	-2.4	Timp1	NM_053819	-3.0
Mpeg1	NM_022617	-2.6	Rasa1	NM_013135	-2.1	Tnfrsf11b	NM_012870	-4.7
Mrc1_pred	XM_225585	-4.4	Rasip1_pred	XM_214916	-2.4	Tpbp	NM_031807	-2.2
Ms4a11_pred	XM_342028	-4.4	Rbbp7	NM_031816	-2.3	Tpm4	NM_012678	-3.9
Ms4a6b	NM_001006975	-3.3	Rcn_pred	XM_342481	-4.1	Tspan3	NM_001005547	-2.3
Mthfs	NM_001009349	-2.4	Rcn2	NM_017132	-2.4	Ttpa	NM_013048	-2.1
Mx1	NM_173096	-2.5	Rcn3_pred	NM_001008694	-2.5	Tuba1	NM_022298	-5.6
Napsa	NM_031670	-2.7	Reck_pred	XM_233371	-3.7	Txndc1_pred	XM_343076	-2.0
Nfib	XM_342854	-2.6	Reln	NM_080394	-9.2	Txnip	NM_001008767	-2.5
Nid2_pred	XM_573694	-2.2	RGD1308143_pred	XM_237468	-2.1	Tyropb	NM_212525	-2.8
Nkg7	NM_133540	-3.0	RGD1308373_pred	XM_344268	-2.6	Ube1c	NM_057205	-2.1
Nol5	NM_021754	-2.0	RGD1310191_pred	XM_341102	-2.4	Ucp2	NM_019354	-4.2
Npy	NM_012614	-2.6	Rgs10	XM_341936	-2.5	Ugcg	XM_579533	-2.3
Nritp	XM_341519	-2.2	Rgs18_pred	XM_222692	-2.4	Vcam1	NM_012889	-3.4
Nrp1	NM_145098	-3.9	Rgs2	NM_053453	-2.7	Vim	NM_031140	-13.6
Oasl2_pred	XM_579310	-2.0	Rock1	NM_031098	-2.4	Vwf	XM_342759	-2.3
Ogn_pred	XM_214441	-6.1	RT1-Ba	XM_579226	-2.9	Waspip	NM_057192	-3.9
Oit3	NM_001001507	-4.6	RT1-Da	XM_579241	-8.3	Wfdc1	NM_133581	-3.1
Pam	NM_013000	-4.6	RT1-Db1	XM_579272	-2.7	Xlkd1_pred	XM_219001	-4.5
Pde2a	NM_031079	-2.1	S100a11	XM_215598	-5.8	Zfp354a	NM_052798	-3.3
Pdia3	NM_017319	-2.9	S100a6	NM_053485	-4.4			
Pf4	NM_001007729	-3.2	Sart2_pred	XM_345110	-3.1			
Pfc	XM_216784	-2.7	Scd2	NM_031841	-3.1			
Pigr	NM_012723	-3.4	Sdcbp	NM_031986	-2.1			
Pla2g2a	NM_031598	-2.3	Sdccag1_pred	XM_216724	-2.3			
Pla2g4a	NM_133551	-2.6	Sema6a_pred	XM_341612	-2.3			
Plac8_pred	XM_341188	-4.9	Serpinb6	NM_199085	-4.0			
Plat	NM_013151	-2.5	Serpine2	XM_343604	-2.1			
Plek_pred	XM_344267	-3.3	Slc25a4	NM_053515	-3.7			
Plscr1	NM_057194	-2.2	Slc28a2	NM_031664	-3.4			
Pltp_pred	XM_215939	-2.3	Slfn3	NM_053687	-5.1			
Plvap	NM_020086	-3.6	Slpi	NM_053372	-6.3			
Plxdc2_pred	XM_341567	-2.2	Smoc2_pred	XM_214777	-4.9			
Plxnd1_pred	XM_232283	-2.5	Snx5_pred	XM_215872	-2.1			
Pmp22	NM_017037	-2.4	Sod3	NM_012880	-7.3			
Pnutl2_pred	XM_573172	-3.0	Sparc	NM_012656	-6.6			
Ppt	NM_022502	-2.1	Sparcl1	NM_012946	-4.8			
Prkcb1	NM_012713	-3.3	Ssg1	XM_573284	-5.9			
Prkch	NM_031085	-2.2	Sv2b	NM_057207	-3.6			
Pmp	XM_579340	-3.8	Tacc1a	NM_001004107	-2.9			

Gene Symbol	Accession Nr.	Susp 1 d	Slices 1 d	M+ 1 d	M+ 6 d	M+ 10 d	M- 1 d	M- 6 d	M- 10 d	S+ 1 d	S+ 6 d	S+ 10 d	S- 1 d	S- 6 d	S- 10 d	FaO
Acox1	NM 017340	-15.8	2.8	-2.2	-2.1	-2.6								2.6	2.2	
Actn1	NM 031005	-3.7	8.7	6.8	195.4	140.3	3.8	89.9	79.4	2.1	37.4	35.6	2.3	21.1	15.7	6.4
Adk	NM 012895	-3.2		-2.2		-2.0	2.3			-2.1			2.3			-2.2
Afp	NM 012493		3.0				3.6			-2.8	-2.3		5.2		5.5	23.7
Nr1i3	NM 022941	-5.9		-4.1				-2.6		-5.5	-11.4	-5.1	-4.0	2.5	3.6	-18.7
Cdh1	NM 031334	-6.4	2.0	5.5	5.8	5.1		7.0	6.9	4.0	3.4	3.9		4.6	6.0	
Cebpa	NM 012524	-3.3		-2.5		-3.3		-2.1					-2.3			-2.0
Cebpb	NM 024125	2.7	6.2				2.5		2.0				2.2	2.4	2.5	2.4
Cpt1a	NM 031559	-19.7	2.9	-5.1		2.9			2.3	-6.1		2.4	-5.6		2.0	2.1
Ccnd1	NM 171992				12.6	20.7	-7.8		2.2		5.6	8.2	-13.4	-2.3	-3.4	6.4
Ccnq1	NM 012923		6.4	14.0	25.5	23.1	16.0	30.1	22.2	9.3	7.4	9.1	13.1	7.4	4.8	3.7
Cyp1a2	NM 012541	-4.7	3.5	-2.7	-72.5	-51.5		-153.7	-57.0	-4.9	-107.2	-95.7	-2.2	-154.6	-101.0	-194.5
Cyp2c	NM 019184	-27.7	-4.7	-5.5	-869.8	-347.5	-5.1	-6.7	-13.6	-7.1	-126.0	-352.6	-5.3	-5.1	-4.4	68.3
Cyp3a3	NM 013105	-8.4			-883.7	-2208.5				-2.3	-96.2	-498.6		8.5	7.1	-3539.8
Fabp2	NM 013068		4.9	2.6		-2.3	-4.1	2.7	3.3		4.3	7.2	-4.7	3.3	2.1	-4.9
Fbp1	NM 012558	-43.8			-18.1	-28.7	-3.4	-3.5	-3.6		-2.3	-2.5	-4.1			-16.2
Gadd45a	NM 024127	4.5	14.8	45.5	67.8	38.8	28.7	35.8	23.2	33.2	25.1	19.7	32.3	15.5	9.6	2.8
Gsn	NM 001004080		2.0	-6.7	8.1	18.5	-13.2		2.5	-6.7		5.1	-19.5		-2.7	-67.2
Gsta3	NM 031509	-11.3														
Gstp2	NM 138974	13.9	13.6	16.1	53.4	37.8	2.9	15.5	28.8	10.7	54.6	54.1		10.4	10.0	58.7
Hmox1	NM 012580	12.2	84.6	49.5	38.0	37.3	30.3	10.4	8.1	58.0	16.3	31.2	47.3	3.8		38.8
Tcf1	NM 012669		3.9		2.2		2.6	2.2								5.2
Hnf4a	NM 022180	-43.2	4.6				2.2									
Hspa1b mapped	NM 212504	472.9	43.8	10.6	16.9	13.5	8.2	7.7	9.5	17.2	3.6	3.6	7.6	5.5	4.4	72.4
Jund	XM 579658	4.4	6.5	7.9	13.0	11.3	6.6	10.6	9.7	4.7	6.2	5.2	6.8	6.5	6.2	17.3
Abcb1	NM 012623	51.1	1187.0	343.0	1295.3	490.8	143.2	1523.4	951.8	184.4	788.8	822.4	101.2	570.6	246.1	58.9
Abcb4	NM 012690				-2.0	-2.2	-2.2				-3.1		-2.2	2.4	2.2	-2.2
Abcc2	XM 577883	-5.3						3.1	3.0							
Abcc3	NM 080581		25.1	12.6	24.2	16.6	4.1	31.1	34.3	11.0	20.0	21.5	2.3	31.5	37.9	21.6
Myc	NM 012603	13.5	78.3	76.6	117.7	36.0	47.9	50.9	37.5	42.8	39.5	27.4	52.8	33.1	28.2	49.9
OATP1	XM 579394	-32.1	-2.7	-8.1	-70.9	-68.4	-5.0	-4.0	-7.0	-11.4	-4.2	-4.9	-5.0	-2.4	-3.4	-9041.6
Cdkn1a	NM 080782	2.1	6.0	8.2	26.0	18.5	14.5	17.1	14.9	4.4	5.7	5.3	11.3	9.2	7.1	4.4
Pck1	NM 198780	-120.2	-8.8	-244.8	-119.7	-300.0	-165.7	-77.5	-31.4	-101.1	-177.3	-104.9	-79.7	-120.4	-95.4	-4.7
Alpi	NM 022665		27.6	26.2	8.1	5.1	25.2	15.9	16.6	37.4	15.3	17.3	28.6	20.0	23.0	4.1
Nr1i2	NM 052980	-11.4		-2.3		-2.3	2.6			-2.1				2.7		-4.3
Rgn	NM 031546	-185.6	-16.6	-14.7	-37.6	-62.8	-18.2	-42.5	-57.4	-19.5	-59.5	-60.8	-14.1	-90.4	-129.4	-11.1
Sod2	NM 017051	-10.9	11.3	14.1	5.3	2.2	14.0	3.9		14.5	4.6	3.3	8.9	4.0		-3.5
Tafa	NM 012671		4.1	5.6	9.6	6.5	4.1	5.9	4.8	2.6	3.0	3.2	2.8	7.2	4.8	7.1
Tgfb1	NM 021578	-14.4	3.5	-5.0	7.7	10.6	-6.0			-5.2		3.8	-9.1	-6.1	-3.3	
Timp1	NM 053819	3.3	16.3	8.9	68.0	60.5	4.0	9.7	12.0		17.1	28.8		3.2	3.1	-3.7
Tnf	NM 012675		387.4	114.7	338.0	507.1	16.3		23.3	368.1	170.4	312.1	6.3			30.8
Txn2	NM 053331	-18.1	2.1											2.3		2.0
Ugt1a1	NM 012683	-3.6	5.7	3.5			6.5	6.7	5.1				5.1	14.9	12.2	2.1

Appendix 9: Summary of gene expression changes in primary rat hepatocytes culture measured with TaqMan PCR. Only genes 2-fold deregulated are shown.

Gene Symbol	Accession Nr.	Susp 1 d	Slices 1 d	M+ 1 d	M+ 6 d	M+ 10 d	M- 1 d	M- 6 d	M- 10 d	S+ 1 d	S+ 6 d	S+ 10 d	S- 1 d	S- 6 d	S- 10 d	FaO
Acox1	NM 017340			-2.7	-4.6	-4.1				-2.5			-3.3			-3.2
Actn1	NM 031005			2.2	4.9	5.1		4.0	4.3		2.8	2.1				
Adk	NM 012895			-3.2	-3.0	-4.0				-3.4	-2.0	-2.3				
Afp	NM 012493		-2.6	-2.7	-4.7	-5.9	-2.0		-2.1	-2.4	-2.4	-2.7	-2.4			
Nr1i3	NM 022941		-5.2	-5.7	-13.1	-13.1	-2.5	-6.6	-4.8	-4.7	-8.2	-8.0	-4.6			-9.0
Cdh1	NM 031334	-5.6														-7.3
Cebpa	NM 012524				-6.1	-6.0										-5.2
Cebpb	NM 024125						2.1						2.2			
Cpt1a	NM 031559	-2.0	-4.0	-8.2	-2.2		-3.0	-2.2		-5.5			-5.8			-2.2
Ccnd1	NM 171992	-3.0			2.6	5.4	-8.8	-2.3				2.6	-10.3	-4.8	-4.1	2.1
Ccng1	NM 012923	2.5	4.4	7.1	8.5	10.9	7.8	9.8	9.9	5.5	5.1	5.6	11.0	6.1	4.9	2.3
Cyp1a2	NM 012541			-5.4	-138.7	-100.4	-3.5	-103.5	-70.8	-8.4	-92.6	-83.9	-4.3	-64.7	-69.2	-53.9
Cyp2c	NM 019184	-4.7	-3.7	-2.6	-276.3	-188.6	-2.5	-4.7	-7.0	-2.8	-36.8	-119.5	-2.4	-3.0	-2.4	-448.8
Cyp3a3	NM 013105	-3.7	-5.4	-2.4	-278.7	-233.4				-2.4	-47.1	-78.9				-254.1
Fabp2	NM 013068				-4.0	-4.1	-3.7				2.2	2.5	-4.0			-4.1
Fbp1	NM 012558	-2.7	-5.1	-3.5	-54.1	-61.8	-6.0	-8.1	-7.4	-2.4	-3.5	-4.0	-6.2	-3.2	-2.5	-17.2
Gadd45a	NM 024127	6.2	6.5	13.8	11.4	10.4	9.8	8.3	6.9	14.5	9.7	6.6	12.1	5.3	3.8	2.5
Gsn	NM 001004080					3.0										
Gsta3	NM 031509															
Gstp2	NM 138974	4.2		17.6	29.7	34.8	4.1	15.3	21.4	18.3	38.0	40.5	2.4	10.9	10.8	22.0
Hmox1	NM 012580	8.4	4.8	11.3	4.3	7.0	7.3			22.9	4.1	7.9	17.0			3.7
Tcf1	NM 012669				-2.1	-3.1							-2.0			
Hnf4a	NM 022180				-4.3	-3.8					-2.4	-2.2				
Hspa1b mapped	NM 212504															
Jund	XM 579658			2.5	2.4	2.2	2.5	2.3	2.4	2.2	2.2	2.1	2.3	2.3	2.4	2.1
Abcb1	NM 012623	73.7	25.9	49.9	98.0	61.7	17.6	97.4	95.1	29.2	91.4	81.5	8.4	54.0	38.5	12.2
Abcb4	NM 012690		-2.5		-4.8	-4.2					-4.5	-3.9	-2.2			-2.5
Abcc2	XM 577883				-2.2	-2.4				-2.2		-2.1	-2.1		-2.1	
Abcc3	NM 080581	3.6		3.2	3.6	2.7		5.5	6.2	4.0	4.7	4.4		6.4	7.8	6.6
Myc	NM 012603	6.3	7.7	12.9	11.8	6.0	9.8	7.0	6.8	10.6	8.6	5.7	12.2	6.1	7.4	4.9
OATP1	XM 579394															
Cdkn1a	NM 080782				2.1	2.5	3.9	2.8	2.7				5.1	2.4	2.3	
Pck1	NM 198780	-9.2	-31.9	-82.1	-126.8	-180.5	-65.4	-60.0	-25.0	-52.6	-120.7	-91.8	-41.5	-51.3	-59.8	-3.8
Alpi	NM 022665															
Nr1i2	NM 052980	-2.3	-3.8	-4.0	-5.7	-5.7				-2.9	-2.7	-2.7				-10.5
Rgn	NM 031546	-41.4	-53.9	-16.8	-69.3	-71.7	-19.2	-62.6	-69.6	-21.1	-48.3	-53.8	-11.1	-71.8	-69.9	-12.8
Sod2	NM 017051	3.4		4.0			3.3			7.2			4.0			
Tafa	NM 012671														2.1	2.1
Tgfb1	NM 021578	2.4			3.4	4.6										
Timp1	NM 053819	7.5		2.3	11.2	13.4			2.6		4.9	7.3	-2.4	-2.4		
Tnf	NM 012675															
Txn2	NM 053331			-2.2	-2.7	-2.6		-2.0	-2.2							
Ugt1a1	NM 012683													8.5		

Appendix 10: Summary of gene expression changes in primary rat hepatocytes culture measured with Illumina BeadChips. Only genes 2-fold deregulated and with a pValue lower than 0.05 are shown.

Gene Symbol	Accession Nr.	HepaRG_DMSO 1 d	HepaRG_DMSO 2 d	HepaRG_DMSO 9 d	HepaRG_basal 1 d	HepaRG_basal 2 d	HepaRG_basal 9 d	Susp_24h	M_-2 d	M_-7 d	M_-11 d	S_-2 d	S_-7 d	S_-11 d
ACTN1	NM_001102				3.3	3.2			2.4	3.0	3.3		2.1	2.8
ADK	NM_001123							-4.6	-2.7	-2.4	-3.0	-6.5	-3.8	-4.6
AFP	NM_001134	-2.0		-3.6				-10.2		-21.1	-15.5	-67.2		
ALPI	NM_000478	-5.4	-7.2					-6.1	-3.8	-10.2	-6.7	-2.8	-5.3	-5.1
CEBPA	NM_004364								-4.1			2.3		3.6
CEBPB	NM_005194										2.1			
CPT1A	NM_0010318						-2.0	-7.5	-7.7	-3.1		-13.8	-5.2	-3.2
CCND1	NM_053056	-2.9	-2.4	-3.6				-5.0	-5.2	-2.4	-2.5	-8.8	-5.3	-4.5
CCNG1	NM_004060					2.1	2.1					-3.7	-2.9	-3.3
CYP1A2	NM_000761	-280.5	-357.8	-151.0	-588.5	-1009.6		-11.4	-17.7	-2.0		-14.0		
CDH1	NM_004360	-4.2	-3.3	-4.5				-9.9	-3.6	-3.4	-4.7	-5.6	-3.8	-3.4
FABP2	NM_001443	-7.5	-5.1	-22.2	-3.6	-3.9	-4.5	-10.8	-134.2	-15.9	-15.4	-83.7	-9.1	-7.9
GADD45A	NM_001924	11.2	14.7	10.2	12.0	11.5	8.5	-2.7		4.3	3.5		6.3	6.4
FBP1	NM_000507		-2722.9	-3427.4		-1613.6		-11.4	-16.3	-9.0	-8.5	-11.6	-3.8	-4.4
GSN	NM_000177	5.7	3.9	5.8	13.6	11.7	6.9		2.9	5.0	4.3	2.8	5.1	8.1
GSTA3	NM_145740							-9.4	-11.3	-12.1	-9.1	-15.0	-11.6	-9.0
HMOX1	NM_002133					-2.1		3.9		3.5	2.9	2.2	2.3	2.1
TCF1	NM_000545													
HNF4A	NM_000457							-2.0						
JUND	NM_005354												2.1	2.1
ABCB1	NM_000927											-5.5	-2.2	
ABCB4	NM_000443	-3.0	-3.1	-3.8	-3.6		-3.0	-13.4	-20.4	-35.5	-42.1	-37.7	-63.7	-55.2
ABCC2	NM_000392						-2.1	-2.3				-4.2	-2.1	
ABCC3	NM_003786	2.8	3.0	2.9	5.3	4.9	2.8	-3.8				-2.2		
MYC	NM_002467				2.1				3.7	3.1	4.4	3.0		2.2
CDKN1A	NM_000389	2.6	2.3	2.4	3.7	1.9			3.0	7.2	11.8		5.9	12.7
RGN	NM_004683	-6.7	-5.2	-8.1	-4.7	-6.7	-7.4	-13.0	-21.0	-14.4	-16.5	-21.1	-10.7	-12.5
SOD2	NM_000636	2.3		2.1	4.4	5.4	2.2	9.7	14.1	4.8	3.5	8.9	2.6	2.4
TGFA	NM_003236	3.6	3.8	3.7	5.4	6.4					2.5			2.6
TGFB1	NM_000660	3.7	3.3	3.9	6.5	7.0	5.6		-2.6	-2.3		-2.2	-2.2	
TXN2	NM_003329	2.7	2.2	2.7	8.1	4.5	4.7		3.4	3.2	3.2	2.8	3.1	3.6
TIMP1	NM_003254	6.3	5.5	5.5	8.8	7.5	5.0		-2.1			-2.2		
TNF	NM_000594								-3.2		-3.9	-2.2		
UGT1A1	NM_001072		2.2					-4.2	-3.8			-6.4		

Appendix 11: Summary of gene expression changes in primary human hepatocytes culture measured with TaqMan PCR. Only genes 2-fold deregulated are shown.

Gene Symbol	Accession Nr.	HepaRG_DMSO 1 d	HepaRG_DMSO 2 d	HepaRG_DMSO 9 d	HepaRG_basal 1 d	HepaRG_basal 2 d	HepaRG_basal 9 d	Susp_24h	M_-2 d	M_-7 d	M_-11 d	S_-2 d	S_-7 d	S_-11 d
ACTN1	NM_001102													
ADK	NM_001123													
AFP	NM_001134	-4.8	-4.9	-4.6	-3.4	-4.8	-2.6	-4.5	-6.5			-5.7		
ALPI	NM_000478													
CEBPA	NM_004364	-3.0	-2.1	-2.9	-3.6		-2.3		-3.4					
CEBPB	NM_005194													
CPT1A	NM_0010318													
CCND1	NM_053056	-3.6	-2.6	-3.3				-3.4	-4.5	-3.4	-4.6	-5.3	-6.4	-5.6
CCNG1	NM_004060											-2.8	-2.3	
CYP1A2	NM_000761	-47.5	-37.0	-39.5	-49.3	-62.8	-54.5	-8.0	-13.1	-2.4	-3.0	-7.0		-3.2
CDH1	NM_004360													
FABP2	NM_001443													
GADD45A	NM_001924								2.3					
FBP1	NM_000507	-273.0	-220.1	-234.5	-250.3	-275.3	-268.2	-5.5	-14.3	-11.1	-13.3	-7.1	-6.1	-7.6
GSN	NM_000177	7.6	6.4	8.4	11.0	10.3	7.2	2.2	4.4	5.4	4.5	4.9	6.5	3.4
GSTA3	NM_145740													
HMOX1	NM_002133	-3.3	-3.3	-2.4	-4.0	-4.9	-5.5	2.6						
TCF1	NM_000545													
HNF4A	NM_000457													
JUND	NM_005354	-2.0			-2.6		-2.4							
ABCB1	NM_000927													
ABCB4	NM_000443	-2.8	-2.8	-3.1	-4.4	-2.2	-3.5	-5.9	-7.1	-7.0	-10.5	-8.3	-8.6	-8.1
ABCC2	NM_000392					-2.2								
ABCC3	NM_003786													
MYC	NM_002467							2.2	2.2			2.5		
CDKN1A	NM_000389	2.6	2.6	3.1	2.6	2.5	2.6	2.6	3.9	4.4	5.2	3.2	3.7	4.3
RGN	NM_004683	-4.3	-2.9	-6.0	-4.6	-6.3	-9.0	-3.6	-14.1	-12.3	-15.0	-7.3	-8.4	-10.5
SOD2	NM_000636	5.4	4.5	5.8	7.4	7.5	5.9	15.3	12.1	9.0	7.7	13.4	8.0	9.0
TGFA	NM_003236													
TGFB1	NM_000660													
TXN2	NM_003329													
TIMP1	NM_003254	3.3	3.8	4.1	3.6	2.9	3.3							
TNF	NM_000594													
UGT1A1	NM_001072	2.6	3.5	2.8			-2.1						3.2	

Appendix 12: Summary of gene expression changes in primary human hepatocytes culture measured with Illumina BeadChips. Only genes 2-fold deregulated and with a pValue lower than 0.05 are shown.

Appendix 13: Gene set with the 724 top ranked genes of the predictive model giving the best classification results of the experiments 9 d after treatment

Gene Symbol	Accession-Nr	Gene Symbol	Accession-Nr	Gene Symbol	Accession-Nr
Abca3_predicted	XM_220219	Clic5	NM_053603	Frg1_predicted	XM_341442
Abca8a_predicted	XM_221100	Cnot6l_predicted	XM_341191	Fusip1_predicted	XM_342948
Abcg4_predicted	XM_236186	Cobll1_predicted	XM_229988	Fxc1	NM_053371
Abl1	XM_231137	Col18a1	XM_241632	G2an_predicted	XM_215144
Acbd3	NM_182843	Colec10_predicted	XM_235330	Gata4	NM_144730
Adar	NM_031006	Commd5	NM_139108	Gbp2	NM_133624
Aer61	XM_579302	Cops5_predicted	XM_232615	Gcipip	NM_133417
Aes	NM_019220	Coq3	NM_019187	Ghitm	NM_001005908
Akna_predicted	XM_342848	Cox7b	NM_182819	Gla	XM_343817
Akt1s1_predicted	XM_238103	Cryl1	NM_175757	Gluld1	NM_181383
Alg5_predicted	XM_215561	Csprs_predicted	XM_237360	Gm83_predicted	XM_343231
Amid_predicted	XM_342137	Ctla4	NM_031674	Gnb1	NM_030987
Ankrd24_predicted	XM_216841	Cubn	NM_053332	Gpr61_predicted	XM_227581
Ankrd5_predicted	XM_215854	Cxxc1_predicted	XM_238016	Gps2_predicted	XM_220615
Anpep	NM_031012	Cycs	NM_012839	Grtp1_predicted	XM_341463
Ap1g1	XM_341686	Cyp11a1	NM_017286	Gsta4_predicted	XM_217195
App	NM_019288	Cyp17a1	NM_012753	Gtf2b	NM_031041
Aprin_predicted	XM_221833	Cyp1a1	NM_012540	Gucy1b2	NM_012770
Areg	NM_017123	Cyp2e1	NM_031543	Hadh2	NM_031682
Arhgap21_predicted	XM_225628	Cyp2r1_predicted	XM_341909	Hagh	NM_033349
Arhgap8_predicted	XM_576323	Dclre1b_predicted	XM_227537	Hdh	XM_573634
Arsb	XM_345140	Ddt	NM_024131	Herc2_predicted	XM_218720
Arvcf_predicted	XM_221276	Ddx24	NM_199119	Hexa	NM_001004443
Ascc1	NM_001007632	Ddx3x	XM_228701	Hgd_predicted	XM_573291
Atad2_predicted	XM_235326	Dgka	NM_080787	Hibch_predicted	XM_217395
Atp13a_predicted	XM_214310	Diablo	NM_001008292	Hmgb1	NM_012963
Atp5g1	NM_017311	Dnm2	NM_013199	Hoxc4	XM_235703
Atp5h	NM_019383	Dnmt1	NM_053354	Hpd	NM_017233
Atp6ap1	NM_031785	Drap1_predicted	XM_215177	Hsd17b9	NM_173305
Bap1_predicted	XM_224614	Dscr1	NM_153724	ldh1	NM_031510

Gene Symbol	Accession-Nr	Gene Symbol	Accession-Nr	Gene Symbol	Accession-Nr
Bat2	NM_212462	Dzip1_predicted	XM_344460	Igfbp1	NM_031624
Bcl2l2	NM_021850	Echs1	NM_078623	Igf2r	NM_012756
Bmp4	NM_012827	Egf	NM_012842	Ikbkap	NM_080899
Bmp7	XM_342591	Ehmt1_predicted	XM_342379	Ikbkb	NM_053355
Brd2	NM_212495	Eif4b	NM_001008324	Inpp1	NM_022944
Btc	NM_022256	Elmo2_predicted	XM_342579	Ipo13	NM_053778
Bwk1	NM_198743	Eml1_predicted	XM_343109	Itm2b	NM_001006963
Cacnb4	XM_215742	Eno3	NM_012949	Itpa	XM_230604
Cadps	NM_013219	Ensa	NM_021842	Jam3	NM_001004269
Calmbp1_predicted	XM_213891	Entpd4_predicted	XM_341346	JSAP1	XM_220232
Camta2_predicted	XM_213362	Epb4	XM_345535	Kcng1	XM_215951
Ccr7	NM_199489	Eps8l3_predicted	XM_215677	Kctd5_predicted	XM_220224
Cd59	XM_579359	Exosc5_predicted	XM_218343	Khdrbs1	NM_130405
Cdc14a_predicted	XM_227618	Fadd	NM_152937	Kidins220	NM_053795
Cdc26_predicted	XM_345540	Fah	NM_017181	Kif3b_predicted	XM_215883
Cdk7	XM_215467	Falz_predicted	XM_221050	L3mbtl2_predicted	XM_235769
Cdk9	NM_001007743	Fbxo33_predicted	XM_234205	Lactb2_predicted	XM_216316
Cetn2	XM_215222	Fdx1	NM_017126	Lama5	XM_215963
Chd4	XM_232354	Fkbp4	XM_342763	Laptm4b_predicted	XM_235393
Chd7_predicted	XM_232671	Fkbp9	NM_001007646	Ldhb	NM_012595
Cipar1	NM_173114	Fkbp1	NM_001002818	Leng1_predicted	XM_214797
Ckap4_predicted	XM_343189	Flrt2_predicted	XM_234361	Lnk	XM_579519
Clasp2	NM_053722	Frap1	NM_019906	LOC245925	NM_139093
Cldn10_predicted	XM_214250	Freq	NM_024366	LOC287101	XM_213222
LOC287115	XM_213235	LOC298842	XM_216656	LOC317604	XM_229179
LOC287250	XM_220370	LOC299179	XM_216763	LOC360531	XM_340803
LOC287388	XM_213328	LOC299199	XM_234416	LOC360596	XM_340876
LOC287477	XM_213394	LOC299264	XM_216764	LOC360664	XM_340940
LOC287541	XM_213403	LOC299315	XM_238474	LOC360668	XM_340943
LOC287962	XM_213588	LOC299713	XM_235021	LOC360681	XM_340953
LOC288089	XM_221431	LOC299949	XM_216928	LOC360760	XM_346914
LOC288309	XM_213675	LOC300126	XM_217016	LOC360826	XM_341099
LOC288396	XM_221799	LOC300160	XM_235581	LOC361140	XM_341426
LOC288455	XM_213700	LOC300361	XM_217080	LOC361174	XM_341459
LOC288646	XM_222167	LOC300441	XM_217094	LOC361340	XM_341623
LOC288772	XM_222316	LOC300444	XM_235926	LOC361460	XM_341739
LOC288978	XM_213864	LOC300644	XM_217113	LOC361475	XM_341753
LOC289182	XM_213922	LOC300783	XM_217180	LOC361543	XM_341829

Gene Symbol	Accession-Nr	Gene Symbol	Accession-Nr	Gene Symbol	Accession-Nr
LOC289264	XM_222923	LOC300839	XM_217189	LOC361578	XM_341861
LOC290500	XM_214256	LOC301137	XM_236799	LOC361606	XM_341884
LOC290706	XM_214341	LOC301711	XM_237538	LOC361646	XM_341925
LOC290825	XM_212786	LOC302092	XM_229666	LOC361649	XM_341928
LOC290916	XM_225053	LOC302559	XM_217599	LOC361774	XM_342068
LOC290999	XM_214433	LOC302898	XM_579268	LOC361797	XM_347003
LOC291000	XM_214432	LOC303100	XM_220372	LOC361871	XM_342165
LOC291034	XM_214448	LOC303730	XM_221185	LOC361990	XM_342290
LOC291290	XM_225531	LOC304349	XM_221990	LOC362127	XM_342428
LOC291952	XM_226397	LOC304860	XM_222736	LOC362294	XM_347039
LOC291974	XM_214666	LOC304863	XM_222746	LOC362295	XM_342608
LOC292195	XM_217716	LOC305122	XM_223143	LOC362370	XM_342695
LOC292811	XM_214901	LOC305332	XM_223397	LOC362526	XM_342844
LOC293156	XM_215012	LOC305452	XM_223536	LOC362559	XM_342878
LOC293509	XM_219352	LOC306007	XM_224329	LOC362662	XM_575960
LOC293699	XM_212887	LOC306586	XM_224997	LOC362725	XM_343047
LOC293711	XM_219546	LOC307235	XM_225730	LOC362776	XM_343103
LOC294560	XM_215428	LOC308758	XM_218817	LOC362801	XM_343127
LOC294722	XM_226796	LOC308765	XM_218824	LOC362938	XM_343266
LOC294925	XM_226988	LOC309081	XM_219424	LOC363000	XM_343330
LOC295015	XM_227132	LOC310137	XM_226853	LOC363069	XM_343397
LOC295090	XM_215580	LOC311114	XM_230006	LOC363129	XM_343464
LOC295161	XM_215594	LOC311218	XM_230305	LOC363162	XM_343501
LOC295234	XM_215630	LOC311355	XM_230503	LOC363289	XM_343631
LOC295952	XM_215788	LOC311382	XM_230560	LOC363309	XM_343649
LOC296050	XM_215787	LOC311591	XM_230798	LOC363332	XM_343670
LOC296300	XM_215885	LOC312728	XM_232372	LOC363476	XM_343795
LOC296318	XM_215910	LOC312946	XM_232647	LOC363555	XM_343870
LOC296320	XM_215906	LOC313346	XM_233144	LOC363611	XM_343905
LOC296761	XM_216066	LOC313373	XM_233199	LOC363817	XM_344036
LOC297388	XM_216181	LOC313842	XM_233805	LOC363937	XM_344119
LOC297402	XM_216190	LOC313982	XM_233989	LOC363962	XM_573437
LOC297514	XM_238368	LOC314196	XM_234264	LOC363974	XM_344134
LOC297890	XM_216348	LOC314660	XM_234947	LOC364006	XM_577273
LOC297971	XM_216368	LOC314927	XM_235252	LOC364060	XM_344178
LOC298282	XM_216446	LOC315434	XM_235833	LOC364136	XM_344230
LOC298384	XM_216480	LOC315463	XM_235924	LOC364139	XM_573586
LOC298490	XM_216527	LOC316228	XM_236927	LOC364253	XM_344296
LOC298496	XM_233477	LOC317346	XM_228716	LOC364258	XM_344301
LOC298787	XM_216638	LOC317405	XM_228821	LOC364343	XM_344366
LOC364381	XM_344404	LOC499316	XM_574620	Lpin2_predicted	XM_237521
LOC364535	XM_344495	LOC499401	XM_574716	Lrp10_predicted	XM_224170
LOC364577	XM_573906	LOC499411	XM_579965	Lsm8_predicted	XM_216102
LOC364613	XM_573924	LOC499525	XM_574850	Man2b1	NM_199404
LOC364823	XM_344652	LOC499561	XM_574885	Map3k3_predicted	XM_221034
LOC365300	XM_574483	LOC499581	XM_574906	Mapkapk2	XM_579712
LOC365314	XM_344924	LOC499617	XM_574942	Mark2	NM_021699
LOC365580	XM_577905	LOC499660	XM_574984	Mbd1_predicted	XM_574171

Gene Symbol	Accession-Nr	Gene Symbol	Accession-Nr	Gene Symbol	Accession-Nr
LOC365664	XM_574847	LOC499700	XM_575029	Mcmdc1_predicted	XM_342146
LOC365924	XM_345284	LOC499755	XM_575090	Mcpt114	XM_573784
LOC365949	XM_345296	LOC499809	XM_575149	Mesdc1_predicted	XM_218853
LOC366248	XM_575286	LOC499856	XM_575197	Metap1_predicted	XM_215717
LOC366315	XM_345503	LOC499905	XM_575251	MGC94056	NM_001004258
LOC366461	XM_345576	LOC499931	XM_575276	MGC94221	NM_001004224
LOC366468	XM_345581	LOC499950	XM_575298	MGC94326	NM_001007709
LOC366565	XM_578532	LOC499956	XM_575304	MGC94413	NM_001007745
LOC367030	XM_576362	LOC500005	XM_575359	MGC95208	NM_001005552
LOC367109	XM_345951	LOC500148	XM_575500	MGC95210	NM_001005532
LOC367171	XM_576473	LOC500196	XM_575548	Mgst2_predicted	XM_215562
LOC367205	XM_578768	LOC500382	XM_575740	Mki67_predicted	XM_225460
LOC367761	XM_346284	LOC500506	XM_575868	Mlc3	NM_020104
LOC367806	XM_346310	LOC500553	XM_575916	Mnt_predicted	XM_220698
LOC367944	XM_346362	LOC500606	XM_575979	Mocs1_predicted	XM_236911
LOC497703	XM_579683	LOC500650	XM_576028	Mocs2	NM_001007633
LOC497706	XM_579538	LOC500662	XM_576040	Mrpl22_predicted	XM_213307
LOC497717	XM_579724	LOC500814	XM_576201	Mrpl27_predicted	XM_213439
LOC497754	XM_579458	LOC500819	XM_576208	Mrpl42_predicted	XM_216882
LOC497832	XM_579562	LOC500869	XM_576267	Mrpl49_predicted	XM_219525
LOC497886	XM_573071	LOC500981	XM_576391	Mrps17_predicted	XM_213762
LOC497904	XM_573090	LOC501002	XM_576412	Ms4a8b_predicted	XM_342026
LOC497974	XM_573168	LOC501058	XM_576474	Mss4	NM_001007678
LOC498002	XM_573198	LOC501064	XM_576479	Mybph	NM_031813
LOC498058	XM_573255	LOC501172	XM_576599	Myc	NM_012603
LOC498229	XM_573449	LOC501204	XM_576630	Myo1 d	NM_012983
LOC498230	XM_573451	LOC501326	XM_576737	Myr8	NM_138893
LOC498268	XM_579805	LOC501351	XM_576762	Nap113	NM_133402
LOC498374	XM_573609	LOC501363	XM_576776	Ncdn	NM_053543
LOC498411	XM_573658	LOC501370	XM_576783	Ncor2_predicted	XM_341072
LOC498435	XM_573687	LOC501397	XM_576809	Ndufa8_predicted	XM_216044
LOC498729	XM_574003	LOC501514	XM_576915	Ndufb9_predicted	XM_216929
LOC498747	XM_574026	LOC501534	XM_576934	Ndufs3_predicted	XM_215776
LOC498759	XM_574044	LOC501621	XM_577021	Ndufv2	NM_031064

Gene Symbol	Accession-Nr	Gene Symbol	Accession-Nr	Gene Symbol	Accession-Nr
LOC498805	XM_574089	LOC501655	XM_577050	Nedd4a	XM_343427
LOC498819	XM_574101	LOC501952	XM_577379	Negr1	NM_021682
LOC498837	XM_574121	LOC502201	XM_577662	Neo1	XM_343402
LOC498899	XM_574186	LOC502393	XM_577872	Neu1	NM_031522
LOC499009	XM_574302	LOC502686	XM_578183	Nfatc4_predicted	XM_240184
LOC499018	XM_574311	LOC502743	XM_578243	Nfe2l2	NM_031789
LOC499031	XM_574321	LOC502858	XM_578358	nidd	NM_213627
LOC499071	XM_574352	LOC502935	XM_578437	Nisch_predicted	XM_240330
LOC499087	XM_574374	LOC503000	XM_578512	Nosip_predicted	XM_214926
LOC499255	XM_574549	LOC503197	XM_578721	Notch1	XM_342392
LOC499262	XM_574557	LOC503351	XM_578889	Npl4	NM_080577
LOC499288	XM_574587	Loc65027	XM_573762	Npy	NM_012614
Nr3c1	NM_012576	Prlph	NM_021580	RGD1359460	NM_001006959
Nucb1	NM_053463	Psma2	NM_017279	RGD1359600	NM_001007688
Nudt6	NM_181363	Psma4	NM_017281	Rgs14	NM_053764
Nyw1	XM_230288	Psma5	NM_017282	Rhcg	NM_183053
Ogfrl1_predicted	XM_237000	Psma6	NM_017283	Ripk5	NM_199463
Olr1024_predicted	NM_001000068	Psma7	XM_579184	Rnf111_predicted	XM_236380
Olr1242_predicted	NM_001000450	Psmb1	NM_053590	Rnf153_predicted	XM_215286
Olr1340_predicted	XM_236174	Psmb3	NM_017285	Rpl3l_predicted	XM_213231
Olr1592_predicted	NM_001000084	Psmb4	NM_031629	Rpo2tc1	NM_001009618
Olr1690_predicted	NM_001000274	Psmb6	NM_057099	Rps12	NM_031709
Olr1751_predicted	NM_001000492	Psmb7	NM_053532	Rragc_predicted	XM_216515
Olr29_predicted	NM_001000691	Psmc1	NM_057123	RSB-11-77	NM_182669
Olr495_predicted	NM_001000310	Psmc2	NM_033236	S100a1	XM_579178
Olr535_predicted	NM_001000672	Psmc3	NM_031595	Sdhc	NM_001005534
Olr552_predicted	NM_001001055	Psmc5	NM_031149	Sec14l2	NM_053801
Olr818_predicted	NM_001000844	Psmc7	NM_031978	Sec24b_predicted	XM_215706
Pabpc4_predicted	XM_216517	Psmc11_predicted	XM_220754	Sema3b_predicted	XM_343479
Pacs1	NM_134406	Psmc7_predicted	XM_226439	Sema3f_predicted	XM_236623
Pafah1b3	NM_053654	Pspn	NM_013014	Serpinh1	NM_017173
Pafah2	NM_177932	Ptbp1	NM_022516	Setdb1_predicted	XM_227444
Pam	NM_013000	Ptgfrn	NM_019243	Siahbp1	XM_343268
Pax2_predicted	XM_239083	Ptk2	NM_013081	Skp1a	NM_001007608
Pcdhga8_predicted	XM_344668	Ptms	NM_031975	Slc12a4	NM_019229

Gene Symbol	Accession-Nr	Gene Symbol	Accession-Nr	Gene Symbol	Accession-Nr
Perq1_predicted	XM_222024	Ptpn21	NM_133545	Slc1a3	NM_019225
Pgpep1	NM_201988	Pus1_predicted	XM_222267	Slc24a4_predicted	XM_234470
Phb	XM_579541	Pycs_predicted	XM_342048	Slc25a11	NM_022398
Phr1_predicted	XM_214245	Pygb	XM_342542	Slc28a2	NM_031664
Pias3	NM_031784	Rab6b_predicted	XM_343459	Slc30a8_predicted	XM_235269
Pigh_predicted	XM_343083	Rac2	NM_001008384	Slc35b4_predicted	XM_216122
Pigq	NM_001007607	Rarsl_predicted	XM_216367	Slc35e1_predicted	XM_224707
Pip5k2c	NM_080480	Rasip1_predicted	XM_214916	Slc37a1_predicted	XM_574727
Plcb1	XM_342524	Rassf5	NM_019365	Slc39a6_predicted	XM_214607
Plec1	NM_022401	Rce1_predicted	XM_219685	Slc39a8_predicted	XM_575042
Plekhb2_predicted	XM_217372	Rfx1_predicted	XM_222456	Slc6a8	XM_579415
Plekhf2_predicted	XM_342803	RGD1305327_predicted	XM_343285	Slc7a1	NM_013111
Plekhn2_predicted	XM_233611	RGD1305649_predicted	XM_575926	Slit2	XM_346464
Plk3	XM_342888	RGD1305679_predicted	XM_341511	Smad1	NM_013130
Plod3	NM_178101	RGD1305793_predicted	XM_219958	Smndc1_predicted	XM_213506
Plp2_mapped	NM_207601	RGD1306284	NM_001008283	Snapc1_predicted	XM_234299
Podxl	NM_138848	RGD1307423	NM_001008334	Snx11_predicted	XM_573185
Poldip2_predicted	XM_237790	RGD1307481	NM_001008327	Spr	XM_342714
Pole4_predicted	XM_342710	RGD1307512_predicted	XM_343357	Spred2_predicted	XM_223647
Polr2j_predicted	XM_213753	RGD1307599_predicted	XM_233692	Srd5a1	NM_017070
Pom210	NM_053322	RGD1307648_predicted	XM_215262	Ssr1_predicted	NM_001008891
Pomc	NM_139326	RGD1308009_predicted	XM_226233	Ssrp1	NM_031121
Pp	XM_215416	RGD1308054_predicted	XM_214834	Stard3nl	NM_001008298
Ppie_predicted	XM_216524	RGD1308350_predicted	XM_343116	Sulf2_predicted	XM_230861
Ppm1d_predicted	XM_213418	RGD1308600_predicted	XM_342393	Supt4h2_predicted	XM_213415
Ppp5c	NM_031729	RGD1309207_predicted	XM_343064	Syngn1	NM_019166
Pprc1_predicted	XM_215259	RGD1309256_predicted	XM_214087	Tacc2	NM_001004415
Prcc_predicted	XM_227476	RGD1309721	NM_001009670	Tacc2	NM_001004418
Prdm13_predicted	XM_345509	RGD1309906	NM_001009246	Taok2	NM_022702
Prkaca	XM_341661	RGD1310022_predicted	XM_214983	Tcam1	NM_021673

Gene Symbol	Accession-Nr	Gene Symbol	Accession-Nr	Gene Symbol	Accession-Nr
Prkcdbp	NM_134449	RGD1311745	NM_001008329	Tceb3bp1_predicted	XM_576183
Tcerg1_predicted	XM_225983	Trim21_predicted	XM_219011	Vps13d_predicted	XM_233792
Tcf2	NM_013103	Trim28	XM_344861	Vps39_predicted	XM_575216
Tcf8	XM_341539	Trpv6	NM_053686	Vwf	XM_342759
Tcof1_predicted	XM_214552	Tsga10ip	XM_579136	Wdr22_predicted	XM_234345
Tep1	NM_022591	Tspyl_predicted	XM_228225	Wfdc3_predicted	XM_215938
Terf1_predicted	XM_238387	Tst	NM_012808	Xpo6_predicted	XM_574559
Tex27_predicted	XM_574725	Ttyh3_predicted	XM_221962	Xylt1	XM_341912
Tfdp2_predicted	XM_217232	Tubb5	NM_173102	Zbtb7a	NM_054002
Tfpi	NM_017200	Tubgcp3_predicted	XM_225013	Zc3hdc5_predicted	XM_340939
Tfrc	XM_340999	Txk_predicted	XM_223365	Zc3hdc6_predicted	XM_230592
Tgfb1	NM_021578	Txn2	NM_053331	Zdhhc2	NM_145096
Tgfb2	NM_031131	Txndc9	NM_172032	Zfp262_predicted	XM_233529
Timm17a	NM_019351	Txn15_predicted	XM_213382	Zfp282_predicted	XM_216140
Timm22	XM_340856	Ua20	NM_144742	Zfp367_predicted	XM_573970
Tinf2	NM_001006962	Ube2r2_predicted	XM_216864	Zmynd12_predicted	XM_233458
Tjp4_predicted	XM_236932	Ufc1	NM_001003709	Zmynd15_predicted	XM_213338
Tlr6	NM_207604	Ufd1l	NM_053418	Znf500_predicted	XM_343376
Tmc4_predicted	XM_218186	Uhrf1_mapped	NM_001008882		BC093384
Tmprss7_predicted	XM_221464	Uqcrh	NM_001009480		AY724519
Tnfrsf6	NM_139194	Urod	XM_342887		AY724532
Tnn_predicted	XM_222794	Uros_predicted	XM_574579		BC079376
Tor1b_predicted	XM_231146	Usp12_predicted	XM_341033		BC100083
Tpi1	XM_579468	Usp7_predicted	XM_340747		CO382628
Trim14_predicted	XM_232992	V1rj6	NM_001009507		DN935439
Trim2_predicted	XM_342268	Vmac	XM_579064		DV728079
					BC083830